FACULTY OF SCIENCES

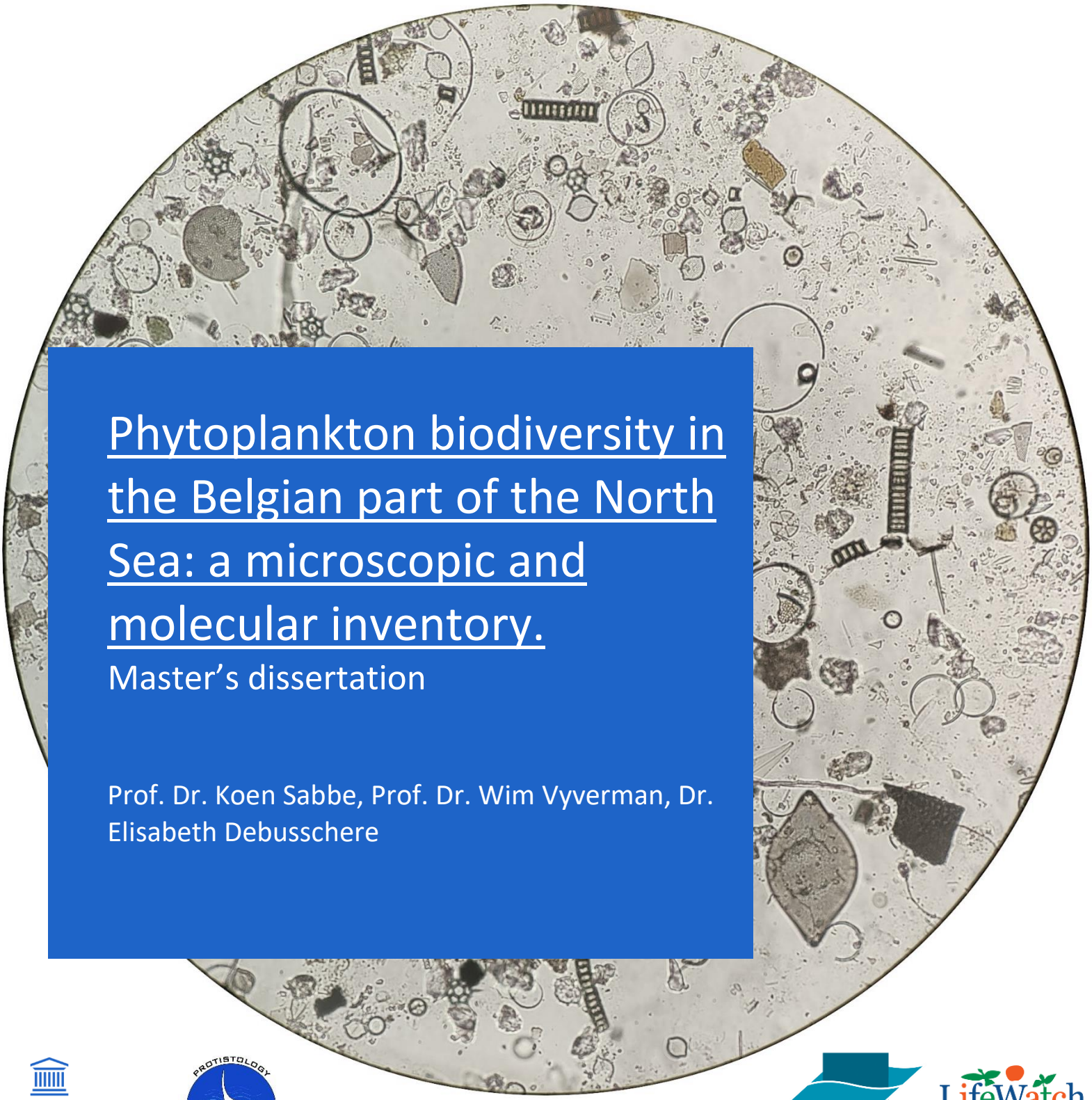

Phytoplankton biodiversity in the Belgian part of the North Sea: a microscopic and molecular inventory.

Master's dissertation

Prof. Dr. Koen Sabbe, Prof. Dr. Wim Vyverman, Dr. Elisabeth Debusschere

GHENT UNIVERSITY

PROTISTOLOGY AQUATIC ECOLOGY

VLIZ

LifeWatch BELGIUM

Biology Department
Research Group Protistology & Aquatic Ecology

Phytoplankton biodiversity in the Belgian part of the North Sea: a microscopic and molecular inventory.

Rune Lagaisse
Studentnumber: 01504232

Supervisor(s): Prof. Dr. Koen Sabbe (promotor)
Prof. Dr. Wim Vyverman (co-promotor)
Dr. Elisabeth Debusschere (co-promotor)
Luz Amadei Martínez (supervisor)
Margarita Bogorad (supervisor)

Master's dissertation submitted to obtain the degree of Master of Science in Biology

Academic year: 2019 – 2020

Table of Contents

List of tables

List of figures

ABSTRACT

Phytoplankton plays a pivotal role in marine ecosystems: it fuels food webs, drives carbon and nutrient cycles and responds rapidly to environmental changes like pollution or global warming. Due to its key function, monitoring of phytoplankton is essential for understanding marine dynamics and in order to preserve the marine environment for the future. In Belgian coastal waters, phytoplankton is currently monitored under the European LifeWatch campaign hosted by the Flanders Marine Institute (VLIZ) in collaboration with the Protistology & Aquatic Ecology (PAE) research group at the University of Gent. In this thesis, we aimed to create an updated inventory of phytoplankton biodiversity in the Belgian part of the North Sea while simultaneously assessing spatial and temporal dynamics. With the creation of an updated inventory accompanied by species descriptions of selected taxa that are challenging to identify, we aimed to produce a reference for future biodiversity assessments. To this end, we opted for a classical microscopic approach in combination with DNA metabarcoding of the microplankton (< 50 µm) community. In contrast with other novel, high-throughoutput assessment techniques like the FlowCam and FlowCytometry, the combination of microscopy and metabarcoding albeit more time-consuming, offers detailed insights into the taxonomic structure of the phytoplankton community. These two complimentary techniques are therefore superior to resolve uncertainties surrounding the biodiversity of phytoplankton in the Belgian part of the North Sea.

Keywords: Phytoplankton; microscopy; NGS; BPNS; BPNS; SEM

Preambule: Covid-19

This thesis was carried out during the Covid-19 pandemic, causing some modules of the research to be ended abruptly or altered. Sampling campaigns were supposed to take place up to April 2020 but ended in December 2019 as no sampling campaigns took place during January and February 2020 due to maintenance of the ship and storms, campaigns from March onwards were cancelled due to the virus. Microscopic counts were originally to be performed using the Utermöhl method and inverted microscopy on 100 ml quantitative samples. Unfortunately, due to the shutdown of the university and its facilities, counts could only be carried out on permanent mounted diatoms. The original quantitative samples for counts are still available at Gent University stored in Lugol's iodine solution and formaldehyde for future analysis. Scanning electron microscopy was supposed to take place on all net samples during the whole campaign, but could only be performed on samples from August and September due to time loss by finding the appropriate fixation methods and subsequent shut down of the university facilities. This likely caused gaps in identification of smaller species through microscopy and limited the number of descriptions of (semi)cryptic species, as for these SEM imagery is required.

INTRODUCTION

1. The Belgian Part of the North Sea

1.1 Physical and chemical characteristics

The Belgian Part of the North Sea (BPNS) is located in the Southern Bight of the North Sea. The Belgian coastline has a length about 65 km and the BPNS extends up to 50 km offshore, generating a surface area of approximately 3 454 km^2 (Belgian State, 2012) (Rousseau et al., 2006). The average depth of the BPNS is 20 m, with a maximum depth up to 30-40 m (De Galan et al., 2004) (Ruddick & Lacroix, 2006). The sea floor is characterized by a complex series of sand banks which are located more or less parallel to the coastline. They can stretch areas of 13-30 km and rise to 20 m above the bottom of the sea. The substrate consists mainly of sand, added clay, silt and gravel (Belgian State, 2012).

The BPNS is a highly dynamic zone, dominated by daily tides varying between 3 m at neap tide and 4.5 m at spring tide. Tidal streams are modified and redirected by the presence of sandbanks, human infrastructure and dredging and shipping activities near the ports of Ostend, Zeebrugge and the Scheldt estuary. The combination of these strong currents and the relative shallowness of the BPNS ensure a permanent mixing of the water column which prevents the formation of pronounced stratifications. Local baroclinic currents are however present at river outflows and estuaries caused by gradients in salinity (Belgian State, 2012) (Van den Eynde et al., 2007). Additionally, hydrodynamics are influenced by storms and winds, which impact water level and transport, salinity, nutrients and suspended matter concentrations (Belgian State, 2012). Atlantic inflow water, which reaches the BPNS through the English Channel (Fig. 2), constitutes up to 95% of Belgian coastal water, the remaining percentages constitute of freshwater river inflow. The influence of these freshwater inflow from the continental rivers Rhine-Meuse (1.9%), Seine (1.3%) and Scheldt (0.8%) is much less pronounced (Belgian State, 2012) (Lacroix et al., 2004) (Ruddick & Lacroix, 2006). The influence of the river Scheldt is highest during February and March (Lacroix et al., 2004). The above mentioned rivers run through industrialized and densely populated areas, causing them to be charged with high nutrient loads and chemical pollutants (Belgian State, 2012). Riverine inputs vary seasonally as well as interannually as a result of river nutrient concentrations and fluctuations in river discharge (Lacroix et al., 2004) (Gypens et al., 2007). Additionally, the BPNS receives nutrients from atmospheric deposition, originating from industrialization (De Galan et al., 2004) (Rousseau et al., 2006).

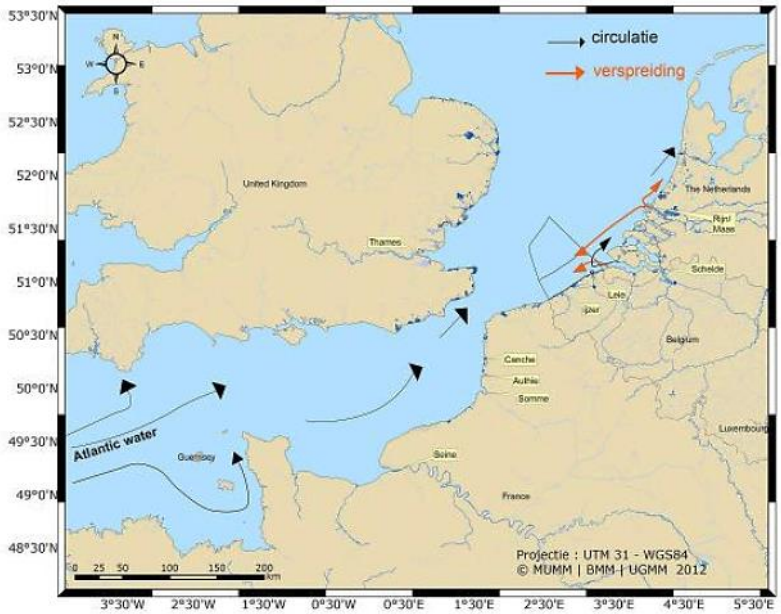

Figure 1: General diagram of the circulation in the Channel and the southern part of the North Sea. The black arrows represent the annual average residual circulation ("circulatie"). The red arrows show the horizontal dispersion ("verspreiding"), caused by the tide, on the transport of the Scheldt and Rhine/Meuse water masses. Source: Belgian state (2012)

The main variability in salinity in the BPNS is horizonal and caused by freshwater inflows from the Scheldt estuary. At the mouths of the estuary, salinity varies between 25 PSU and 32 PSU, while seawater entering the BPNS through the Channel has a mean salinity of 35 PSU (De Galan et al., 2004). Vertical variability in salinity is limited by permanent vertical mixing. Long term variability in salinity is caused by climate variability in wind and precipitation, which either enhances or stops river plumes from advancing into the open sea. Seasonal variability in salinity is mainly caused by seasonal cycles of freshwater inflow and precipitation (Belgian State, 2012).

The availability of light is essential for photosynthesis based food webs, as phytoplankton converts chemical energy to biologically available energy. The vertical attenuation of Photosynthetically Available Radiation (PAR) controls light availability and thus primary production in the water column. The BPNS is characterized by significant variability in PAR mainly seasonally but also caused by spatial variability in suspended particulate matter (SPM) and dissolved organic matter (DOM). Shallow waters close to the coast are more turbid and have higher concentrations of SPM. Secchi depth varies from less than a meter at onshore, turbid locations to 5-15 m at offshore locations. Temporal variability in PAR is caused by resuspension and advection of particulate matter, modified by winds and tides. During winter, the prevalence of stronger winds generates seasonal cycles with higher PAR attenuation in winter, followed by increased settling of SPM in spring which influences the timing of onset of spring phytoplankton blooms (see further). Additional variability in PAR attenuation may be caused by riverine DOM (Rousseau et al., 2006) (Belgian State, 2012).

Sea surface temperature (SST) displays a seasonal cycle, generated by solar radiation, with a difference of about 15°C between summer and winter temperatures. Additionally, an interannual variability in SST of 1-4°C is observed. This variability is correlated with the NAO index (see below), and can obscure long term trends in temperature related to global warming. Vertical temperature differences along the water column are usually only small due to the strong and persistent mixing of the water column. Exceptions are found near the mouths of estuaries where salinity gradients can cause local stratifications (Belgian State, 2012) (Tsimplis et al., 2006).

The North Atlantic oscillation (NAO) causes interannual variability in multiple abiotic factors described above. NAO is the gradient between the Icelandic Low and Azores High atmospheric pressure zones. The magnitude of pressure difference in the atmosphere influences winds, precipitation, air temperatures and clouds (Ruddick & Lacroix, 2006). Periods of positive NAO index are characterized by strong Southwesterly winds, which drive Atlantic inflow water from the Channel into Belgian coastal waters. These winds also influence the spreading of river plumes of the river Scheldt, with positive NAO indices forcing a stronger North-Eastward dispersion of the plume. Additionally, a positive NAO index is correlated with increased precipitation over the Scheldt which impacts nutrient supply to coastal waters (Belgian State, 2012) (Rind et al., 2005).

1.2 BPNS: an anthropogenically impacted area

The BPNS delivers many ecosystem services like food provision, offshore industry and energy production, nutrient cycling, tourism, recreation and education (Belgian State, 2012). The many uses of the BPNS are reflected in the complex Belgian Marine Spatial Plan, which aims to harmonize both economic assets as well as ecological objectives. This includes developing offshore windmill farms, the delimitation of Marine Protected Areas (MPAs), sand and gravel extraction, protection of wrecks with associated high biodiversity, reserving areas for military purposes and much more. The Belgian Marine Spatial Plan is meant to safeguard

the many ecological functions and economic benefits of the BPNS (Pecceu et al., 2016) (Royal Decree, 2014) (Royal Decree, 2020).

However, due to the long history of various human activities taking place in and around the BPNS, the ecosystem services and the present biodiversity are under pressure. The Scheldt basin passes through intensively used anthropogenic areas. Through land runoff, precipitation, atmospheric deposition and sewage and industrial waste water treatment plants, the river Scheldt gets charged with high nutrient loads which partly end up in the BPNS (Desmit et al., 2018) (Prins et al., 2012) (Burson et al., 2016). These anthropogenic inputs skew nutrient ratios compared to the optimal nutrient ratios for phytoplankton (the Redfield ratio for Nitrogen (N), Phosphorus (P) and Silicon (Si): N:P=16 for marine phytoplankton and N:Si= 1 for coastal diatoms), which can modify phytoplankton community composition (Redfield et al., 1963). Since the improvement of waste water management in the 1990s, a de-eutrophication period began, characterized by a significant decrease in P input in the river Scheldt (Burson et al., 2016). Since the de-eutrophication period, N input also decreased although to a lesser extent than the P decrease due to the ongoing intense use of agricultural fertilizers (Burson et al., 2016). These significant decreases in N and P indirectly influenced the Si cycle in the river Scheldt. With decreasing nutrient inputs, Si retention decreased simultaneously caused by lower upstream diatom production, leading to increased Si input in coastal waters (Prins et al., 2012) (Desmit et al., 2018). This unbalanced change in nutrient decreases and retention altered phytoplankton community structure as different species have different nutrient requirements (Burson et al., 2016) (Nohe et al., 2020). Unbalanced changes in nutrients can contribute to Harmful Algal Blooms (HABs), in combinations with changes in environmental variables like increases in sea surface temperatures and changes in community structure altering predation pressure (Anderson et al., 2012)(Nohe et al., 2020).

The BPNS is subjected to multiple forms of exploitation and hosts heavy industry. The construction of offshore windmill farms and the associated dredging activities influence SPM concentrations and turbidity (Philippart et al., 2013). Erosion and organic enrichment is present in the vicinity of the wind turbines (Belgian State, 2012). The construction of the port of Zeebrugge, the expansion of the port of Oostende and the dredging activities performed to deepen the shipping tracks have led to a significant destruction of the seabed and redistribution of fine-grained sediments. Maintenance dredging and subsequent dumping of the sediment at sea, has an effect that extends far beyond the zone of sediment deposition. Especially silt, which makes up 60-70% of the sediment that gets resuspended after deposition, increases turbidity significantly in and around the dumping site. Exploitation by extraction of sand and gravel causes physical damage to the seabed, but the impact usually remains limited in time and space (Belgian State, 2012). Exploitation by heavy fishing industry has also exerted great pressure on the ecosystems of BPNS, with an influence extending beyond the level of fish in food webs. Overexploitation of fish stocks has been observed to cascade down food webs to the lowest levels of primary producers, causing altered phytoplankton community structure (Casini et al., 2008). The effect of fisheries depends on the used fishing technique, the location, timing and post fishing management. Beam trawling, one of the most destructive fishing practices, highly impacts the seabed and its associated diversity and influences turbidity (Belgian State, 2012).

The introduction of invasive species through aquaculture and ballast water from the shipping industry can potentially disrupt communities. Often, invasive phytoplankton species have the potential to dominate entire phytoplankton communities by outcompeting local species for resources and thereby decreasing biodiversity (Reise et al., 1998) (Meier et al., 2015) (Kerckhof et al., 2007).

Another problem for the marine environment constitutes pollution by litter, chemicals and radioactive waste. Agriculture, industry, wastewater management, incineration of fossil fuels and accidental leaking of painting and asphalt are the main sources of hazardous substances in the BPNS. Both attached to particulate matter and in dissolved form, they end up in the BPNS via the river basins of the Seine, Scheldt and Meuse-Rhine. (Belgian State, 2012)(Kersten et al., 1993) .

Lastly, climate change exerts its effect on the North Sea. Sea surface temperatures (SST) have increased with 1.5°C between 1988 and 2014 (Nohe et al.,2020), with the strongest increasing taking place during the last 50 years (Belkin, 2009). An increase in SST may enhance stratification of the water column and influence mixing, SPM concentrations and light availability, and in doing so climate change can even influence the lowest levels of marine producers (Baudron et al., 2014) (Beardall et al., 2009) (Winder & Sommer, 2012) (Beaugrand, 2004). Sea level increase, typically measured at Ostend, has been accelerating since 1992 and now measures up to 4.41 mm per year (Belgian State, 2012). Lastly, NOA is also influenced by climate chance, leading to an increased frequency of positive oscillations, the effects of which have been discussed above (Rind et al., 2005).

The above human-induced changes can lead to increased economic costs, ecosystem shifts and even threats to public health. They pose challenges for management and conservation of the BPNS if we want to ensure marine biodiversity and ecosystem services for future generations (Pecceu et al., 2016).

2. Phytoplankton in the BPNS

Oceans cover about 70% of our planet's surface, making them one of the biggest ecosystems in the world. Their importance is reflected in the key role oceans play in global nutrient and carbon cycling (Hays et al., 2005). Carbon cycling, which activity influences the Earths global climate, is largely driven by phytoplankton primary production (Ducklow et al., 2001). Phytoplankton are responsible for over 45% of the global net primary production, even though they remarkably only represent about 1% of the Earths photosynthetic biomass (Karlusich et al., 2020). They are defined as aquatic photosynthetic ('phyto') microbial organisms which are passively moved by ocean currents ('plankton'). They are generally small in size, going from less than 1 µm up to 1 mm (Winder & Sommer, 2012). Phytoplankton do not only play an important role in the global carbon cycle (Hays et al., 2005), but they also fuel entire food webs through their photosynthetic activity. Due to their high abundances and short generation times, they respond quickly to changes in environmental conditions like oceanic currents, nutrient conditions, temperature, light availability, salinity and pollution and in doing so they influence higher levels of food webs (Hays et al., 2005).

Phytoplankton is a taxonomically highly diverse group comprising both photosynthetic protists and cyanobacteria. Within the Eukaryote domain, phytoplankton mainly belong to a few main groups; SAR (Stramenophila, Alveolata and Rhizaria), Archaeplastida, Haptophyta (especially coccolithophorids) and Cryptophyceae (Burki, 2014) (Pierella Karlusich et al., 2020). In most papers, the dominant phytoplankton groups listed for the BPNS are dinoflagellates (Dinophyceae), diatoms (Bacillariophyceae) and Prymnesiophyceae (Desmit et al.2015) (Lancelot et al.,2009) (Muylaert et al. 2006) (Rousseau et al.,2006).

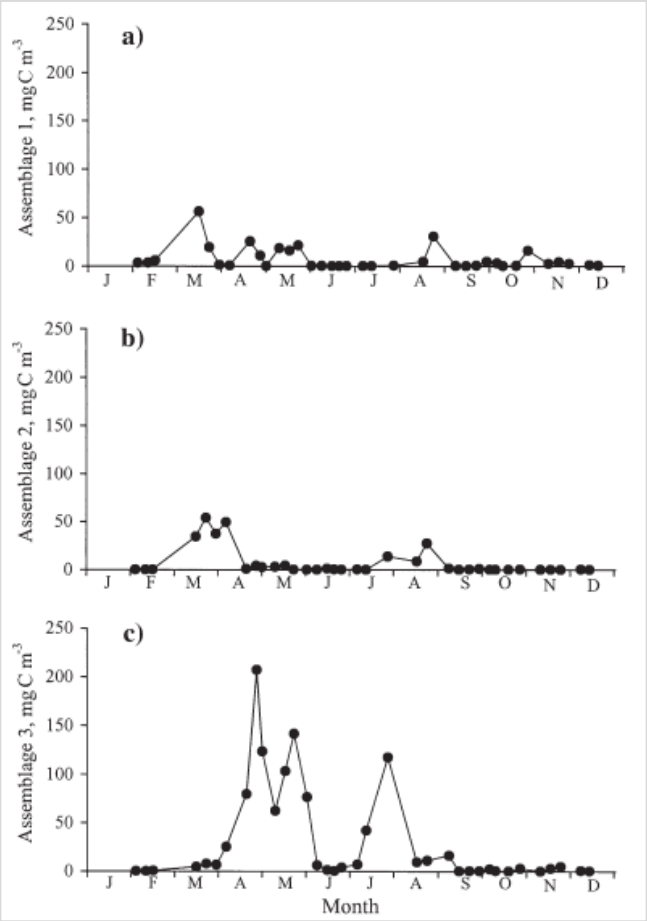

Figure 2: (a) Assemblage 1 (early spring and autumn diatoms); (b) Assemblage 2 (Chaetoceros spp.-Schroederella sp.); and (c) Assemblage 3 (Rhizosolenia spp.) blooming at Station 330 of Belgian coastal waters in 1995. Source Rousseau et al. (2002).

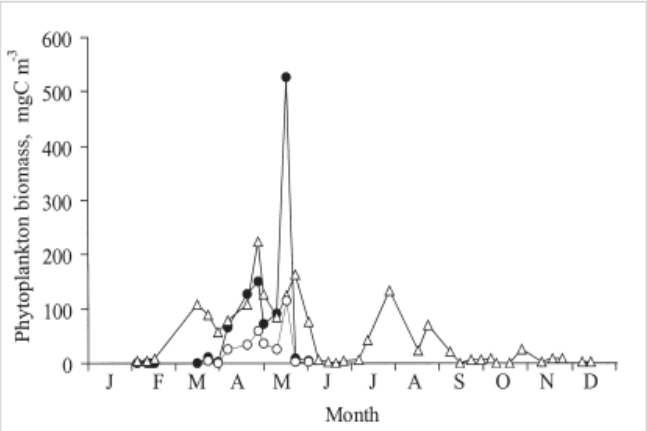

Figure 3: Seasonal changes of diatoms (triangles), Phaeocystis colony (black dots) and cellular (open circles). Source Rousseau et al. (2002).

Temporal dynamics in the phytoplankton community in the BPNS are characterized by an annually recurring seasonal succession of phytoplankton blooms. A typical spring diatom dominated bloom is formed between March and May, but there is interannual variation in the timing, peak abundances and community composition of the bloom (Desmit et al., 2015). Advancement of the bloom is mainly determined by light availability and temperature, but also to a lesser extent by mixing of the water column, nutrient conditions, grazing, and phytoplankton community composition (Behrenfeld & Boss, 2018). This spring bloom is typically followed by a *Phaeocystis globosa* bloom (Fig. 3) and then again by a diatom summer peak, although less intense than the main diatom spring bloom (Rousseau et al., 2006). Dinoflagellates typically reach their peak during the summer months.

Muylaert at al. (2006) and Rousseau et al. (2008) identified three major successive diatom assemblages in the BPNS and their underlying mechanisms (Fig. 2). The fist community dominates from January to March and is characterized by bentho-pelagic species like *Actinocyclus scenarius*, *Paralia* spp., *Odontella aurita*, *Rhaphoneis amphiceros*, *Pelagiogrammopsis vanheurckii* and smaller sized pelagic species like *Thalassiosira* spp. The second community is dominated by *Chaetoceros* spp., *Leptocyclindrus danicus*, *Skeletonema* spp. and *Lithodesmium undulatum.* The third community comprises mainly *Rhizosolenia* spp., *Guinardia* spp., and *Pseudo-nitzschia* spp. These three communities always occur in the same order (1-2-3-2-1), but their timing of onset varies both locally and interannually. Community 2 is never truly dominant but is rather a transition stage between community 1 and 3 during spring and late summer, and it coincides with the *Phaeocystis* bloom. The replacement of community 1 by 2 and 3 is linked to the depletion of dissolved Si, as community 1 contains more heavily silicified species. The reappearance of community 1 at the end of summer, is linked to the reoccurrence of increased

levels of dissolved Si (Rousseau et al., 2002) (Muylaert et al., 2006).
Spatial variability in phytoplankton community biomass and structure is characterized by a coast to offshore gradient, with increased biomasses and chlorophyll a concentrations near the coast, and a higher abundance of smaller dinoflagellate species at offshore locations (Muylaert et al., 2006) (Rousseau et al., 2006). The onset of the spring bloom is observed to occur in March in the South West part of the BPNS while in the North East part the bloom started one month later. The SW part of the BPNS is characterized by shallow and more turbid waters as opposed to the NW part of the BPNS, leading to differences in onset and succession of the diatom communities between the SE and NW part of the BPNS (Muylaert et al., 2006).

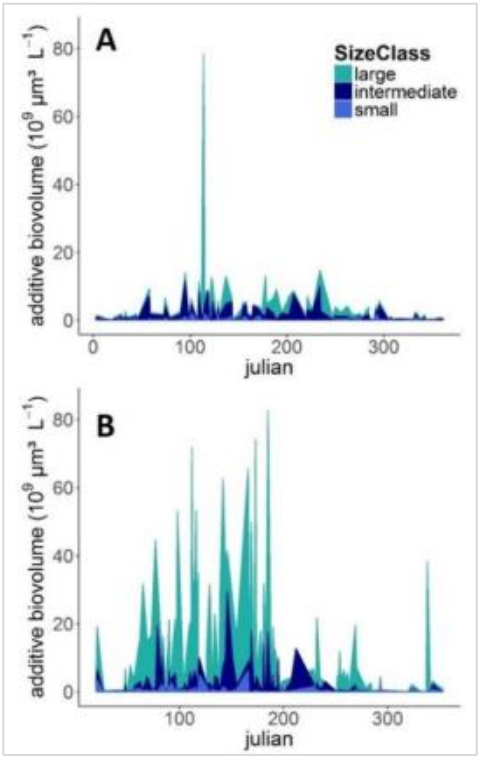

Figure 4:Annual cycle of small, intermediate and large diatoms in the onshore stations of the BPNS averaged for A 1970s and B 2000s. Source Nohe et al. (2019).

With the analysis of the Belgian Phytoplankton Database (Nohe et al., 2018), the above described patterns in phytoplankton communities structure and bloom onset were observed to have changed over the last decades. First, total biovolumes of dinoflagellates and diatoms have increased. Diatom abundances have increased from winter to summer while dinoflagellates have increased in spring and summer. These increases in biomass coincide with increased summer and winter temperatures since the 1970s, but indirect effects like increased stratification, top-down control by grazers and higher light availability are also possible causes. Secondly, the bimodal annual diatom bloom pattern (described above) changed to a single unimodal extended growing season which starts earlier in February and lasts until July and this is mainly dominated by larger diatom species (Fig. 4). Dinoflagellates have also shifted from a bimodal annual bloom pattern to a single bloom from May to September. Earlier onset of and more intense diatom spring bloom correlated with increased water transparency, higher winter SST and more favorable nutrient ratios in late winter and earlier spring. The earlier decline in diatoms in mid-summer might be related to the increase in dinoflagellates who do better under warm and less turbulent conditions. Third, the diatom community has become more seasonally homogenized with a pronounced shift towards larger taxa, potentially related to their lower Si requirements and their higher resistance to grazers. There is a significant increase in *Chaetoceros* spp., which are associated with higher SST and more light availability. Lastly, there is also a significant increase in potentially harmful algal species like *Pseudo-nitzschia* spp. and some harmful dinoflagellate genera, possibly caused by increased SST as dinoflagellates perform better under warmer temperatures (Nohe et al., 2020). The observed shift in phytoplankton phenology is probably linked to the increase in SST of 1.5°C between 1988 and 2014 (Nohe, 2020). A decline in annual mean chlorophyll has been observed since 1988, possibly linked to the de-eutrophication period since the mid-1980s and the increase in SST (Desmit et al., 2020) (Nohe et al., 2020).

3. Phytoplankton as an indicator

Recently, the focus for sustainably managing the marine environment has shifted towards using an ecosystem approach with specific indicators that reflect overall ecosystem health (Borja et al., 2018) (Carstensen et al., 2010) (McQuatters-Gollop et al., 2017) (Van Oostende et al., 2012) (Shephard et al., 2015).

Legislation using water quality to establish both food web and ecosystem health has put forward phytoplankton as a suitable ecosystem indicator (European Commission, 2008) (EEC, 1991). The potential of phytoplankton as an indicator is illustrated by its key role in marine systems, its high diversity and its typical characteristics (Tréguer et al., 2018) (Falkowski et al., 2004). Because of its short turnover time and large abundances, phytoplankton responds quickly to environmental change and as such can function as an early warning signal of climate change (Hays et al., 2005). Additionally, as species ranges are modified due to changes in SST and nutrient conditions, phytoplankton has a great potential for invading new territory and thereby disrupting entire ecosystems. Such changes could also lead to increased occurrence of undesirable and harmful algal blooms (HAB). While toxic blooms are devastating for marine life and its consumers, non-toxic nuisance blooms can also cause mass mortality of marine organisms through oxygen depletion as they start to settle and are being decomposed by bacteria (Pitcher & Probyn, 2016). Hence, phytoplankton monitoring is crucial for public health as well as for economical assets of marine environments (Bill et al., 2018) (EEC, 1991). In order to inform decision making and policy for the BPNS, the accuracy and credibility of phytoplankton data needs to be assured (McQuatters-Gollop et al., 2017).

Examples of the use of phytoplankton as an indicator for ecosystem health can be found in the Marine Water Framework Directive which uses indices for phytoplankton and chlorophyll a as an indicator for eutrophication. Additionally, it is said that phytoplankton as an indicator could also be applicable to fulfill goals in the Marine Strategy Framework directive (MSFD). The MSFD already requires the assessment of the phytoplankton community, as well as zooplankton community, to get an overview of biological communities associated with certain seabed and water column types. But it further states that 'human induced eutrophication and its adverse effects must be minimized', a statement that could use phytoplankton as a suitable assessment tool for the matter, which would integrate the European Marine Strategy Framework and the Water Framework Directive (Carstensen et al., 2010).

4. Monitoring

4.1 Methods for monitoring

A wide selection of techniques is available for phytoplankton identification and/or quantification, including optical (microscopic) techniques, molecular-genetic analyses (DNA/RNA), pigment analyses and techniques based on light scatter like flowcytometry and FlowCam. However, despite this variety of techniques, the phytoplankton community composition of the BPNS still is insufficiently known. The above identification techniques each have benefits and pitfalls which tend to influence the accuracy of biodiversity studies and these are briefly discussed below.

Optical methods like light microscopy have a high taxonomic resolution but are time-consuming and counts often appear to miss or misidentify pico-sized species. Additionally, this technique also requires considerable taxonomic skill to be able to distinguish between similar appearing or even semicryptic species (McQuatters-Gollop et al., 2017). Higher resolution microscopy like Transmission and Scanning Electron Microscopy (TEM and SEM) can be used to resolve the question of pico-sized species or to distinguish between semicryptic species like those belonging to the genera of *Thalassiosira*, *Pseudo-nitzschia* and *Skeletonema* (Navarro & De Peribonio, 2006) (Škaloud et al., 2006) (Hoppenrath, 2004). Epifluorescence microscopy, in combination with DAPI staining of the nucleus and UV filters, can be a good estimator of functional picoplankton community composition (Massana, 2011), but is limited by lower taxonomic resolution.

Techniques based on pigment analysis like High-Performance Liquid Chromatography (HPLC) detects characteristic pigments based on retention times and absorption spectra, which function as biomarkers for different phytoplankton functional groups (S. W. Wright et al., 1991). This technique has a much lower taxonomic resolution but has the advantage of capturing smaller sized groups. HPLC provides a good quantitative estimate of total phytoplankton community biomass but is less reliable for estimating abundances of different functional groups (Eker-Develi et al., 2012).

Flow cytometry measures light scatter and fluorescence with the use of a monochromatic laser. As cells pass through the laser beam, they are counted and parameters like cell width, length and fluorescence are measured (Marie et al., 2005) (Dubelaar & Jonker, 2000). This technique allows for fast counting and detection of smaller sized cells, but is prone to error when dealing with samples low in concentration or samples containing larger sized cells. FlowCAM, in essence, combines light scatter by a laser with imaging microscopy. Imagery output can be studied manually by the researcher or can be analyzed automatically using libraries to reduce time spend on analysis. However, development or selection of appropriate libraries can be both challenging and time consuming. Magnitude and focus of the device need to be adjusted to cell size under study, which can be difficult when dealing with samples that contain species with varying size ranges (Bengt Karlson, 2010).

In recent decades, biodiversity studies have been reshaped by the advent of genetic techniques. They allow to investigate diversity more efficiently by species identification through molecular markers. Metabarcoding uses high-throughoutput sequencing technologies, like Next Generation Sequencing technologies (NGS), allowing for 'en masse' sequencing of amplicons (Taberlet & Coissac, 2012). Analyzed sequences are clustered in so called Operational Taxonomic Units (OTU) which are then assigned to an appropriate taxon, by so-called 'blasting' the sequences to a reference database (Blaxter, 2004) (Ratnasingham & Hebert, 2007). Sequences that cannot be matched with a reference database, due to mismatches or incomplete libraries, can be grouped in Molecular Operational Taxonomic Units (MOTU's) and as such they are still useful in comparative studies (Pavan-Kumar et al., 2015). Another approach is to use Amplicon Sequence Variants (ASVs), individual DNA sequences originating from high-throughoutput marker gene analysis after the removal of erroneous sequences generated during PCR amplification and sequencing. ASVs can differ from one another by as little as a single nucleotide and allow a finer resolution and are more easily comparable between studies than OTUs (Callahan et al., 2017). Metabarcoding allows for the easy detection of small, rare and invasive species by inferring their presence from water samples and gives us a holistic view of ecosystems (Borja et al., 2018) (Creer et al., 2016). However, inferring quantities from sequencing techniques is highly unreliable and these techniques are in urgent need for a standardization of protocols (Elbrecht & Leese, 2015) (Günther et al., 2018) (Borja et al., 2018). Certain groups, like dinoflagellates, exhibit a larger number of SSU copy numbers which skew relative abundance estimates to high number for dinoflagellates. In other groups, cell lysis is more difficult which causes these groups to be underestimated because not all cells break during the extraction process (Medinger et al., 2010).

Choosing identification techniques that are compatible with the aim of our study are thus pivotal as the technique chosen will influence the results or might not provide the required resolution of data.

4.2 Past and present long term monitoring and species checklists

Even though knowledge on phytoplankton is of great value, monitoring is often insufficient. Most monitoring campaigns are short-term because of the financial limits of projects (Lewis & Allen, 2009). Sparse long-term datasets are rare, have gaps or lack temporal and/or taxonomic resolution. It is suggested that monitoring

and timeseries should have timescales of at least 40 years in order to distinguish between natural phenomena and anthropogenic changes (Henson et al., 2010), as biological changes in response to global change occur on time scales of decennia and longer (Lewis & Allen, 2009).

There are several phytoplankton monitoring programs available for the North Sea and adjoining areas, including the Continuous Plankton Recorder in the Northeast Atlantic and North Sea, the Helgoland Roads time series located in the German Bight, the Marsdiep and Rijkswaterstaat monitoring in the Dutch parts of the North Sea, the French programs REPHY and SOMLIT in the English Channel and the British Plymouth L4 time series (Nohe et al., 2019). For the BPNS, phytoplankton community composition has been monitored at station 330 from 1988 to 2008 (Rousseau et al., 2002) (Gypens et al., 2007) (Xavier Desmit et al., 2015) (Breton et al., 2006) (Terseleer et al., 2014). Since 2002, monthly samples are analysed under the European LifeWatch program, mainly focusing on pigment data (Muylaert et al., 2006). In the period 2003-2010 and in 2016 phytoplankton community structure has been studied in more detail. The 4DEMON project (https://www.4demon.be/, accessed 2/6/2020), running from 2014 to 2018 aimed at integrating and centralizing marine data collected in the BPNS over the last four decades. Under this program, a phytoplankton community composition dataset named the 'Belgian Phytoplankton Database' was constructed, which is freely accessible online (http://www.vliz.be/en/imis?module=dataset&dasid=5717, accessed 2/6/2020). The database is a compilation of technical reports, projects, thesis and PhD studies and monitoring dating back to 1968 that were submitted to various control stages. The database provides high quality phytoplankton count data with updated and standardized taxonomy, information about sampling location, date, depth and methodology and associated abiotic environmental variables. The database contains 681 unique IDs of which 93% were identified at genus level (Nohe A., et. al 2018). The leftover 7% were identified at higher taxonomic level and 1% could not be matched. This implies that the database is trustworthy up to genus level for the majority of the entries.

Although the above mentioned long term studies often report biodiversity, the main focus is often on higher taxonomic groups or nuisance algae like *Phaeocystis*, by identification through pigment composition or microscopic counts, limiting the taxonomic resolution of datasets (Nohe, 2020) (Muylaert et al., 2006)(Breton et al., 2006). Species diversity is less often studied in detail, including micro-, nano- and picoplankton fractions of the phytoplankton community. Especially the smallest size fractions of phytoplankton remains largely understudied and in this way, an important part of biodiversity is overlooked (Karlusich et al., 2020).

When we want an intensive taxonomic overview of present phytoplankton diversity, we need detailed species checklists. In Europe, there are a few checklist with most complete and accessible data coming from Helgoland, with one of the most recent studies being Kraberg et al. (2019) as an update to Hoppenrath et al. (2004). This work compares species found during the research period with older checklists of the same area by Dresbes (1974), Dresbes & Elterbrächter (1976) and Harms (1993). Other checklists for Europe include Parke and Dixon (1976) and Hendey (1974) for the British Isles, Kuylenstierna and Karlson (2000) for Kattegat and Skagerrak, Hansen and Larsen (1992) for Kattegat, Heimdal et al. (1973) for Norway, Leewis (1985) for the Dutch coast and Hällfors (2004) and Pankow (1990) both for the Baltic Sea. The majority of the above mentioned checklists are not of recent origin and some are hard to access because they are not available online and/or written in writers native languages, making it difficult for researchers to use these checklists in biodiversity studies. The Helgoland checklist is an exception, with the Helgoland Roads time series being one of the longest and richest phytoplankton dataset in Europe dating back to 1962. However, the high frequency quantitative Helgoland time series phytoplankton assessment is mostly based on Lugol's iodine fixed samples. This causes a large number of the taxa to remain unidentified to species level and rare species might be missed because of low volumes processed. Kraberg et al. (2019) provides an update for the 2004

Helgoland checklist with 11 new records and arguments that the best results are obtained by combining the core Helgoland time series with additional SEM surveys and molecular studies and vows for this combination in future species inventories. For the time series, imagery has been added to data management and archives on www.planktonnet.awi.de (Alfred Wegener Institute for Polar and Marine Research, accessed 25/04/2020), and these are linked to the datasets, which is especially recommended when new taxa are reported.

4.3 Knowledge gaps in phytoplankton species monitoring in the BPNS

Due to updates in taxonomy, description of new species, changes in species distributions and more detailed identification methods that reveal previously overlooked species, checklists should not be seen as an end product. This calls for regular updates to existing species checklists.

At the moment, there is no recent and extensive checklist similar to the Helgoland checklist (2019) available for the BPNS. Both parts of the North Sea differ considerably in prevailing environmental and climatic conditions, meaning that the Helgoland checklist is not necessarily representative of the biodiversity in the BPNS. There is also an added probability that the Helgoland checklist is incomplete because the taxonomic resolution of the inventory is mainly limited to Bacillariophyceae and Dinophyceae as it is currently based on microscopic identifications. The checklist is in need of metabarcoding additions, to reveal rare and small sized species. Although metabarcoding has proved to be a very effective and time-efficient way to process a large number of samples, this does not overthrow the need for a classic microscopic approach when assessing biodiversity, as studies using mock communities have proven that metabarcoding can be biased and cannot be trusted for quantitative estimations (Piwosz et al., 2020). Species sequences that are not present in libraries might skew results and less well-known species might be overlooked. Therefore, metabarcoding and microscopic counts and identifications are complimentary and together, they give a better insight in phytoplankton community structure. Their combination covers both qualitative and quantitative estimations and they can be used to cross verify new or uncertain observations (Piwosz et al., 2020).

As Kraberg et al. (2019) stated, inventories are more valuable if they can be quality checked and revised in the future. Continuously updating checklists is necessary since taxonomy and species distributions are everchanging and because taxonomist will always introduce a bias. If an inventory is accompanied with imagery, species identifications can be quality checked, updated and standardized according to the appropriate taxonomic consensus at that moment in time if necessary. Additionally, imagery data has a great value for future species identifications, to train new taxonomists and in order to facilitate further research.

AIM

Because of the above-mentioned gaps in our knowledge of the phytoplankton community, we applied a selection of identification techniques in order to get a more detailed view of the biodiversity and abundances of phyto- and microplankton species in the BPNS. We opted for a classic microscopic approach (Light Microscopy and Scanning Electron Microscopy (LM and SEM)) combined with DNA-based metabarcoding analyses, focused on the smallest fractions (<50 µm) of the community, in order to identify as many taxa as possible. To obtain quantitative estimates of the community, microscopic counts we performed on permanent diatom mounted materials. We aimed to create an updated inventory of phytoplankton community composition, while also assessing the spatial and temporal dynamics in phyto- and microplankton community structure in the BPNS in relation to environmental parameters from August to December 2019[1]. Every entry in the microscopic inventory is accompanied by imagery for future verification and in order to provide a baseline for future research. For some taxa that are more challenging to identify, we provided more detailed morphological descriptions based on SEM and LM imagery. We then compared the microscopic inventory with taxonomic inventories from adjoining areas.

MATERIALS AND METHODS

1. Study area and sampling

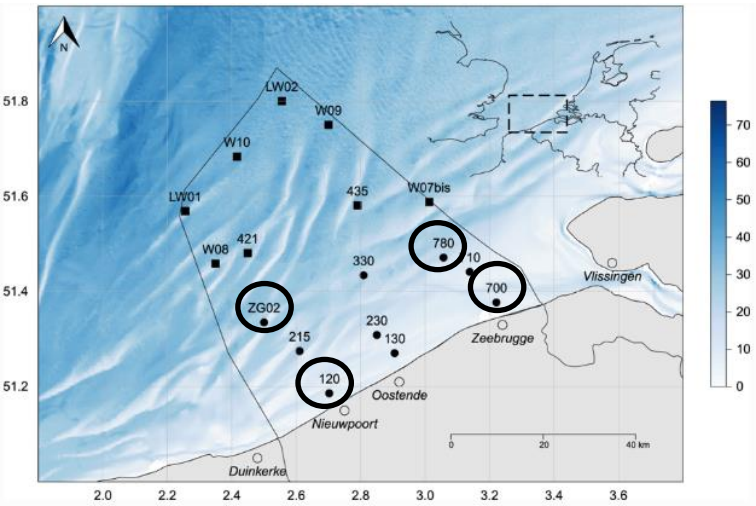

Figure 5: LifeWatch stations in the Belgian part of the North Sea. Sampled stations are indicated by circles.

For the sampling campaign we joined the monthly Belgian LifeWatch monitoring cruises of the Flanders Marine Institute (VLIZ) with RV Simon Stevin. We selected two onshore stations, 120 and 700, and two offshore stations, ZG02 and 780, on opposite sides of the Belgian Coast (Fig. 5, Table 1) in order to get the full range of spatial dynamics related to coastal dynamics, outflow of the river Scheldt and the influence of Atlantic inflow waters (Belgian State, 2012). Stations were originally going to be sampled from August 2019 to April 2020, with the exception of January when RV Simon Stevin is under maintenance. In reality, sampling could not be carried out in

[1] The original aim was to sample from august 2019 to April 2020, but this was not possible due to Covid-19.

February due to stormy weather and from March onwards sampling was not possible due to the Covid-19 pandemic.

Table 1: Coordinates and depth of the sampling stations.

Station	Latitude (N)	Longitude (E)	Depth (m)
120	51.1850	2.7012	14.5
ZG02	51.3333	2.5000	17.5
700	51.3767	3.2200	12.1
780	51.4712	3.0580	23.0

Figure 6: Niskin bottles and CTD mounted on a carousel on board of RV Simon Stevin.

At each of the four stations, three types of samples were taken using Niskin bottles (Fig. 6), which were closed at 3 m below the seasurface. First, two 100 ml replicate samples were taken for planned quantitative estimations using the Utermöhl counting method (J. W. G. LUND, C. KIPLING, 1958) (Bengt Karlson, 2010). One replicate sample was stored in 1% final concentration of Lugol's iodine solution (Paxinos, 2000) and the second replicate sample was stored in 3% final concentration of formaldehyde for long term preservation. Secondly, two replicate net samples were taken using a net with a 10 µm mesh size for qualitative investigation. Here, the sampling volume was as much as possible, depending on the prevailing environmental conditions like turbidity and sediment suspension in the water column. One of the net sample replicates was stored in 1% final concentration of Lugol's iodine solution and the second replicate sample was kept as a live sample for live microscopy. Both the 100 ml and the net samples were stored at 4°C on board and onshore. The live sample was later stored in 3% final concentration of formaldehyde after it was studied. Lastly, two DNA samples were taken. A prefilter of 50 µm was used to eliminate larger organisms whose DNA could otherwise swamp the DNA extract (Gran-Stadniczeñko et al., 2019). This filtrate was then filtered over a 3 µm and 0.8 µm filter which were put in series after one another, to capture two size fractions of phytoplankton. We sampled as much as possible, depending on the environmental conditions like SPM and kept track of the volume. Filters were immediately stored in liquid nitrogen on board and in -80°C in the lab until further analysis. Unlike the other samples, DNA samples were planned only from August up to December 2019, because otherwise there was not enough time to sequence the samples and analyze the data. During each sampling campaign, environmental data were collected using a CTD device mounted on the same carousel as the Niskin bottles. Metadata collected were sampling time, latitude and longitude, ammonium (µmol NH_4/L), nitrate (µmol NO_3/L), nitrite (µmol NO_2/L), phosphate (µmol PO_4/L), silicate (µmol SiO_4/L), conductivity (mS/cm), Photosynthetic Active Radiation (PAR), Density (kg/m^3) and fluorescence mg/m^3) and are available online; For CTD data: Flanders Marine Institute (VLIZ);(2017): Marine Information and Data Acquisition System: underway and cruise data. (MIDAS), and for nutrients a fixed dataset is available via: Flanders Marine Institute (VLIZ), Belgium (2019): LifeWatch observatory data: nutrient, pigment, suspended matter and Secchi measurements in the Belgian Part of the North Sea. https://doi.org/10.14284/393. More detailed sampling protocols can be found in Appendix 1.

2. Microscopy

2.1 Light microscopy

i. Qualitative analysis

Morphological identifications of live 10 µm net sample material were performed using a Zeiss Axiophot microscope (Carl Zeiss, Germany) equipped with Nomarski interference contrast and mounted with a Axiocam digital camera. First, live samples were observed to detect and study motile species, after which these samples were stored in 3% final concentration formaldehyde for long term preservation. Live observations took place between 4-6 days after sampling because they were only received after that time period after sampling. Next, Lugol's iodine fixed net samples were used to observe additional phytoplankton species. Finally, subsamples were oxidized to prepare permanent diatom slides which enable in depth identifications based on morphology of the diatom silica cell wall. To this end, Falcon tubes containing 15 ml of sample material were centrifuged at 1000 RPM for 30 min. The supernatant was removed and the tubes were filled with 30% hydrogen peroxide and left at 60°C for 5-7 days. Hereafter, a rinsing series with demineralized water was performed three times to remove leftover peroxide. Fixed slides were made using a droplet of oxidized material that was left to dry on a cover slip. Slides were then heated on a hotplate at 150°C with a droplet Naphrax on top and covered with the cover slip.

Imagery from LM were used in the microscopic inventory. All images were edited with Gimp 2.10.14. Edits consisted of standardizing the scale to a solid bar, adding unique photo numbering to link photos to identification, cropping and combining images in plates and adjusting brightness. Name tags are always in the format of station_month_fraction, in the table below and in the figures and datasets.

ii. Quantitative analysis

For quantitative cell counts, 100 ml samples were supposed to be used. Quantitative counts would have been obtained using the Utermöhl counting method (J. W. G. LUND, C. KIPLING, 1958) and a Zeiss Axiovert 135 (Carl Zeiss, Germany) inverted microscope. Prior to counting, samples would need to settle first in a sedimentation chamber (Paxinos & Mitchell, 2015). Full description of the protocol and standardization formulas can be found in the UNESCO manual chapter 2 (Bengt Karlson, 2010). These counts were scheduled for April, once I would have a good scope of species diversity in samples through microscopic identification. Unfortunately, due to the Covid-19 pandemic, counts could not be performed because the lab was closed (see Preambule: Covid-19). Instead, relative abundance counts were performed on the permanent diatom slides that were originally made for LM morphological identification. The oxidation method, using 35% H_2O_2, selects for siliceous structures, so mainly diatoms and silicoflagellates are visible. The treatment and centrifugation during the oxidation process can cause certain bigger species and filamentous species and colonies to break up and lightly silicified species to dissolve.

Apart from the above mentioned issues, microscopic counts in itself have some inherent issues. Some cells could only be identified up to genus level or higher taxonomic level. A few *Thalassiosira* species were identified to species level, but often the resolution would be too low or the samples would be too dense to identify *Thalassiosira* to species level. Colonial and filamentous species can also form a challenge and in this case a certain 'unit' of counting should be set beforehand.

UNESCO (Bengt Karlson, 2010) advises to take the unit of the colony as 1 count for colonial species and to take a fixed length (e.g. 100 µm) as 1 unit for filamentous species. However, because we are working on oxidized material, valves were counted separately as colonies broke up during the oxidation process. This explains the high count numbers for colonial taxa like *Paralia*, *Eucampia*, *Bellerochea* and *Pseudo-nitzschia* for some samples.

For counting, an OLYMPUS BX51TF (Olympus optical co. LTD, Japan) was used. Magnification used was 60x overall, while for some smaller species, observations were temporarily switched to 100x magnification.

2.2 Scanning Electron microscopy

Since oxidations with hydrogen peroxide were not powerful enough to get a clear view of the cell wall in the SEM, we opted for a different protocol using nitric acid (69%) and hydrogen peroxide (35%) in a 1:1:3 ratio nitric acid:hydrogen peroxide:sample. The volume of sample used was dependent on the density and the available volume of the sample. Samples treated with acid were placed at 60°C for 5-7 days after which they were rinsed 3 times with distilled water at 1000 RPMfor 30 min. Droplets of the oxidized material were left to dry on stubs after which they were coated with gold for 90 s at 25 mA. Stubs were analysed using a Scanning electron Microscope Jeol JSM-5600LV at 20 kV.

Imagery from SEM were used in the microscopic inventory for the species descriptions of selected taxa. All imagery was edited with Gimp 2.10.14 as described above for LM.

2.3 Identification literature

The following literature was used to identify species:

- Carmelo R. J. (1996). Identifying Marine Diatoms and Dinoflagellates. Academic Press.
- Hoppenrath, M. (2009). Marine Phytoplankton. Selected microphytoplankton species from the North Sea aroung Helgoland and Sylt. Kleine Senckenberg-Reihe 49.
- Throndsen J., H. G. R. & T. K. (2007). Phytoplankton of Norwegian coastal waters. Almater Forlag AS.
- Hartley B. (1996). *An atlas of British Diatoms*. Biopress Ltd.
- Hoppenrath et al. (2007) for *Thalassiosira*
- Sar et al. (2013) for *Pleurosigma*
- MacGillivary & Kaczmarska (2015)
- Sims et al. (2018) for *Odontella* & *Zygoceros*
- Wilks & Armand (2017) for *Shionodiscus*
- Ferrario et al. (2012) for *Stephanopyxis*
- Sarno et al. (2005) for *Skeletonema*
- McCartney et al. (2014) & Maliverno et al. (2016) for silicoflagellates

For the correct taxonomy and internationally accepted species names, we used AlgaeBase (https://www.algaebase.org/, accessed 03/06/2020). This is an open access reference base for marine species comprising the most recent taxonomic data as well as synonyms and basionyms.

3. DNA extraction and sequencing

DNA extraction was performed using the DNeasy Powerlyzer Microbial Kit from Qiagen (Hilden, Germany, see Appendix 2) following the manufacturers protocol with some minor adjustments. The first steps of the process were replaced by adding the microbeads to the DNA filters in an Eppendorf tube, after which the PowerBead solution and the SL solutions was added before shaking the tubes in a beadbeater for 3 min at a frequency of 30 Hz. Following, these Eppendorf tubes were centrifuged for 30 sec at 10 000 RPM and the supernatant was collected for further steps according to the protocol (see Appendix 2).

For PCR, we used the Faststart High fidelity PCR system (03553400001, Sigma-Aldrich, USA) containing the following primers; TAReuk454FWD (CCAGCASCYGCGGTAATTCC) and TAReukREV3 (ACTTTCGTTCTTGATYRA), which select the ribosomal small unit 18s rDNA gene (V4 region). For each sample, the PCR mix contained 2.5 µl PCR buffer (Qiagen), 2.5 µl dNTP's (Qiagen), 2 µl of each primer (Qiagen), 14.75 µl distilled water, 0.25 µl Taq DNA polymerase (Qiagen) and 1 µl of template DNA. The PCR program consisted of a denaturation step at 97°C for 5 min, followed by 35 cycles of denaturation at 94°C for 1 min, annealing at 57-52°C for 1 min, elongation at 72°C for 3 min. This was followed by a final elongation at 72°C for 20 min. We performed an initial PCR of 35 cycles, using a Biometa T Professional Thermocycle, (GmbH, Göttingen, Germany) and a Veriti 96 well Thermal cycle (Applied biosystems, Waltham, USA). Following, gel electrophoresis was performed at 100 V for 30 min and results were visualized by ethidium bromide staining of 30 min. For samples that gave no signal after 35 cycles we repeated the process but let the PCR run for 40 cycles on double the amount of template DNA (2 µl and 13.75µl distilled water instead) after which the results were visualized again by gel electrophoresis and ethidium bromide staining. When all samples gave a clear signal, either after 35 or 40 cycles, we ran an additional but identical PCR with the appropriate number of cycles for each sample in order to become two duplicate PCR products for each sample. This was done to reduce error in the PCR since the detection of strands is a random chance process. So by replicating the PCR multiple times, different strands will be picked up first and amplified more. We keep the number of replicate PCRs at two to reduce cost while still being effective in reducing error. For 4 of the samples taken during November we couldn't get a second replicate PCR: ZG02 0.8 µm, 120 3 µm, 120 0.8 µm, 700 0.8 µm. Both replicate PCR products for each sample are used to preform library prep. Following, we purified the PCR product using an Eppendorf epMotion 5073 (Hamburg, Germany), Ampure beads, 1xTe buffer and 80% ethanol. DNA is bound to the beads and washed with ethanol after which 1x TE buffer is used to dissolve the DNA again. Lastly, we performed a library prep using Faststart high fidelity PCR system, N & S tags and dNTP's. A PCR of 14 cycles was performed to anneal the tags. Detailed protocol and type of tags used for each sample can be found in Appendix 4. Now we performed a second purification of the library prep, which is identical to the PCR purification. We measured the concentration of DNA with Qubit and if the measured concentration of DNA was too low (< 40 ng/ml), the PCR with the tags was run again for 16 cycles. Lastly, the amount of DNA in each sample was made equimolar by adding distilled water, based on concentration values given by the Qubit. Finally, 5 µl of equimolar DNA for each sample was pooled together in an Eppendorf tube and checked one last time by the bio-analyser to detect the presence of chimeras. Once all quality control steps were passed without trouble, pooled DNA was sent to Genewiz Europe (Leipzig, Germany) for Illumina sequencing.

4. Data processing

4.1 Microscopic inventory

The microscopic taxonomic inventory was compared to the updated version of the Helgoland checklist (Kraberg et al., 2019) as well as to the Belgian Phytoplankton Database (Nohe et al., 2020). Each species in the microscopic inventory has a unique photo tag that links it to the displayed plates in order to verify their identification in the future. A pie chart was made to display the diversity at genus level for diatoms and higher taxonomic level for silicoflagellates, Chlorophyta and dinoflagellates. For a selected number of species of (semi)cryptic nature, detailed species descriptions were made and accompanied by detailed LM and SEM images. Measurements used in descriptions are obtained in ImageJ 1.8.0 and averaged over all observations.

4.2 Microscopic count data statistics

All diatoms in each diatom mounted slide were identified and enumerated, and the counts were converted into relative abundances. To display the most abundant species found over all samples, a table is displayed with all species found during microscopic counting and their total relative abundance over all samples. Following, a number of pie charts were made; a general pie charts which shows the 10 diatom species with the highest relative abundances during the microscopic counts, followed by a two pie charts which displays the most abundant species per month and per station.

The data were then log (x+1) transformed and Principal Component Analysis (in CANOCO for Windows) was applied to the dataset as the log of gradient metric was lower than 2 which suggests that most species display linear responses to the underlying environmental gradients. In the diagram, the 25 best fitted species (i.e. who varied most along the axes shown) are plotted. The environmental variables temperature, salinity, PAR and fluorescence are plotted as supplementary variables (i.e. their coordinates represent their correlation with the axes).

4.3 Amplicon sequencing data processing & statistics

For the data analysis of the amplicon sequencing the DADA2 pipeline (Callahan et al., 2016) in Rstudio version 1.2.5033. A tutorial of the pipeline we followed is available online at: https://benjjneb.github.io/dada2/tutorial.html (accessed 04/2020). We start with Illumina-sequenced paired-end fastq files and in the end we obtain an amplicon sequence variant (ASV table), to which we assign taxonomy before further downstream analysis. We opted to work with ASVs instead of OTUs as this makes the results more precise, traceable, reusable across studies and reproducible in the future and not limited by incomplete reference databases. ASVs have an intrinsic biological meaning as opposed to OTUs, meaning that studies using the same primer set can simply be merged and compared (Callahan et al., 2017).

First, after importing fastq files, the quality of reads was inspected visually and primer sequences and tails were trimmed with the filterAndTrim command, trimLeft was set at 21 bases for the forward reads and 29 bases for the reverse reads, truncLen was set to 250 for forward reads and 240 for reverse reads. maxEE sets the maximum number of expected errors allowed in a read, was set at 2 by default, trunQ was set to 1. Next, error models were constructed with the learnErrors function. Once these are known, sample interference

are applied using the dada function and we obtain a number of ASVs from a higher number of unique sequences. This dada function can resolve errors as little as 1 nucleotide (indels and substitutions). Reads are now denoised and forward and reverse reads are merged using the mergPairs function, which happens by default if the forward and reverse reads overlap by at least 12 bases, and are identical in the overlap region. Now, a sequence table is constructed, a matrix with rows corresponding to samples and columns corresponding to sequence variants. As a last step before assigning taxonomy, chimeras are removed with the removeBimeraDenovo function as the dada function does not do this inherently even though it makes it easier to identify chimeras after denoising. As a last control step, reads are tracked through the pipeline to see if one of the above steps significantly decreased the number of reads for a samples, if so the above steps had to be revised but this was not necessary. Now, taxonomy was assigned using the assignTaxonomy function using a fitting library. For the appropriate library selection I tried both Silva (138 and 132) and PR2, but only PR2 (version 4.12.0 18S DADA2) gave results up to species level. ASVs were matched to the library based on Naïve Bayesian classifier method explained by Wang et al. (2007). The used function, assignTaxonomy, takes as input a set of sequences to be classified and a training set of reference sequences with known taxonomy, and outputs taxonomic assignments with bootstrap confidence. Classifications using this Naïve Bayesian Classifier have high confidence estimates from domain to genus level. The majority of species assignments using this method of classifications were of high estimated confidence (>95%) and high accuracy (98%) and the majority of errors made in experimental studies are due to anomalies in current taxonomy (Wang et al., 2007). Using this classifier, error rates are highest for short segments of bases, and for these short segments (<50 bp) the method is proven most accurate, having least errors, for V2 and V4 regions (the latter used in this thesis) (Wang et al., 2007). This supports the use of this Naïve Bayesian Classifier here. Following, samples were submitted to a manual control to check the number of reads and the number of species/taxa matched. This caused some samples to be omitted from the analysis because they had extremely low number of reads or taxa assigned to them compared to other samples. Table 2 list the samples that were omitted from the analysis for these reasons.

Table 2: Samples deleted from the dataset due to the reasons: insufficient (relative) number of reads, insufficient number of taxa or extreme outlier in ordinations. Name tag consists of station_month_fraction.

Name tag	Number of reads	Reason of removal
700_10_08	31661	Low number of reads
700_09_3	178679	Extreme outlier in ordination
700_12_3	315185	Insufficient number of taxa
ZG02_11_3	6	Low number of reads
120_09_3	41064	Insufficient number of taxa
120_11_08	12	Low number of reads
700_11_3	113785	Extreme outlier in ordination
700_11_08	71421	Extreme outlier in ordination
700_12_3	25754	Insufficient number of reads
780_08_08	120553	Insufficient number of taxa
120_09_08	46	Low number of reads
700_08_3	17394	Insufficient number of taxa
780_09_08	72	Low number of reads

After removal of these low quality samples, the taxonomic table was manipulated manually by inspecting the count table of ASVs, meaning we looked at ASVs with a high abundance and checked if they had a meaningful

taxonomic assignment. ASVs that had a high abundance but did not have a match to species level with the PR2 library (and only had higher taxonomic level matches assigned) were blasted manually using Nucleotide BLAST (National Center for Biotechnology Information (NCBI). Bethesda (MD): National Library of Medicine (US), National Center for Biotechnology Information; [1988], cited 06/2020. Available from: https://www.ncbi.nlm.nih.gov/). This led to the identification of following species: *Teleaulax acuta, Teleaulax amphioxeia, Shionodiscus oestrupii var. vernickiae, Gyrodinium jinhaense, Thalassiosira eccentrica, Thalassiosira oceanica, Chaetoceros jonquieri* and *Minidiscus variabilis.* After this, some manual changes were made to taxonomic table by updating names of some taxa to their recent taxonomy (so they could be run against WoRMS taxonomy - see further). When species names were unknown but genus names where known the species name was set to the genus name followed by "sp." After this, the taxonomic table was ran again World Register of Marine Species (WoRMS) (http://www.marinespecies.org/, accessed 3/06/2020) to retrieve more Aphia information through the package "worms" using the WoRMS RESTful Webservice aiming to obtain taxonomic consistency. As a last step, ASVs that only had a match up to division levels, but had an 'NA' for higher taxonomic levels were omitted from the analyses, as well as ASVs belonging to the Metazoa and Embryophyta as we are not interested in these taxa and they might influence the analysis. The amplicon sequencing data thus comprises all eukaryote micro-organisms, amongst which a lot of heterotrophic taxa (Protozoa).

As a normalization before statistical analysis, the ASV count table was transformed to relative abundances (also called proportions) as it seemed most appropriate for our purposes (Kellogg et al., 2017). Rarefying, another commonly used technique based on random subsampling without replacement, induces a loss of power (type-II errors) by decreasing the number of observations (library size) to the lowest size and in doing so increases the width of the confidence interval because samples were discarded or because part of the fraction of the original library is discarded. Additional to losing data, rarifying also adds artificial uncertainty through random subsampling. Rarefied counts also remain overdispersed relative to Poisson distribution, meaning an increase in Type-I error, and estimating overdispersion is difficult in rarified counts (McMurdie & Holmes, 2014). Although proportions also have their downsides, for our purposes they are a better alternative than rarifying and the loss of statistical power through proportions is less than using rarefying (McMurdie & Holmes, 2014)(Weiss et al., 2017). Novel techniques like DESeq Variance Stabilization Transformation through the DESeq packages make ecological interpretation of data more difficult and are generally not necessary in our case (McMurdie & Holmes, 2014).

4.4 Amplicon sequencing based inventory

For the amplicon sequencing inventory a dual taxonomic inventory was created: one of all unique ASVs found and one of all unique species found in the unfiltered amplicon sequencing dataset. We saw that multiple ASVs would often match to the same species leading to a discrepancy between number of ASVs and number of species found (see results), and therefore we decided to retain both the ASV and the species information. The taxonomic tables for these two inventories underwent some manual changes based on Adl et al.(2019) when taxonomy was outdated or uncertain. For the taxonomic inventory on species level we made some pie charts of the community composition and abundances of supergroups and divisions found, based on diversity (percentage of species) and relative abundances found for each supergroup or division. For Ochrophyta

(mainly diatoms here) and dinoflagellates some additional pie charts were made on class and order level to display community composition based on number of species found per class or order for these two groups.

4.5 Amplicon sequencing spatial and temporal statistical analysis

As a filter, ASVs with relative abundances below 1% for all samples were omitted from the spatial and temporal statistical analyses. Following, the relative abundances were calculated again without the low abundance ASVs so the ASVs that passed the filter add up to 100 again. Next, the taxonomic table (ASVs and their taxonomic information) and filtered relative abundance count table were merged into a matrix with species names as rows and samples as columns, while the matrix was filled with relative abundance values. All further analyses are done on species level, not on ASV level. This matrix then had to be transformed to deal with zero values and arch effects. Different ordination methods and transformations were tried in order to choose the appropriate technique. Ordinations were run on Hellinger transformed and log transformed relative abundance count tables, with species identifications (not ASVs). Since there was no crucial difference between the two transformation methods, Hellinger transformation was chosen as this is a commonly used method to deal with zero values in count data sets to avoid arch effects.

Following Principal Component Analysis (PCA) and Nonmetric MultiDimensional Scaling (NMDS) were both run on the Hellinger transformed count matrix and on a presence/absence matrix. The latter was done because amplicon sequencing tends to be biased for abundances, so we wanted to see if there was a difference in patterns by trying both methods. The ordination technique that showed most straightforward patterns was the PCA run on Hellinger transformed relative abundance. The results of this PCA graphs based on relative abundances of species identifications is shown below in results. The additional graphs, NMDS on relative abundance and PCA and NMDS on presence/absence are displayed in Appendix 5. The number of significant axes for the ordinations was chosen with the help of a Broken Stick diagram. A Shepard diagram for the PCA shows how the ordination fits in the reduced space in comparison to the original distances in the unreduced space after defining the number of axes. Graphs were produced displaying samples colored according to station, month and fraction for visual purposes. Additional graphs display for each ordination the species structure the community. These species are for PCA the species with the highest summed values for the significant axes. The species arrows are colored according to the division they belong to. For the PCA displayed in results, the 30 most important species are plotted. In order to display the full community, additional ordinations with all other species used in the PCA can be found in Appendix 5. Samples that showed extreme outliers in the ordinations were omitted from the analysis as they compressed the ordination and patterns became invisible (Table 2).

In order to see if there is a correlation between the ordination axes and the environmental variables, a Spearman rank correlation coefficient was calculated based on the scores for each sample in the ordination diagram and the measured values of the environmental parameters for each sample. Correlation coefficients were correlated were calculated for temperature, PAR, fluorescence and salinity. Significance was examined for these correlation coefficients by a permutation function that produces an empirical distribution of correlation coefficients under the null hypothesis (no correlation), and by subsequently calculating the fraction of correlation coefficients of that empirical distribution that are equal to or more extreme than the correlation values of our data, hence a p-value was obtained.

Lastly, a Permutational multivariate analysis of variance (PERMANOVA) was performed on the Hellinger transformed Euclidean distance matrix to detect for significant differences between stations, months, fractions and their interaction effects.

4.6 Packages used for the amplicon sequencing data analysis

- phyloseq: An R package for reproducible interactive analysis and graphics of microbiome census data. Paul J. McMurdie and Susan Holmes (2013) PLoS ONE 8(4):e61217.
- Jari Oksanen, F. Guillaume Blanchet, Michael Friendly, Roeland Kindt, Pierre Legendre, Dan McGlin, Peter R. Minchin, R. B. O'Hara, Gavin L. Simpson, Peter Solymos, M. Henry H. Stevens, Eduard Szoes and Helene Wagner (2019). vegan: Community Ecology Package. R package version 2.5-6. https://CRAN.R-project.org/package=vegan
- H. Wickham. ggplot2: Elegant Graphics for Data Analysis. Springer-Verlag New York, 2016.
- Tal Galili (2015). dendextend: an R package for visualizing, adjusting, and comparing trees of hierarchical clustering. Bioinformatics. DOI:10.1093/bioinformatics/btv428
- Hadley Wickham and Lionel Henry (2020). tidyr: Tidy Messy Data. R package version 1.0.2. https://CRAN.R-project.org/package=tidyr
- Simon Garnier (2018). viridis: Default Color Maps from 'matplotlib'. R package version 0.5.1. https://CRAN.R-project.org/package=viridis
- H. Wickham. Reshaping data with the reshape package. Journal of Statistical Software, 21(12), 2007.
- John Fox and Sanford Weisberg (2019). An {R} Companion to Applied Regression, Third Edition. Thousand Oaks CA: Sage. URL:https://socialsciences.mcmaster.ca/jfox/Books/Companion/
- Erich Neuwirth (2014). RColorBrewer: ColorBrewer Palettes. R package version 1.1-2. https://CRAN.R-project.org/package=RColorBrewer
- Hadley Wickham (2020). forcats: Tools for Working with Categorical Variables (Factors). R package version 0.5.0. https://CRAN.R-project.org/package=forcats
- John Baumgartner and Russell Dinnage (2019). hues: Distinct Colour Palettes Based on 'iwanthue'. R package version 0.2.0. https://CRAN.R-project.org/package=hues
- Robert J. Hijmans (2020). raster: Geographic Data Analysis and Modeling. R package version 3.1-5. https://CRAN.R-project.org/package=raster
- *Jan Holstein (2018). Worms: Retrieving Aphia Information from World Register of Marine Species. https://cran.r-project.org/web/packages/worms/index.html*

4.7 High-Performance Liquid Chromatography (HPLC) Pigment analysis

In order to verify some patterns seen in the results we chose to have a brief look at pigment compositions of the phyto- and microplankton community. Pigments are routinely studied under LifeWatch and the most recent publication is under Mortelmans et al. (2019). The HPLC method selected for the routine monitoring of pigments uses methanol/TBAA 28mM 70/30 and methanol as solvents. The column used is an Agilent Eclipse XDB-C8 column. Pigments are analysed with a Diode Array Detection (DAD) at 450 nm (all chlorophyll pigments and carotenoids) and 665 nm (only chlorophyll pigments) to detect absorbance spectra for individual pigment peaks. Then, pigments are identified by comparing retention times and absorption spectra to pure pigment standards provided by Danish company DHI. Further downstream analysis of biological pigments generally happens with CHEMical TAXonomy (CHEMTAX) to estimate the taxonomic abundances of phytoplankton and eukaryote micro-organisms. However, here we made some simple graphs displaying the course of pigment concentrations over the months August to December 2019, for station 120, ZG02, 700 and 780 as detailed CHEMTAX analysis is not the objective of this thesis.
The pigments we chose to visualize are chlorophyll a (overall biomass of photosynthetic community), chlorophyll b (Chlorophyta, Cyanobacteria, Prasinophytes, dinoflagellates group IV and Euglenophyta to

lesser extent), fucoxanthin (diatoms mainly, also other Ochrophyta, *Phaeocystis,* dinoflagellates, Pinguiophytes, Prymnesiophytes), chlorophyll c3 (*Phaeocystis*, diatoms, dinoflagellates group II, Prymnesiophytes), chlorophyll c2 (diatoms, Dictyochophytes, dinoflagellates, Pavlovophytes, Prymnesiophytes), alloxanthin (Cryptophyta), peridine (dinoflagellates group I) and diato- and diadinoxanthin (dinoflagellates, Dictyophytes, Prymnesiophytes, Pavlovophytes and diatoms) (S. Wright & Jeffrey, 1996).

4.8 Nutrient data

During the LifeWatch campaigns, nutrient data is also routinely collected by VLIZ. Around 200 ml of seawater is filtered through a 0.2 µm cellulose-acetate filter and 150 ml of filtered water is stored at -24°C until further analysis (Mortelmans et al., 2019). Nutrients analyzed are NH_4= Ammonium, NO_3=Nitrate, NO_2=Nitrite, PO_4=Phosphate, SiO_4= Silicate. Measurements missing for whole month of December and station 700 in September.

RESULTS

1. Phytoplankton inventory of the BPNS

1.1 Microscopic inventory

All species observed using a combination of microscopic techniques, LM of live material, Lugol's iodine fixed and oxidized material and SEM, are listed in Table 3. A separate inventory for each sample taken during the campaign is also available through the Marine Data Archives. Figures 7 to 17 show images of every species identified, organized in plates that display similar species together so they can be compared more easily. All species identifications in the table below are linked to a unique photo tags.

Table 3: Microscopic inventory of species found in Lugol's iodine fixed samples and permanent slides LM and/or SEM. Species occurrences in the Helgoland checklist (Kraberg et al., 2019) and the Belgian Phytoplankton Database (BPD) (Nohe et al.,2018) are indicated. For each species photo tags are provided to verify identifications in plates 7 to 17 below.

Species name	Helgo-land	BPD	Photo tag
Chlorophyta			
Pseudopediastrum boryanum (Turpin) Hegewald, 2005		x	1
Ciliophora			
*Favela ehrenberghii (*Claparère & Lachmann) Jörgensen, 1858			2
Tintinnopsis campanula Ehrenberg, 1840		x	3
Dinoflagellata			
Tripos fusus (Ehrenberg) Gómez, 2013	x	x	4
Akashiwo spp.			5
Gyrodinium spp.			10

Protoperidinium spp.			8, 9
Prorocentrum spp.			6, 7
Noctiluca scintillans (Macartney) Kofoid & Swezy, 1921	x	x	12
Bacillariophyta			
Eunotogramma spp.			13
Bacillaria paxillifer (O.F. Müller) Marsson, 1901	x	x	14, 15
Cylindrotheca closterium (Ehrenberg) Reinmann & Lewin, 1964	x	x	16
Psammodictyon panduliforme Gre(gory), Mann, 1857		x	17
Nitzschia thermalis (Ehrenberg) Auerswald, 1861			18
Pseudo-nitzschia pungens (Grunow ex Cleve) Hasle, 1993	x	x	19, 20
Bellerochea horologicales Stosh, 1977		x	22, 23
Bellerochea malleus (Brightwell) Van Heurck, 1885	x	x	21
Biddulphia alternans (Bailey) Van Heurck, 1885			24, 25
Bacteriastrum mediterraneum Pavillard, 1916			26, 26b
Bacteriastrum hyalinum Lauder 1864	x	x	27, 27b
Chaetoceros affinis Lauder, 1864	x	x	28
Chaetoceros brevis Schütt, 1895		x	37
Chaetoceros curvisetus Cleve, 1889		x	29
Chaetoceros constrictus Gran, 1897		x	38
Chaetoceros danicus Cleve, 1889	x	x	30
Chaetoceros debilis Cleve, 1894	x	x	31
Chaetoceros decipiens Cleve, 1873	x	x	32
Chaetoceros didymus Ehrenberg, 1845	x	x	33
Chaetoceros lorenzianus Grunow, 1863	x		36
Chaetoceros socialis Lauder, 1864	x	x	35
Chaetoceros teres Cleve, 1896	x	x	34
Cerataulina pelagica (Cleve) Hendey, 1937	x	x	68
Coscinodiscus centralis Ehrenberg, 1839	x	x	39
Coscinodiscus connicus Smith, 1856	x	x	40
Coscinodiscus radiatus Ehrenberg 1840	x	x	41
Coscinodiscus wailesii Gran & Angst, 1931	x		42
Ralfsiella smithii (Ralfs in Pritchard) Sims, Williams & Ashworth, 2018		x	43, 44
Stellarima stellaris (Roper) Hasle & Sims, 1986	x	x	45
Actinoptychus senarius (Ehrenberg) Ehrenberg, 1843	x	x	48
Actinoptychus splendens (Shadbolt) Ralfs, 1861	x	x	49
Actinocyclus curvatulus Janisch, 1878	x		50
*Actinocyclus normanii (*Gregory ex Greville) Hustedt, 1957			51
Actinocyclus octonarius Ehrenberg, 1837	x		52
Azpeitia nodulifera (Schmidt) Fryxell & Sims, 1986		x	47
Roperia tessellata (Roper) Grunow ex Pelletan, 1889	x	x	53, 54
Cymatosira belgica Grunow, 1881		x	56
Cymatosira lorenzianus Grunow, 1862			55
Brockmanniella brockmannii (Hustedt) Hasle, Stosch & Syvertsen, 1983	x	x	57

Plagiogrammopsis vanheurckii (Grunow) Hasle, Stoch & Syvertsen, 1983	x	x	58
Odontella rhombus (Ehrenberg) Kützing, 1849		x	59, 59b
Odontella rhombus f. trigona (Cleve ex Van Heurck) Ross in Hertly, 1986	x	x	60
Ralfsiella minima (Grunow) Sims & Williams, 2018	x	x	63
Hobaniella longicruris (Greville) Sims & Williams, 2018	x		61
Trieres sinensis (Greville) Ashworth & Theriot, 2013	x	x	64
Trieres mobiliensis (Bailey) Ashworth & Theriot, 2013	x	x	62
Asterionella kariana (Grunow) Gardner & Crawford, 1880	x	x	65
Eucampia zodiacus Ehrenberg, 1839	x	x	66
Eucampia zodiacus var. cornigera Grunow, 1882	x	x	67
Leptocylindrus danicus Cleve, 1889	x	x	69
Leptocylindrus convexus Nanjappa & Zingone, 2013			77
Tenuicylindrus belgicus (Meunier) Nanjappa & Zingone, 2013			70
Ditylum brightwellii (West) Grunow, 1885	x	x	71, 71b
Lithodesmium spp.			72
Diploneis bombus (Ehrenberg) Ehrenberg, 1853		x	73
Diploneis didyma (Ehrenberg) Ehrenberg, 1844		x	74
Navicula palpebralis Bébisson ex Smith, 1853		x	76
Trachyneis aspera (Ehrenberg) Cleve, 1894		x	75
Meuniera membranaceae (Cleve), Silva, 1996		x	78
Pleurosigma intermedium Smith, 1853		x	79, 80, 80b
Pleurosigma spp.			81, 81b
Paralia marina (Smith) Heiberg, (1863)	x		82
Asterionella glacialis (Castracane) Round, 1990	x	x	86
Delphineis surirella (Ehrenberg) Andrews, 1981	x	x	84, 85
Rhaphoneis amphiceros (Ehrenberg) Ehrenberg, 1844	x	x	86
Proboscia alata (Brightwell) Sundström, 1986	x	x	87
Guinardia flaccida (Castracane) Peragallo, 1892	x	x	88, 89
Guinardia delicatula (Cleve) Hasle & Syvertesen, 1997	x	x	91
Guinardia striata (Stolterfoth) Hasle, 1996	x	x	90
Neocalyptrella robusta (Norman ex Ralfs) Hernández-Becerril & del Castillo, 1997	x	x	92
Rhizosolenia decipiens Sundström, 1986			93
Rhizosolenia imbricata Brightwell, 1858	x	x	94
Rhizosolenia setigera Brightwell, 1858	x	x	95
Epithemia adnata (Kützing) Brébisson, 1838		x	96
Epithemia sorex Kützing, 1844		x	97, 98
Cyclotella atomus Hustedt, 1937			100
Cyclotella choctawhatcheeana Pasad, 1990			99
Eupyxidicula turris (Greville) Blanco & Wetzel, 2016	x	x	101, 102
Cymatopleura solea (Brébisson) Smith, 1851		x	103, 104
Thalassionema nitzschioides (Grunow) Mereschowsky, 1902	x	x	105, 106
Amphora commutata Grunow Van Heurck, 1880		x	107

Detonula pumila (Castracane) Gran, 1900	x	x	109
Lauderia annulata Cleve, 1873	x	x	108
Skeletonema marinoi Sarno &Zingone, 2005	x		110, 111
Minisdiscus spp.			123
Thalassiosira anguste-lineata (Schmidt) Fryxell & Hasle, 1977	x	x	122
Thalassiosira curviseriata Takano, 1981	x	x	114
Shionodiscus oestruppii var. vernickae (Ostenfeld) Alverson, Kang & Theriot, 2006			112, 124
Thalassiosira decipiens (Grunow ex Van Heurck) Jørgensen , 1905	x	x	115
Thalassiosira eccentrica (Ehrenberg) Cleve 1904	x	x	116, 125
Thalassiosira hendeyi Hasle & Fryxell, 1971	x		117
Thalassiosira lundiana Fryxell, 1975	x		118
Thalassiosira punctigera (Castracane) Hasle, 1983	x		119
Thalassiosira rotula Meunier, 1910	x	x	120
Thalassiosira tenera Proschina-Lavrenko, 1961	x	x	121, 123
Triceratium favus Ehrenberg, 1839	x	x	126, 127
Ochrophyta			
Dictyocha spp.			130
Dictyocha spp.			131
Occtactis speculum Chang, Grieve & Sutherland 2017		x	128, 129
Unknown			
Unknown dinoflagellate			11
Unknown diatom			132
Unknown diatom			133
Unknown diatom			134
Unknown diatom			136
Unknown tintinnid cilliate			135

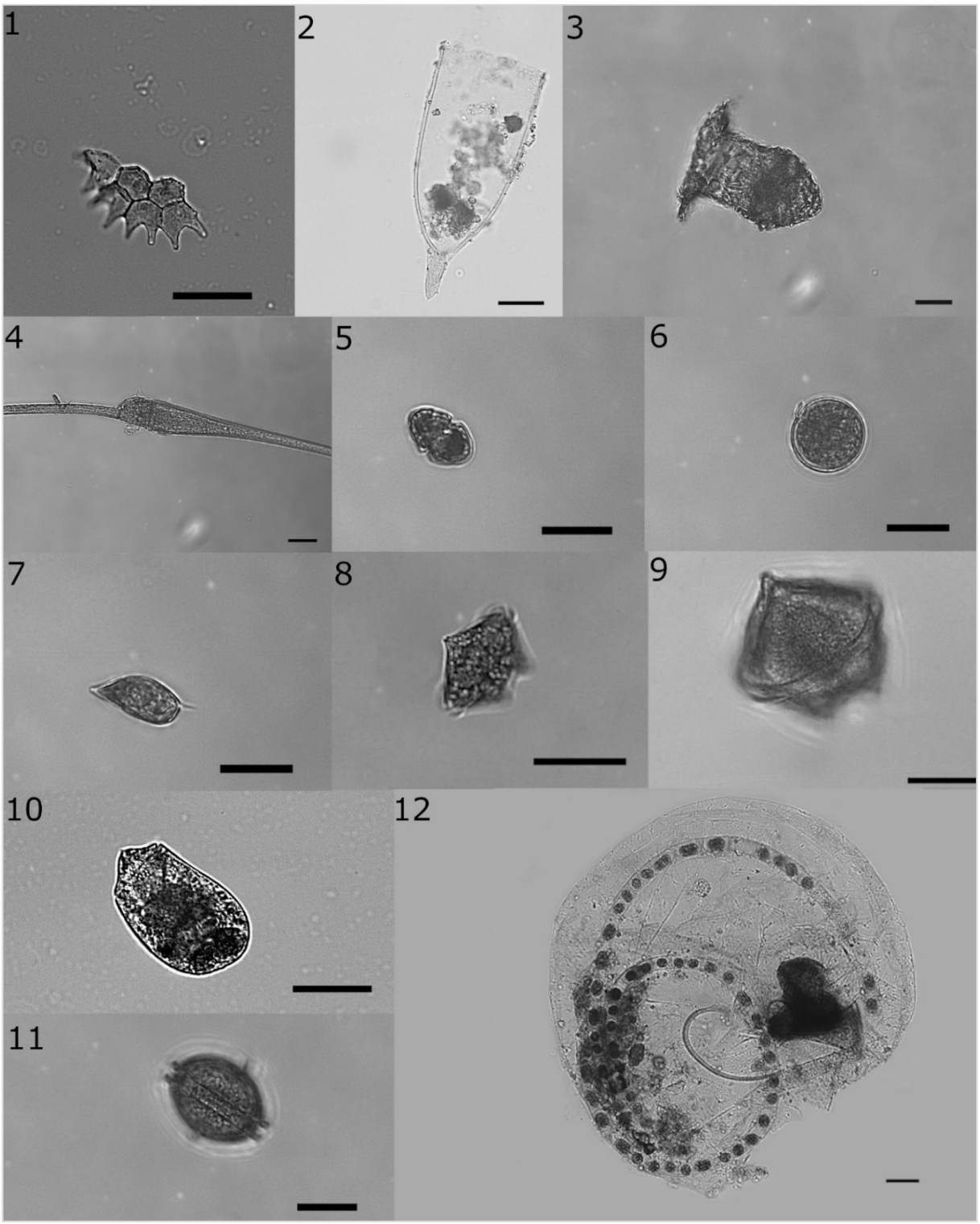

Figure 7: Plate1.1. Pseudopediastrum boryanum 120_08_20, scale bar is 50µm.2. Favella ehrenberghii 120_09_87, scale bar is 50µm. 3. Tintinnopsis campanula, 700_09_44, scale bar is 20µm. 4. Tripos fusus 120_09_16, scale bar is 50µm. 5. Akashiwo spp. 120_09_20, scale bar is 20µm. 6. Prorocentrum spp. 120_09_20, scale bar is 20µm. 7. Prorocentrum spp. 120_09_23, scale bar 20µm. 8. Protoperidinium spp. 700_09_49, scale bar is 50µm. 9. Protoperidinium spp. 780_09_58, scale bar is 50µm. 10. Gyrodinium spp. 230_08_18, scale bar 50µm. 11. Unknown dinoflagellate ZG02_09_25, scale bar is 20µm. 12. Noctiluca scintillans 780_09_43, scale bar is 50µm.

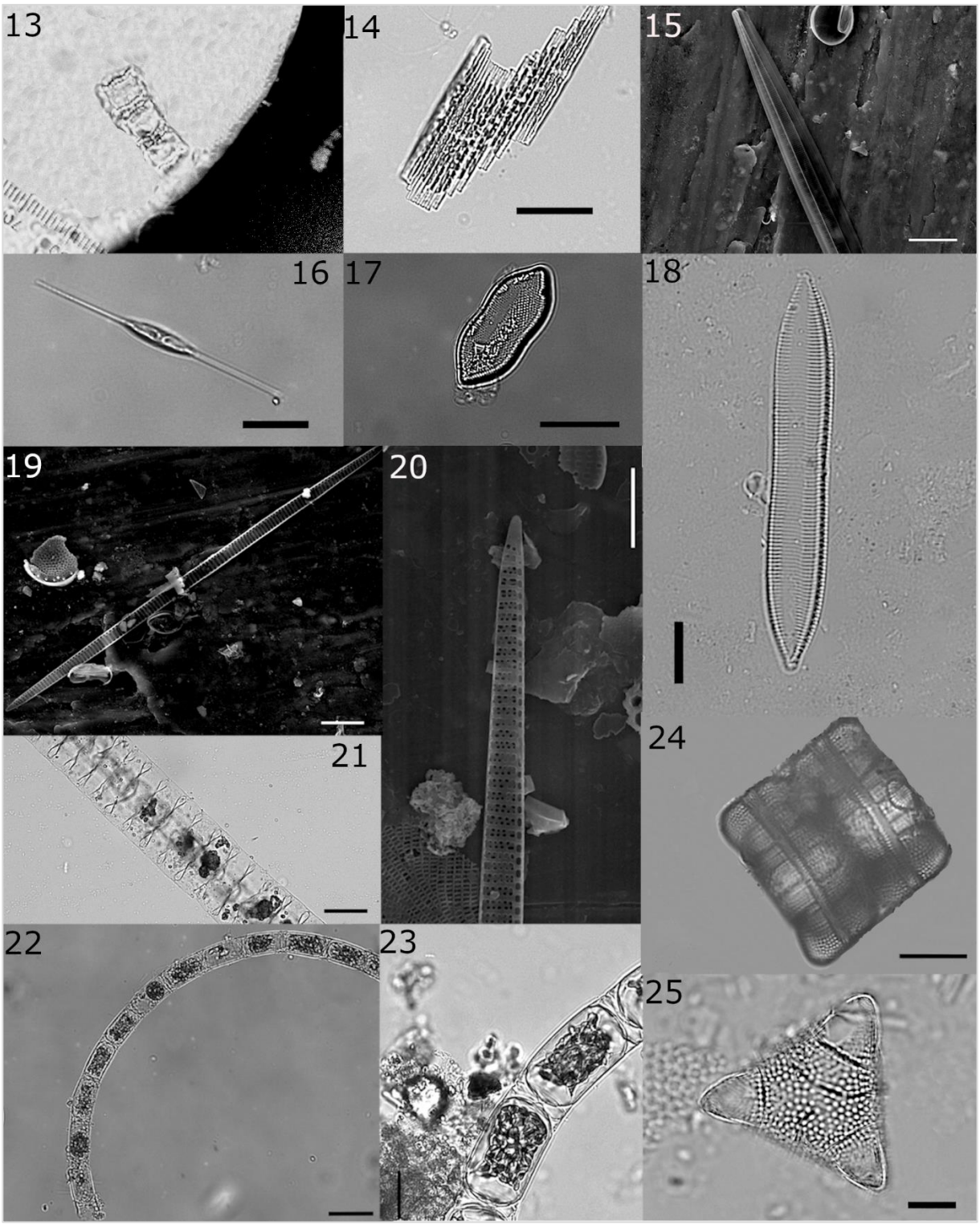

Figure 8: Plate 2. 13. Eunotogramma spp. 700_11_93, magnification 100x. 14. Bacillaria paxillifer 780_09_61, scale bar 50µm.15. Bacillaria paxillifer ZG02_09_27, scale bar 10µm. 16. Cylindrotheca closterium 120_11_11, scale bar 20µm. 17. Psammodictyon panduliforme, ZG02_09_61, scale bar 20µm. 18. Nitzschia thermalis 700_11_43, scale bar is 10µm. 19 & 20. Pseudo-nitzschia pungens ZG09_09_07, scale bar is 10µm. Oostende_08_14, scale bar 5µm. 21. Bellerochea malleus 120_08_19, scale bar is 50µm. 22. Bellerochea horologicales 780_09_68, scale bar is 50µm. 23. Bellerochea horologicales 700_08_5, scale bar is 20µm. 24. Biddulphia alternans 120_12_46, scale bar is 20µm. 25. Biddulphia alternans 120_12_35, scale bar is 10µm.

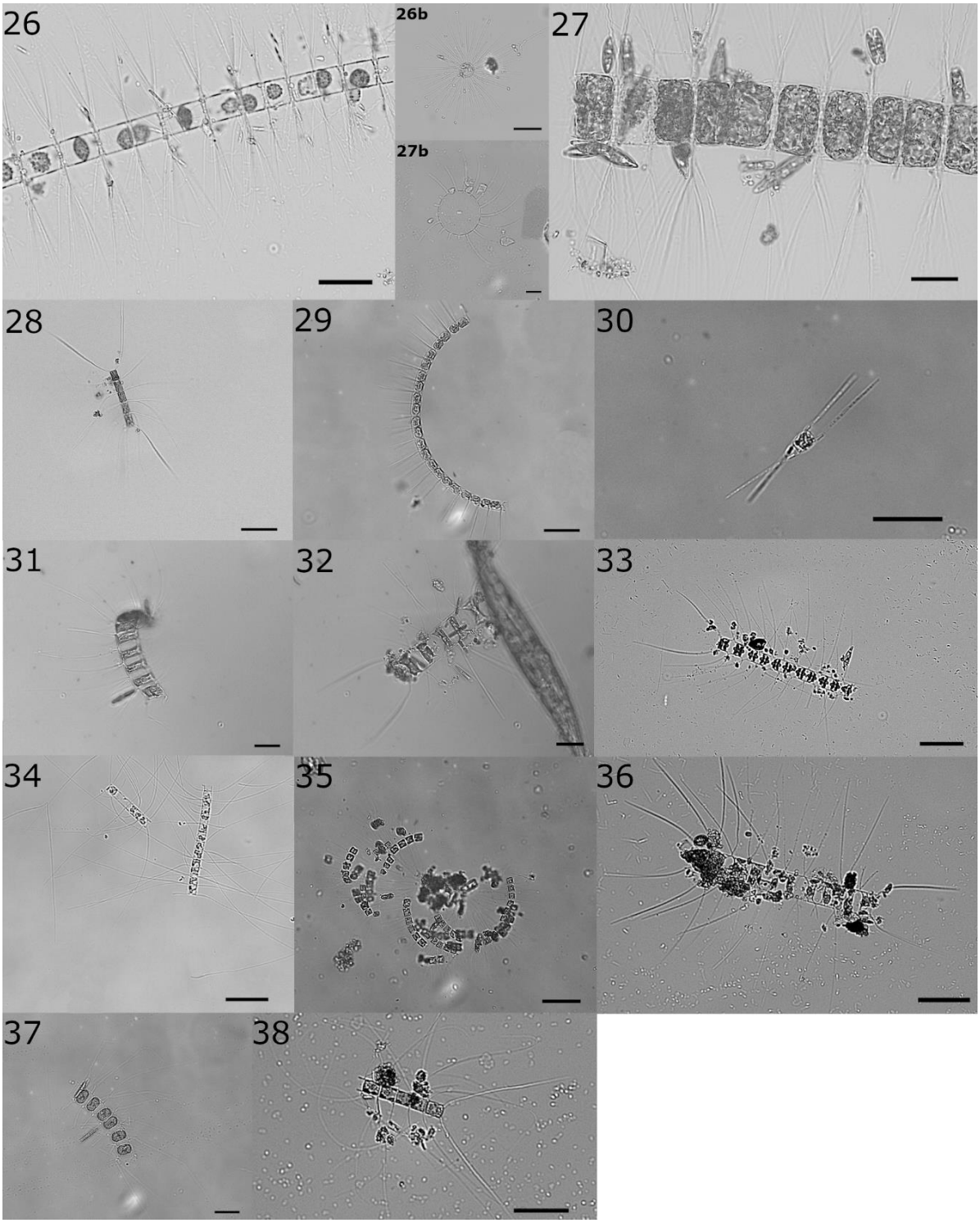

Figure 9: Plate 3. 26. Bacteriastrum mediterraneum ZG02_09_100, scale bar is 50µm. 26b. Bacteriastrum mediterraneum,780_08_35, scale bar is 50µm. 27. Bacteriastrum hyalinum 780_08_9, scale bar is 50µm. 27b. Bacteriastrum hyalinum 700_12_37, scale bar is 10µm. 28. Chaetoceros affinis 130_08_10, scale bar is 50µm. 29. Chaetoceros curvisetus, ZG02_09_21, scale bar is 50µm. 30. Chaetoceros danicus 700_09_2, scale bar is 20µm. 31. Chaetoceros debilis 700_09_54, scale bar is 20µm. 32. Chaetoceros decipiens 780_09_36, scale bar is 20µm. 33. Chaetoceros didymus 120_08_17, scale bar is 50µm. 34. Chaetoceros teres 230_08_3, scale bar is 50µm. 35. Chaetoceros socialis 120_11_9, scale bar is 50µm. 36. Chaetoceros lorenzianus 120_080_11, scale bar is 50µm. 37. Chaetoceros brevis 700_08_12, scale bar is 20µm. 38. Chaetoceros constrictus ZG02_09_21, scale bar is 50µm.

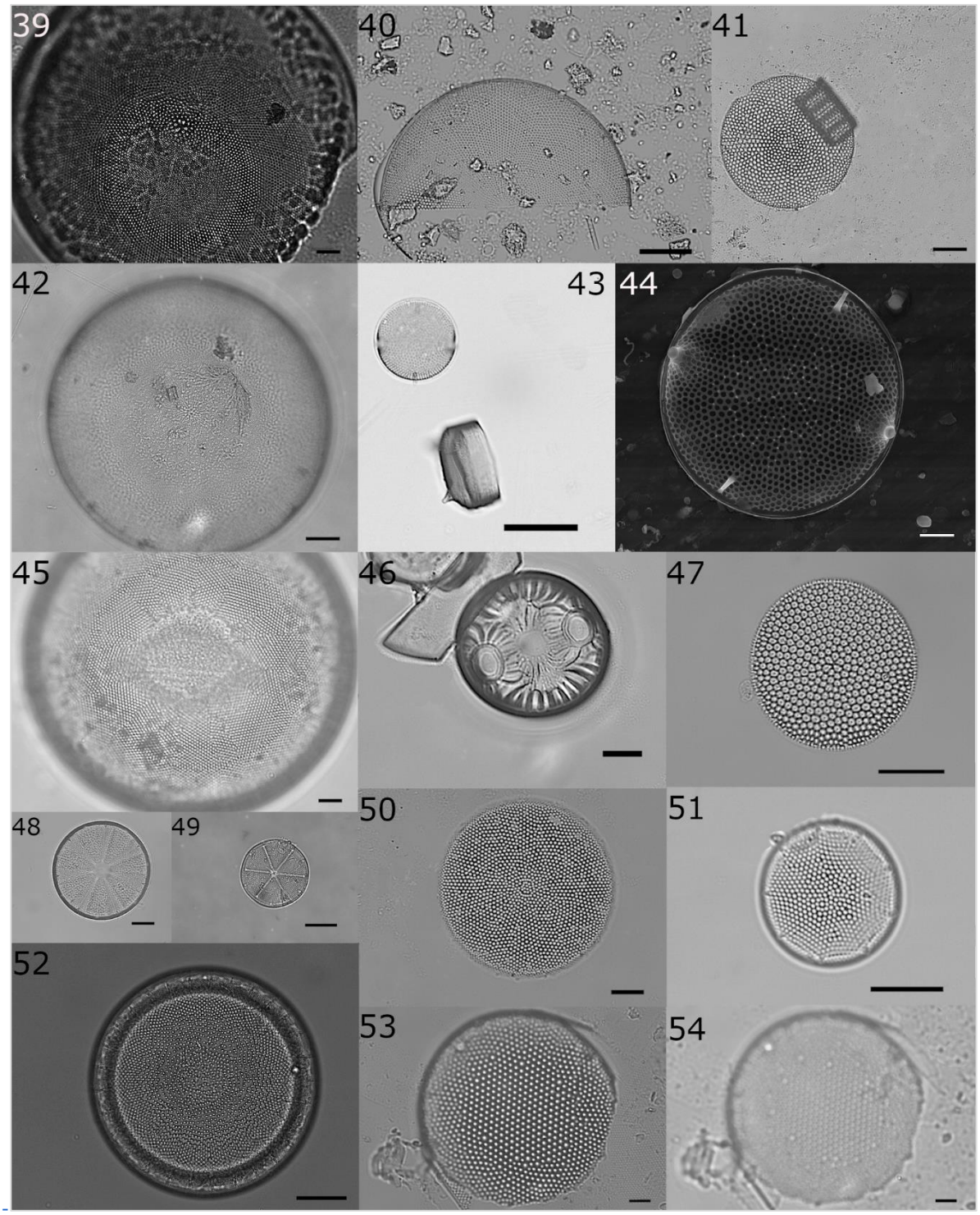

Figure 10: Plate 4. 39. Coscinodiscus centralis 780_10_30, scale bar is 10µm. 40. Coscinodiscus connicus, 700_08_61, scale bar is 50µm. 41. Coscinodiscus radiatus 120_12_30, scale bar is 20µm. 42. Coscinodiscus wailesii 120_09_61, scale bar is 20µm. 43. Ralfsiella smithii ZG02_08_49, scale bar is 50µm. 44. Ralfsiella smithii 120_09_41, scale bar is 10µm. 45. Stellarima stellaris 780_12_47scale bar is 10µm. 46. Auliscus sculptus 780_12_55, scale bar is 10µm. 47. Azpeitia spp. 780_08_44, scale bar is 20µm. 48. Actinoptychus splendens 120_09_12, scale bar is 20µm. 49. Actinoptychus senarius ZG02_09_45, scale bar is 50µm. 50. Actinocyclus curvatulus 700_12_33, scale bar is 10µm. 51. Actinocyclus normanii 780_09_20 scale bar is 20µm. 52. Actinocyclus octonarius 780_09_2, scale bar is 20µm. 53 & 54. Roperia telessata 780_12_44, scale bar is 10µm.

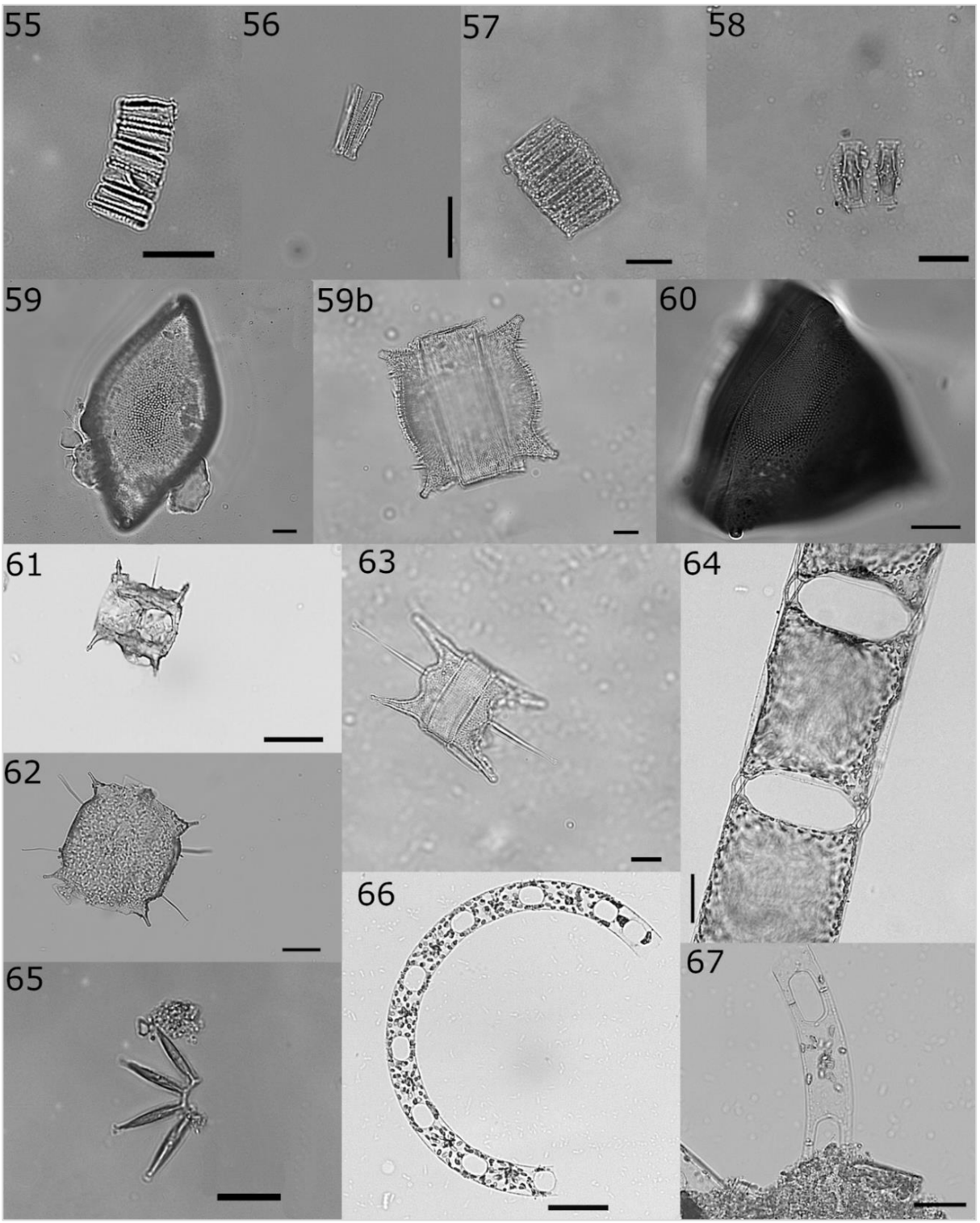

Figure 11: Plate 5. 55. Cymatozia lorenziana 700_09_71, scale bar is 10µm. 56. Cymatosira belgica 780_09_8, scale bar is 20µm. 57. Brockmanniella brockmannii. 780_12_03, 58, scale bar is 20µm. 58. Plagiogrammopsis vanheurckii 700_12_17, scale bar is 20µm. 59. Odontella rhombus 700_11_17, scale bar is 10µm. 59b. Odontella rhombus 120_11_41, scale bar is 10µm. 60. Odontella rhombus f. trigona 780_09_9, scale bar is 20µm. 61. Hobaniella longicruris 780_08_20, scale bar is 50µm. 62. Trieris mobiliensis 780_08_29, scale bar is 50µm. 63. Ralfsiella minima, 120_10_21, scale bar is 10µm. 64. Trieres sinensis 130_08_9, scale bar is 50µm. 65. Asterionella kariana 700_12_2, scale bar is 20µm. 66. Eucampia zodicus 130_08_5, scale bar is 50µm. 67. Eucampia zodiacus var. cornigera ZG02_08_12, scale bar is 50µm.

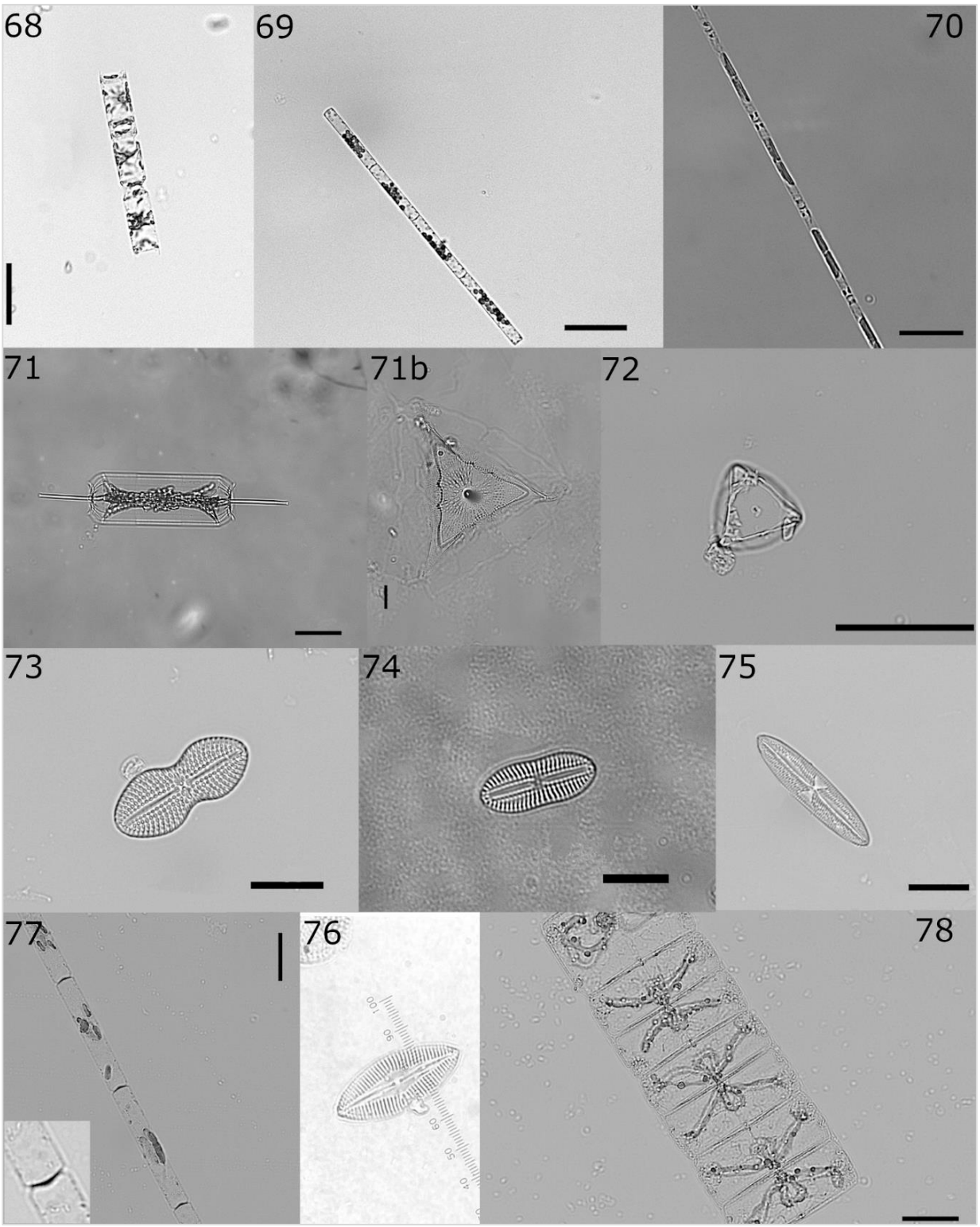

Figure 12: Plate 6. 68. Cerataulina pelagica 700_08_27, scale bar is 50µm. 69. Leptocylindrus danicus 230_08_4, scale bar is 50µm. 70. Tenuicylindrus danicus 780_09_31, scale bar is 20µm. 71. Ditylum brightwellii 120_11_1, scale bar is 50µm. 71b. Ditylum brightwellii 120_11_33, scale bar is 10µm. 72. Lithodesmium spp. 780_09_21, scale bar is 20µm. 73. Diploneis bombus ZG02_08_57, scale bar is 20µm. 74. Diploneis didyma 780_10_20, scale bar is 10µm. 75. Trachyneis aspera ZG02_08_38, scale bar is 20µm. 76. Navicula palpebralis 120_09_102, magnification is 60x. 77. Leptocylindrus convexus ZG02_08_10, scale bar is 50µm. 78. Meuniera membranaceae ZG02_08_16, scale bar is 50µm.

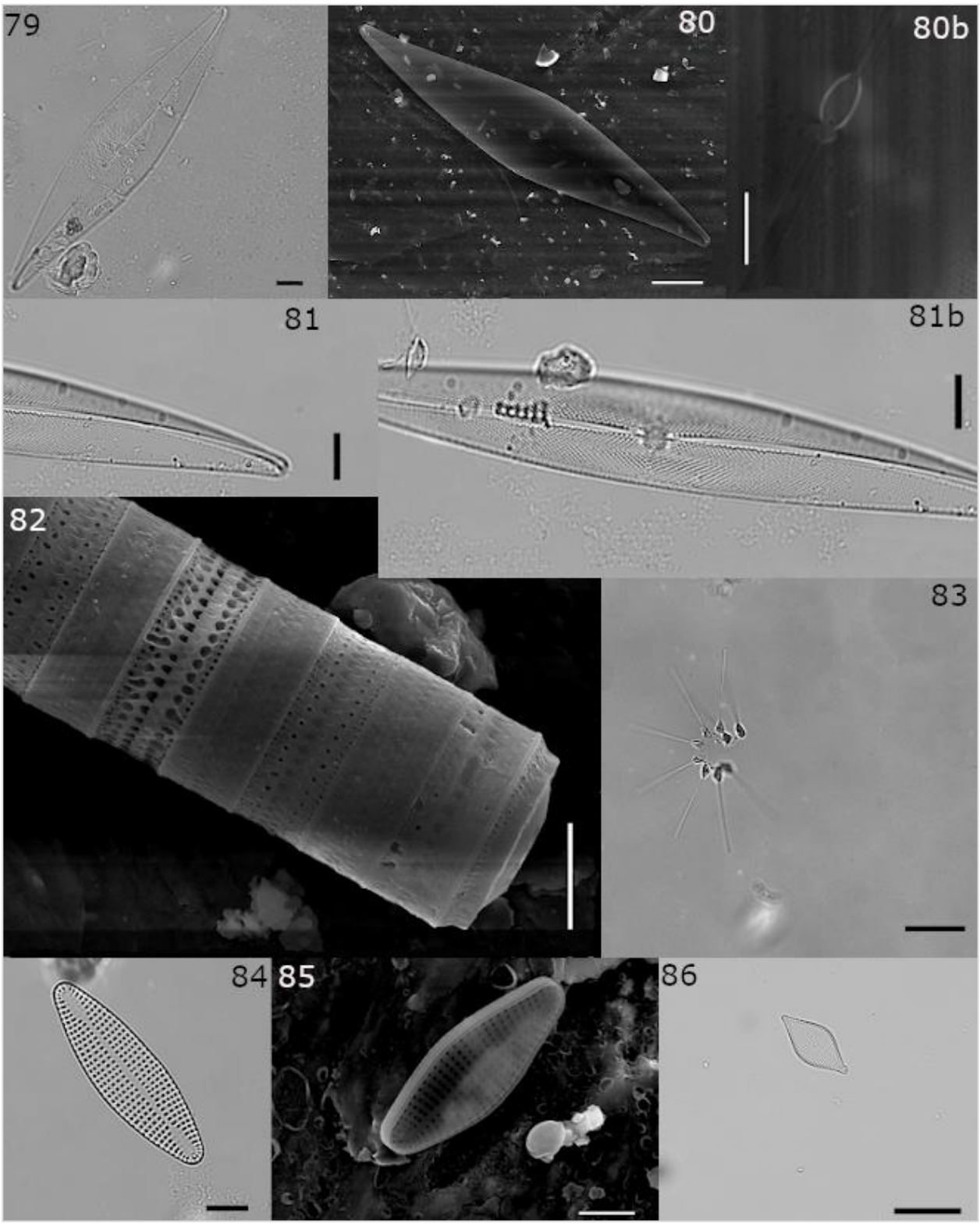

Figure 13: Plate 7. 79. Pleurosigma intermedium 700_11_52, scale bar is 10µm. 80. Pleurosigma intermedium 120_09_44, scale bar is 20µm. 80b. Pleurosigma intermedium 120_09_45, scale bar is 5µm. 81 & 81b. Pleurosigma spp. 700_12_44, scale bar is 10µm. 82. Paralia marina ZG02_09_36, scale bar is 5µm. 83. Asterionella glacialis 700_09_05, scale bar is 50µlm. 84. Delphineis surirella 120_12_57, scale bar is 10µm. 85. Delphineis surirella ZG02_09_36, scale bar is 5µm. 86. Rhaphoneis amphiceros 780_08_31, scale bar is 50µm.

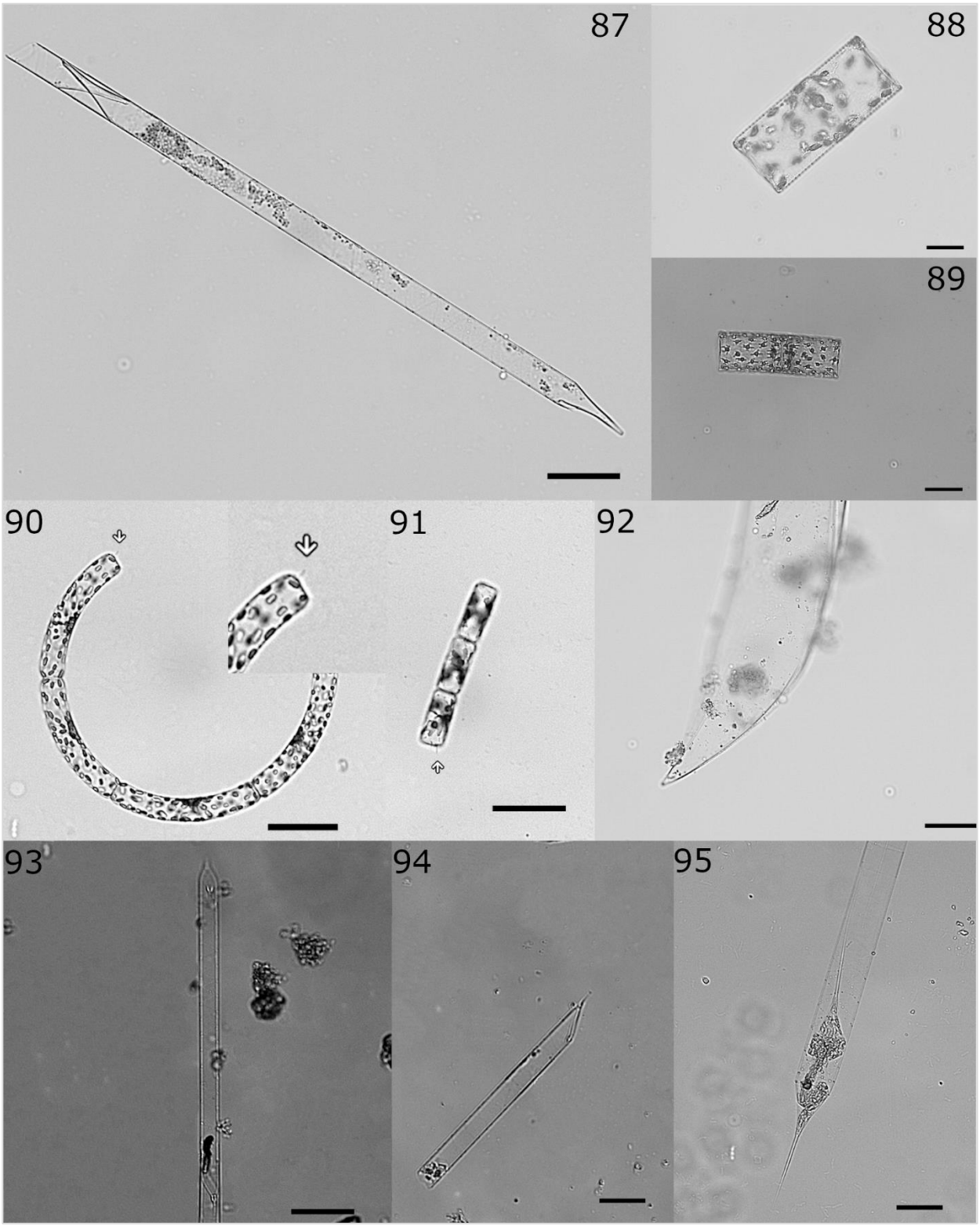

Figure 14: Plate 8. 87. Proboscia alata ZG02_09_96, scale bar is 50µm. 88, 89. Guinardia flaccida ZG02_08_26, scale bar is 50µm. 90. Guinardia striata 130_08_4, scale bar is 50µm . 91. Guinardia delicatula 130_08_1, scale bar is 50µm. 92. Neocalyptrella robusta ZG02_09_102, scale bar is 50µm. 93. Rhizosolenia decipens 700_12_20, scale bar is 50µm.. 94. Rhizosolenia imbricata 780_12_19 ,scale bar is 50µm. 95. Rhizosolenia setigera 120_08_16, scale bar is 20µm.

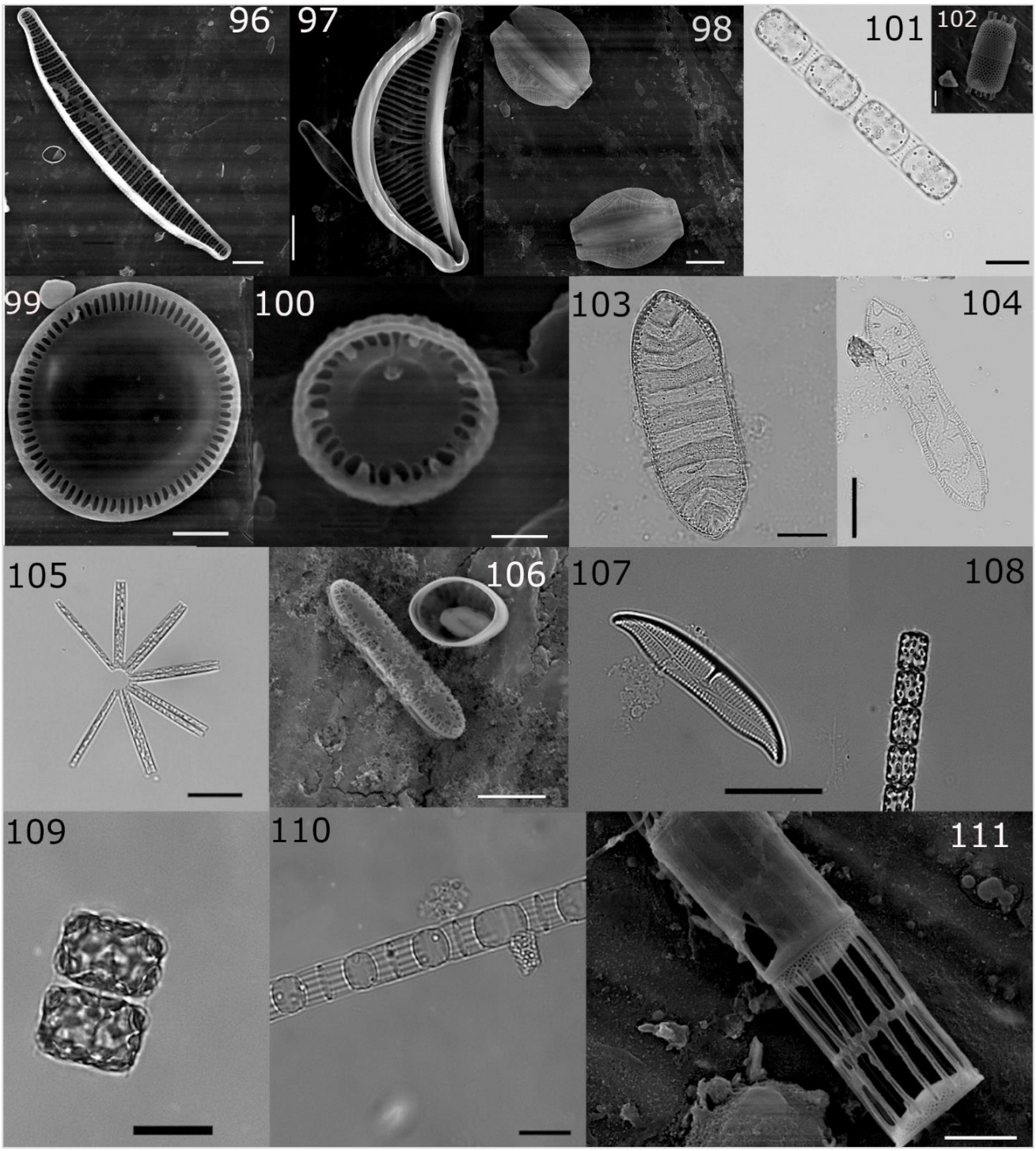

Figure 15: Plate 9. 96 Epithemia adnata 120_08_4, scale bar is 10µm. 97. Epithemia sorex 120_08_20.90, scale bar is 5µm. 98. Epithemia spp. 120_08_22, scale bar is 10µm. 99. Cyclotella choctawhatcheeana 120_09_35, scale bar 5µm. 100. Cyclotella atomus Oostende_08_10, scale bar is 1µm. 101. Eupyxidicula turris ZG02_94. 91, scale bar is 50µm. 102. Eupyxidicula turris, 120_09_03, scale bar is 10µm. 103. Cymatopleura solea 700_12_58, scale bar is 10µm. 104 Cymatopleura solea 700_08_54, scale bar is 20µm. 105. Thalassionema nitzschioides 780_09_40, scale bar is 50µm. 106. Thalassionema nitzschioides ZG02_09_28, scale bar is 5µm. 107. Amphora comutata 780_09_13, scale bar is 20µm. 108. Lauderia annulata 230_08_12, scale bar is 50µm. 109. Detonula pumila 700_09_50, scale bar is 20µm. 110. Skeletonema marinoi 120_09_55, scale bar is 10µm. 111. Skeletonema marinoi 780_09_49, scale bar is 5µm.

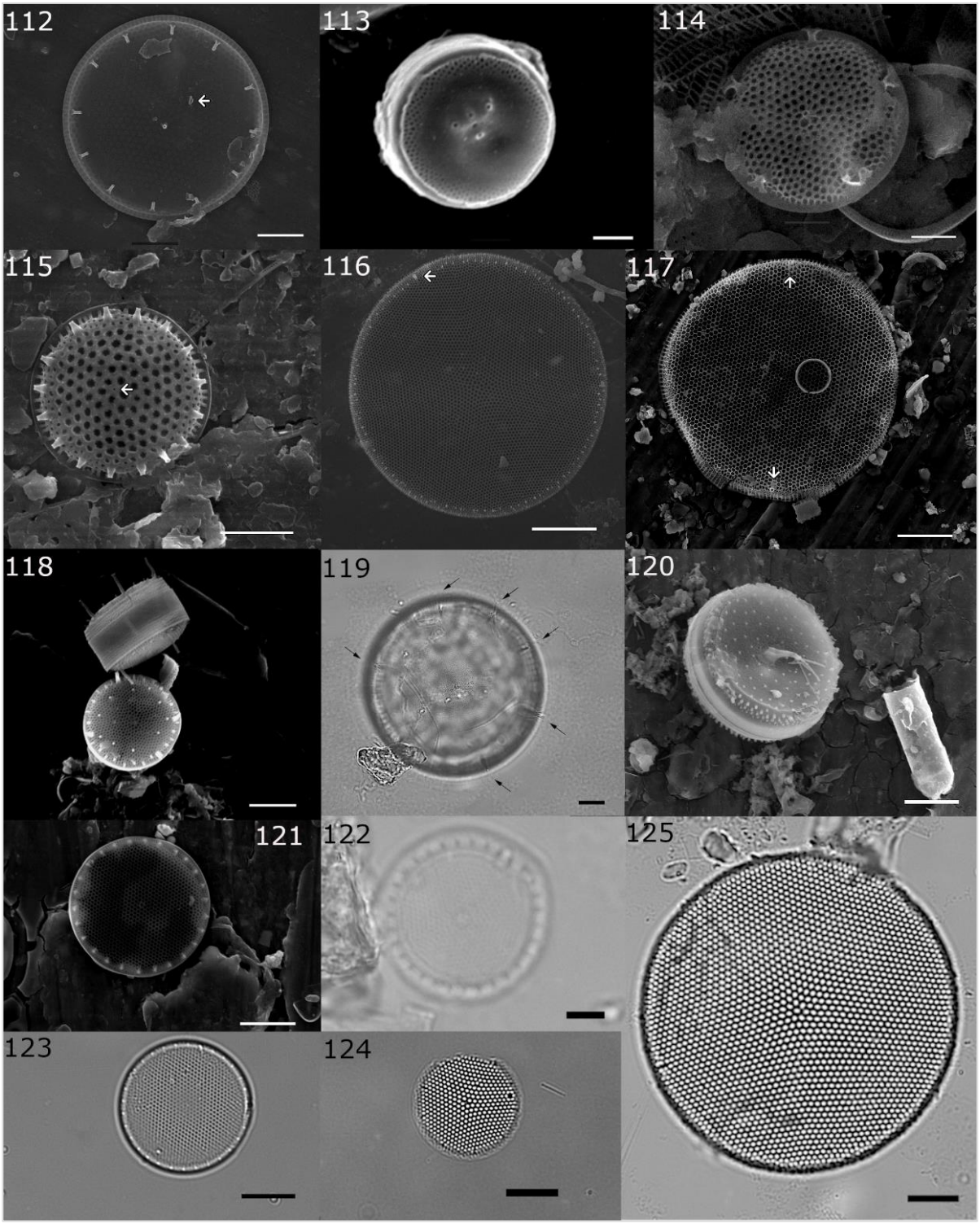

Figure 16: Plate 10. 112. Shionodiscus oestrupii var. vernickae Oostende_08_6, scale bar is 5µm. 113. Minidiscus spp. ZG02_09_08, scale bar is 1µm. 114. Thalassiosira curviseriata ZG02_08_15, scale bar is 2µm. 115. Thalassiosira decipiens 700_08_2, scale bar is 5µm. 116. Thalasiosira eccentrica 780_08_7, scale bar is 10µm. 117. Thalassiosira hendeyi 780_08_28, scale bar is 20µm. 118. Thalassiosira lundiana ZG02_09_24, scale bar is 5 µm. 119. Thalassiosira punctigera 120_11_32, scale bar is 10µm. 120. Thalassiosira rotula 120_09_3, scale bar is 10µm. 121. Thalassiosire tenera ZG02_09_25, scale bar is 10µm. 122. Thalassiosira anguste-lineata 780_12_68, scale bar is 5µm. 123. Thalassiosira tenera 780_09_15, scale bar is 10µm. 124. Shionodiscus oestruppii var. vernickae ZG02_09_52, scale bar is 10µm. 125. Thalassiosira eccentrica 700_12_21, scale bar is 10µm.

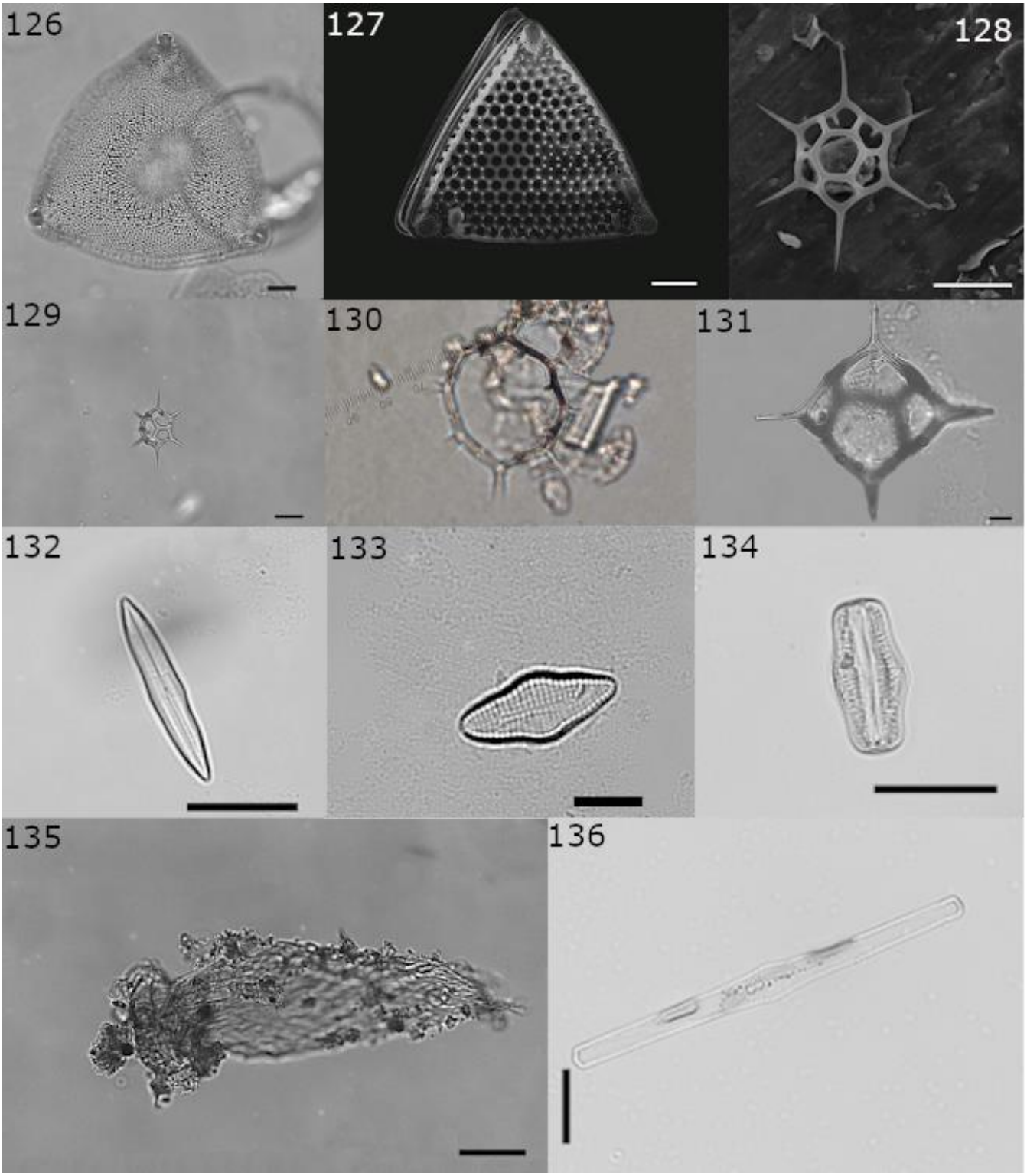

Figure 17: Plate 11. 126. Triceratium favus 700_12_57, scale bar is 10µm. 127. Triceratium favus Oostend_08_16, scale bar is 20µm.128. Occtactis speculum 120_09_30, scale bar is 20µm. 129. Occtactis speculum ZG02_12_16, scale bar is 20µm. 130. Dictyocha spp. 120_09_99, magnification is 100x. 131. Dicytocha spp. 780_12_50, scale bar is 10µm. 132. Unknown diatom ZG02_12_34, scale bar is 10µm. 133 Unknown diatom ZG02_12_50, scale bar is 20µm. 134. Unknown diatom 120_08_44, scale bar is 20µm. 135. Unknown tintinnid ZG02_09_2, scale bar is 50µm. 136. Unknown diatom ZG02_08_23, scale bar 50µm.

Of the 108 identifications listed in Table 3, 98 were identified to species level. The remaining 10 identifications were only identified up to genus level because they were observed only once in LM, which was insufficient to distinguish between different species in the respective genera. Out of these 98 species 65% are also present in the checklist for Helgoland (Hoppenrath, 2004) (Kraberg et al., 2019), while 76 % of the species are recorded in the Belgian Phytoplankton Database (BPD, Nohe et al., 2018). Species that were not found in the BPD are *Actinocylus curvatulus, Actinocyclus normanii, Actinocyclus octonarius, Bacteriastrum mediterraneum, Coscinodiscus wailesii, Cyclotella atomus , Cyclotella choctawhatcheeana, Cymatosira lorenziana, Eucampia zodiacus var. cornigera, Favella ehrenberghii, Leptocylindrus convexus, Nitzschia thermalis, Odontella longicruris, Paralia marina, Rhizosolenia decipiens, Shionodiscus oestupii var. vernickae, Skeletonema marinoi, Tenuicylindrus belgicus, Thalassiosira hendeyi,, Thalassiosira lundiana, Thalassiosira punctigera and Thalassiosira tenera.* Thamarasi (2016) however did detect *Actinocyclus* spp., *Cymatosira lorenziana*, *Skeletonema* spp. and *Thalassiosira hendeyi* in the BPNS. The BPD detected *Paralia sulcata* and *Skeletonema costatum* species complexes in the BPNS (Nohe et al., 2018), which have now been resolved and under which *Paralia marina* and *Skeletonema marinoi* fall respectively.

Of the 10 identifications up to genus level, only the genus *Minidiscus* is not reported in the BPD, the remaining 9 genera have been reported in the BPD.

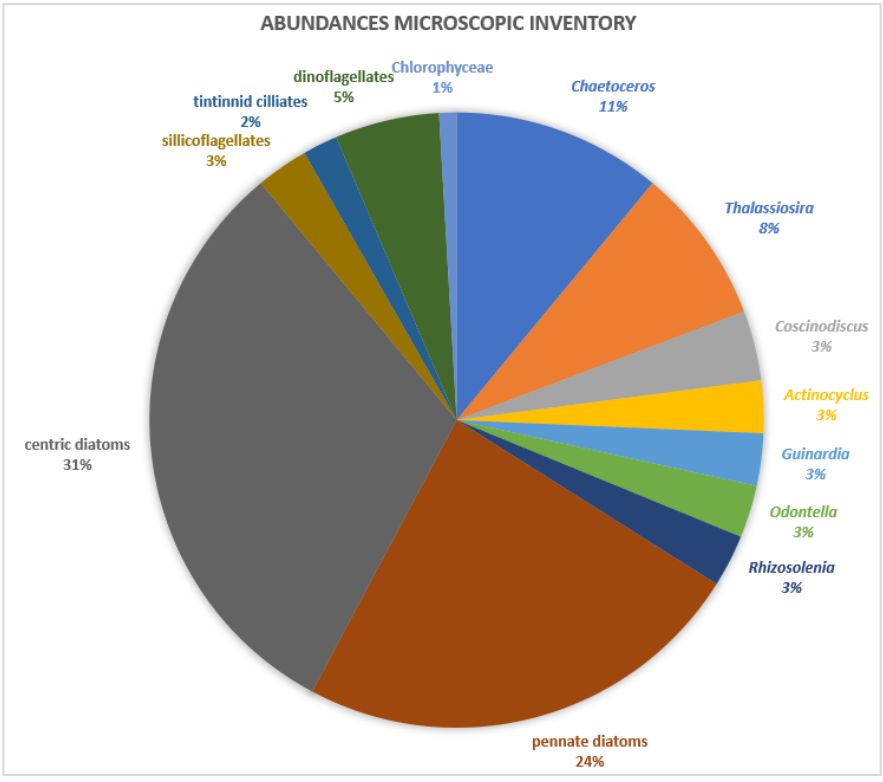

Figure 18: Number of species in major genera and higher order grouping, based on LM and SEM inventory. Total number of species is 101. Diatom genera that had an abundance of less than 2 species were grouped in centric or pennate diatoms for display purposes. Non-diatom groups found are silicoflagellates, tintinnid cilliates, dinoflagellates and Chlorophyta.

Diatoms comprised the most diverse group (96 species), followed by dinoflagellates (6 species), silicoflagellates (3 species), tintinnid cilliates (2 species) and Chlorophyta (1 species). In Fig. 18 the diatom genera diatoms for which most species were observed in the microscopic inventory are shown, together with non-diatom groups silicoflagellates, dinoflagellates, tintinnid cilliates and Chlorophyta. The diatom genus *Chaetoceros* comprises most species (12) followed by *Thalassiosira* (9), *Coscinodiscus* (4), *Actinocyclus* (3), *Guinardia* (3), *Odontella* (3) and *Rhizosolenia* (3). All other genera found had only 2 or less species and hence they are grouped under centric and pennate diatoms. Silicoflagellates comprise 3 species, dinoflagellates comprise 6 species, tintinnid cilliates comprise 2 species and Chlorophyta comprise 1 species.

Some species listed in Table 3 are freshwater species, like *Pseudopediastrum boryanum, Cymatopleura solea* and various *Epithemia* species. They originate from the following samples (station_month):

- *Pseudopediastrum boryanum*: 120_08
- *Cymatopleura solea*: 700_08, 700_12
- *Epithemia spp.:* ZG02_08, 120_08, 780_09, 700_11
- *Epithemia adnata*: 120_08, 120_09
- *Epithemia sorex*: 120_08, 120_09
- *Epithemia turgida*: 120_09

The majority of the species are located at station 120, near the mouth of the Yser river in front of Nieuwpoort. *Pseudopediastrum boryanum* was observed alive, *Cymatopleura solea* was observed in oxidized material, *Epithemia* species were identified in SEM mostly in combination with some identifications in oxidized material. The freshwater diatom species may therefore been dead upon sampling.

1.2 Descriptions

For 9 species which are difficult to identify (e.g. because of their semicryptic nature) detailed descriptions are provided below. The descriptions are accompanied by detailed LM and/or SEM images and measurements. 'Seasonality' describes in which samples these species were detected using metabarcoding, with the exception of *Thalassiosira decipiens* which was not observed in amplicon sequencing but only in SEM. Note that 'Seasonality' is thus not the full seasonal distribution of these species but rather when they were seen during the sample period August to December 2019. Since SEM could only be performed on August and September 2019 samples, *Thalassiosira decipiens* could only be mentioned during these two months. Previous records are not an exhaustive list of previous observations, but rather a reference to a previous observation of that species in the BPNS.

Pseudo-nitzschia pungens (Grunow ex Cleve) Hasle 1993 (Fig. 19)

Basionym: *Nitzschia pungens* Grunow ex Cleve

Previous North Sea records: Casteleyn et al. (2008).

Seasonality: August, September, October, November and December.

Identification: Hasle, G.R. and Syvertsen, E.E. *1997*. Marine diatoms. In: C.R. Tomas (ed.) Identifying Marine Phytoplankton. Academic Press, Inc., San Diego, California.

Description: Cells 2.5 ± 0.9 µm width and 116.7 ± 13.5 µm apical length. Linear valves with acute apices. Outline of valve symmetrical in apical axis (Fig. 1.1 & Fig. 1.2). Central larger interspace absent. 10.36 ± 1.9 striae per 10 µm and 10.3 ± 2.0 fibulae per 10 µm. Two rows of poroids per stria (Fig.1.3 & Fig. 1.4) and 2.9 ± 0.4 poroids per 1 µm. Central striae and fibulae not more widely spaced (Fig. 1.2 & Fig. 1.4). Values based on measurements of 14 observations.

Remarks: Transapical axis wider than 3 µm, characteristic for the *Pseudo-nitzschia* seriata complex to which *Pseudo-nitzschia pungens* belongs (Casteleyn et al., 2008).

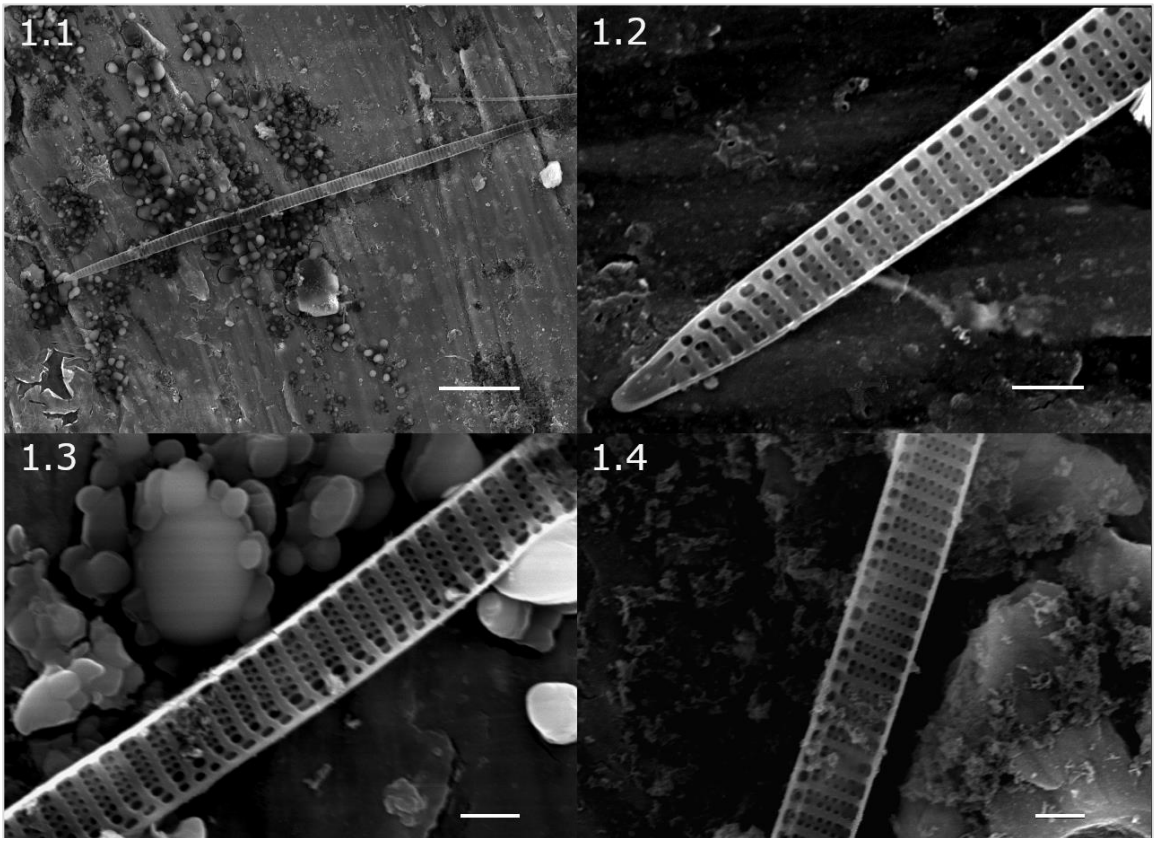

Figure 19: Pseudo-nitzschia pungens in SEM, sample ZG02_08. Fig. 1.1 Valve view. Scale bar 20µm. Fig. 1.2 Valve inside view of valve apex. Scale bar 2µm. Fig. 1.3 Valve inside view. Scale bar 2µm. Fig. 1.4 Valve inside view. Equal number of striae and fibulae. Scale bar 2µm.

Skeletonema marinoi Sarno & Zingone 2015 (Fig. 20)

Previous North Sea records: Sjöqvist et al. (2015)

Seasonality: August, September, October, November and December.

Identification: Sarno et al. (2005)

Description: Valve face slightly convex (Fig. 2.2). Sibling cells linked in linear chains by intercalary fultoportulae which are open along their entire length (Fig 2.2). Fultoportulae are located near the valve face margin (Fig. 2.2). Intercalary fultoportulae linked by 1:2 junctions in a plain joint without knuckles (Fig. 2.2). Intercalary rimoportulae are short and located near the valve face margin (Fig 2.2).

Remarks: *Skeletonema marinoi* and *Skeletonema dohrnii* are not entirely morphological and genetically distinct (Ellegaard et al., 2008). Measurements for valve diameter were not possible, since the species was only seen once in SEM in griddle view.

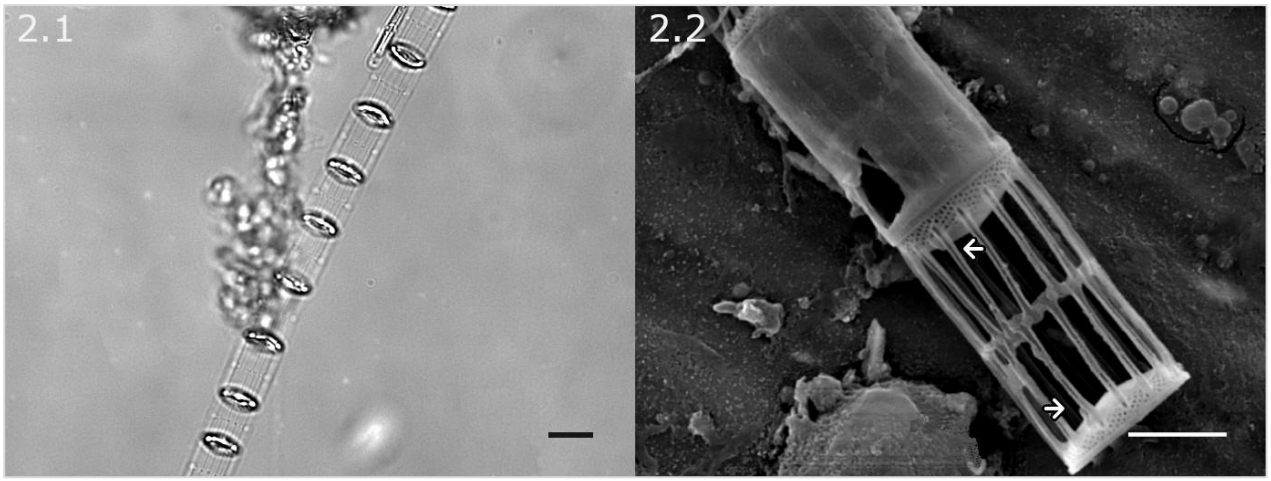

Figure 20: Skeletonema marinoi. Fig 2.1 Griddle view, sample 120_09 in light microscope. Chain of sibling cells. Scale bar 10µm. Fig. 2.2 Griddle view, sample 780_09 in SEM. Linking of sibling valves by open intercalary fultoportulae. Intercalary rimoportulae indicated by arrows. Scale bar 5µm.

Eupyxidicula turris (Greville) Blanco & Wetzel 2016 (Fig. 21)

Basionym: *Creswellia turris* Greville

Synonym: *Stephanopyxis turris,* (Greville) Ralfs 1861

Previous North Sea records: Hoppenrath et al. (2004)

Seasonality: August, September, October, November and December.

Identification: Ferrario et al. (2012)

Description: Cylindrical cells connected by rimoportulae, fusing midway between sibling cells and uniting them into long filaments (Fig. 3.1). Rimoportulae truncate and arranged in a ring on the valve face margin (Fig. 3.2). Transition between mantle and valve surface gradual. Areolae on valve surface and mantle hexagonal (Fig 3.4) and of similar size (Fig 3.3).

S

Remarks: *Eupyxidicula turris* can be distinguished from *Stephanopyxis palmeriana* by areolae of similar size on valve surface and margin. Measurements of valve diameter were not possible because all valves seen appeared under an angle.

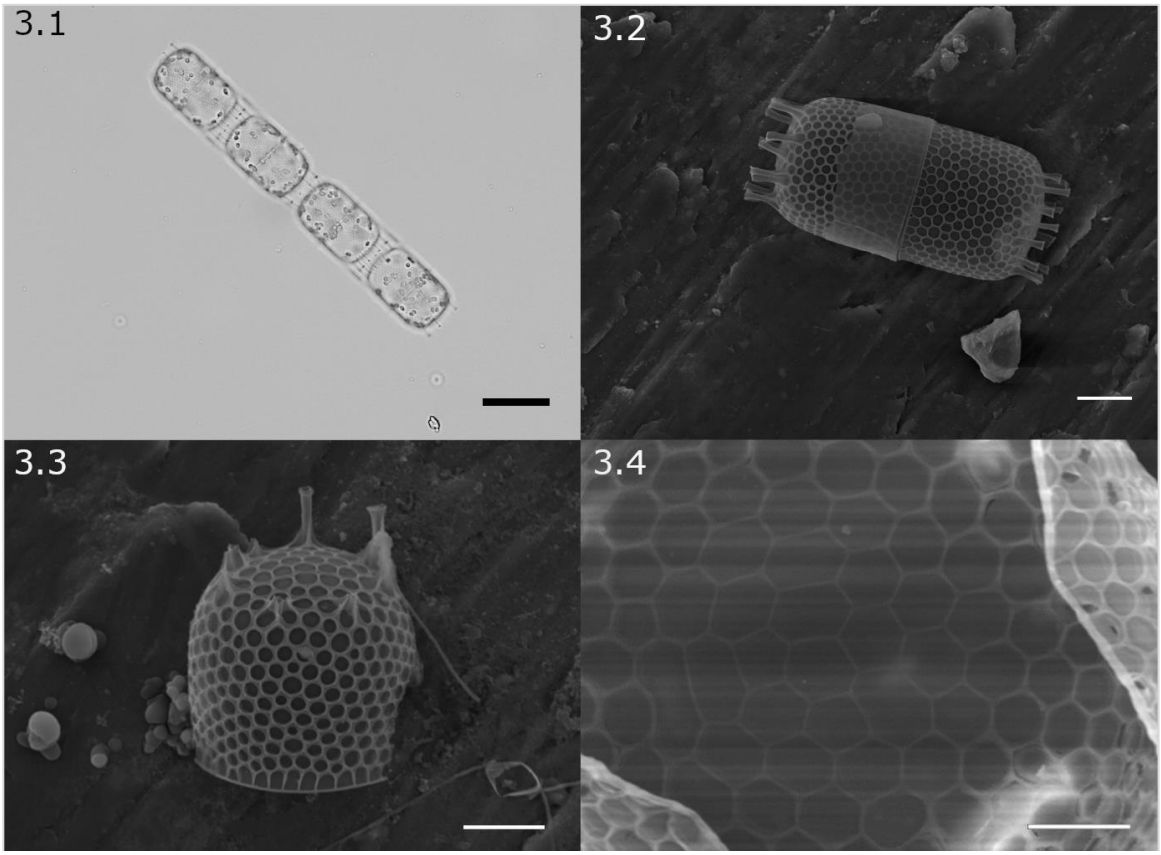

Figure 21: Eupyxidicula turris. Fig 3.1 Griddle view, sample ZG02_09 in SEM. Midway fusion of cells in light microscope. Scale bar 50µm. Fig. 3.2. Griddle view, sample 120_09 in SEM. Scale bar 10µm. Fig. 3.3 Valve in oblique side view, sample 120_09 in SEM. Scale bar 10µm. Fig. 3.4 Valve inside view, sample 780_09 in SEM. Scale bar 5µm..

Shionodiscus oestrupii var. *vernickae* (Ostenfeld) Alverson, Kang & Theriot 2006 (Fig. 22)

Basionym: *Coscinosira oestrupii* Ostenfeld, 1900

Previous North Sea records: Oksman et al. (2019)

Seasonality: August, September, October, November and December.

Identification: Wilks & Armand (2017)

Description: Cells 17.3 ± 2.4 µm in diameter. Valves with eccentric areolation pattern (Fig. 4.1). 13 ± 1.3 number of areolae per 10 µm. One trifultate central process and one labiate central process (Fig. 4.2) separated by 2.7 ± 0.5 areolae on average. One ring of 9.3 ± 1.1 marginal fultoportulae in which processes are 5.5 ± 0.7 µm apart. Values based on measurements of 7-14 observations.

Remarks: Marginal fultoportulae are more closely spaced in *Shionodiscus oestrupii* var. *oestrupii* than in *Shionodiscus oestrupii* var. *vernickae*.

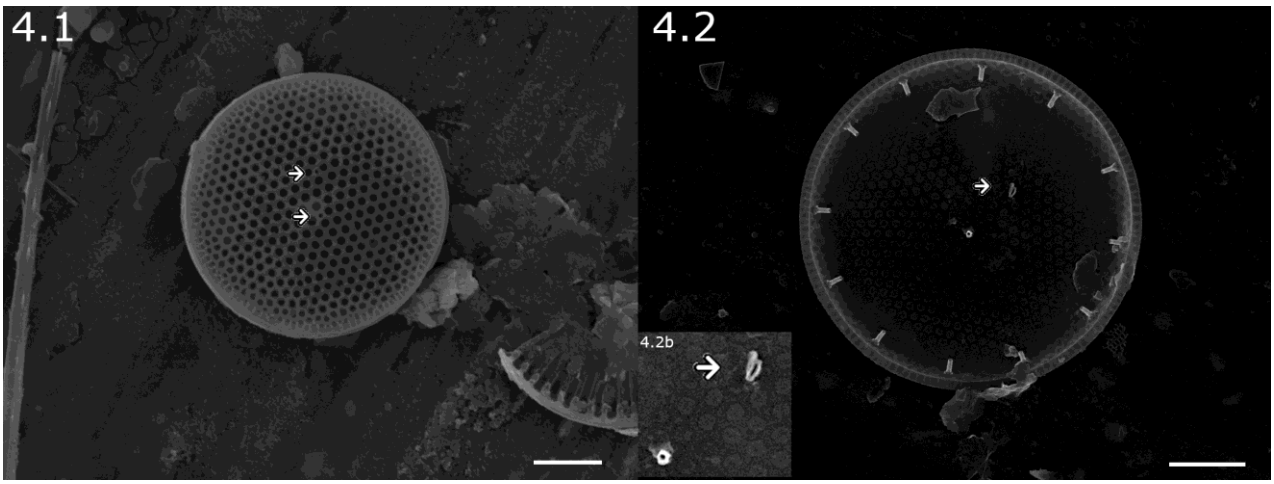

Figure 22: Shionodiscus oestrupii var. vernickae in SEM. Scale bars 5µm. Fig. 4.1 Valve view sample, sample 120_09. Central fultoportula and trifultate process indicated by arrows. Fig. 4.2 Valve view sample, sample Oostende_08. Trifultate process indicated by arrow. Fig. 4.2b, zoomed in on trifultate process indicated by arrow.

Thalassiosira tenera Proschina-Lavrenko 1961 (Fig. 23)

Previous North Sea records: Hoppenrath et al. (2004)

Seasonality: August, September, October, November and December.

Identification: Hoppenrath et al. (2007)

Description: Cells 25.6 ± 1.0 µm in diameter. Valves with linear areolation pattern. Areolae hexagonal in shape (Fig 5.1). 15.1 ± 0.7 areolae per 10 µm. One central fultoportula surrounded by a larger areola (Fig 5.1 & Fig. 5.2). Marginal ring of toothed fultoportulae, with 5.4 ± 0.5 marginal fultoportulae in 10 µm. One rimoportula next to a marginal fultoportula inside the ring of marginal fultoportulae (Fig. 5.2). Values based on measurements of 7 observations.

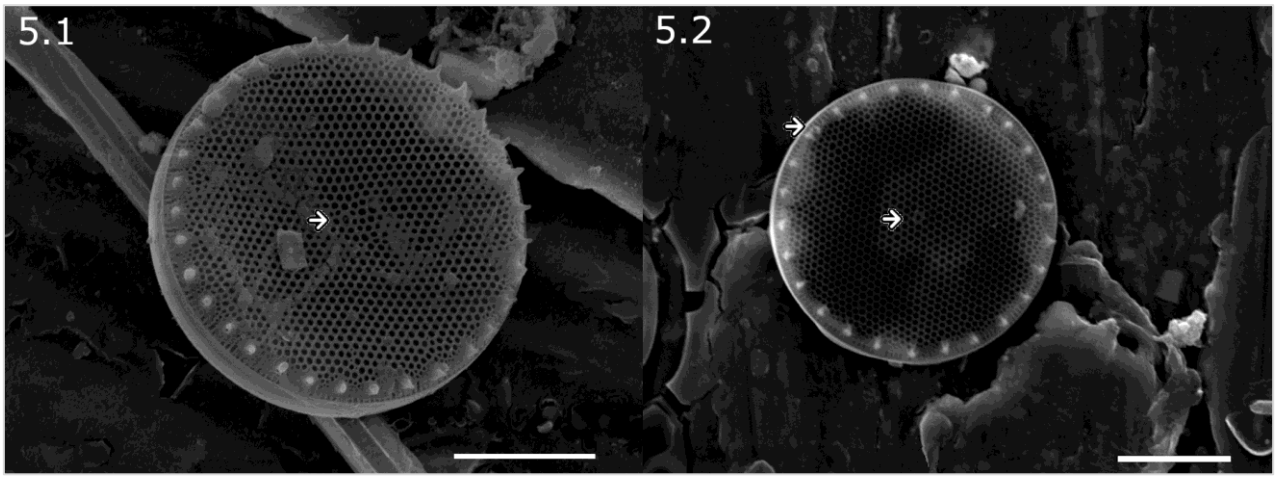

Figure 23: Thalassiosira tenera in SEM. Scale bars 10µm. Fig. 5.1 Valve outside view, sample 780_09. Larger central areola indicated by arrow. Fig. 5.2 Valve outside view, sample ZG02_25. Central fultoportula and rimoportula in rim of marginal fultoportulae.

Thalassiosira hendeyi Halse & Fryxell 1971 (Fig. 24)

Synonym: *Coscinodiscus hustedtii* Müller-Melchers

Previous North Sea records: Hoppenrath et al.(2004)

Seasonality: August, September, October, November and December.

Identification: Hoppenrath et al. (2007)

Description: Cells 42.1 ± 0.3 µm in diameter. Valve with linear areolation pattern with hexagonal areolae (Fig. 6.2). 8 ± 1 areolae per 10 µm. Two prominent rimoportulae on opposite sides of the valve face margin (Fig. 6.1 & Fig. 6.2). One small fultoportula in the centre of the valve face surface (Fig. 6.3). Values based on measurements of 3 observations.

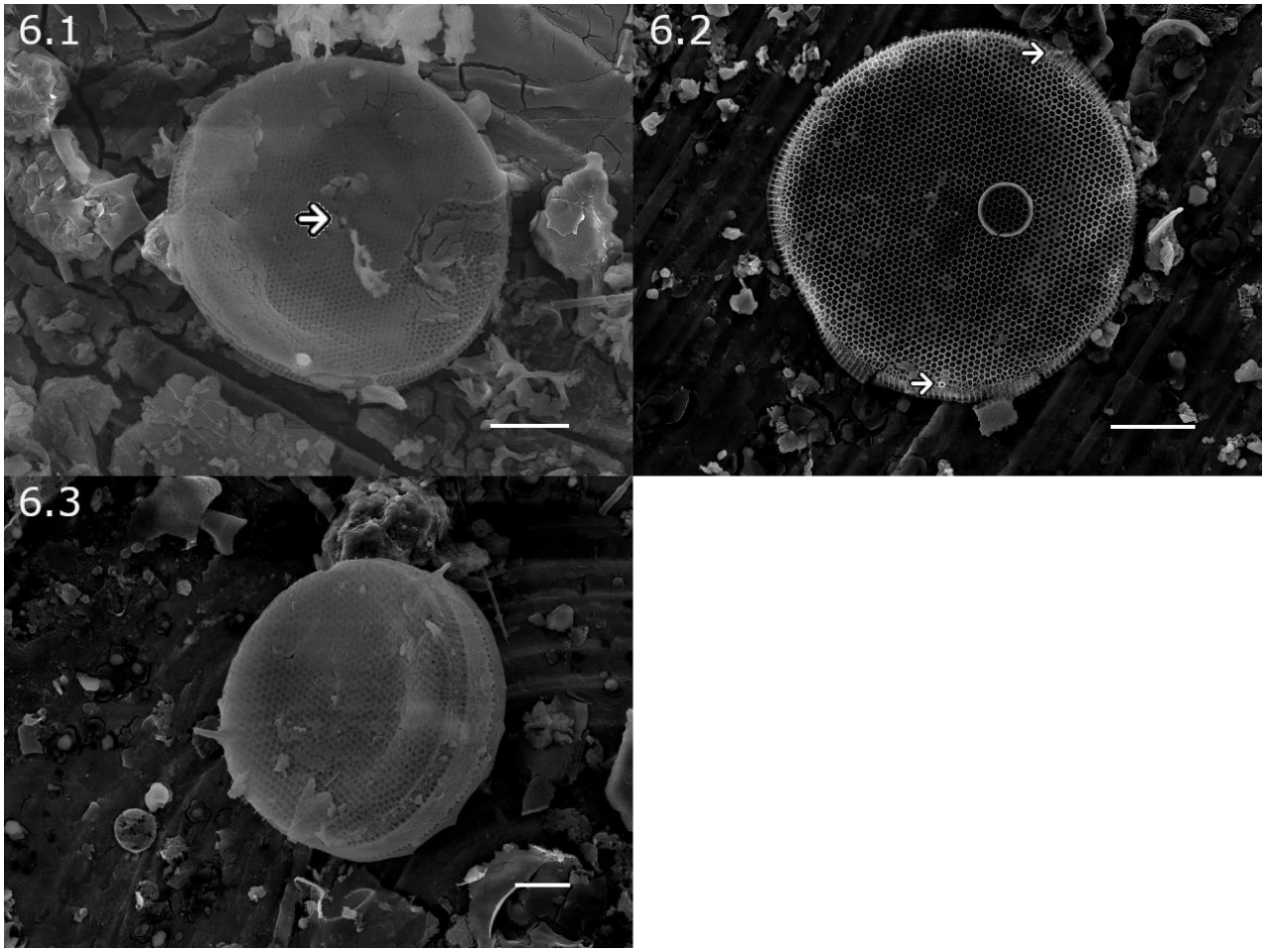

Figure 24: Thalassiosira hendeyi in SEM, sample 780_09. Fig. 6.1 Valve outside view. Two rimoportulae on opposite sides of the valve face margin and one central fultoportula indicated by arrow. Scale bar 20µm. Fig. 6.2 Valve outside view. Two rimoportulae indicated by arrows. Scale bar 20µm. Fig. 6.3. Oblique side view. Concave valve surface. Scale bar 10µm.

Thalassiosira curviseriata Takano 1981 (Fig.25)

Previous North Sea records: Hoppenrath et al. (2004)

Seasonality: August, September, October, November and December.

Identification: Hoppenrath et al. (2007)

Description: Cells 7.1 ± 0.8 µm in diameter. Valves with radial areolation (Fig. 7.1). 3.7 ± 0.6 in 1 µm. One (Fig. 7.1) or two (Fig 7.2) central fultoportulae. One marginal ring with 3.7 ± 0.6 winged fultoportulae, each ending in two wings, which divide into two additional branches each (Fig 7.1). One rimoportula next to a fultoportula inside the ring of marginal fultoportulae (Fig. 7.2). Values based on measurements of 3 observations.

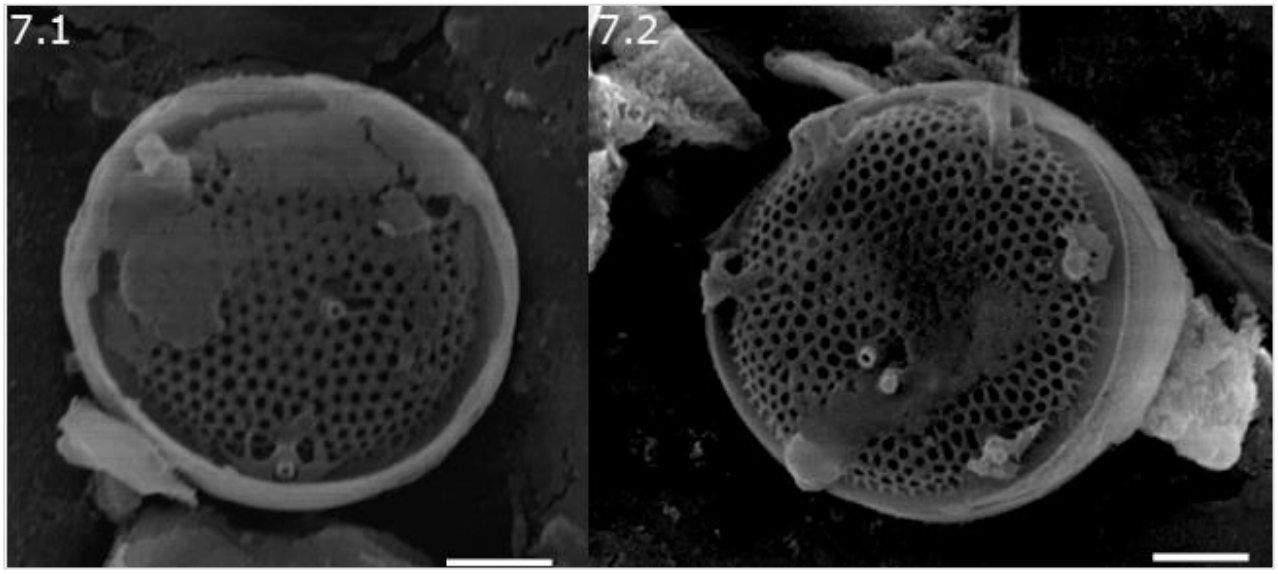

Figure 25: Thalassiosira curviseriata in SEM, sample 780_09. Scale bars 2µm. Fig 7.1 Valve outside view. One central fultoportula. Wings of marginal fultoportulae split into two branches. Fig. 7.2 Valve outside view. Two central fultoportulae. One marginal rimoportula inside ring of marginal fultoportulae.

Thalassiosira eccentrica (Ehrenberg) Cleve 1904 (Fig. 27)

Basionym: *Coscinodiscus eccentricus* Ehrenberg

Previous North Sea records: Hoppenrath et al. (2004)

Seasonality: August, September, October, November and December.

Identification: Hoppenrath et al. (2007)

Description: Cells 59.1 ± 12.9 µm in diameter. Valves with eccentric areolation pattern (Fig. 8.1) with 8.4 ± 0.6 hexagonal areolae per 10 µm. One smaller central fultoportula next to a central areola which is surrounded by 7 areolae (Fig. 8.4). Two rings of marginal fultoportulae (Fig. 8.1) and additional fultoportulae scattered over valve face (Fig. 8.2). 5.8 ± 0.5 fultoportulae per 10 µm inside marginal ring and 3 additional scattered fultoportulae in 10 µm. One rimoportula next to a marginal fultoportula inside the ring of marginal fultoportulae (Fig. 8.3). Values based on measurements of 1-6 observations.

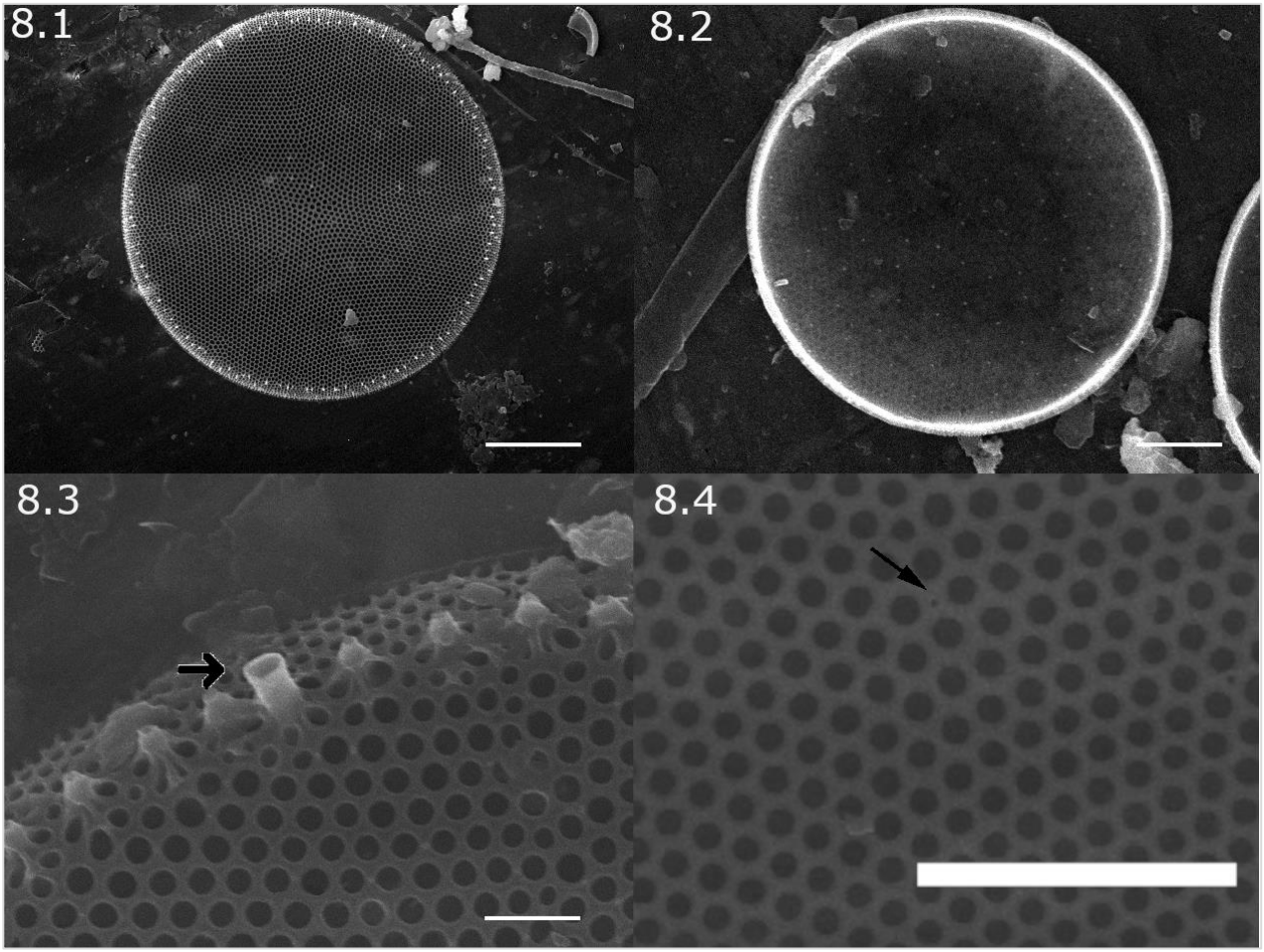

Figure 26: Thalassiosira eccentrica in SEM, sample 780_09. Fig. 8.1 Valve outside view. Eccentric pattern. Scale bar 20µm. Fig 8.2 Valve inside view. Fultoportulae scattered over valve. Scale bar 10µm. Fig 8.3 Valve outside view. Marginal rimoportula indicated by arrow. Scale bar 2µm. Fig 8.4 Valve outside view. Central fultoportula indicated by arrow and right above central areola, which in turn is surrounded by 7 areolae. Scale bar 10µm

Thalassiosira decipiens (Grunow ex Van Heurck) Jørgensen 1905 (Fig. 9)

Basionym: *Coscinodiscus decipiens* Grunow ex Van Heurck

Previous North Sea records: Hoppenrath et al. (2004)

Seasonality: August and September (SEM).

Identification: Hoppenrath et al. (2007)

Description: Cells 10.2 ± 0.9 µm in diameter. One valve surface convex (Fig. 9.1) and the other valve surface concave (Fig. 9.2). Valves with eccentric areolation pattern (Fig. 9.1), with 7.8 ± 0.8 areolae per 10 µm. One central fultoportula (Fig. 9.1). One marginal ring of fultoportulae with one rimoportula inside the marginal ring of fultoportulae (Fig. 9.2), 6.3 ± 0.5 fultoportulae in 10 µm. Values based on measurements of 6 observations.

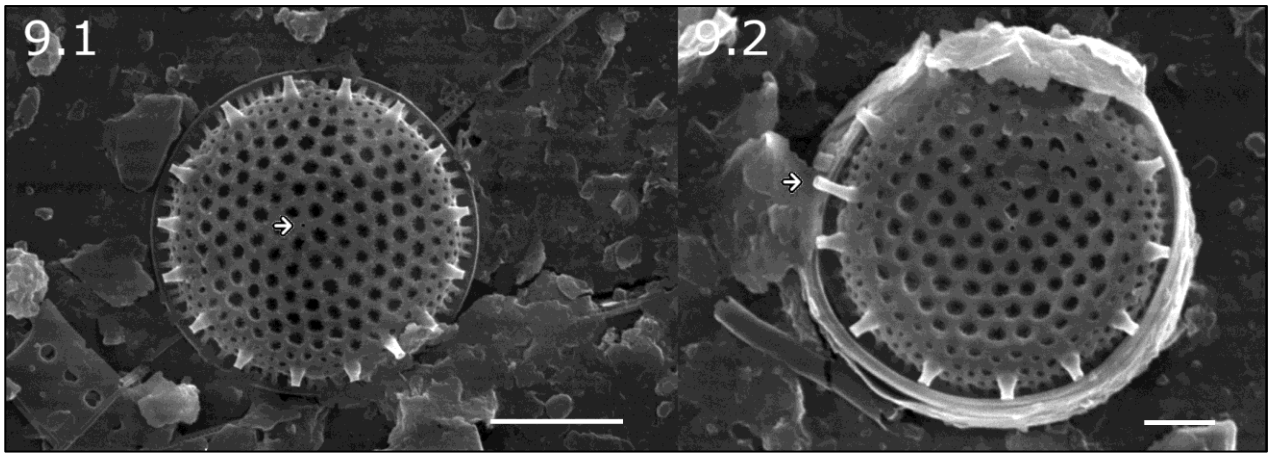

Figure 27: Thalassiosira decipiens in SEM. sample 700_08. Fig. 9.1 Valve outside view. Central fultoportula indicated by arrow. Scale bar 5µm. Fig. 9.2 Valve outside view. Marginal rimoportula inside rind with fultoportulae indicated by arrow. Scale bar is 10 µm.

1.3 Amplicon sequencing based inventory

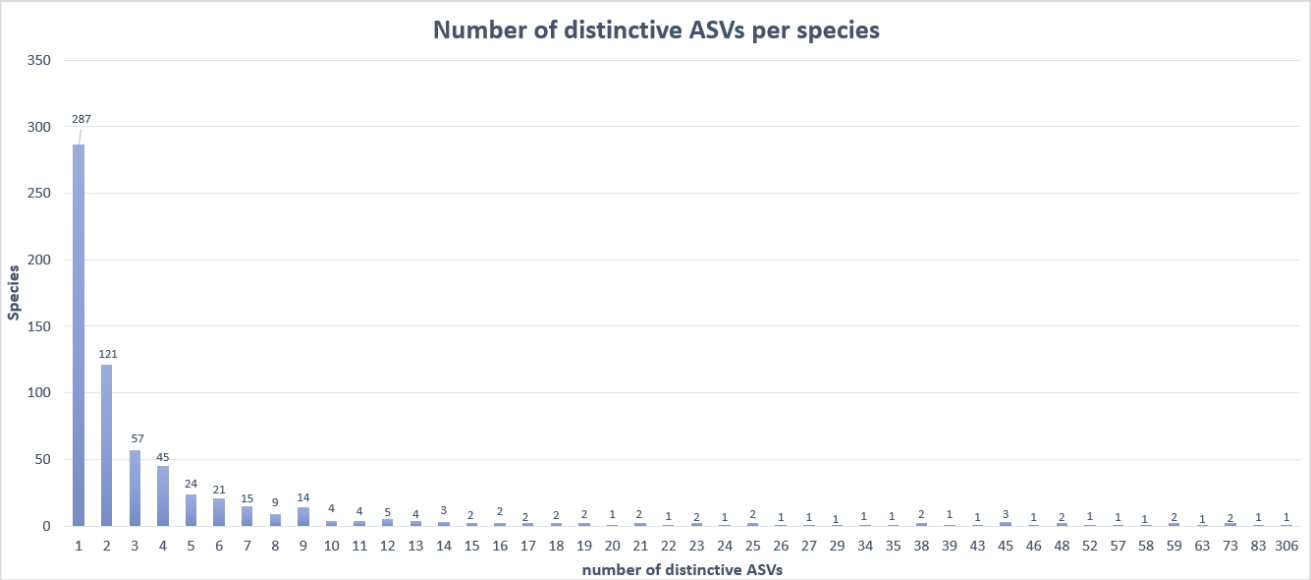

Figure 28: Number of ASVs per species for the amplicon sequencing inventory. X-axis depicts the number of ASVs found for certain species. Y-axis depicts how many species had a certain amount of unique ASVs matched to them.

Amplicon sequencing revealed 3 498 unique ASVs belonging to 657 unique species. The difference in the number of ASVs vs species is mainly caused by a few species having a very high number of ASVs. The majority of the species have 1 to 2 ASVs (Fig. 28). About 90% of all species found in the microscopic inventory, have 10 ASVs or less. The highest number of ASVs per species is 306, found on the right side of the graph for unknown Dino-Group-II, the second highest number of ASVs, 83, is found for unknown Chrysophyceae. This is followed by two times 73 ASVs, 63 ASVs and 59 ASVs for unknown Cercozoans, 59 ASVs for an unknown Bacillariophyceae, 58 ASVs for an unknown Telonema, 57 and 52 ASVs for unknown Dino-Group-I and unknown Dinophyceae. Most of the species matches 'unknown' to species level and only have higher taxonomic level matches. This could imply that these species with a number of ASVs assigned to them stem from eDNA, are mainly dinoflagellates or small species.

For the following analyses, figures and numbers are based on the species-based amplicon sequencing inventory, not the ASV based inventory. The amplicon sequencing based species based inventory can be found in Appendix 7. The full ASV-based inventory for amplicon sequencing is reported separately on the Marine Data Archives due to its size.

Fig. 29 shows the diversity in terms of number of species per supergroup (larger, central pie chart) and per division (surrounding figures) in the amplicon sequencing based species based inventory. Stramenopila is the most diverse supergroup containing 35% of all species found, followed by Alveolata which contains 30.2% of all species found. Supergroups Archaeplastida (9.9%), Rhizaria (8.6%), Hacrobia (7.4%), Opisthokonta (4.3%), Amoebozoa (2.5%), Apusozoa (1.6%) and Excavata (0.2%). Stramenopila are dominated by the class Ochrophyta (73%), Alveolata are dominated by dinoflagellates (Myzozoa + Dinoflagellata) (50%) and Ciliophora (40%), Archaeplastida are dominated by Chlorophyta (95%), Rhizaria are dominated by Cercozoa (91%), Hacrobia are dominated by Cryptophyta (61%), Opisthokonta are dominated by Fungi (55%), Amoebozoa are dominated by class Amoebozoa (47%), Apusozoa are dominated by Apusomonadidae (55%), Excavata only comprise two species *Diplonema* sp. and *Heteramoeba clara*.

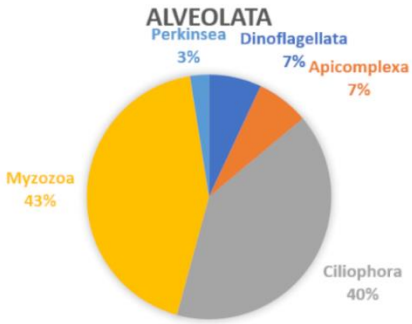

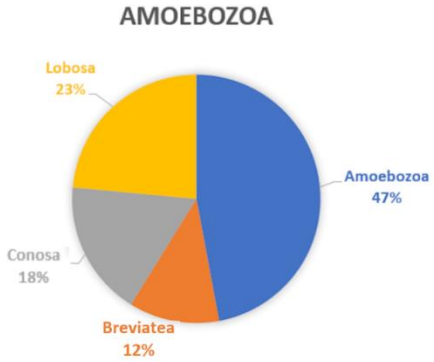

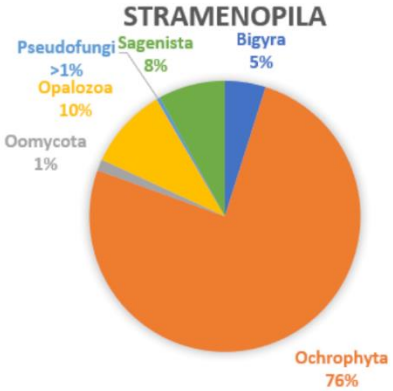

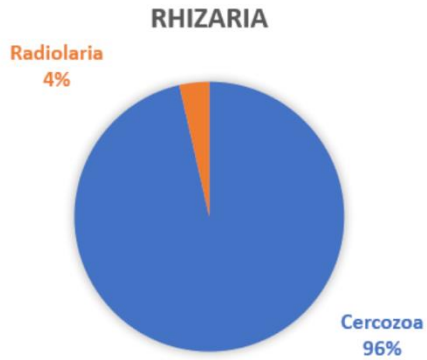

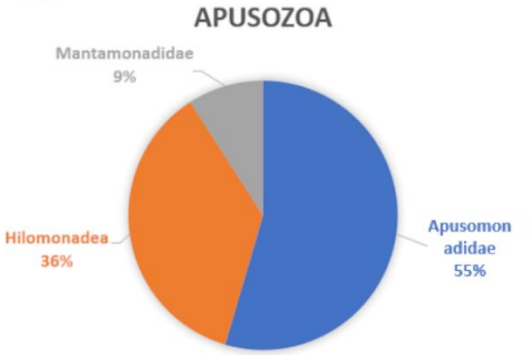

SUPERGROUPS

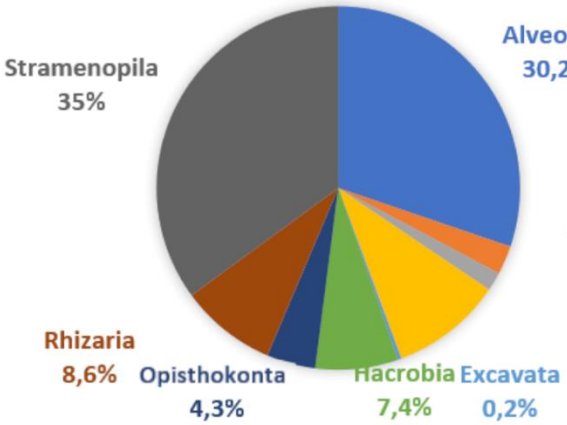

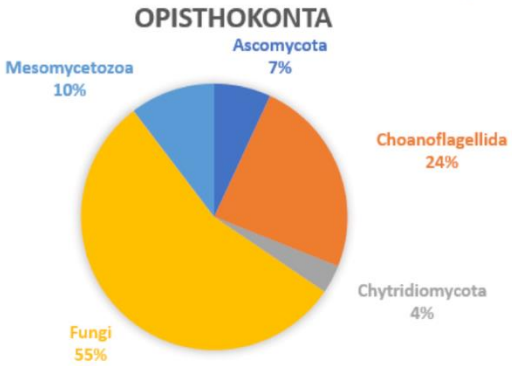

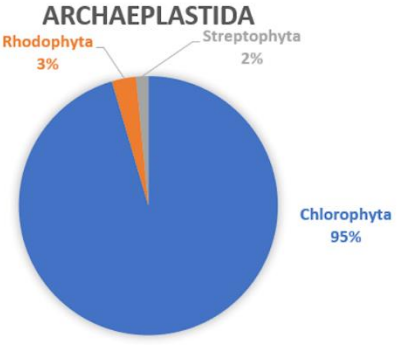

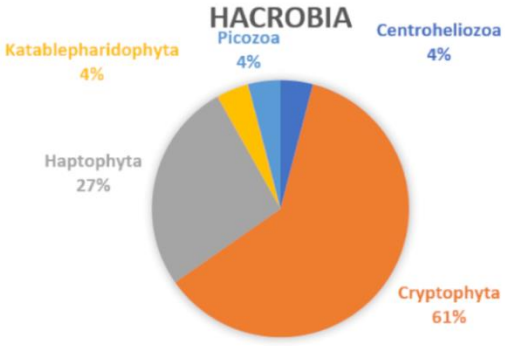

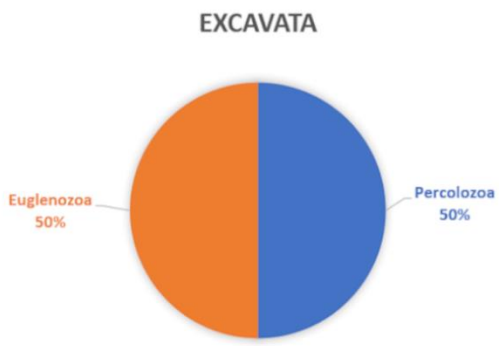

Figure 29: Species diversity per supergroup (central pie chart) and per division (surrounding pie charts). In the amplicon sequencing species-based inventory.

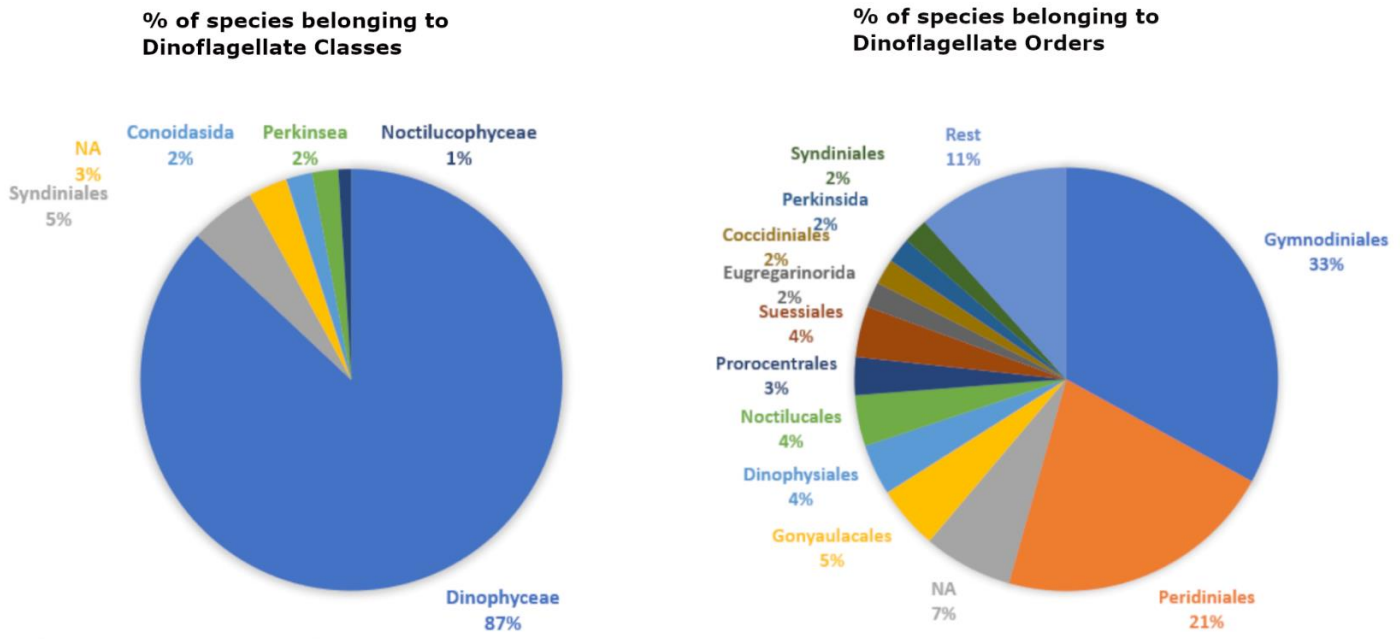

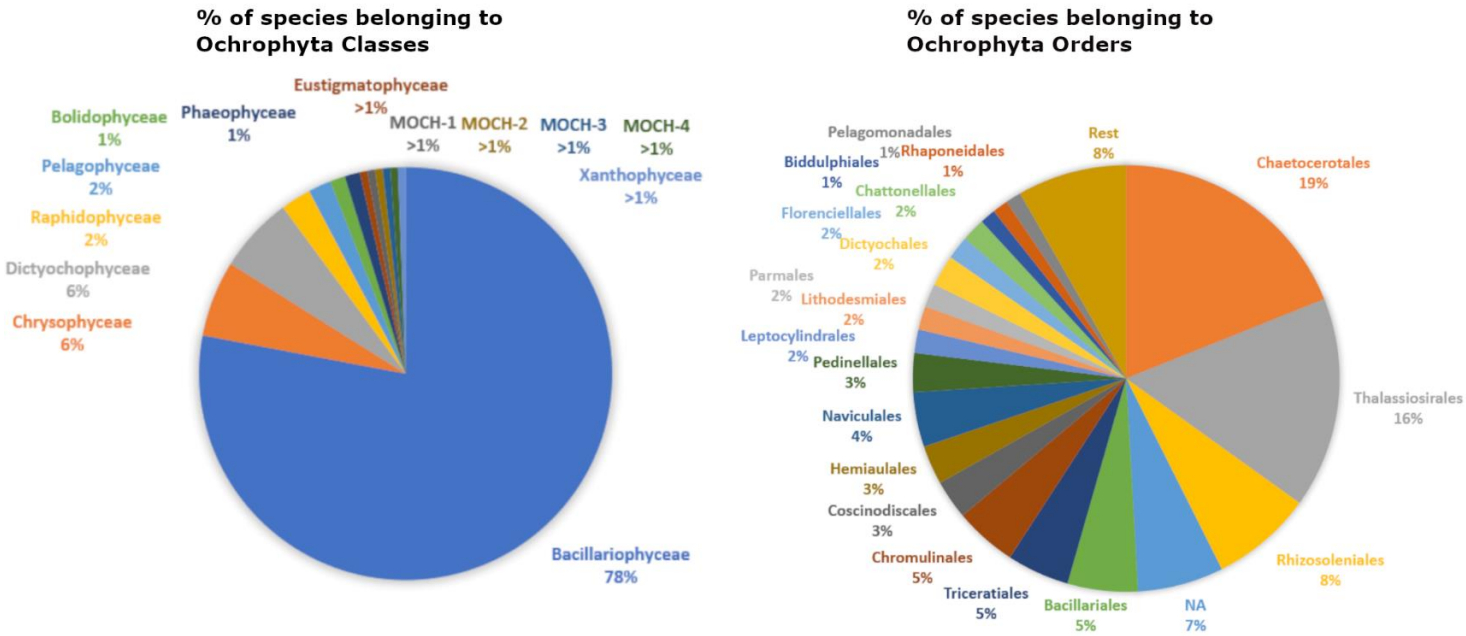

Figure 30: Top: Species diversity in the dinoflagellates (Dinoflagellata+Myzozoa) as percentage of species per Class and Order. Rest dinoflagellates consist of Suessiales, Dino-Group-I to IV, Blastodiniales, Lophodiniales, Oxyrrhinales, Pyrocystales, Syndiniales, Thracosphaerales, Torodinales, Tovelliales, which each comprise only 1 species and thus they are grouped together. Bottom: species diversity of Ochrophyta as percentage of species per Class and Order. Rest Ochrophyta consist of Achnanthales, Anaulales, Corethrales, Cymatosirales, Cymbellales, Ethmodiscales, Fragilariales, Melosirales, Paraliales, Surirellales, Thalassionematales, Eustigmatales, Sarcinochrysidales and Mischococcales each of these groups comprise only 1 species. NA groups contain species which did not have a taxonomic match up to the respective taxonomic level in the figures, so the class or order level is unknown/uncertain.

Fig. 30 explores community composition at class and order level for dinoflagellates (Dinoflagellata + Myzozoa) and Ochrophyta, since dinoflagellates and diatoms are dominant groups in the microplankton community of the BPNS (Nohe et al., 2020). Dinoflagellates mainly consist of the class Dinophyceae, followed by Syndiniales, unknown species (NA) with unknown or uncertain class-level matches, Conoidasida, Perkinsea and Noctilucophyceae. At the order level, most species matches occur under orders Gymnodiniales and Peridiniales, followed by some species with unknown or uncertain order-level matches, Gonyaulacales, Dinophysiales, Noctilucales, Prorocentrales, Suessiales, Eugregarinorida, Coccidiniales, Perkinsida and Syndiniales. When looking at Ochrophyta in detail, the majority of species matches belong to class Bacillariophyceae, followed by Chrysophyceae, Dictyochophyceae, Raphidophyceae, Pelagophyceae, Bolidophyceae, Phaeophyceae, Eustigmatophyceae, Xanthophyceae and Marine OCHrophyte (MOCH) groups I to IV. Looking even more into detail at order level for Ochrophyta, most species belong to Chaetocerotales, Thalassiosirales and Rhizosoleniales, followed by species with unknown or uncertain order-level matches (NA), Bacillariales, Triceratiales, Chromulinales, Coscinodiscales, Hemiaulales, Naviculales, Pedinellales, Leptocylindrales, Lithodesmiales, Parmales, Florenciellales, Chatonellales, Biddulphiales, Rhaphoneidales, Pelagomodales.

Instead of looking at diversity, we now look at relative abundances (Table 4). Supergroup Alveolata has the highest relative abundance (56%), followed by Stramenopila (16.5%), Hacrobia (16%), Archaeplastida (7%), Rhizaria (3%), Opisthokonta (0.5%), Apusozoa (0.06%), Amoebozoa (0.04%) and Excavata (0.0007%) (Fig. 31). Dinoflagellates (Dinoflagellata+Myzozoa) have a relative abundance of 48%, diatoms (Bacillariophyta) have a relative abundance of 14% and both dominate their respective supergroups in relative abundance.
The top 10 species with highest relative abundances over all samples are Unknown Dino-group II, *Gyrodinium* sp., *Plagioselmis prolonga,* Unknown Dino-group I, *Gyrodinium fusiforme, Gyrodinium dominans, Gyrodinium spirale,* Unknown Strombidiida B, *Teleaulax acuta* and *Heterocapsa pygmae*.

Table 4: Relative abundances (RA) of supergroups and divisions found in amplicon sequencing species based inventory.

Supergroup	Division	RA (%)	Supergroup	Division	RA (%)
Alveolata	Dinoflagellata	18,24975	Opisthokonta	Ascomycota	1,29E-03
	Apicomplexa	0,06132		Choanoflagellida	3,10E-01
	Ciliophora	7,474438		Choanozoa	2,78E-02
	Myzozoa	30,22857		Chytridiomycota	1,93E-03
	Perkinsea	0,015431		Fungi	9,63E-02
	Alveolata total	**56,02951**		Mesomycetozoa	6,21E-02
Amoebozoa	Amoebozoa	0,035166		Opisthokonta total	**4,99E-01**
	Breviatea	0,000858	Rhizaria	Cercozoa	3,36E+00
	Conosa	0,00176		Euglenozoa	1,56E-03
	Lobosa	0,00515		Ochrophyta	4,45E-02
	Amoebozoa total	**0,042934**		Radiolaria	3,26E-02
Apusozoa	Apusomonadidae	0,049802		Rhizaria total	**3,44**
	Hilomonadea	0,014322	Stramenopila	Bigyra	0,03083
	Mantamonadidae	7,12E-05		Ochrophyta	13,6262
	Apusozoa total	**0,064196**		Oomycota	0,00612
Archaeplastida	Chlorophyta	7,07899		Opalozoa	1,268
	Rhodophyta	0,071435		Pseudofunghi	0,712992
	Streptophyta	0,00276		Sagenista	0,8537
	Archaeplastida total	**7,153185**		Stramenopila total	**16,49784**
Hacrobia	Centroheliozoa	0,084214	Excavata	Percolozoa	0,000305
	Cryptophyta	13,20452		Euglenozoa	0,000398

	Haptophyta	0,213765		Excavata total	0,000703
	Katablepharidophyta	0,314389			
	Picozoa	2,176879			
	Hacrobia total	15,99377			

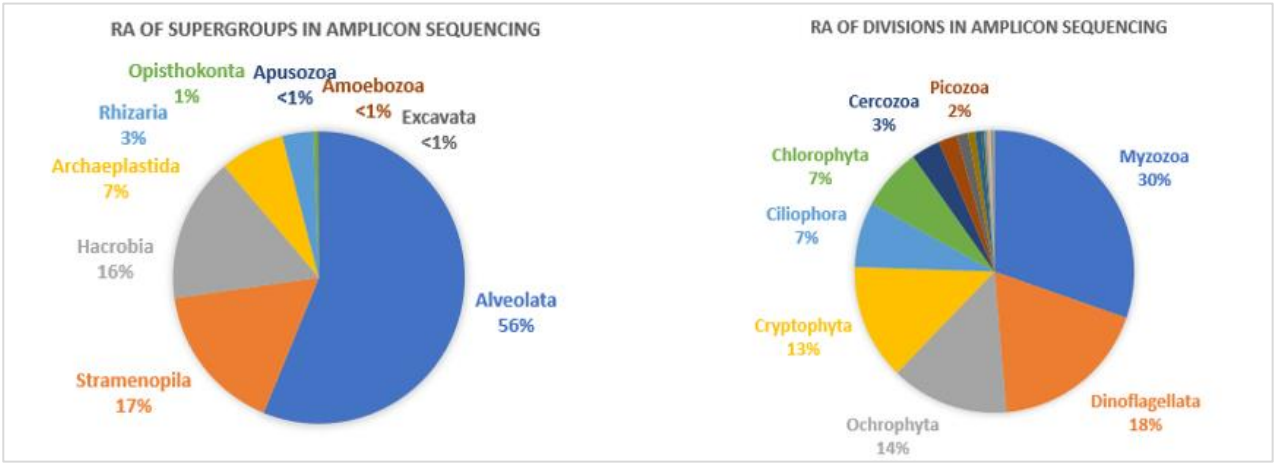

Figure 31: Top: Relative abundances of supergroups in amplicon sequencing inventory. Bottom: Relative abundance of most abundant divisions in amplicon sequencing.

2. Structure and temporal dynamics of planktonic diatom communities in the BPNS in the period August-December 2019

All species found during the LM counts of the oxidized materials, their valve numbers per liter and their mean relative abundance, are shown in Table 5. They are displayed in decreasing order of relative abundance. During the microscopic counts of the oxidized materials, 74 species were identified. *Paralia* spp. species were most abundant, followed by *Delphineis surirella*, *Cymatosira belgica*, *Thalassiosira* spp., *Chaetoceros* spp. (although these are often lost during oxidation) *Rhaphoneis amphiceros*, *Pseudo-nitzschia* spp., *Ditylum brightwelli*, *Bacillaria paxillifer* and *Hobaniella longicruris* (Fig. 32). All other species take up less than 2% of the counts.

Table 5: Species identified for microscopic count based on oxidized material and their mean relative abundances (RA) valve numbers per L over all samples from August 2019 to December 2020. Species displayed in decreasing total relative abundance.

Species	counts/L	RA (%)	Species	counts/L	RA (%)
Paralia spp.	633,057	22,90105	*Coscinodiscus centralis*	5,986081	0,216549
Delphineis surirella	476,6652	17,24353	*Nitzschia thermalis*	5,466667	0,197759
Cymatosira belgica	224,2267	8,111477	*Thalassiosira tenera*	5,366667	0,194141
Thalassiosira spp.	164,3589	5,945739	*Thalassiosira lundiana*	5,166667	0,186906
Rhaphoneis amphiceros	154,294	5,581638	*Actinoptychus splendens*	3,916153	0,141668
Chaetoceros spp.	145,0677	5,247873	*Skeletonema* spp.	3,733333	0,135055
Pseudo-nitzschia spp.	116,4849	4,213881	*Pleurosigma* spp.	3,67442	0,132923
Ditylum brightwellii	99,96879	3,616405	*Rhizosolenia setigera*	3,186328	0,115267
Bacillaria paxillifer	78,99615	2,857713	*Biddulphia alternans*	3,114286	0,11266
Hobaniella longicruris	64,50159	2,333367	*Actinocyclus octonarius*	3,061904	0,110765

Cymatosira lorenziana	61,35837	2,21966	*Diploneis bombus*	3,05349	0,110461
Centric diatom	50,85128	1,839562	*Cerataulina pelagica*	2,282608	0,082574
Pennate diatom	50,65778	1,832562	*Epithemia* spp.	1,82657	0,066077
Eucampia zodicus	34,66145	1,25389	*Navicula palpebralis*	1,663614	0,060182
Bellerochea horologicales	33,36447	1,206971	*Eunotogramma* spp.	1,653419	0,059813
Bacteriastrum hyalinum	29,50171	1,067234	*Stellarima stellaris*	1,540476	0,055727
Actinoptychus senarius	28,45372	1,029323	*Coscinodiscus* spp.	1,511111	0,054665
Eupyxidicula turris	26,2906	0,951071	*Coscinodiscus radiatus*	1,361904	0,049267
Thalassiosira punctigera	24,45189	0,884555	*Coscinodiscus connicus*	1,066667	0,038587
Occtactis speculum	23,92424	0,865468	*Trachyneis aspera*	1,009523	0,03652
Psammodictyon panduliforme	21,08354	0,762704	*Azpeitia* spp.	0,912271	0,033002
Zygoceros rhombus	17,62033	0,637421	*Basteriastrum spp.*	0,780953	0,028251
Ralfsiella smithii	13,59866	0,491936	*Rhizosolenia imbricata*	0,772947	0,027962
Thalassiosira hendeyi	12,96667	0,469074	*Actinocyclus* spp.	0,705128	0,025508
Actinocyclus curvatulus	12,28472	0,444404	*Gyrodinium* spp.	0,53333	0,019293
Trieres sinensis	11,73213	0,424414	*Cylindrotheca clostridium*	0,52657	0,019049
Thalassionema spp.	11,30342	0,408905	*Lithodesmium* spp.	0,4	0,01447
Thalassionema nitzschioides	11,24445	0,406772	*Odontella mobiliensis*	0,38779	0,014028
Thalassiosira anguste-lineata	11,20635	0,405394	*Thalassiosira decipiens*	0,333333	0,012058
Navicula spp.	10,58675	0,382979	*Triceratium favus*	0,325189	0,011764
Diploneis didyma	9,091111	0,328874	*Brockmanniella brockmannii*	0,193237	0,00699
Thalassiosira rotula	7,987254	0,288942	*Odontella* spp.	0,13333	0,004823
Ralfsiella minima	7,234859	0,261723	*Cymbella solea*	0,114286	0,004134
Thalassiosira eccentrica	6,504152	0,23529	*Eupodiscus sculptus*	0,068376	0,002474
Rhizosolenia spp.	6,255557	0,226297	*Roperia tessellata*	0,068376	0,002474
Plagiogrammopsis vanheurckii	6,221002	0,225047			

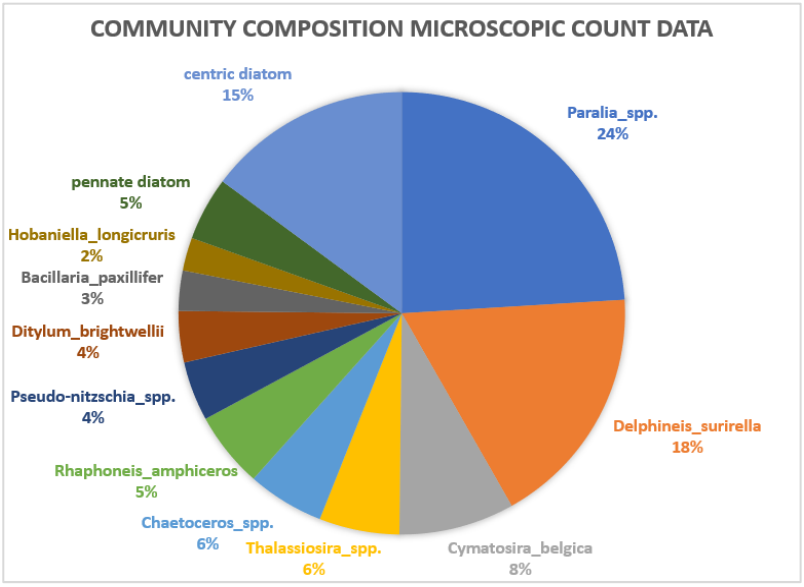

Figure 32: Top 10 most abundant diatom taxa within the microscopic counts of the oxidized materials. Remaining species are grouped under centric or pennate diatoms.

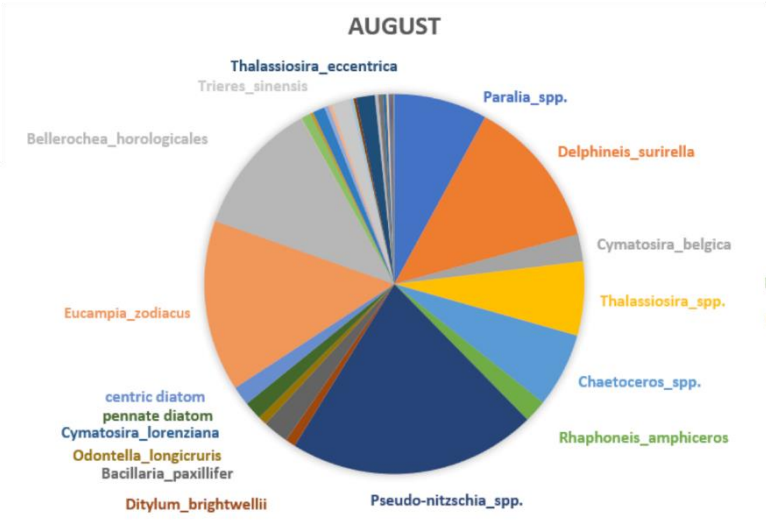
AUGUST
Thalassiosira_eccentrica
Trieres_sinensis
Paralia_spp.
Bellerochea_horologicales
Delphineis_surirella
Cymatosira_belgica
Thalassiosira_spp.
Eucampia_zodiacus
Chaetoceros_spp.
centric diatom
pennate diatom
Cymatosira_lorenziana
Rhaphoneis_amphiceros
Odontella_longicruris
Bacillaria_paxillifer
Ditylum_brightwellii
Pseudo-nitzschia_spp.

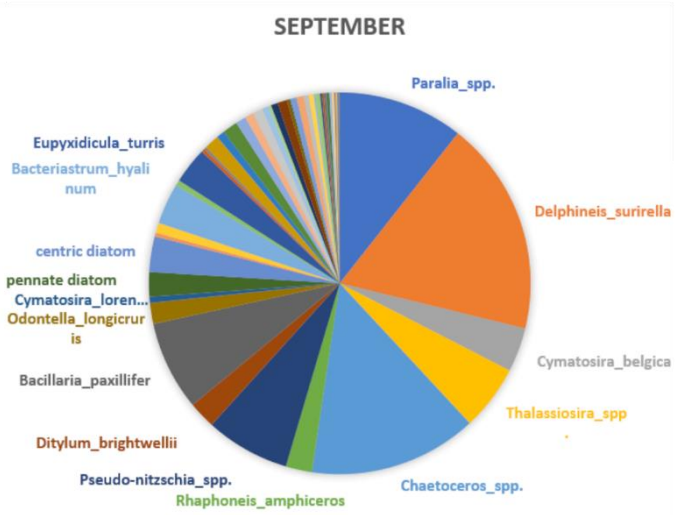
SEPTEMBER
Paralia_spp.
Eupyxidicula_turris
Bacteriastrum_hyali
num
Delphineis_surirella
centric diatom
pennate diatom
Cymatosira_loren...
Odontella_longicrur
is
Cymatosira_belgica
Bacillaria_paxillifer
Thalassiosira_spp
Ditylum_brightwellii
Pseudo-nitzschia_spp.
Chaetoceros_spp.
Rhaphoneis_amphiceros

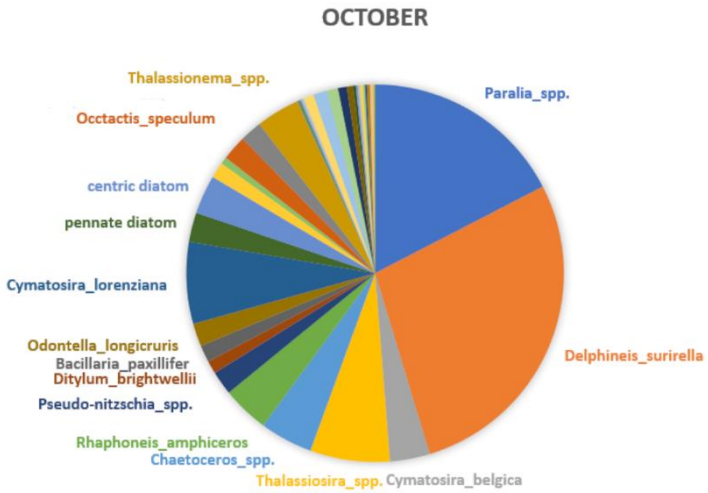
OCTOBER
Thalassionema_spp.
Paralia_spp.
Occtactis_speculum
centric diatom
pennate diatom
Cymatosira_lorenziana
Delphineis_surirella
Odontella_longicruris
Bacillaria_paxillifer
Ditylum_brightwellii
Pseudo-nitzschia_spp.
Rhaphoneis_amphiceros
Chaetoceros_spp.
Thalassiosira_spp.
Cymatosira_belgica

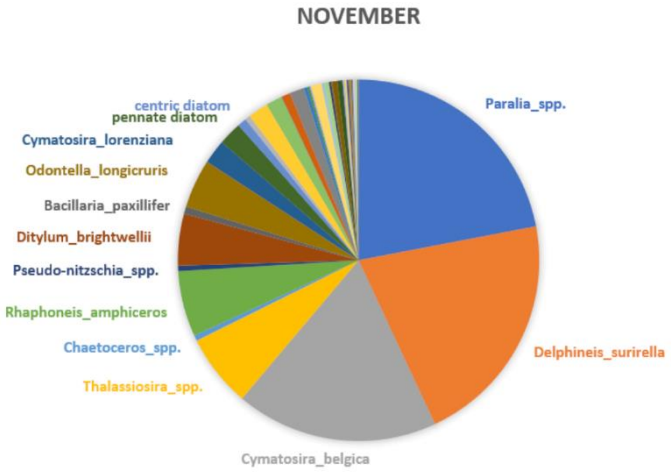
NOVEMBER
centric diatom
pennate diatom
Paralia_spp.
Cymatosira_lorenziana
Odontella_longicruris
Bacillaria_paxillifer
Ditylum_brightwellii
Pseudo-nitzschia_spp.
Rhaphoneis_amphiceros
Chaetoceros_spp.
Delphineis_surirella
Thalassiosira_spp.
Cymatosira_belgica

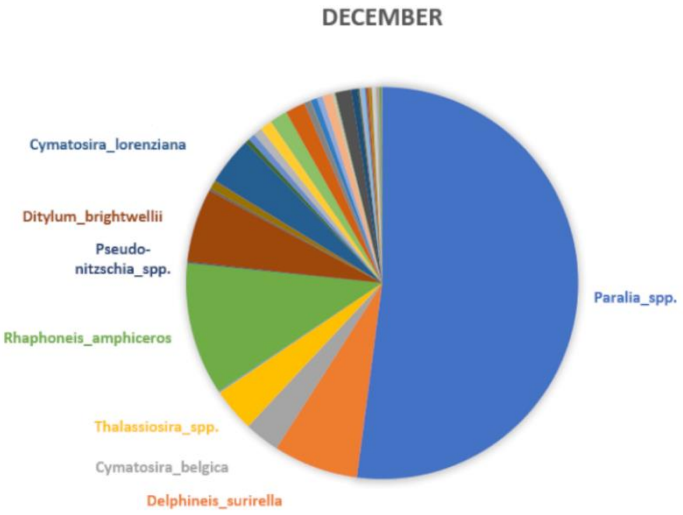
DECEMBER
Cymatosira_lorenziana
Ditylum_brightwellii
Pseudo-
nitzschia_spp.
Paralia_spp.
Rhaphoneis_amphiceros
Thalassiosira_spp.
Cymatosira_belgica
Delphineis_surirella

Figure 33: Community composition and relative species abundances per month, only most abundant species or species whose abundances change over months are displayed by name. Species whose abundances don't clearly fluctuate over the months have been discarded from the figures for visual purposes.

Looking at the seasonal distribution of species and their relative abundances in microscopic count data, *Eucampia zodicacus* and *Bellerochea horologicales* appear to be more abundant in August (Fig. 33). *Pseudo-nitzschia* spp. appear more dominant in August, after which it gradually decreases through autumn and winter. *Paralia* spp. make up more than half of all the diatoms found in December, and its relative abundance seems to increase from August to December. *Cymatosira belgica* and *Ditylum brightwelii* seem most abundant in November. *Chaetoceros* spp. show a peak abundance in September, with lower abundances in August and October and very low abundances in November and December. However, because *Chaetoceros* easily disappear during oxidation, this trend is probably less trustworthy. Relative abundances of species distributions per stations show no obvious patterns between onshore and offshore stations or between stations in the NE and SW part of the BPNS and thus they are displayed in Appendix 5.

Next, a Principle Component Analysis (PCA) was performed on the microscopic count data based on oxidized materials, the output of the which is shown in Table 6. The first two axes explain about 41% of the variation in the ordination. In Fig. 34 the top two ordination diagrams are colored according to months and stations, while the environmental variables PAR, temperature, salinity and fluorescence are plotted as supplementary variables. Nutrient measurements are not incorporated in the ordinations but instead are displayed in Fig. 36, because data are incomplete. The bottom diagram shows the 25 species which are best fitted by the first two PCA axes.

Table 6: Results PCA on log-transformed relative abundance data for North Sea diatoms and silicoflagellates.

Analysis 'Unconstrained-suppl-vars'				
Method: PCA with supplementary variables				
Summary Table:				
Statistic	Axis 1	Axis 2	Axis 3	Axis 4
Eigenvalues	0.2628	0.1496	0.1189	0.0861
Explained variation (cumulative)	26.28	41.25	53.14	61.75
Pseudo-canonical correlation (suppl.)	0.9398	0.6929	0.7563	0.653

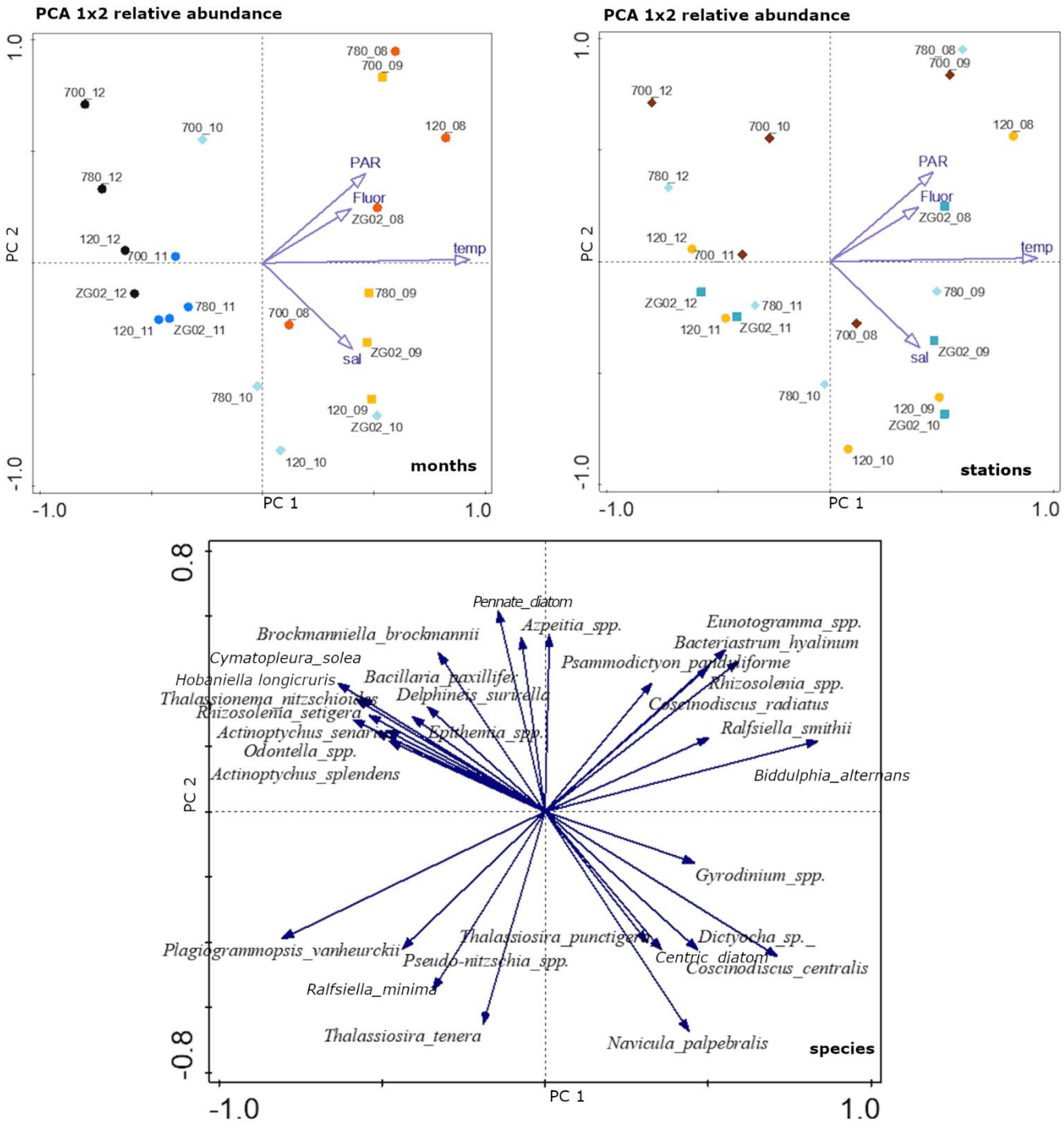

Figure 34: PCA on log (x+1) transformed microscopic count data. Top: left graph indicates months and right graphs indicates stations as indicated in the bottom right corner. Sample codes depict station_month. Bottom graphs shows 25 best fitted species structuring the ordinations. Environmental data temperature, salinity, PAR and fluorescence are plotted on the top two graphs.

The PCA of the diatom count data (Fig. 34, top) reveals a clear seasonal pattern, with the summer months August and September clustered together on the positive side of the first axis and November and December clustered together on the negative side of the first axis. The samples from October are mainly separated from the other months along the second axis. The eastern stations 120 and ZG02 are mainly situated on the negative size of the second axis, while stations 700 and 780 are mainly found mainly on the positive size of the second axis, although this spatial pattern is less straightforward.

Temperature is positively correlated with the first axis. PAR and fluorescence are positively correlated with the positive side of the first axis and the positive side of the second axis. Salinity is positively correlated to the positive side of the first axis and the negative side of the second axis. September and August samples seem to be positively correlated to temperature, PAR and fluorescence and, to a lesser extent, salinity. December and November samples are negatively correlated to the plotted environmental variables.

The 25 taxa whose variation is best captured along the first two axes, are shown at the bottom of Fig. 34. Centric and pennate diatoms comprise diatoms that could not be identified to genus level and were thus generally assigned to the pennate or centric group (based on their morphology). Note however that while they are displayed in the PCA, these groups are treated as a distinct taxon, they include different species which may not all behave in the same way in the data set. *Thalassiosira tenera, Ralfsiella minima, Pseudo-nitzschia* spp*., Navicula palpebralis, Coscinodiscus centralis* and *Thalassiosira punctigera* appear to be more abundant in the October samples. *Brockmaniella brockmanii, Cymatopleura solea, Hobaniella longicruris, Thalassionema nitzschioides, Rhizosolenia setigera, Actinoptychus senarius, Actinoptychus splendens, Delphineis surirella, Bacillaria paxillifer, Epithemia* spp. and *Odontella* spp. are relatively more important in November and December samples. *Eunotogramma* spp*., Bacteriastrum hyalinum, Psammodictyon panduliforme, Rhizosolenia* spp*., Coscinodiscus centralis, Ralfsiella smithii, Gyrodinium* and *Dichtyocha* spp. are more important in August and September.

3. Microplankton dynamics in the BPNS based on amplicon sequencing analyses

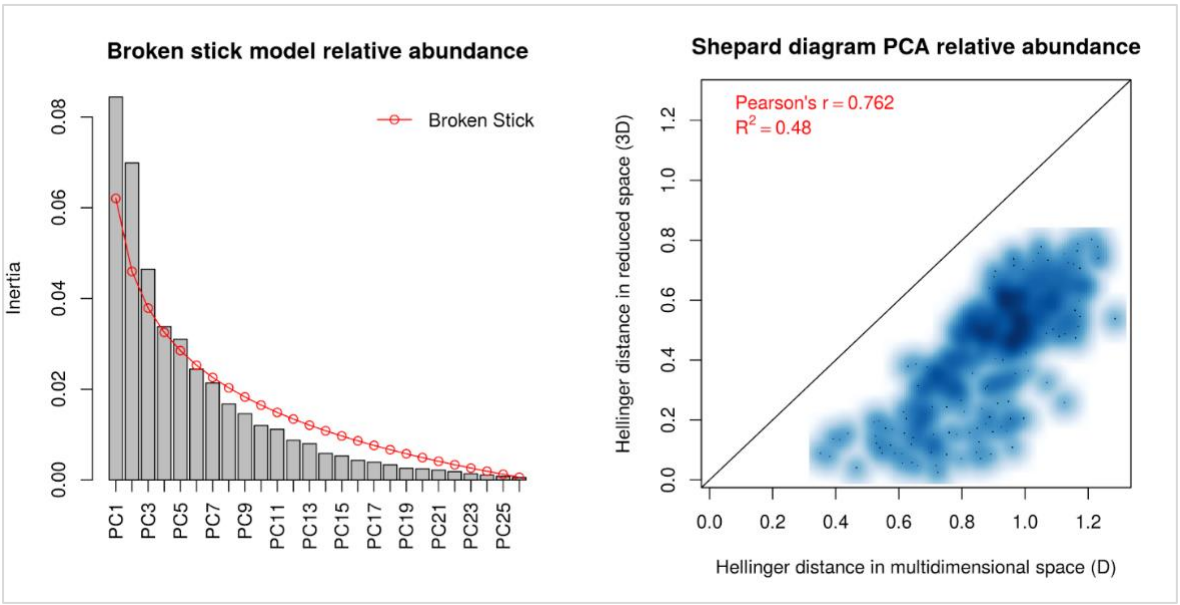

Figure 35:Broken stick diagrams and Shepard diagrams for relative abundance.

Different ordination methods and transformations were tried on species count tables in order to choose the appropriate ordination technique. The ordination that showed most straightforward patterns was the PCA run on Hellinger transformed relative abundance for the first two axes. According to the Broken stick diagrams shown in Fig. 33, the first 2 axes are most important and explain the majority of the clustering. The The PCA graphs based on relative abundances are shown below in Fig. 35. The additional graphs, PCA on relative abundance for the 1st and 3rd axis, NMDS on relative abundance and PCA and NMDS on presence/absence of species are displayed in Appendix 6 (Fig. 41). In Fig. 35 samples are coloured according to station, month and fraction to be able to distinguish between patterns. The 30 most fitted species are plotted to visualise how they structure the community. In order to display the full community, which is 104 species after filtering on relative abundance of 1%, the rest of the species (31-104) are displayed in the Appendix 6 (Fig. 42). Names and arrows of all species plotted are coloured according to the bigger taxonomic group they belong to.

For the environmental variables, Spearman Rank correlation coefficients were calculated with the first two axes based on the coordinates of the samples in the ordination diagram and the measured value for the environmental values temperature, PAR, salinity and fluorescence for each sample. Results are displayed in Table 7 and none of the environmental variables seem to be significantly correlated to the first two ordination axes. Nutrient measurements are displayed separately in Fig. 37, because data is incomplete.

*Table 7: Spearman rank correlation (rho) and calculated p-values for environmental variables and the first two axes of the ordination. Significant p-values are indicated by an *.*

		Temperature	PAR	Fluorescence	Salinity
PC1	ρ_S	0.08835229	0.002759069	0.01926019	0.1062141
	P-value	0.679375	0.98625	0.920000	0.590625
PC2	ρ_S	0.06817495	-0.068363597	-0.30052007	0.2923182
	P-value	0.716875	0.74250	0.125625	0.140000

The patterns in community structure in the ordination (Fig. 36) are not readily interpretable. There is no clear separation between the two size fractions (also confirmed by Appendix 6, Fig. 43). Samples from the onshore stations (700 and 120) are located mainly on the negative side of the second axis (with the exception of one sample from station 120), but they are overall mixed with samples from the offshore stations. ZG02 seems to be mainly located on the negative side of the first axis, with two exceptions on the positive side of the first axis. Station 780 displays no clear pattern. September, October and November are located mainly on the positive side of the first axis, with the exception of a single September sample. December samples are mainly located on the negative side of the first and the second axis, with the exception of one sample, and they are predominantly located towards the 3rd quadrant.

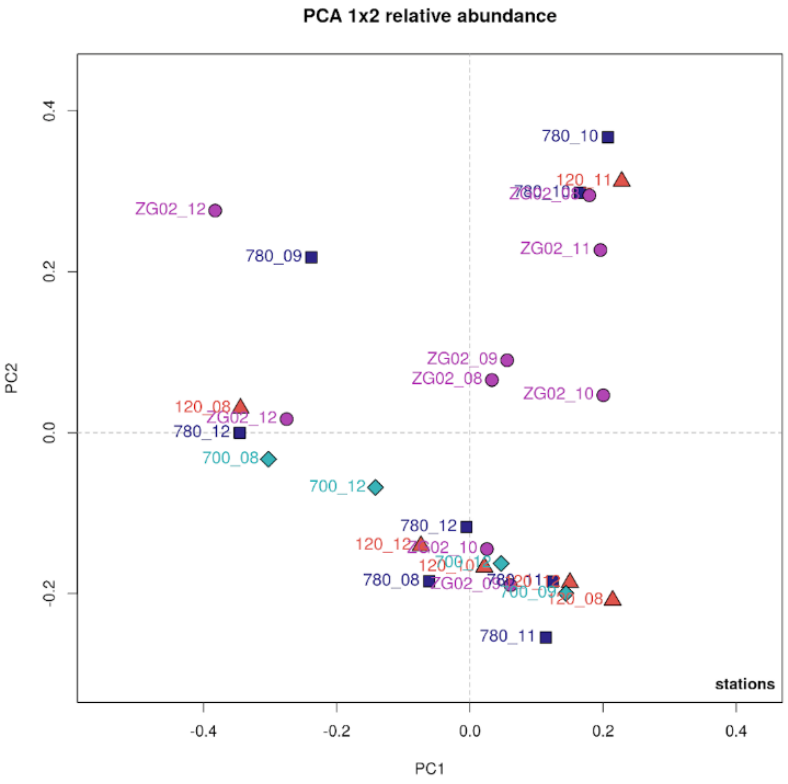
PCA 1x2 relative abundance
780_10
120_11
ZG02_12
780_09
ZG02_11
ZG02_09
ZG02_08
ZG02_10
120_08
780_12
700_08
700_12
780_08
780_11
stations
PC1
PC2

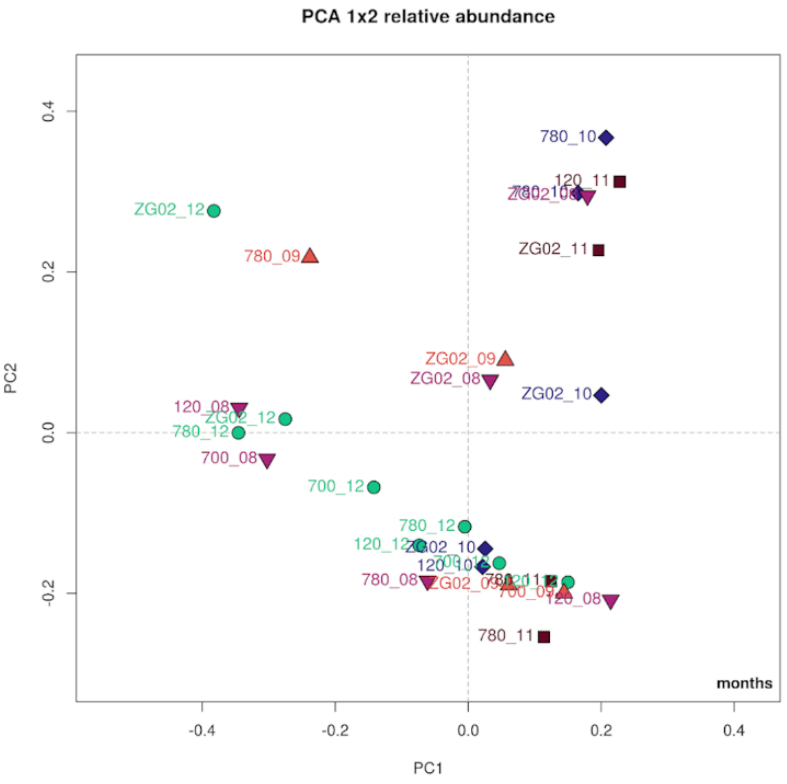
PCA 1x2 relative abundance
780_10
120_11
ZG02_12
780_09
ZG02_11
ZG02_09
ZG02_08
ZG02_10
120_08
780_12
700_08
700_12
780_08
780_11
months
PC1
PC2

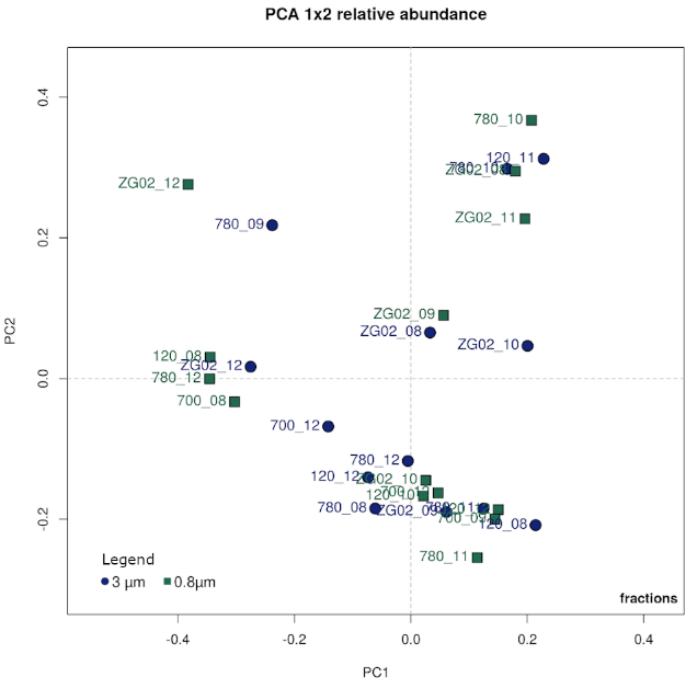
PCA 1x2 relative abundance
780_10
120_11
ZG02_12
780_09
ZG02_11
ZG02_09
ZG02_08
ZG02_10
120_08
780_12
700_08
700_12
780_08
780_11
Legend
3 µm
0.8µm
fractions
PC1
PC2

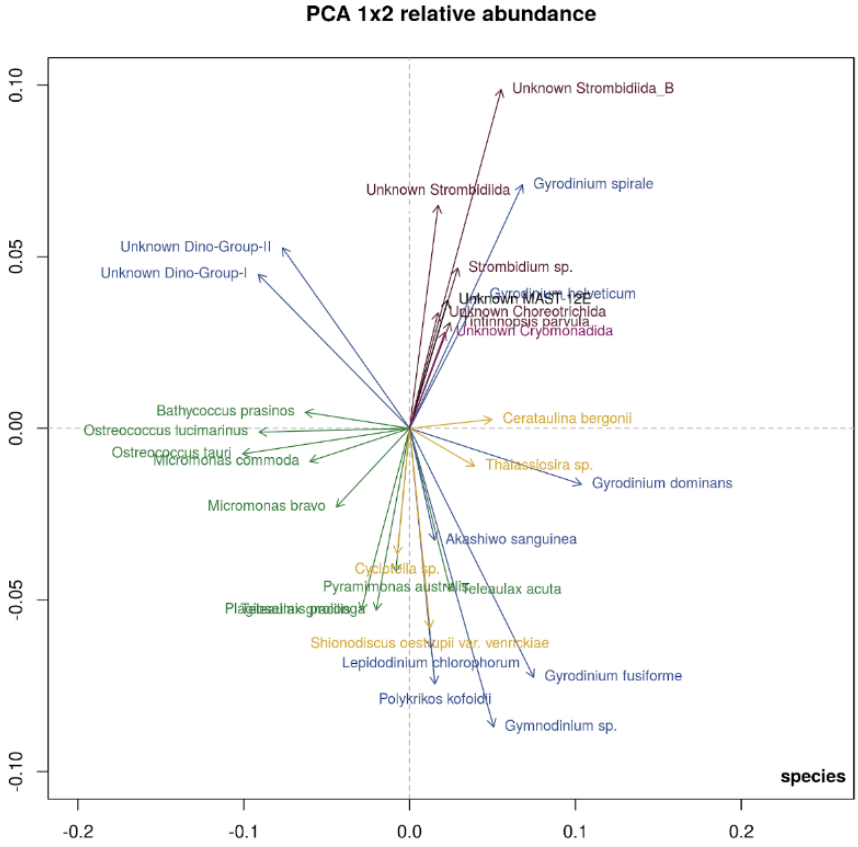
PCA 1x2 relative abundance
Unknown Strombidilida_B
Unknown Strombidilida
Gyrodinium spirale
Unknown Dino-Group-II
Unknown Dino-Group-I
Strombidium sp.
Gyrodinium helveticum
Unknown MAST-12E
Unknown Choreotrichida
Tintinnopsis parvula
Unknown Cryomonadida
Bathycoccus prasinos
Ostreococcus lucimarinus
Ostreococcus tauri
Micromonas commoda
Cerataulina bergonii
Thalassiosira sp.
Gyrodinium dominans
Micromonas bravo
Akashiwo sanguinea
Cyclotella sp.
Pyramimonas australis
Teleaulax acuta
Shionodiscus oestrupii var. venrickiae
Lepidodinium chlorophorum
Gyrodinium fusiforme
Polykrikos kofoidii
Gymnodinium sp.
species

Figure 36: PCA of Hellinger transformed relative abundance species derived from the amplicon sequencing, symbols and colours for stations, months and size fractions. The 30 best fitted species are plotted in the bottom right graph, species labels are colour-coded on the basis of higher taxonomic affiliation. Ochrophyta are displayed in yellow, Chlorophyta are displayed in green, Dinoflagellata are displayed in pastel blue/purple, Cercozoa are displayed in fuchsia, Cilliophora are displayed in dark red, Picozoa are displayed in bright blue, leftover groups like Bigyra, Choanoflagellida, Haptophyta, Katablepharidophyta, Pseudo-fungi, Rhodophyta, Haptophyta and Sagenista are displayed in black since there were only 1 or 2 species under these divisions.

If we look at the species diagram, there appears to be a clear clustering of species per higher taxonomic level. Most of the Chlorophyta increase in the direction of the 3rd quadrant. Diatoms and many dinoflagellates mainly increase along the second axis (negative side), although dinoflagellates also appear in the 1st and 2nd quadrant. Cryptophyceae and Ciliophora are located in the 1st quadrant. For the graphs of the other species (Appendix 6), this general pattern (i.e. similar distribution of species belonging to the same higher order taxonomic level) remains more or less similar. It seems like the species plotted are grouped based on higher taxonomic level, with some separations based on size as well i.e. small green algae cluster together, while larger-sized diatoms and dinoflagellates in less extent cluster together separately from the small pico-sized plankton. When we look at the consistency of Chlorophyta in the amplicon sequencing inventory, the majority consists of Mamiellophyceae (83% RA within Chlorophyta), followed by Pyramimonadophyceae (13%) and minor concentrations of Ulvophyceae (1.5%), Florideophyceae (1.1%), Nephrosemidophyceae (0.7%) Synurophyceae (0.01%), Streptophyta_X (0.04%), Chlorophyceae (0.09%) Chlorodendrophyceae (0.1%), Prasinophyceae (0.2%) and Palmophyllophyceae (0.2%). The majority of Mamiellophyceae consists of *Ostreococcus* (44% RA within Chlorophyta) and *Micromonas* (23% RA withing Chlorophyta) species.

To test whether the variation patterns in community structure were significantly different between stations, months or size fractions, PERMANOVA were run on the Hellinger transformed relative abundance species data. Table 8 indicates that PERMANOVA did not reveal any significant differences in community structure between stations, months, size fractions or their interaction terms.

*Table 8: Results of PERMANOVA, significant p-vales are indicated by an *. Df= degrees of freedom, SumOfSqs= sum of squares, R2= sum of squares divided by total (=amount of variation explained by this factor), F=F-value , P= p-value (Pr(>F)).*

Terms added sequentially (first to last)					
adonis2(formula = physeq_eucl ~ station + month + fraction + station:month + station:fraction + month:fraction, data = sampledf)					
	Df	**SumOfSqs**	**R2**	**F**	**P**
station	3	2.2130	0.12341	1.0097	0.489
month	4	2.4725	0.13788	0.8461	0.810
fraction	1	0.5810	0.03240	0.7953	0.736
station: month	8	5.9968	0.33442	1.0261	0.463
station: fraction	3	1.6988	0.09473	0.7751	0.865
month: fraction	4	2.7783	0.15494	0.9508	0.589
Residual	3	2.1917	0.12222		
Total	26	17.9321	1.00000		

4. Supporting environmental and pigment data

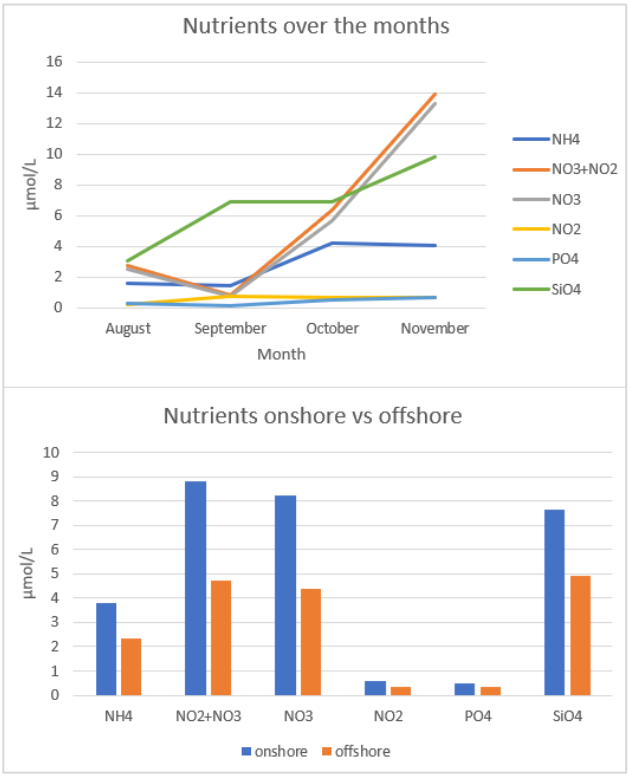

Figure 37: Nutrient measurements. Top: Mean measurements over all stations per month. Bottom: mean measurements over all months for onshore (120 and 700) vs offshore (ZG02 and 780) stations. NH_4= Ammonium, NO_3=Nitrate, NO_2=Nitrite, PO_4=Phosphate, SiO_4= Silicate. Measurements missing for December and station 700 September.

The top of Fig. 37 shows the concentrations of the main nutrients over the sampling period (although no measurements are available for December). All nutrients seem to be low in August and many reach their lowest values in September, with the exception of SiO_4 which increases again after August. Concentrations of all nutrients seem to be highest in November. In the bottom graph, nutrient concentrations are depicted over onshore and offshore stations and concentrations are clearly higher at onshore stations, which is to be expected.

The course of pigment concentrations over the months is displayed in Fig. 38. Looking at microscopic count data October samples are situated somewhat odd in the ordinations space (Fig. 34). While August and September samples are clustered on the positive side of the first axis and November and December are clustered on the negative side of the first axis, October samples are located on the negative side of the second axis. During microscopic observation of live and Lugol's iodine fixed samples, October samples seemed to be sparse in terms of number of cells compared to earlier samples and even later samples from November and December seemed to noticeably have more cells. This is more or less confirmed by the concentration of some the measured pigments from the research period, which have low concentrations in October (Fig. 38) compared to other months. Chlorophyll a, which is a proxy for the biomass of the full phytoplankton community, shows a slight dip in concentration in October. This dip is more visible in chlorophyll c2 (diatoms, dino-group II, Prymnesiophytes) and chlorophyll c3 (*Phaeocystis*, Dictyochophytes, dinoflagellates) concentrations as well as in alloxanthin (Cryptophytes), peridine (dino-group I), fucoxanthin (diatoms mainly, but also *Phaeocystis*, dinoflagellates, Prymnesiophytes, Pinguiophytes) and diadino- dinoxanthin (both dinoflagellates, diatoms, Dictyochophytes, Prymnesiophhtes, Pavlovophytes). Why exactly this is, is uncertain. Nutrients in October seem to be on the rise and not at the lowest point in during the sampling period (Fig. 36). Another unexpected results for amplicon sequencing is the clustering of species by higher taxonomic level (Fig. 36), especially the clustering of small green algae in the 3rd quadrant. This lightly coincides with December (ZG02_12, 780_12, 700_12, 780_12, 120_12) and August samples (120_8, 700_8, 780_8) and 700 and 780 samples (both mainly but not exclusively). When we want to see green algae in pigments we need to look at chlorophyll c2 concentrations. These are all below the detection limit (shown as 0 µg/L) in December and highest in August (0.18µg/L on average), except for station 700. The average concentration for station 700 is 0.05µg/L, for 780 is 0.10µg/L, for 120 is 0.11 µg/L and for ZG02 is 0.08 µg/L. According to chlorophyll b, green algae (and other taxa) have highest monthly abundant in August and highest abundance at station 780 and 120. This lightly resembles our results for August samples and 780 samples, but not for December samples or 700 samples in amplicon sequencing regarding small green algae.

Figure 38: Pigment measurements for the research period for stations 120, ZG02, 700 and 780 are shown over the course of the research period for each station individually. Chlorophyll a (overall biomass of photosynthetic community), chlorophyll b (Chlorophyta, Cyanobacteria, Prasinophytes, dino-group V and Euglenophyta to a lesser extent), fucoxanthin (diatoms mainly, also other Ochrophyta, Paeocyctis, dinoflagellates, Pinguiophytes, Prymnesiophytes), chlorophyll c3 (Phaeocystis, diatoms, dinoflagellates group II, Prymnesiophytes), chlorophyll c2 (diatoms, Dictyochophytes,dinoflagellates, Pavlovophytes, Prymnesiophytes), alloxanthin (Cryptophyta), peridine (dino-group 1) and diato- and diadinoxanthin (dinoflagellates, Dictyophytes, Prymnesiophytes, Pavlovophytes and diatoms) are displayed.

DISCUSSION

1. Phyto- and microplankton diversity during summer-autumn 2019 in the BPNS

While microscopy focussed on revealing phytoplankton (and mainly diatom) diversity, amplicon sequencing investigated the full eukaryotic microplankton community, including mixo- and heterotrophic taxa.

Using LM and SEM, 98 taxa were identified to species level in the microscopic inventory, the remaining 10 taxa were identified to genus level. Diatoms comprised the biggest group (96 species), followed by dinoflagellates (6 species), silicoflagellates (3 species), tintinnid cilliates (2 species) and Chlorophyta (1 species). Out of the 101 species in the microscopic inventory, 65% were also present in the checklist for Helgoland (Kraberg et al., 2019), 76 % of the species were present in the Belgian Phytoplankton Database (Nohe et al., 2018). According to diatom counts on oxidized materials, *Paralia* spp. is most abundant, followed by *Delphineis surirella*, *Cymatosira belgica, Thalassiosira* spp*., Chaetoceros* spp*., Rhaphoneis amphiceros, Pseudo-nitzschia* spp*., Ditylum brightwellii, Bacillaria paxillifer* and *Hobaniella longicruris. Chaetoceros* and *Thalassiosira* are also the most diverse species rich genera in the microscopic inventory, followed by *Coscinodiscus*, *Actinocyclus*, *Guinardia*, *Odontella* and *Rhizosolenia*.

In amplicon sequencing, the species with the highest relative abundances are Unknown Dino-group-II, *Gymnodinium* spp*., Plagioselmis prolonga,* Unknown Dino-Group I, *Gyrodinium fusiforme, Gyrodinium dominans, Gyrodinium spirale,* Unknown Strombidiida*, Teleaulax acuta* and *Heterocapsa pygmaea*. At first there aren't any similar results between the 10 most abundant species in amplicon sequencing and the most abundant species in the microscopic counts. This is because the microscopic counts were performed on oxidized slides, selecting for silicified species. Looking at Bacillariophyceae (diatoms) in the amplicon sequencing data set, *Ceratulina bergonii, Thalassiosira* spp*., Shionodiscus oestrupii var. vernickae, Cyclotella* spp*., Rhizosolenia delicatula, Chaetoceros* spp*., Chaetoceros tenuissimus,* Unknown Bacillariophyceae*, Chaetoceros danicus and Bellerochea polymorpha* are the 10 most abundant species in decreasing order. Now we see some more similarities: *Thalassiosira* spp. and *Chaetoceros* spp*.* are amongst the 10 most abundant taxa in both amplicon sequencing for Bacillariophyceae and in diatom counts and they are also the most diverse genera in the microscopic inventory. *Shionodiscus oestrupii var. vernickae* and *Cyclotella* spp., while being abundant in amplicon sequencing data for Bacillariophyceae and present in the microscopic inventory, are not present in the microscopic count data on oxidized materials at all because they are too small to identify properly in light microscopy, certainly to distinguish between *Shionodiscus oestrupii* and smaller *Thalassiosira* species as *T. minima*. *Rhizosolenia delicatula* is not present in the microscopic inventory and is also not present in the microscopic count data on oxidized materials because *Rhizosolenia* tend to be hard to identify in LM because the griddle bands are often not visible and because their cells break during the oxidation process. *Chaetoceros tenuissimus* is also not present in the microscopic inventory or the microscopic counts on oxidized materials. This might have been overlooked on my part as it can be hard to distinguish *T. tenuissimus* from single *Chaetoceros* valves in LM. *Bellerochea polymorpha* is also not present in the microscopic inventory and microscopic counts on oxidized materials. A more correct name for this species is *Lithodesmioides polymorpha*, but this species was never observed in microscopy. Perhaps, in order to visualized this species additional SEM protocols are necessary as described by Yahia-Kéfi et al. (2005) as the species seems to be easily overlooked. *Cerataulina bergonii,* the most abundant diatom species according to amplicon sequencing of Bacillariophyceae, is a synonym of *Cerataulina pelagica*. The latter is found in the microscopic inventory and also in the microscopic count data but is far less abundant, perhaps because the

cells collapsed during the oxidation process (most valves seen during the microscopic counts of oxidized materials were deformed). This species seemed to occur in long chains mainly in summer samples if I recall from looking at Lugol's iodine fixed samples. *Paralia* spp., the most abundant species according to microscopic count data on oxidized slides, is only ranked as the 73rd most abundant Bacillariophyceae species according to amplicon sequencing. This could be because *Paralia* spp. were counted per valve, since chains broke up during the oxidation process. Generally diatoms have low abundances in amplicon sequencing because they are overshadowed by abundance of species with high copy numbers.

Thalassiosira spp., *Chaetoceros* spp., *Pseudo-nitzschia* spp. and *Ditylum brightwellii* are amongst the most abundant species/genera in diatom counts on oxidized materials and they have been observed to have increased in abundance in the BPNS between 1970-2000 by Nohe et al. (2020) for the BPNS. *Thalassionema* spp., *Rhizosolenia* spp., *Plagiogrammopsis* spp., *Lithodesmium* spp. and *Brockmaniella* spp. have also been observed to have increased in last decades by Nohe et al. (2020), although they are observed less in the microscopic count data here. The dominance of *Paralia* spp. found in this thesis is not confirmed by the study of Thamarasi (2016) for the research period 2015-2016 in the BPNS, where the most abundant taxa counted for April 2015 - March 2016, were *Thalassiosira* spp., pennate diatoms species, *Leptocylindrus* spp. and *Guinardia* spp. The fact that *Paralia* spp. are very abundant in our study but not in Thamarasi (2016) is probably because Thamarasi (2016) performed counts using the Utermöhl method on qualitative samples (using the UNESCO manual), so they counted *Paralia* spp. likely as colonies while I counted them as individual valves. Töpke (2009) found other species to be most abundant in the BPNS for the period 2003-2008 compared to Thamarasi (2016), in decreasing order of abundance: *Pseudo-nitzschia pungens, Rhizosolenia setigera, Pseudo-nitzschia delicatissima, Asterionellopsis glacialis, Rhizosolenia hebeata, Thalassiosira* spp. *Chaetoceros* spp., *Paralia sulcata, Guinardia delicatula* and *Plagiogrammopsis vanheurckii.* Here, we do see *Paralia sulacata* which coincides with *Paralia* spp. in this study as we labelled the *P. sulcata* complex as *Paralia* spp. as the *Paralia* species are impossible to distinguish in LM. Further, *Thalassiosira* spp. and *Pseudo-nitzschia* spp. were abundant according to Töpke (2009) just like observed in this thesis. *Rhizosolenia hebeata* and *Pseudo-nitzschia delicatissima* were never observed in microscopy in this thesis. Hernández-Fariñas et al. (2013) found for the EEC that *Guinardia, Chaetoceros, Rhizosolenia, Pseudo-nitzschia, Paralia, Skeletonema* and *Leptocylindrus* were amongst the most abundant genera in Utermöhl counts for 1992-2011 water samples along the French coast (Bay of Somme, Boulogne and Dunkerque), again resembling of what we found for *Chaetoceros, Pseudo-nitzschia* and *Paralia*. *Guinardia*. *Rhizosolenia* and *Leptocylindrus* species are vulnerable to oxidations and are thus underestimated in the microscopic counts on oxidized materials.

For amplicon sequencing, supergroup Alveolata has the highest relative abundance (56%), followed by Stramenopila (16.5%), Hacrobia (16%), Archaeplastida (4%), Rhizaria (3%), Opisthokonta (0.5%), Apusozoa (0.06%), Amoebozoa (0.04%) and Excavata (0.0007%). On division level, the highest relative abundance is for dinoflagellates (48%) followed by diatoms (14%) and both dominate their respective supergroups in terms of relative abundance. In terms of diversity, Stramenopila is the most diverse supergroup containing 35% of all found species, followed by Alveolata which contains 30.2% of all species found. Supergroups Archaeplastida (9.9%), Rhizaria (8.6%), Hacrobia (7.4%), Opisthokonta (4.3%), Amoebozoa (2.5%), Apusozoa (1.6%) and Excavata (0.2%) contain less species. Stramenopila are dominated by the class Ochrophyta (73%), Alveolata are dominated by dinoflagellates (Myzozoa + Dinoflagellata) (50%) and Ciliophora (40%), Archaeplastida are dominated by Chlorophyta (95%), Rhizaria are dominated by Cercozoa (91%), Hacrobia are dominated by Cryptophyta (61%), Opisthokonta are dominated by Fungi (55%), Amoebozoa are dominated by class Amoebozoa (47%), Apusozoa are dominated by Apusomonadidae (55%), Excavata only comprise two species. Dinoflagellates mainly consist of the class Dinophyceae, followed by Syndiniales (MALV: Marine ALVeolata), species with unknown or uncertain class-level matches, Conoidasida, Perkinsea

and Noctilucophyceae. At the order level, most species matches occur under orders Gymnodiniales and Peridiniales. Looking at Ochrophyta, the majority of species matches belong to class Bacillariophyceae, followed by Chrysophyceae, Dictyochophyceae, Raphidophyceae, Pelagophyceae, Bolidophyceae, Phaeophyceae, Eustigmatophyceae, Xanthophyceae and Marine OCHrophyte (MOCH) groups 1 to 4. Looking at order level for Ochrophyta, most species belong to Chaetocerotales, Thalassiosirales and Rhizosoleniales. Just like in microscopic counts where *Thalassiosira* and *Chaetoceros* comprised most species.

Thamarasi (2016) also performed NGS for the BPNS in 2015-2016 and found dinoflagellates (80%) to have the highest abundance, followed by Ciliophora (8%), just like here Alveolata had the highest relative abundance (56%) here and is dominated by dinoflagellates and Ciliophora. Thamarasi (2016) further found relative abundances for cryptophytes (5%), diatoms (4%), chlorophytes (2%) and *Phaeocystis* (1%). Dinoflagellates are in both studies the most abundant group unlike in this study where the abundance of dinoflagellates is a lot less, perhaps because we are dealing with late summer to early winter samples. In this study, diatoms are the second most abundant groups, unlike in Thamarasi (2016), just like Chlorophyta and Cercozoa are more important here as well. Further, here *Phaeocystis* (*P. globosa* +*P. cordata* + unknown Phaeocystaceae) have a relative abundance of 0.18%, 10 times less than in Thamarasi (2016), but the full seasonal scope is included in Thamarasi (2016) results, while here we only look at late summer to early winter species abundances, when *Phaeocystis* are typically low in abundance (Rousseau et al., 2002). Genitsaris et al. (2016) performed NGS in the eastern English Channel (EEC) and found Alveolata to have the highest number of OTUs, followed by Stramenopila, Opisthokonta, Hacrobia, Rhizaria, Archaeplastida, Amoebozoa, Apusozoa and Excavata in decreasing order. This is more or less comparable to what we found for the relative abundances of supergroups in amplicon sequencing, except that in this study Opisthokonta is less abundant than Hacrobia, Rhizaria and Archaeplastida as opposed to Genitsaris et al. (2016). Genitsaris et al. (2015) study in the EEC found Dinophyceae the most diverse group, comprising the majority of OTUs and it was also the dominant group in terms of number of reads. In terms of abundance, Dinophyceae (13%) and MALV (13%) are the most abundant groups, followed by and Ciliophora (8%) and Cercozoa (8%) and Fungi (8%), MAST (6%) and Chlorophyta (5%). In terms of OTUs, the majority of OTUs belonged to Dinophyceae (38%), followed by Bacillariophyta (16%), very comparable to our study, followed by MALV (9%), MAST (8%) and Haptophyta (8%), and Ciliophora (5%). In this thesis, marine Alveolates (MALV), comprising of Syndiniales here, have a RA of 5%, Marine Straminopila (MAST) comprise Opalozoa, Sagenista and Pseudofungi here and together have a RA of 22%. Rachik et al. (2018) also reported that Dinophyceae showed the highest number of reads in the EEC. In terms of diversity Ciliophora was most diverse, followed by Dinophyceae, Syndiniales, Fungi and Bacillariophyta. The most abundant species was *Gyrodinium spirale*, which is the 7th most abundant species here in amplicon sequencing. Hernández-Fariñas et al. (2013) found *Gyrodinium* the major dinoflagellate genera present in Utermöhl counts for the French coast along the EEC between 1992-2011 and *Gyrodinium* even showed a strong increase and doubled in terms of abundance between 2002 and 2007.

As opposed to the microscopic inventory where diatoms seem most abundant and diverse, dinoflagellates are more abundant and diverse in amplicon sequencing. This could be because dinoflagellate species were hard to identify in microscopy and need different protocols to be able to stain and visualize the thecae in armoured species, which is crucial for species identification. However, even though their diversity might have been underestimated in microscopy, the fact that dinoflagellates seem so abundant according to amplicon sequencing needs to be interpreted with caution. Although I underestimated diversity of dinoflagellates in the microscopic inventory due to identification issues, they were generally more rare in microscopy and they would only occur in certain samples in low numbers, while diatoms always dominated every sample in microscopy. Dinoflagellates also show a high number of unique ASVs matched to a single species in the amplicon sequencing inventory. This could be due the fact that dinoflagellate often have resting stages, or

because of their high SSU rDNA copy numbers (Medinger et al., 2010) (Not et al., 2009). The under-representation of diatoms in the amplicon sequence data set can also be explained by difficulties in DNA extraction (difficulty of breaking silica skeletons in diatoms) (Medinger et al., 2010). Our data thus appear to confirm that amplicon sequencing is not ideal for quantitative estimations (Piwosz et al., 2020), certainly when dinoflagellates are present.

Only 45 out of the 98 species observations in the microscopic inventory were also found in the amplicon sequencing species based inventory. This illustrates that classic microscopy cannot be fully replaced by high throughoutput sequencing techniques like amplicon sequencing and that microscopic techniques and metabarcoding are complementary. A good example is the *Skeletonema costatum* complex of which species are (semi)cryptic in microscopic observations. The species I saw in SEM was identified as *S. marinoi*, and LM observation pointed in that direction as well. However, *S. marinoi* and *S. dohrnii* are not entirely morphologically and genetically distinct (Ellegaard et al., 2008). Amplicon sequencing also found *S. marinoi,* in addition to *S. pseudocostatum and S. menzellii* which were never observed during microscopy. Since both microscopy and amplicon sequencing point in the direction of *S. marinoi* and not *S. dohrnii*, we can be quite certain that the observation of *S. marinoi* is correct. For some (semi)cryptic species or first time observed species microscopy and amplicon sequencing can be used to cross-validate identifications and help rule out uncertainties. For one *Cyclotella* species observation I doubted between *C. meneghiniana* and *C. choctawhatcheeana* in SEM because the species was only seen on one occasion. However, amplicon sequencing only found *C. choctawhatcheeana,* which indeed is logical as this is an estuarine species while *C. menegheniana* is more a freshwater species (Muylaert et al., 2006).

In conclusion, while the microscopic inventory focused mainly on diatoms, the amplicon sequencing species based inventory covers many more phytoplankton groups, amongst which small (pico-) sized and (semi)cryptic species which are hard to identify with microscopy. Without amplicon sequencing, the importance of mixo- and heterotrophic groups and small sized groups like Cercozoa would have been underestimated. Karlusich et al. (2020) also noted that mixotrophs is a quite ubiquitous and an underestimated part of the phytoplankton community, and that photosynthesis is not sharply defined but rather is a continuum that fades into heterotrophy, meaning that these heterotrophic groups are important to include. Amplicon sequence abundances seemed to be skewed towards high dinoflagellate abundances. Thus, to get a view of the full diversity and abundances of the full community, a combination of microscopy and metabarcoding techniques is recommended.

2. Ecological patterns in microscopic count data and amplicon sequencing analysis

The diatom counts on oxidized materials revealed a pronounced seasonal pattern, with August and September samples clearly differentiated from November and December samples along the first ordination axis. *Eunotogramma* spp*., Bacteriastrum hyalinum, Psammodictyon panduliforme, Rhizosolenia* spp*., Coscinodiscus centralis, Ralfsiella smithii, Gyrodinium* spp. and *Dichtyocha* spp. are more important in August and September. *Brockmaniella brockmanii, Cymatopleura solea, Hobaniella longicruris, Thalassionema nitzschioides, Rhizosolenia setigera, Actinoptychus senarius, Actinoptychus splendens, Delphineis surirella, Bacillaria paxillifer, Epithemia* spp. and *Odontella* spp. are relatively more important in November and December samples. October samples differ from both groups of samples and are predominantly located on the negative side of the second axis. *Thalassiosira tenera, Ralfsiella minima, Navicula palpebralis,*

Coscinodiscus centralis and *Thalassiosira punctigera* appear to be more abundant in October samples. September and August samples seem to be positively correlated to temperature, PAR and fluorescence and, to a lesser extent, salinity.

Rhizosolenia species are found near August and September samples and Nohe et al. (2020) also found *Rhizosolenia* to appear in the C3 summer assemblage from June to August. *Gyrodinium* is more common in August and September and Rousseau et al. (2002) and Nohe et al. (2020) also found dinoflagellates to peak predominantly during summer months. Although the oxidation method removed most of the dinoflagellates, a few *Gyrodinium* cells survived and these were all found in September; ZG02_09, 780_09 and 700_10. Additionally, unidentified dinoflagellates were also observed in August and September; 120_08 and 120_09. They are clearly found more often during summer months, and they were never found during the months November and December. *Thalassiosira* species are found near October samples in this study and Thamarashi (2016) also mainly observed that *Thalassiosira* species are typically found in autumn. Rousseau et al. (2008) appoint *Thalassiosira* species as typical for the C1 community which is a community found in August/September/October (Rousseau et al., 2002), but which also extends to autumn and early winter (Muylaert et al. 2006). *Coscinodiscus* species are relatively more abundant in October (*C. centralis*) and summer (*C. radiatus* and *C. centralis*) samples in this study. Rousseau et al. (2008) typically found *Coscinodiscus* species during September and October. November and December samples were characterized by the predominance of species typical for the C1 community according to (Muylaert et al., 2006) such as *Brockmanniella brockmannii, Thalassionema nitzschioides, Actinoptychus senarius* and *Actinoptychus splendens,* and Nohe et al. (2020) also found these species typical for the autumn-winter assemblage. Fig. 33 shows that some species have higher abundances during some months compared to others. *Eucampia zodicacus* and *Bellerochea horologicales* seem abundant in August only. *Pseudo-nitzschia* spp. seem most important in August, after which they gradually decrease during subsequent months. *Pseudo-nitzschia* species are characteristic for community C3 according to Muylaert et al. (2006), occurring from mid-April to July. Nohe et al. (2020) found *Pseudo-nitzschia* species to have an extended growing season to September, which is seen in our data as well. *Paralia* spp. take up more than half of the diatom abundance of species found in December, and its relative abundance seems to increase from August to December. Nohe et al. (2020) found *Paralia* spp. to be typical for the autumn-winter assemblage as well. *Chaetoceros* spp. show peak abundance in September, with lower abundances in August and October and very low abundances in November and December. However, the majority of *Chaetoceros* spp. do not survive the oxidation so this might be an artefact. In general, we can see a gradual transition between the typical communities for the BPNS in our samples as they move from summer assemblages with *Rhizosolenia, Pseudo-nitzschia* and *Gyrodinium*, to the intermediate assemblage with *Thalassiosira* and *Coscinodiscus*, to an autumn-winter assemblage with *Actinoptychus, Paralia, Brockmaniella* and *Thalassionema.*

No clear differences in diatom community composition were observed between onshore and offshore station or between NE stations (700 and 780) and SW stations (120 and ZG02). The pattern for species occurrences between the different stations show no straightforward patterns. *Gyrodinium* spp. seemed to be predominantly found at offshore stations ZG02 and 780, although not exclusively. Töpke (2009) found *Gyrodinium* spp. more frequently at offshore stations as well. However, to draw conclusions about dinoflagellate occurrences we need a microscopic count of the full community on quantitative samples using the Utermöhl counting method on quantitative samples.

Remarkably, the October samples take a peculiar position in the PCA of the diatom counts (Fig.34), being separated from the other samples by the second axis, while summer and winter samples are separated from each other by the first axis. During the microscopic observations on the Lugol's iodine fixed samples, overall

phytoplankton abundance seemed much lower in October samples than for the other months. This appears to be confirmed by the pigment data (Fig. 38) where there is a dip in chlorophyll a, a proxy of overall photosynthetic biomass of the whole phytoplankton community, chlorophyll c3 (*Paeocystis,*diatoms, dinoflagellates group II, Prymnesiophytes), fucoxanthin (mainly diatoms, but also other Ochrophyta, dinoflagellates and *Paeocystis)*, alloxanthin (Cryptophytes), peridine (dinoflagellates group I) and diato- and diadinoxanthin (dinoflagellates, diatoms and Dictuochophyceae and Prymnesiopytes) concentrations for October.

In contrast to diatom counts, seasonal patterns are less obvious in amplicon sequencing data. The most striking pattern in these data is the clear clustering of species based on higher taxonomic level, but without an obvious signal linked to season, station or size fraction. This is confirmed by the PERMANOVA results which show no significant differences, and also by the lack of significant correlations between the ordination axes and the environmental variables. The reason that there might be no clear pattern is because we are dealing with late summer/autumn/early winter. The study period is relatively limited, and only a selection of stations was sampled, also limiting the scale of the study. This means that differences between stations or months will have to be large before they are visible. Including spring and early summer samples would have shown more patterns because the bloom events and successional stages tend to be more obvious during the springtime. Our results coincide with Louchart et al. (2020) where no seasonal patterns were found in late summer and autumn in the English Channel for the full phytoplankton community (incl. microphytoplankton, nanoeukaryotes and picophytoplankton, Cryptophyte-like cells). It seems like seasonal patterns are visible in the diatom fraction of the phytoplankton community, gets masked when observing the full microplankton community perhaps caused by the presence of many mixo- and heterotrophic groups in the amplicon sequencing data.

In the amplicon sequencing ordinations August and December samples and 700 and 780 samples seem to have more small green algae (120_08, ZG02_12, 780_12, 700_08, 700_12, 780_12, 120_12, 780_08 are located nearby the cluster of green algae in Fig. 36). Chlorophyll b is found in small green algae but also in Euglenophytes; the latter however are seen only once in the amplicon sequencing based inventory so they seem to be way less abundant than pico-sized green algae, the latter likely influenced chlorophyll b measurements most. Fig. 36 shows highest levels of chlorophyll c2 in August, except for station 700, chlorophyll b concentrations are zero for all stations in December. When we look at the consistency of Chlorophyta in the amplicon sequencing inventory, the majority consists of Mamiellophyceae, followed by Pyramimonadophyceae. The majority of Mamiellophyceae consists of *Ostreococcus* and *Micromonas* species. Töpke (2009) also found that CHEMTAX identified chlorophytes as an important component of the phytoplankton community. Karlusich et al. (2020) also appointed that chlorophytes are important in phytoplankton communities where the most prominent lineages are clade VII Prasinophyceae and Mamiellophyceae. Tragin et al. (2020) found the majority of Chlorophyta species to belong to Mamiellophyceae for SOMLIT (Brest and Roscoff) and Helgoland. Just like we found in this thesis, *Micromonas* and *Osterococcus* were the two dominant genera in Tragin et al. (2017). Bolaños et al. (2020) as part of the NAAMES study, found that in the North Atlantic small phytoplankton taxa were unexpectedly common. Here, winter phytoplankton communities were dominated in terms of ASVs by cyanobacteria and pico-sized phyto-eukaryotes in the western North Atlantic, in the subpolar region Cyanobacteria, Synechococcus clades I and IV, *Bathycoccus* and *Micromonas* dominated*,* in subtropical regions Cyanobacteria, *Synechococcus* IV, *Prochlorococcus*, *Bathycoccus* and *Micromonas* dominated while *Osterococcus* also had noticeably high contributions. Overall, Bolaños et al. (2020) found that these pico-sized phytoplankton dominated winter conditions and these transitioned to more diverse and dynamic spring communities in which pico- and nanosized phyto-eukaryotes dominated. Metfies et al. (2020) for Helgoland

found that there was an increase in relative abundance of pico-eukaryotes, like Chlorophyta mainly belonging to *Bathycoccus* and *Micromonas*, after the spring bloom in 2016. Widdicombe et al. (2010) as part of the L4 time series observed that phytoflagellates (2µm-10µm diameter and recognizable flagellae and/or plastids that were not diatoms or dinoflagellates) dominated Utermöhl counts from 1992-2007 for the Western English Channel. In that study phytoflagellates accounted for 86.98% RA, while diatoms accounted for 5.04%, *Phaeocystis* for 3.41%, dinoflagellates for 2.90%, coccolithophorids for 2.75% and ciliates for 0.17%. This highlights the numerical abundance of small cells opposed to groups like diatoms and dinoflagellates.

Looking at the amplicon sequencing ordinations for fractions and the bar graphs for fraction (Fig. 35 and Appendix 5 Fig. 41), it seem like the filtering method was not effective in fractionating. Perhaps the biggest filter got clogged, also retaining smaller groups. Larger cells may have been broken in the filtration process, which could cause them to show up in the smallest fraction. Since we are not only looking at autotrophs here but also mixotrophs, heterotrophs and parasites it could be that predation introduced smaller species in the biggest fraction. Environmental/extracellular DNA after cell death could also be a cause. Filtering with a peristaltic pump might be more successful in fractionating in the future.

The fact that none of the environmental parameters show significant Spearman Rank correlation coefficients, is possibly due to the sampling period from August to December. However it could also be that, when looking at the full microplankton community, environmental variables are not the main drivers, but instead inter-taxa relations structure assemblages (Genitsaris et al., 2015). Taxon specific trophic traits as trophic role and specialization level may provide an understanding of protist community organisation. Genitsaris et al. (2016) also describes the importance of microbial interactions in counterbalancing environmental variables in two closely located stations.

In conclusion, microscopic counts on oxidized materials showed a clear seasonal pattern and a gradual transition between the typical communities for the BPNS as they move from summer assemblages with *Rhizosolenia, Pseudo-nitzschia* and *Gyrodinium*, to the intermediate assemblage with *Thalassiosira* and *Coscinodiscus*, to an autumn-winter assemblage with *Actinoptychus, Paralia, Brockamniella* and *Thalassionema.* There was no clear pattern found for stations in the microscopic count data. In the amplicon sequencing count data no seasonal, spatial or size fraction dependent pattern was visible and none of the environmental variables had a significant correlation with the ordination axes. This could be because we are dealing with late summer to autumn and early winter samples and because we are incorporating the full microplankton community in the amplicon sequencing analysis as opposed the diatom community in the microscopic counts on oxidized materials. There was however a remarkable pattern in species clustering by higher taxonomic level. Small green algae for a pronounced cluster, separated from plotted diatoms, dinoflagellates and Ciliophora. Other studies in the North Sea also appointed small green algae as an important group in the area, especially at the end of the year.

3. Future perspectives

To get a better scope of the full phytoplankton community with microscopic counts, 100 ml quantitative samples should be counted using the Utermöhl counting method. In this way, dinoflagellates and larger sized Chlorophyta, which now almost fully disappeared during the oxidation procedure, would be incorporated in the count data. For diatoms this would lead to more balanced counts of colonial species, which break up during the oxidation process, as well as better represent some taxa which are vulnerable to oxidation like *Leptocylindrus, Chaetoceros, Rhizosolenia* and *Trieres* species and tend to disappear after oxidation. To visualize dinoflagellates better for the microscopic inventory, specific protocols can be applied for LM and SEM. For LM dinoflagellate cells can be isolated if they are in low abundances, and stained with Calcofluor White M2R or Solophenyl Flavine 7GFE500 (Direct Yellow 96), however these stains are only shortly active. For SEM filtering and dehydration with 1:1 HMDS:EtOH (Tillmann et al., 2019)(Tillmann et al., 2016) should help to visualize dinoflagellates.

Because sampling ended in December, we missed big part of the seasonal pattern in the phytoplankton community, more specifically the spring bloom. If spring months would have been sampled as planned, the seasonal pattern probably might have been clearer in amplicon sequencing temporal analysis. Differences in seasonal succession between stations might have been visible as well as a significant effects of environmental variables.

CONCLUSION

In conclusion, we provided an updated inventory of the BPNS, with a microscopic observations of 108 observations focusing mainly on the diatom community and amplicon sequencing identifications of 657 species of the whole microplankton community. The latter showed the importance of heterotrophic groups and smaller microplankton species in the BPNS, during late summer, autumn and early winter. Microscopic counts on oxidized materials showed a clear seasonal pattern in the diatom community, with abundances of dominant species aligning with previous observations of the typical seasonal succession and environmental variables. On the contrary, amplicon sequencing showed no clear patterns. Instead, a clustering of species by higher taxonomic level was observed which shows the importance of small green algae during late summer/autumn/early winter.

SUMMARY

Phytoplankton is of great interest: it is known to fuel photosynthetic reliant food webs, it has a high diversity including toxic and harmful species and it has a short generation time allowing them to respond quickly to environmental changes in nutrients, light availability and so on. Due to its key function, monitoring of phytoplankton is essential for understanding marine dynamics and in order to preserve the marine environment for the future. Dynamics in the phytoplankton community in the Belgian Part of the North Sea (BPNS) are characterized by an annually recurring seasonal succession of phytoplankton blooms, but this typical succession of communities has changed over the last couple of decades. The previously observed bimodal annual diatom bloom pattern has changed to a single unimodal extended growing season with an earlier onset. Total biovolumes of dinoflagellates and diatoms have increased; diatoms have increased from winter to summer while dinoflagellates have increased in spring and summer. The diatom community has become more seasonally homogenized with a pronounced shift towards larger taxa as well as a significant increase in potential harmful species.

Although there are long term studies available for the Belgian Part of the North Sea and adjoining areas, species diversity is less often studied in detail by including micro-, nano- and picoplankton fractions of the phytoplankton community. Especially the smallest size fractions of phytoplankton remains largely understudied and in this way an important part of biodiversity is overlooked. Therefore, we applied a selection of identification techniques in order to get a more detailed view of the biodiversity and abundances of phyto- and microplankton species for the BPNS. We opted for a classic microscopic approach (LM and SEM) combined with metabarcoding analysis, focusing on the smallest fractions (<50 µm) of the community in order to create a species inventory for the BPNS to assess biodiversity. Subsequently, in order to obtain quantitative estimates of the community microscopic counts were performed. These counts, together with amplicon sequencing relative abundance estimates, help us assess the spatial and temporal dynamics in late summer to early winter in the phyto- and microplankton community in the BPNS as we sampled at onshore and offshore locations on opposite sides of the coast during the period August to December 2019.

In terms of diversity, the LM and SEM observations led to a microscopic inventory of 108 identification accompanied by imagery for future verification and descriptions of a few selected species of (semi)cryptic nature. Diatoms comprised the most diverse group (96 sp.), followed by dinoflagellates (6 sp.), silicoflagellates (3 sp.), tintinnid cilliates (2 sp.) and Chlorophyta (1 sp.). The diatom genus *Chaetoceros* comprised most species in the microscopic inventory followed by, *Thalassiosira*, *Coscinodiscus*, *Actinocyclus*, *Guinardia*, *Odontella* and *Rhizosolenia*. 76% of the identified species has been detected in the BPNS before (Nohet et al. 2020) and 65% of the identified species has been detected in the Helgoland checklist (Kraberg et al., 2019). While microscopy focussed on revealing phytoplankton (and mainly diatom) diversity, amplicon sequencing investigated the full eukaryotic microplankton community, including mixo- and heterotrophic taxa. The amplicon sequencing inventory led to 657 species identifications with the majority belonging to Stramenopila (35%) and Alveolata (30.2%), followed by Archaeplastida (9.9%), Hacrobia (7.4%), Rhizaria (8.6%), Opisthokonta (4.3%), Amoebozoa (2.5%), Apusozoa (1.6%) and Excavata (0.2%). Stramenopila are dominated by the class Ochrophyta, Alveolata are dominated by dinoflagellates and Ciliophora, Archaeplastida are dominated by Chlorophyta, Rhizaria are dominated by Cercozoa, Hacrobia are dominated by Cryptophyta, Opisthokonta are dominated by Fungi, Amoebozoa are dominated by class Amoebozoa, Apusozoa are dominated by Apusomonadidae, Excavata only comprise two species.

During the microscopic counts of the oxidized materials 74 species were identified. *Paralia* species were most abundant, followed by *Delphineis surirella*, *Cymatosira belgica*, *Thalassiosira* spp., *Chaetoceros* spp., *Rhaphoneis amphiceros*, *Pseudo-nitzschia* spp., *Ditylum brightwelli*, *Bacillaria paxillifer* and *Hobaniella longicruris. Paralia, Thalassiosira* spp., *Chaetoceros* spp., *Pseudo-nitzschia* spp. and *Ditylum brightwellii* are amongst the most abundant species/genera in diatom counts on oxidized materials and they have been observed to have increased in abundance in the BPNS between 1970-2000 (Nohe et al., 2020). Töpke et al. (2009) also found high abundances of *Paralia* for the research period 2003-2008 for the BPNS and also *Thalassiosira* and *Pseudo-nitzschia* were found to be abundant then. Hernández-Fariñas et al. (2013) also found *Paralia, Chaetoceros* and *Pseudo-nitzschia* abundant in the EEC between 1992 and 2011.

For amplicon sequencing in terms of relative abundances supergroup Alveolata has the highest abundance (56%), followed by Stramenopila (16.5%), Hacrobia (16%), Archaeplastida (7%), Rhizaria (3%), Opisthokonta (0.5%), Apusozoa (0.06%), Amoebozoa (0.04%) and Excavata (0.0007%) (Fig. 31). Dinoflagellates had a relative abundance of 48%, diatoms (Bacillariophyta) had a relative abundance of 14% and both groups dominate their respective supergroups in terms of relative abundance. The top 10 species with highest relative abundances over all samples are Unknown Dino-group II, *Gyrodinium* spp*., Plagioselmis prolonga,* Unknown Dino-group I*, Gyrodinium fusiforme, Gyrodinium dominans, Gyrodinium spirale,* Unknown Strombidiida B*, Teleaulax acuta* and *Heterocapsa pygmae*. Genitsaris et al. (2015) and Rachik et al. (2018) also found Dinophyceae the most diverse group, comprising the majority of reads or OTUs for the Eastern English Channel (EEC). *Gyrodinium* species are amongst the most abundant species as well in these studies.

At first there aren't any similar results between the 10 most abundant species in amplicon sequencing and the most abundant species in the microscopic counts of oxidized materials. But looking at Bacillariophyceae (diatoms) fraction in the amplicon sequencing data set *Ceratulina bergonii, Thalassiosira* spp*., Shionodiscus oestrupii var. vernickae, Cyclotella* spp*., Rhizosolenia delicatula, Chaetoceros* spp*., Chaetoceros tenuissimus, Unknown Bacillariophyceae, Chaetoceros danicus and Bellerochea polymorpha* are 10 most abundant species in decreasing order. Now we see more similarities: *Thalassiosira* spp. and *Chaetoceros* spp. are amongst the 10 most abundant taxa in both amplicon sequencing for Bacillariophyceae and in diatom counts and they are also the most diverse genera in the microscopic inventory. The remaining species were either too small to count in the microscopic counts or did not survive the oxidation process. *Paralia* spp., the most abundant species in microscopic count data, is not abundant at all in amplicon sequencing, probably because *Paralia* spp. were counted as valves instead of chains. Generally diatoms have low abundances in amplicon sequencing because they are overshadowed by other taxa with high abundances. As opposed to the microscopic inventory where diatoms seem most abundant and diverse, dinoflagellates are more abundant and diverse in amplicon sequencing. This could be because dinoflagellate species were hard to identify in microscopy and need additional protocols to get a full scope of dinoflagellate diversity in microscopy. However, the fact that they seem so abundant according to amplicon sequencing needs to be interpreted with caution. Dinoflagellates often have resting stages and they have high SSU rDNA copy numbers (Medinger et al., 2010) (Not et al., 2009) which makes them appear disproportionally abundant in amplicon sequencing. The under-representation of diatoms in the amplicon sequence data set can also be explained by difficulties in DNA extraction in diatoms (Medinger et al., 2010).

Only 45 out of the 98 species observations in the microscopic inventory were also found in the amplicon sequencing species based inventory. This illustrates that classic microscopy cannot be fully replaced by high throughoutput sequencing techniques like amplicon sequencing and that microscopic techniques and metabarcoding are complementary. Without amplicon sequencing, the importance of heterotrophic groups and small sized groups like Cercozoa would have been underestimated. Karlusich et al. (2020) also noted that mixotrophs is an quite ubiquitous and an underestimated part of the phytoplankton community, and that photosynthesis is not sharply defined but rather is a continuum that fades into heterotrophy, meaning that these heterotrophic groups are important to include. Thus, to get a view of the full community in detail, a combination of microscopy and metabarcoding techniques is recommended.

In terms of spatial and temporal dynamics, microscopic count data on oxidized materials revealed a pronounced seasonal pattern, but no clear spatial pattern between onshore and offshore stations or between NW or SE stations. August and September samples showed a clear cluster, separated from November and December samples which clustered together. Both groups showed different characteristic species structuring these seasonal communities, ranging from a summer assemblage with *Rhizosolenia, Pseudo-nitzschia* and *Gyrodinium*, to an intermediate assemblage with *Thalassiosira* and *Coscinodiscus*, to an autumn-winter assemblage with *Actinoptychus, Paralia, Brockmaniella* and *Thalassionema,* October samples are located somewhat odd in the ordination space on the negative side of the second axis, which is confirmed by pigment data from the research period. September and August samples seem to be positively correlated to temperature, PAR and fluorescence and, to a lesser extent, salinity

Amplicon sequencing data showed no seasonal, spatial or size fraction dependent pattern and none of the environmental showed to be significant. The reason for this is likely that we are dealing with late summer/autumn/early

winter. Including early summer and spring months in sampling would perhaps have shown more patterns because the bloom events and successional stages tend to be more obvious during the springtime. These results coincide with Louchart et al. (2020) where no seasonal patterns were found in late summer and autumn in the English Channel for the full phytoplankton community (incl. microphytoplankton, nanoeukaryotes and picophytoplankton, Cryptophyte-like cells). It seems like seasonal patterns are visible in the diatom fraction of the phytoplankton community, gets masked when observing the full microplankton community perhaps caused by the presence of mixo- and heterotrophic groups in the amplicon sequencing data. Remarkably, there appears to be a clear clustering of species per higher taxonomic level, with separations based on cell size as well. Small green algae cluster together, separated from larger sized diatoms and dinoflagellates. When we look at the consistency of Chlorophyta in the amplicon sequencing inventory, the majority consists of Mamiellophyceae and Pyramimonadophyceae, followed by minor concentrations of Ulvophyceae, Florideophyceae, Nephrosemidophyceae, Synurophyceae, Chlorodendrophyceae, Prasinophyceae and Palmophyllophyceae. The majority of Mamiellophyceae consists of *Ostreococcus* and *Micromonas* species. Töpke (2009) also found that CHEMTAX identified chlorophytes as an important component of the phytoplankton community in the BPNS. Karlusich et al. (2020) also appointed that chlorophytes are important in phytoplankton communities where the most prominent lineages are clade VII Prasinophytes and Mamiellophyceae. Tragin et al. (2020) found the majority of Chlorophyta species to belong to Mamiellophyceae for SOMLIT (Brest and Roscoff) and Helgoland, with minor contributions of Trebouxiophyceae, Ulvophycea and Pyramimonadales. *Micromonas* and *Osterococcus* were the two dominant genera in Tragin et al. (2017). Bolaños et al. (2020) as part of the NAAMES study, found that in the North Atlantic small phytoplankton taxa were unexpectedly common.

The fact that none of the environmental parameters were significant for amplicon sequencing is possibly because the sampling period ranged from August to December. However, it could also be that when looking at the full microplankton community, environmental variables are not the main drivers (or environmental variables structuring the community were not included in this study), but instead inter-taxa relations might structure community assemblages (Genitsaris et al., 2015). Taxon specific trophic traits as trophic role and specialization level may provide an understanding of protist community organisation. Genitsaris et al. (2016) also describes the importance of microbial interactions in counterbalancing environmental variables in two closely located stations.

In conclusion, we provided an updated inventory of the BPNS, with a microscopic observations of 108 observations focusing mainly on the diatom community and amplicon sequencing identifications of 657 species of the whole microplankton community. The latter showed the importance of heterotrophic groups and smaller microplankton species in the BPNS, during late summer, autumn and early winter. Microscopic counts on oxidized materials showed a clear seasonal pattern in the diatom community, with abundances of dominant species aligning with previous observations of the typical seasonal succession and environmental variables. On the contrary, amplicon sequencing showed no clear patterns. Instead, a clustering of species by higher taxonomic level was observed which shows the importance of small green algae during late summer/autumn/early winter.

SAMENVATTING

Fytoplankton speelt een cruciale rol in mariene ecosystemen: ze liggen aan de basis van fotosynthetische voedselwebben, de groep kent een grote diversiteit waaronder giftige en schadelijke soorten en fytoplankton heeft een korte generatietijd waardoor deze snel kunnen reageren op veranderingen in omgevingsfactoren als nutriënten, temperatuur en beschikbaarheid van licht. Vanwege hun sleutelfunctie is monitoring van fytoplankton essentieel om mariene ecosystemen te begrijpen en om deze te beschermen in de toekomst. Temporele dynamieken in de fytoplanktongemeenschap in het Belgische Noordzee (BNZ) wordt gekenmerkt door een jaarlijks terugkerende seizoenale cyclus van drie gemeenschappen, maar deze cyclus heeft de afgelopen jaren veranderingen ondergaan. Het vroeger geobserveerde bimodale jaarlijkse bloeipatroon van diatomeeën en dinoflagellaten veranderde in een enkel unimodaal verlengd groeiseizoen dat eerder begint en voornamelijk wordt gedomineerd door grote soorten. Verder zijn de totale bio volumes van dinoflagellaten en diatomeeën toegenomen, waarbij diatomeeën zijn toegenomen van winter tot zomer, en dinoflagellaten zijn toegenomen in de lente en de zomer. Verder is de diatomeeëngemeenschap meer gehomogeniseerd dan vroeger en is er een significante toename van potentieel schadelijke soorten.

Hoewel er langetermijn studies beschikbaar zijn voor het Belgische deel van de Noordzee en aangrenzende gebieden, wordt soortendiversiteit vaak niet in detail bestudeerd. De micro-, nano- en picoplankton fracties van de fytoplanktongemeenschap zijn tot nu toe onvoldoende bestudeerd en op deze manier wordt een belangrijk deel van de biodiversiteit over het hoofd gezien. Daarom hebben we een selectie van identificatietechnieken toegepast om een meer gedetailleerd beeld te krijgen van de biodiversiteit van fyto- en microplankton soorten in de BNZ. We kozen voor een klassieke microscopische benadering (LM en SEM) gecombineerd met DNA analyses, gericht op de kleinste fracties van de gemeenschap (<50 µm). Dit om diversiteit te bestuderen en een soortinventaris op te stellen voor de Belgische Noordzee. Om ook kwantitatieve schattingen van de gemeenschap te verkrijgen, worden microscopische tellingen uitgevoerd. Deze tellingen, samen met amplicon sequenering gebaseerde abundantie schattingen, helpen ons de ruimtelijke en temporele dynamiek in de fyto- en microplankton gemeenschapsstructuur te bestuderen tijdens het najaar. Om dergelijke patronen te onderzoeken, bemonsterden we zowel onshore en offshore locaties aan weerszijden van de kust in de periode augustus tot december 2019.

In termen van diversiteit leidden de licht- en scanning elektron microscopische observaties tot een microscopische inventarisatie van 108 taxa, vergezeld van beeldmateriaal voor toekomstige verificatie en beschrijvingen van enkele geselecteerde soorten van (semi) cryptische aard. Diatomeeën zijn de meest diverse groep (96 soorten), gevolgd door dinoflagellaten (6 soorten), silicoflagellaten (3 soorten), tintinniden (2 soorten) en Chlorophyta (1 soort). Het diatomeeën geslacht *Chaetoceros* omvatte de meeste soorten in de microscopische inventaris (12), gevolgd door *Thalassiosira* (9), *Coscinodiscus* (4), *Actinocyclus* (3), *Guinardia* (3), *Odontella* (3) en *Rhizosolenia* (3). 76% van de geïdentificeerde soorten werd al eerder gedetecteerd in de Belgische Noordzee (Nohet et al. 2020) en 65% van de geïdentificeerde soorten werd gedetecteerd in de Helgoland checklist (Kraberg et al., 2019). Terwijl microscopie zich concentreerde op het bestuderen van fytoplankton (en voornamelijk diatomeeën) diversiteit, onderzocht amplicon sequenering de volledige eukaryote microplankton gemeenschap, inclusief mixo- en heterotrofe taxa. De inventarisatie m.b.v. amplicon sequenering leidde tot 657 soortidentificaties, waarvan het merendeel behoort tot supergroepen Stramenopila (35%) en Alveolata (30,2%), gevolgd door Archaeplastida (9,9%), Hacrobia (7,4%), Rhizaria (8,6%), Opisthokonta (4,3%), Amoebozoa (2,5%), Apusozoa (1,6%) en Excavata (0,2%). Stramenopila worden gedomineerd door de klasse Ochrophyta, Alveolata worden gedomineerd door dinoflagellaten en Ciliophora, Archaeplastida worden gedomineerd door Chlorophyta, Rhizaria worden gedomineerd door Cercozoa, Hacrobia wordt gedomineerd door Cryptophyta, Opisthokonta wordt gedomineerd door Fungi, Amoebozoa wordt gedomineerd door klasse Amoebozoa, Apusozoa wordt gedomineerd door Apusomonadidae, Excavata omvat slechts twee soorten.

Tijdens de microscopische tellingen van de geoxideerde stalen werden 74 soorten geïdentificeerd. *Paralia* spp. toonde de hoogste relatieve abundantie, gevolgd door *Delphineis surirella, Cymatosira belgica, Thalassiosira* spp*., Chaetoceros* spp*., Rhaphoneis amphiceros, Pseudo-nitzschia* spp*., Ditylum brightwelli, Bacillaria paxillifer en Hobaniella longicruris. Paralia, Thalassiosira* spp*., Chaetoceros* spp*., Pseudo-nitzschia* spp*.* en *Ditylum brightwellii* behoren tot de meest voorkomende soorten/geslachten in diatomeeëntellingen op geoxideerde materialen en deze zijn toegenomen tijdens de periode 1970-2000 in de Belgische Noordzee (Nohe et al. 2020). Töpke et al. (2009) observeerde ook hoge abundanties van *Paralia* in de Belgische Noordzeee tijdens de onderzoeksperiode 2003-2008 en *Thalassiosira* en *Pseudo-nitzschia* bleken toen ook aanwezig te zijn in hoge getallen. Hernández-Fariñas et al. (2013) observeerden ook dat *Paralia, Chaetoceros* en *Pseudo-nitzschia* tussen 1992 en 2011 in overvloed aanwezig waren in het Kanaal.

Voor amplicon sequenering in termen van relatieve abundanties heeft supergroep Alveolata de hoogste abundantie (56%), gevolgd door Stramenopila (16,5%), Hacrobia (16%), Archaeplastida (7%), Rhizaria (3%), Opisthokonta (0,5%) , Apusozoa (0,06%), Amoebozoa (0,04%) en Excavata (0,0007%) (Fig.31). Dinoflagellaten hadden een relatieve abundantie van 48%, diatomeeën hadden een relatieve abundantie van 14% en beide groepen domineren hun respectievelijke supergroepen in termen van relatieve abundantie. De top 10 soorten met de hoogste relatieve abundanties over alle stalen zijn Onbekende Dino-groep II, *Gyrodinium* spp*., Plagioselmis verlenga,* Onbekende Dinogroep I, *Gyrodinium fusiforme, Gyrodinium dominans, Gyrodinium spirale*, Onbekende Strombidiida B, *Teleaulax acuta* en *Heterocapsa pygmae*. Genitsaris et al. (2015) en Rachik et al. (2018) observeerde ook Dinophyceae als de meest diverse groep, die de meerderheid van de reads of OTU's voor het Engels Kanaal omvat. *Gyrodinium* soorten behoren ook in deze onderzoeken tot de meest voorkomende soorten. In eerste instantie zijn er geen vergelijkbare

resultaten tussen de 10 meest voorkomende soorten in amplicon sequencing en de meest voorkomende soorten in de microscopische tellingen. Echter, kijkend naar de Bacillariophyceae (diatomeeën) fractie in de amplicon sequencing dataset, zijn *Ceratulina bergonii, Thalassiosira* spp*., Shionodiscus oestrupii var. vernickae, Cyclotella* spp*., Rhizosolenia delicatula, Chaetoceros spp., Chaetoceros tenuissimus,* Unknown Bacillariophyceae*, Chaetoceros danicus* en *Bellerochea polymorpha* zijn 10 meest voorkomende soorten in afnemende volgorde. Nu zien we wat meer overeenkomsten; *Thalassiosira* spp. en *Chaetoceros* spp. behoren tot de 10 meest voorkomende taxa in zowel amplicon sequencing voor Bacillariophyceae als in diatomeeën tellingen en ze zijn ook de meest diverse geslachten in de microscopische inventaris. De overige soorten waren ofwel te klein om in de microscopische tellingen te tellen of verdwenen tijdens het oxidatieproces. *Paralia* spp., de meest voorkomende soort in microscopische tellingen, komt helemaal niet abundant voor in amplicon sequencing, dit omdat *Paralia* spp. werden geteld per valve. Over het algemeen hebben diatomeeën een lage abundantie in amplicon sequenering data omdat ze worden overschaduwd door taxa die overvloedig zijn in abundanties. In tegenstelling tot de microscopische inventaris waar diatomeeën het meest overvloedig en divers lijken, zijn dinoflagellaten overvloediger en diverser bij amplicon sequenering. Dit kan zijn omdat dinoflagellaten soorten moeilijk te identificeren waren in microscopie en andere protocollen vereisen om de volledige diversiteit aan dinoflagellaten te bestuderen in microscopie. Het feit dat dinoflagellaten volgens amplicon sequenering zo overvloedig lijken, moet echter met de nodige voorzichtigheid worden geïnterpreteerd. Dinoflagellaten hebben vaak ruststadia en vanwege hun hoge SSU-rDNA-kopieaantallen in dinoflagellaten cellen worden hun relatieve abundanties vaak overschat bij metabarcoding (Medinger et al., 2010) (Not et al., 2009). De ondervertegenwoordiging van diatomeeën in de amplicon sequenering data kan ook worden verklaard door problemen bij de DNA-extractie bij diatomeeën (Medinger et al., 2010).

Slechts 45 van de 98 waarnemingen in de microscopische inventaris werden ook gevonden in de amplicon sequenering gebaseerde inventaris. Dit illustreert dat klassieke microscopie niet volledig vervangen kan worden door metabarcoding technieken en dat microscopische technieken en amplicon sequenering eerder complementair zijn. Zonder amplicon sequencing zou het belang van mixo- en heterotrofe groepen en kleine groepen als Cercozoa onderschat worden. Karlusich et al. (2020) merkte ook op dat mixotrofen een vrij alomtegenwoordig en een onderschat onderdeel zijn van de fytoplanktongemeenschap, en dat fotosynthese eerder een continuüm is dat overgaat in heterotrofie, wat betekent dat deze groepen een belangrijk deel uitmaken van de microplankton gemeenschap dat zeker niet over het hoofd mag gezien worden in studies. Om een gedetailleerd beeld te krijgen van de volledige gemeenschap is een combinatie van microscopie en metabarcoderingstechnieken aangeraden.

In termen van ruimtelijke en temporele dynamiek, toonden microscopische telgegevens op geoxideerde materialen een uitgesproken seizoenaal patroon, maar geen duidelijk ruimtelijk patroon tussen onshore en offshore stations of tussen NW of ZO stations. Augustus en september stalen vertoonden een duidelijke cluster, gescheiden van stalen november en december stalen ook samen die gegroepeerd waren. Beide groepen vertoonden verschillende karakteristieke soorten die deze seizoenale gemeenschappen structureerden, variërend van een zomerassemblage met *Rhizosolenia*, *Pseudo-nitzschia* en *Gyrodinium*, tot een tussen assemblage met *Thalassiosira* en *Coscinodiscus*, tot een herfst-winterassemblage met *Actinoptychus, Paralia, Brockmaniella* en *Thalassionema*. Oktober stalen bevinden zich enigszins onverwacht in de ordinatie, aan de negatieve kant van de tweede as. Stalen van september en augustus lijken positief gecorreleerd te zijn met temperatuur, PAR en fluorescentie en, in mindere mate, saliniteit.

Amplicon sequenering data vertoonden geen seizoensgebonden, ruimtelijk of groottefractie afhankelijk patroon en ook geen enkel van de omgevingsvariabelen bleken significant. De reden hiervoor is waarschijnlijk dat we te maken hebben met nazomer/herfst/vroege winter stalen. Zomer en lentemaanden in de staalname op nemen, zou misschien meer patronen vertoond hebben, omdat bloeien en successiestadia duidelijker zijn tijdens het voorjaar. Deze resultaten vallen samen met Louchart et al. (2020) waar geen seizoenale patronen werden gevonden in de late zomer en herfst in het Engelse Kanaal voor de volledige fytoplanktongemeenschap (incl. microfytoplankton, nano-eukaryoten en picofytoplankton, cryptofyt-achtige cellen). Het lijkt erop dat seizoenale patronen zichtbaar zijn in de diatomeeënfractie van de fytoplanktongemeenschap, en dat deze worden gemaskeerd bij het observeren van de volledige microplanktongemeenschap, wat misschien veroorzaakt wordt door de aanwezigheid van mixo- en heterotrofe groepen in de amplicon sequenering data. Opvallend is een duidelijke clustering van soorten per hoger taxonomisch niveau, met scheidingen op basis van celgrootte. Kleine groene algen clusteren samen, gescheiden van grotere groepen

als diatomeeën en dinoflagellaten. Als we kijken naar de diversiteit van Chlorophyta in de amplicon sequenering gebaseerde inventaris, bestaat de meerderheid uit Mamiellophyceae, gevolgd door Pyramimonadophyceae en kleine hoeveelheden van Ulvophyceae, Florideophyceae, Nephrosemidophyceae, Synurophyceae, Chlorodendrophyceae, Prasinophyllophyceae en Palmophyllophyceae. Het merendeel van de Mamiellophyceae bestaat uit *Ostreococcus* en *Micromonas* soorten. Töpke (2009) ontdekte ook dat CHEMTAX chlorofyten identificeerde als een belangrijk onderdeel van de fytoplanktongemeenschap in de Belgische Noordzee. Karlusich et al. (2020) stelden ook vast dat chlorofyten belangrijk zijn in fytoplanktongemeenschappen waar de meest prominente lijnen clade VII Prasinophyta en Mamiellophyceae zijn. Tragin et al. (2020) ontdekten dat de meeste Chlorophyta-soorten behoren tot Mamiellophyceae voor SOMLIT (Brest en Roscoff) en Helgoland, met kleine bijdragen van Trebouxiophyceae, Ulvophycea en Pyramimonadales. *Micromonas* en *Osterococcus* waren de twee dominante geslachten in Tragin et al. (2017). Bolaños et al. (2020) als onderdeel van de NAAMES studie, ontdekten dat in de Noord-Atlantische Oceaan kleine fytoplankton taxa onverwacht veel voorkwamen.

Het feit dat geen van de omgevingsparameters significant was voor amplicon sequenering is mogelijk te wijten aan de staalname periode van augustus tot december. Het kan echter ook zijn dat wanneer we kijken naar de volledige microplankton gemeenschap, omgevingsvariabelen niet de belangrijkste drijfveren zijn (of de cruciale omgevingsvariabelen niet werden getest in deze studie), maar in plaats daarvan inter-taxa structuurassemblages de gemeenschap structureren (Genitsaris et al., 2015). Taxon specifieke trofische eigenschappen als trofische rol en specialisatieniveau kunnen inzicht verschaffen in de organisatie van protisten in de gemeenschap. Genitsaris et al. (2016) beschrijft ook het belang van microbiële interacties bij het compenseren van de invloed van omgevingsvariabelen in twee dicht bij elkaar gelegen stations.

In conclusie, we hebben een bijgewerkte inventaris van het BNZ bekomen, met microscopische waarnemingen van 108 taxa die zich voornamelijk richten op de diatomeeëngemeenschap en amplicon sequenering gebaseerde identificaties van 657 taxa van de hele microplanktongemeenschap. Dit laatste toonde het belang aan van heterotrofe groepen en kleinere microplankton soorten in het Belgische Noordzee tijdens de nazomer, herfst en vroege winter. Microscopische tellingen op geoxideerde materialen lieten een duidelijk seizoenaal patroon zien in de diatomeeëngemeenschap, met een overvloed aan dominante soorten. Dit is in lijn met eerdere waarnemingen van de typische seizoenale soortenopvolging in de gemeenschap gelinkt aan omgevingsvariabelen. Daarentegen vertoonde amplicon sequenering geen duidelijke seizoenale of ruimtelijke patronen. In plaats daarvan werd een clustering van soorten naar hoger taxonomisch niveau waargenomen, wat het belang van kleine groene algen aantoont tijdens het najaar.

ACKNOWLEDGEMENT

This thesis was supported by the infrastructure (RV Simon Stevin) provided by VLIZ as part of the Flemish contribution to LifeWatch. In relation to this, a big thank you to Dr. Elisabeth Debusschere for proofreading and making crucial equipment and resources available through VLIZ and LifeWatch.

First and foremost, I would like to thank my promotor Prof. Dr. Koen Sabbe for the help and advice during the year, for organising everything, for correcting text and for being very open to answer any questions, whether smart or stupid and for giving me the trust to work more independently. Secondly, a big thanks to Prof. Dr. Olivier De Clerck for lending me the microscope so I could perform the microscopic counts. Lastly, I would like to thank Prof. Dr. Wim Vyverman for providing equipment and facilities within the research groups.

Also a huge thanks to Rita and Alex for their patience and the countless hours we spend on Skype and email trying to figure out the amplicon sequencing data processing and statistics and to Luz for helping me with microscopic identifications, providing a huge amount of identification literature and joining me on my first campaign with RV Simon Stevin. At least also thanks to Dr. Bjorn Tytgat for the advice in the statistics department.

Of course I would also like the thank the lab staff for helping me with the different aspects of my thesis throughout the year. I would also like to thank Renaat for showing how to work with the SEM as well as for his help in the lab trying to figure out the appropriate oxidation techniques and how to clean the mess afterwards, especially after my most spectacular, and final, attempt. Also a big thanks to Peter for showing me how to work the microscopes and for this help with the many technological issues that can be grouped under 'Ornette', and Ilse for her help in the lab, providing pigment data, searching through Reinhout's samples and showing me where the -80°C freezer was after I had been on the search for a whole afternoon. Last but not least, a big thanks to Sophie for the help in the lab explaining the whole procedure and her patience as I ran countless PCRs and gels.

REFERENCES

Adl, S. M., Bass, D., Lane, C. E., Lukeš, J., Schoch, C. L., Smirnov, A., Agatha, S., Berney, C., Brown, M. W., Burki, F., Cárdenas, P., Čepička, I., Chistyakova, L., del Campo, J., Dunthorn, M., Edvardsen, B., Eglit, Y., Guillou, L., Hampl, V., … Zhang, Q. (2019). Revisions to the Classification, Nomenclature, and Diversity of Eukaryotes. *Journal of Eukaryotic Microbiology*, *66*(1), 4–119. https://doi.org/10.1111/jeu.12691

Anderson, D. M., Cambella, A. D., & Hallegraeff, G. M. (2012). Progress in understanding harmful algal blooms (HABs): Paradigm shifts and new technologies for research, monitoring and management. *Annual Review of Marine Science*, *4*, 143–176. https://doi.org/10.1146/annurev-marine-120308-081121

Baudron, A. R., Needle, C. L., Rijnsdorp, A. D., & Tara Marshall, C. (2014). Warming temperatures and smaller body sizes: Synchronous changes in growth of North Sea fishes. *Global Change Biology*, *20*(4), 1023–1031. https://doi.org/10.1111/gcb.12514

Beardall, J., Stojkovic, S., & Larsen, S. (2009). Living in a high CO2 world: Impacts of global climate change on marine phytoplankton. *Plant Ecology and Diversity*, *2*(2), 191–205. https://doi.org/10.1080/17550870903271363

Beaugrand, G. (2004). The North Sea regime shift: Evidence, causes, mechanisms and consequences. *Progress in Oceanography*, *60*(2–4), 245–262. https://doi.org/10.1016/j.pocean.2004.02.018

Behrenfeld, M. J., & Boss, E. S. (2018). Student's tutorial on bloom hypotheses in the context of phytoplankton annual cycles. *Global Change Biology*, *24*(1), 55–77. https://doi.org/10.1111/gcb.13858

Belgian State. (2012). Initial Assessment for the Belgian marine waters. -Art 8 lid 1a & 1b. *BMM, Federale Overheidsdienst Volksgezondheid, Veiligheid van de Voedselketen En Leefmilieu, Brussel, België*, 1–80.

Belkin, I. M. (2009). Rapid warming of Large Marine Ecosystems. *Progress in Oceanography*, *81*(1–4), 207–213. https://doi.org/10.1016/j.pocean.2009.04.011

Bengt Karlson, C. C. and E. B. (2010). Intergovernmental Oceanographic Commission of ©UNESCO. MICROSCOPIC AND MOLECULAR METHODS FOR QUANTITATIVE PHYTOPLANKTON ANALYSIS. *IOC Manuals and Guides*, *55*, 110.

Bill, B. D. B., Moore, S. K. S., Batten, S., Trainer, V. V. L., Stern, R., Fischer, A., Moore, S. K. S., Trainer, V. V. L., Bill, B. D. B., Fischer, A.,

Batten, S., Moore, S. K. S., Batten, S., Trainer, V. V. L., Stern, R., & Fischer, A. (2018). Spatial and temporal patterns of Pseudo-nitzschia genetic diversity in the North Pacific Ocean from the Continuous Plankton Recorder survey. *Marine Ecology Progress Series*, *606*, 7–28. https://doi.org/10.3354/meps12711

Blaxter, M. L. (2004). The promise of a DNA taxonomy. *The Royal Society*, *March*, 669–679. https://doi.org/10.1098/rstb.2003.1447

Bolaños, L. M., Karp-Boss, L., Choi, C. J., Worden, A. Z., Graff, J. R., Haëntjens, N., Chase, A. P., Della Penna, A., Gaube, P., Morison, F., Menden-Deuer, S., Westberry, T. K., O'Malley, R. T., Boss, E., Behrenfeld, M. J., & Giovannoni, S. J. (2020). Small phytoplankton dominate western North Atlantic biomass. *ISME Journal*, *14*(7), 1663–1674. https://doi.org/10.1038/s41396-020-0636-0

Borja, A., Kahlert, M., Iwan Jones, J., Cordier, T., Zimmerman, J., Sagova-Mareckova, M., Trobajo, R., Pinna, M., Sousa-Santos, C., Barquín, J., Vasselon, V., Moritz, C., Domaizon, I., Bouchez, A., Filipe, A. F., Weigand, A., van der Hoorn, B., Specchia, V., Rinkevich, B., … Pawlowski, J. (2018). The future of biotic indices in the ecogenomic era: Integrating (e)DNA metabarcoding in biological assessment of aquatic ecosystems. *Science of The Total Environment*, *637–638*, 1295–1310. https://doi.org/10.1016/j.scitotenv.2018.05.002

Breton, E., Rousseau, V., Parent, J. Y., Ozer, J., & Lancelot, C. (2006). Hydroclimatic modulation of diatom/Phaeocystis blooms in nutrient-enriched Belgian coastal waters (North Sea). *Limnology and Oceanography*, *51*(3), 1401–1409. https://doi.org/10.4319/lo.2006.51.3.1401

Burki, F. (2014). The eukaryotic tree of life from a global phylogenomic perspective. *Cold Spring Harbor Perspectives in Biology*, *6*(5), 1–18. https://doi.org/10.1101/cshperspect.a016147

Burson, A., Stomp, M., Akil, L., Brussaard, C. P. D., & Huisman, J. (2016). Unbalanced reduction of nutrient loads has created an offshore gradient from phosphorus to nitrogen limitation in the North Sea. *Limnology and Oceanography*, *61*(3), 869–888. https://doi.org/10.1002/lno.10257

Callahan, B. J., McMurdie, P. J., & Holmes, S. P. (2017). Exact sequence variants should replace operational taxonomic units in marker-gene data analysis. *ISME Journal*, *11*(12), 2639–2643. https://doi.org/10.1038/ismej.2017.119

Callahan, B. J., McMurdie, P. J., Rosen, M. J., Han, A. W., Johnson, A. J. A., & Holmes, S. P. (2016). DADA2: High-resolution sample inference from Illumina amplicon data. *Nature Methods*, *13*(7), 581–583. https://doi.org/10.1038/nmeth.3869

Carstensen, J., Borja, Á., Heiskanen, A.-S., van de Bund, W., & Elliott, M. (2010). Marine management – Towards an integrated implementation of the European Marine Strategy Framework and the Water Framework Directives. *Marine Pollution Bulletin*, *60*(12), 2175–2186. https://doi.org/10.1016/j.marpolbul.2010.09.026

Casini, M., Lövgren, J., Hjelm, J., Cardinale, M., Molinero, J. C., & Kornilovs, G. (2008). Multi-level trophic cascades in a heavily exploited open marine ecosystem. *Proceedings of the Royal Society B: Biological Sciences*, *275*(1644), 1793–1801. https://doi.org/10.1098/rspb.2007.1752

Casteleyn, G., Chepurnov, V. A., Leliaert, F., Mann, D. G., Bates, S. S., Lundholm, N., Rhodes, L., Sabbe, K., & Vyverman, W. (2008). Pseudo-nitzschia pungens (Bacillariophyceae): A cosmopolitan diatom species? *Harmful Algae*, *7*(2), 241–257. https://doi.org/10.1016/j.hal.2007.08.004

Creer, S., Deiner, K., Frey, S., Porazinska, D., Taberlet, P., Thomas, W. K., Potter, C., & Bik, H. M. (2016). The ecologist ' s field guide to sequence-based identification of biodiversity. *Methods in Ecology and E*, *4*, 1008–1018. https://doi.org/10.1111/2041-210X.12574

De Galan, S., Elskens, M., Goeyens, L., Pollentier, A., Brion, N., & Baeyens, W. (2004). Spatial and temporal trends in nutrient concentrations in the Belgian Continental area of the North Sea during the period 1993–2000. *Estuarine, Coastal and Shelf Science*, *61*(3), 517–528. https://doi.org/10.1016/j.ecss.2004.06.015

Desmit, X., Thieu, V., Billen, G., Campuzano, F., Dulière, V., Garnier, J., Lassaletta, L., Ménesguen, A., Neves, R., Pinto, L., Silvestre, M., Sobrinho, J. L., & Lacroix, G. (2018). Unbalanced reduction of nutrient loads has created an offshore gradient from phosphorus to nitrogen limitation in the North Sea. *Science of the Total Environment*, *635*(3), 1444–1466. https://doi.org/10.1002/lno.10257

Desmit, Xavier, Nohe, A., Borges, A. V., Prins, T., De Cauwer, K., Lagring, R., Van der Zande, D., & Sabbe, K. (2020). Changes in chlorophyll concentration and phenology in the North Sea in relation to de-eutrophication and sea surface warming. *Limnology and Oceanography*, *65*(4), 828–847. https://doi.org/10.1002/lno.11351

Desmit, Xavier, Ruddick, K., & Lacroix, G. (2015). Salinity predicts the distribution of chlorophyll a spring peak in the southern North Sea continental waters. *Journal of Sea Research*, *103*, 59–74. https://doi.org/10.1016/j.seares.2015.02.007

Dubelaar, G. B. J., & Jonker, R. R. (2000). Flow cytometry as a tool for the study of phytoplankton. *Scientia Marina*, *64*(2), 135–156. https://doi.org/10.3989/scimar.2000.64n2135

Ducklow, H. W., Steinberg, D. K., William, C., Point, M. G., & Buesseler, K. O. (2001). *Upper Ocean Carbon Export and the Biological PumpDucklow, H. W., Steinberg, D. K., William, C., Point, M. G., & Buesseler, K. O. (2001). Upper Ocean Carbon Export and the Biological Pump, 14(4). 14*(4).

EEC. (1991). Council Directive 91/493/EEC of 22 July 1991 laying down the health conditions for the production and the placing on the market of fishery products. *Official Journal of the European Communities*, *24.9.91*(No L 268/15), 20. http://eur-lex.europa.eu/legal-content/EN/TXT/?uri=CELEX%3A31991L0493

Eker-Develi, E., Berthon, J. F., Canuti, E., Slabakova, N., Moncheva, S., Shtereva, G., & Dzhurova, B. (2012). Phytoplankton taxonomy

based on CHEMTAX and microscopy in the northwestern Black Sea. *Journal of Marine Systems*, *94*, 18–32. https://doi.org/10.1016/j.jmarsys.2011.10.005

Elbrecht, V., & Leese, F. (2015). Can DNA-Based Ecosystem Assessments Quantify Species Abundance ? Testing Primer Bias and Biomass — Sequence Relationships with an Innovative Metabarcoding Protocol. *PLOS ONE*, *10*(7), 1–16. https://doi.org/10.1371/journal.pone.0130324

Ellegaard, M., Godhe, A., Härnström, K., & McQuoid, M. (2008). The species concept in a marine diatom: LSU rDNA-based phylogenetic differentiation in Skeletonema marinoi/dohrnii (Bacillariophyceae) is not reflected in morphology. *Phycologia*, *47*(2), 156–167. https://doi.org/10.2216/07-09.1

European Commission, Marine Strategy Framework Directive/56/EC2008, 2008. (2008). https://eur-lex.europa.eu/legal-content/EN/TXT/?uri=CELEX%3A32008L0056

Falkowski, P. G., Katz, M. E., Knoll, A. H., Quigg, A., Raven, J. A., Schofield, O., & Taylor, F. J. R. R. (2004). The evolution of modern eukaryotic phytoplankton. *Science*, *305*(5682), 354–360. https://doi.org/10.1126/science.1095964

Ferrario, M. E., Almandoz, G. O., & Cefarelli, A. O. (2012). Stephanopyxis species (Bacillariophyceae) from shelf and slope waters of the Argentinean Sea : Ultrastructure and distribution Stephanopyxis species (Bacillariophyceae) from shelf and slope waters of the Argentinean Sea : Ultrastructure and distributi. *Nova Hedwigia*, *96*(1–2), 249–263. https://doi.org/10.1127/0029-5035/2012/0077

Flanders Marine Institute (VLIZ); (2017): Marine Information and Data Acquisition System: underway and cruise data. (n.d.).

Genitsaris, S., Monchy, S., Breton, E., Lecuyer, E., & Christaki, U. (2016). Small-scale variability of protistan planktonic communities relative to environmental pressures and biotic interactions at two adjacent coastal stations. *Marine Ecology Progress Series*, *548*, 61–75. https://doi.org/10.3354/meps11647

Genitsaris, S., Monchy, S., Viscogliosi, E., Sime-Ngando, T., Ferreira, S., & Christaki, U. (2015). Seasonal variations of marine protist community structure based on taxon-specific traits using the eastern English Channel as a model coastal system. *FEMS Microbiology Ecology*, *91*(5), 1–15. https://doi.org/10.1093/femsec/fiv034

Gran-Stadniczeñko, S., Egge, E., Hostyeva, V., Logares, R., Eikrem, W., & Edvardsen, B. (2019). Protist Diversity and Seasonal Dynamics in Skagerrak Plankton Communities as Revealed by Metabarcoding and Microscopy. *Journal of Eukaryotic Microbiology*, *66*(3), 494–513. https://doi.org/10.1111/jeu.12700

Günther, B., Knebelsberger, T., Neumann, H., Laakmann, S., & Martínez Arbizu, P. (2018). Metabarcoding of marine environmental DNA based on mitochondrial and nuclear genes. *Scientific Reports*, *8*(1), 1–13. https://doi.org/10.1038/s41598-018-32917-x

Gypens, N., Lacroix, G., & Lancelot, C. (2007). Causes of variability in diatom and Phaeocystis blooms in Belgian coastal waters between 1989 and 2003: A model study. *Journal of Sea Research*, *57*(1), 19–35. https://doi.org/10.1016/j.seares.2006.07.004

Hartley, B. (1996). *An atlas of British diatoms* (P. A. Sims (Ed.)). Biopress Ltd.

Hays, G. C., Richardson, A. J., & Robinson, C. (2005). Climate change and marine plankton. *TRENDS in Ecology and Evolution*, *20*(6), 337–344. https://doi.org/10.1016/j.tree.2005.03.004

Henson, S. A., Sarmiento, J. L., Dunne, J. P., Bopp, L., Lima, I., Doney, S. C., John, J., & Beaulieu, C. (2010). Detection of anthropogenic climate change in satellite records of ocean chlorophyll and productivity. *Biogeosciences*, *7*(2), 621–640. https://doi.org/10.5194/bg-7-621-2010

Hernández-Fariñas, T., Soudant, D., Barillé, L., Belin, C., Lefebvre, A., & Bacher, C. (2013). Temporal changes in the phytoplankton community along the French coast of the eastern English Channel and the southern Bight of the North Sea. *ICES Journal of Marine Science*, *71*(4), 821–833. https://doi.org/10.1093/icesjms/fst192

Hoppenrath, M. (2004a). *A revised checklist of planktonic diatoms and dinoflagellates from Helgoland (North Sea , German Bight)*. 243–251. https://doi.org/10.1007/s10152-004-0190-6

Hoppenrath, M. (2004b). A revised checklist of planktonic diatoms and dinoflagellates from Helgoland (North Sea, German Bight). *Helgoland Marine Research*, *58*(4), 243–251. https://doi.org/10.1007/s10152-004-0190-6

Hoppenrath, M., Beszteri, B., Drebes, G., Halliger, H., Van Beusekom, J. E. E., Janisch, S., & Wiltshire, K. H. (2007). Thalassiosira species (Bacillariophyceae, Thalassiosirales) in the North Sea at Helgoland (German Bight) and Sylt (North Frisian Wadden Sea) - A first approach to assessing diversity. *European Journal of Phycology*, *42*(3), 271–288. https://doi.org/10.1080/09670260701352288

J. W. G. LUND, C. KIPLING, and E. D. L. C. (1958). *The inverted microscope method of estimating algal numbers and the statistical basis of estimations by counting*. *11*(2), 143–170. https://doi.org/10.1007/BF00007865

Kellogg, C. T. E., McClelland, J. W., Dunton, K. H., Crump, B. C., Weiss, S., Xu, Z. Z., Peddada, S., Amir, A., Bittinger, K., Gonzalez, A., Lozupone, C., Zaneveld, J. R., Vázquez-Baeza, Y., Birmingham, A., Hyde, E. R., Knight, R., Bond, S. L., Timsit, E., Workentine, M., … Léguillette, R. (2017). Upper and lower respiratory tract microbiota in horses: Bacterial communities associated with health and mild asthma (inflammatory airway disease) and effects of dexamethasone. *BMC Microbiology*, *5*(1), 1–11. https://doi.org/10.1186/s40168-017-0237-y

Kerckhof, F., Haelters, J., & Gollasch, S. (2007). Alien species in the marine and brackish ecosystem: The situation in Belgian waters. *Aquatic Invasions*, *2*(3), 243–257. https://doi.org/10.3391/ai.2007.2.3.9

Kersten, M., Dicke, M., Kriews, M., Naumann, K., Schmidt, D., Schulz, M., Schwikowski, M., & Steiger, M. (1993). Distribution and

Fate of Heavy Metals in the North Sea. *Pollution of the North Sea*, 300–347. https://doi.org/10.1007/978-3-642-73709-1_19
Kraberg, A., Kieb, U., Peters, S., & Wiltshire, K. H. (2019). An updated phytoplankton check-list for the Helgoland Roads time series station with eleven new records of diatoms and dinoflagellates. *Helgoland Marine Research*, *73*(1). https://doi.org/10.1186/s10152-019-0528-8
Lacroix, G., Ruddick, K., Ozer, J., & Lancelot. (2004). Modeling the impact of the Scheldt/Meuse plumes on the salinity distribution in Belgian waters (soutern North Sea). *Journal of Geophysical Research D: Atmospheres*, *110*(52), 149–163. https://doi.org/10.1029/2004JD005103
Lewis, K., & Allen, J. I. (2009). Validation of a hydrodynamic-ecosystem model simulation with time-series data collected in the western English Channel. *Journal of Marine Systems*, *77*(3), 296–311. https://doi.org/10.1016/j.jmarsys.2007.12.013
Louchart, A., Lizon, F., Lefebvre, A., Didry, M., Schmitt, F. G., & Artigas, L. F. (2020). Phytoplankton distribution from Western to Central English Channel, revealed by automated flow cytometry during the summer-fall transition. *Continental Shelf Research*, *195*(September 2019), 104056. https://doi.org/10.1016/j.csr.2020.104056
MacGillivary, M. L., & Kaczmarska, I. (2015). Paralia (Bacillariophyta) stowaways in ship ballast: implications for biogeography and diversity of the genus. *Journal of Biological Research-Thessaloniki*, *22*(1), 1–26. https://doi.org/10.1186/s40709-015-0024-5
Maliverno, E., Karatsolis, B. T., Dimiza, M. D., Lagaria, A., Psarra, S., & Triantaphyllou, M. V. (2016). Silicoflagellés actuels de la mer Egée du Nord-Est (Mer Méditerranée orientale) : morphologies et squelettes doubles. *Revue de Micropaleontologie*, *59*(3), 253–265. https://doi.org/10.1016/j.revmic.2016.06.001
Marie, D., Simon, N., & Vaulot, D. (2005). Phytoplankton Cell Counting by Flow Cytometry. *Algal Culturing Techniques*, *January*, 253–267. https://doi.org/10.1016/b978-012088426-1/50018-4
Massana, R. (2011). Eukaryotic Picoplankton in Surface Oceans. *Annual Review of Microbiology*, *65*(1), 91–110. https://doi.org/10.1146/annurev-micro-090110-102903
McCartney, K., Witkowski, J., Jordan, R. W., Daugbjerg, N., Malinverno, E., van Wezel, R., Kano, H., Abe, K., Scott, F., Schweizer, M., Young, J. R., Hallegraeff, G. M., & Shiozawa, A. (2014). Fine structure of silicoflagellate double skeletons. *Marine Micropaleontology*, *113*, 10–19. https://doi.org/10.1016/j.marmicro.2014.08.006
McMurdie, P. J., & Holmes, S. (2014). Waste Not, Want Not: Why Rarefying Microbiome Data Is Inadmissible. *PLoS Computational Biology*, *10*(4). https://doi.org/10.1371/journal.pcbi.1003531
McQuatters-Gollop, A., Johns, D. G., Bresnan, E., Skinner, J., Rombouts, I., Stern, R., Aubert, A., Johansen, M., Bedford, J., & Knights, A. (2017). From microscope to management: The critical value of plankton taxonomy to marine policy and biodiversity conservation. *Marine Policy*, *83*(May), 1–10. https://doi.org/10.1016/j.marpol.2017.05.022
Medinger, R., Nolte, V., Pandey, R. V., Jost, S., Ottenwälder, B., Schlötterer, C., & Boenigk, J. (2010). Diversity in a hidden world: Potential and limitation of next-generation sequencing for surveys of molecular diversity of eukaryotic microorganisms. *Molecular Ecology*, *19*(SUPPL. 1), 32–40. https://doi.org/10.1111/j.1365-294X.2009.04478.x
Meier, S., Muijsers, F., Beck, M., Badewien, T. H., & Hillebrand, H. (2015). Dominance of the non-indigenous diatom Mediopyxis helysia in Wadden Sea phytoplankton can be linked to broad tolerance to different Si and N supplies. In *Journal of Sea Research* (Vol. 95). Elsevier B.V. https://doi.org/10.1016/j.seares.2014.10.001
Metfies, K., Hessel, J., Klenk, R., Petersen, W., Wiltshire, K. H., & Kraberg, A. (2020). Uncovering the intricacies of microbial community dynamics at Helgoland Roads at the end of a spring bloom using automated sampling and 18S meta-barcoding. *PloS One*, *15*(6), e0233921. https://doi.org/10.1371/journal.pone.0233921
Mortelmans, J., Deneudt, K., Cattrijsse, A., Beauchard, O., Daveloose, I., Vyverman, W., Vanaverbeke, J., Timmermans, K., Peene, J., Roose, P., Knockaert, M., Chou, L., Sanders, R., Stinchcombe, M., Kimpe, P., Lammens, S., Theetaert, H., Gkritzalis, T., Hernandez, F., & Mees, J. (2019). Nutrient, pigment, suspended matter and turbidity measurements in the Belgian part of the North Sea. *Scientific Data*, *6*(1), 1–8. https://doi.org/10.1038/s41597-019-0032-7
Muylaert, K., Gonzales, R., Franck, M., Lionard, M., Van der Zee, C., Cattrijsse, A., Sabbe, K., Chou, L., & Vyverman, W. (2006). Spatial variation in phytoplankton dynamics in the Belgian coastal zone of the North Sea studied by microscopy, HPLC-CHEMTAX and underway fluorescence recordings. *Journal of Sea Research*, *55*(4), 253–265. https://doi.org/10.1016/j.seares.2005.12.002
Navarro, J. N., & De Peribonio, R. G. (2006). A light and scanning electron microscope study of the centric diatom Polymyxus coronalis (Bacillariophyta) . *European Journal of Phycology*, *28*(3), 167–172. https://doi.org/10.1080/09670269300650261
Nohe A., Knockaert C., Goffin A., Dewitte E., De Cauwer K., Desmit X., Vyverman W., Tyberghein L., Lagring R., S. K. (2018). *Marine phytoplankton community composition data from the Belgian part of the North Sea, 1968-2010.* VLIZ. https://doi.org/https://doi.org/10.14284/320
Nohe, A. (2020). *Long-term trends in phytoplankton biomass , composition and dynamics in the Belgian part of the North Sea*.
Nohe, A., Goffin, A., Tyberghein, L., Lagring, R., De Cauwer, K., Vyverman, W., & Sabbe, K. (2020). Marked changes in diatom and dinoflagellate biomass, composition and seasonality in the Belgian Part of the North Sea between the 1970s and 2000s. *Science of the Total Environment*, *716*. https://doi.org/10.1016/j.scitotenv.2019.136316
Nohe, A., Knockaert, C., Goffin, A., Dewitte, E., De Cauwer, K., Desmit, X., Vyverman, W., Tyberghein, L., Lagring, R., Sabbe, K., Knockaert, C., Lagring, R., Sabbe, K., Vyverman, W., Nohe, A., Desmit, X., Dewitte, E., & Goffin, A. (2018). Data Descriptor: Marine phytoplankton community composition data from the Belgian part of the North Sea, 1968-2010. *Scientific Data*, *5*, 1–

9. https://doi.org/10.1038/sdata.2018.126
Not, F., del Campo, J., Balagué, V., de Vargas, C., & Massana, R. (2009). New insights into the diversity of marine picoeukaryotes. *PLoS ONE*, *4*(9). https://doi.org/10.1371/journal.pone.0007143
Oksman, M., Juggins, S., Miettinen, A., Witkowski, A., & Weckström, K. (2019). The biogeography and ecology of common diatom species in the northern North Atlantic, and their implications for paleoceanographic reconstructions. *Marine Micropaleontology*, *148*(February), 1–28. https://doi.org/10.1016/j.marmicro.2019.02.002
OVERHEIDSDIENST, F., VOLKSGEZONDHEID, V. VAN DE, & LEEFMILIEU, V. E. (2020). *Koninklijk besluit tot vaststelling van het marien ruimtelijk plan voor de periode van 2020 tot 2026 in de Belgische zeegebieden.* 52.
Pavan-Kumar, A., Gireesh-Babu, P., & Lakra, W. S. (2015). DNA Metabacoding: a new approach for rapid biodiversity assessment. *Journal of Cell Science and Molecular Biology*, *2*(1), 111. http://opensciencepublications.com/fulltextarticles/JCMB-2350-0190-2-111.html
Paxinos, R. (2000). A rapid Utermohl method for estimating algal numbers. *Journal of Plankton Research*, *22*(12), 2255–2262. https://doi.org/10.1093/plankt/22.12.2255
Paxinos, Rosemary, & Mitchell, J. G. (2015). *A rapid Utermöhl method for estimating algal numbers A rapid Utermöhl method for estimating algal numbers*. *February*.
Pecceu, E., Hostens, K., & Maes, F. (2016). Governance analysis of MPAs in the Belgian part of the North Sea. *Marine Policy*, *71*, 265–274. https://doi.org/10.1016/j.marpol.2015.12.017
Philippart, C. J. M., Salama, M. S., Kromkamp, J. C., van der Woerd, H. J., Zuur, A. F., & Cadée, G. C. (2013). Four decades of variability in turbidity in the western Wadden Sea as derived from corrected Secchi disk readings. *Journal of Sea Research*, *82*(September), 67–79. https://doi.org/10.1016/j.seares.2012.07.005
Pierella Karlusich, J. J., Ibarbalz, F. M., & Bowler, C. (2020). Phytoplankton in the Tara Ocean . *Annual Review of Marine Science*, *12*(1), 233–265. https://doi.org/10.1146/annurev-marine-010419-010706
Pitcher, G. C., & Probyn, T. A. (2016). Suffocating phytoplankton, suffocating waters - red tides and anoxia. *Frontiers in Marine Science*, *3*(186). https://doi.org/10.3389/mars.2016.001.186
Piwosz, K., Shabarova, T., Pernthaler, J., Posch, T., Šimek, K., Porcal, P., & Salcher, M. M. (2020). Bacterial and Eukaryotic Small-Subunit Amplicon Data Do Not Provide a Quantitative Picture of Microbial Communities, but They Are Reliable in the Context of Ecological Interpretations. *MSphere*, *5*(2), 14. https://doi.org/10.1128/msphere.00052-20
Prins, T. C., Desmit, X., & Baretta-Bekker, J. G. (2012). Phytoplankton composition in Dutch coastal waters responds to changes in riverine nutrient loads. *Journal of Sea Research*, *73*, 49–62. https://doi.org/10.1016/j.seares.2012.06.009
Rachik, S., Li, L. L., Breton, E., Christaki, U., Monchy, S., & Genitsaris, S. (2018). Diversity and potential activity patterns of planktonic eukaryotic microbes in a mesoeutrophic coastal area (eastern English Channel). *Plos One*, *13*(5), e0196987. https://doi.org/10.1371/journal.pone.0196987
Ratnasingham, S., & Hebert, P. D. N. (2007). The Barcode of Life Data System (www.barcodinglife.org). *Molecular Ecology Notes*, *7*(April 2016), 355–364. https://doi.org/10.1111/j.1471-8286.2006.01678.x
Redfield, a C., Ketchum, B. H., & Richards, F. a. (1963). The influence of organisms on the composition of sea water. *The Sea*, *2*, 26–77.
Reise, K., Gollasch, S., & Wolff, W. J. (1998). Introduced marine species of the North Sea coasts. *Helgolander Meeresuntersuchungen*, *52*(3–4), 219–234. https://doi.org/10.1007/BF02908898
Rind, D., Perlwitz, J., & Lonergan, P. (2005). AO/NAO response to climate change: 1. Respective influences of stratospheric and tropospheric climate changes. *Journal of Geophysical Research D: Atmospheres*, *110*(12), 1–15. https://doi.org/10.1029/2004JD005103
Rousseau, V, Lancelot, C., & Cox, D. (2006). *Current Status of Eutrophication in the Belgian Coastal Zone*. *190*, 1–122.
Rousseau, Véronique, Leynaert, A., Daoud, N., & Lancelot, C. (2002). Diatom succession, silicification and silicic acid availability in Belgian coastal waters (Southern North Sea). *Marine Ecology Progress Series*, *236*(July 2002), 61–73. https://doi.org/10.3354/meps236061
Royal Decree. (2014). *Marine Spatial Plan for the Belgian part of the North Sea*. 1–167. https://www.health.belgium.be/sites/default/files/uploads/fields/fpshealth_theme_file/19094275/Summary Marine Spatial Plan.pdf
Ruddick, K., & Lacroix, G. (2006). Hydrodynamics and meteorology of the Belgian Coastal Zone parameters , time and space scales. *Physical Oceanography*, 1–15.
Samuel Shephard1*, Simon P. R. Greenstreet2, GerJan J. Piet3, Anna Rindorf4, and M. D.-C. (2015). Surveillance indicators and their use in implementation of the Marine Strategy Framework Directive. *Encyclopedia of Environment and Society*, *72*(8), 2269–2277. https://doi.org/10.4135/9781412953924.n678
Sar, E. A., Sterrenburg, F. A. S., Lavigne, A. S., & Sunesen, I. (2013). Diatoms from marine coastal environments of Argentina. Species of the genus Pleurosigma (Pleurosigmataceae). *Boletin de La Sociedad Argentina de Botanica*, *48*(1), 17–51.
Sarno, D., Kooistra, W. H. C. F., Medlin, L. K., Percopo, I., & Zingone, A. (2005). Diversity in the genus Skeletonema (Bacillariophyceae). II. An assessment of the taxonomy of S. costatum-like species with the description of four new species. *Journal of Phycology*, *41*(1), 151–176. https://doi.org/10.1111/j.1529-8817.2005.04067.x

Sims, P. A., Williams, D. M., & Ashworth, M. (2018). Examination of type specimens for the genera Odontella and Zygoceros (Bacillariophyceae) with evidence for the new family Odontellaceae and a description of three new genera. *Phytotaxa*, *382*(1), 1–56. https://doi.org/10.11646/phytotaxa.382.1.1

Sjöqvist C., Godhe A., Johnsson P. R., Sundqvist L., K. A. (2015). Local adaptation and oceanographic connectivity patterns explain genetic differentiation of a marine diatom across the North Sea – Baltic Sea salinity gradient. *Molecular Ecology*, *24*, 2871–2885. https://doi.org/10.1111/mec.13208

Škaloud, P., Řezáčová, M., & Ellegaard, M. (2006). Spatial distribution of phytoplankton in Spring 2004 along a transect in the eastern part of the North Sea. *Journal of Oceanography*, *62*(5), 717–729. https://doi.org/10.1007/s10872-006-0089-8

Taberlet, P., & Coissac, E. (2012). Towards next-generation biodiversity assessment using DNA metabarcoding. *Molecular Ecology*, *21*, 2045–2050.

Terseleer, N., Bruggeman, J., Lancelot, C., & Gypens, N. (2014). Trait-based representation of diatom functional diversity in a plankton functional type model of the eutrophied southern north sea. *Limnology and Oceanography*, *59*(6), 1958–1972. https://doi.org/10.4319/lo.2014.59.6.1958

Tillmann, U., Borel, C. M., Barrera, F., Lara, R., Krock, B., Almandoz, G. O., Witt, M., & Trefault, N. (2016). Azadinium poporum from the Argentine Continental Shelf, Southwestern Atlantic, produces azaspiracid-2 and azaspiracid-2 phosphate. *Harmful Algae*, *51*(December 2015), 40–55. https://doi.org/10.1016/j.hal.2015.11.001

Tillmann, U., Hoppenrath, M., & Gottschling, M. (2019). Reliable determination of Prorocentrum micans Ehrenb. (Prorocentrales, Dinophyceae) based on newly collected material from the type locality. *European Journal of Phycology*, *54*(3), 417–431. https://doi.org/10.1080/09670262.2019.1579925

Töpke. (2009). *An analysis of phytoplankton dynamics in the Belgian Coastal Zone of the North Sea based on microscopical cell counts and pigment analysis* .

Tragin, M., Zingone, A., Vaulot, D., Hernández-Fariñas, T., Soudant, D., Barillé, L., Belin, C., Lefebvre, A., Bacher, C., Thyssen, M., Alvain, S., Lefèbvre, A., Dessailly, D., Rijkeboer, M., Guiselin, N., Creach, V., Artigas, L. F., Lefebvre, A., Guiselin, N., … Barnes, M. K. (2020). Temporal changes in the phytoplankton community along the French coast of the eastern English Channel and the southern Bight of the North Sea. *ICES Journal of Marine Science*, *68*(January 2015), e0233921. https://doi.org/10.1016/j.seares.2012.06.009

Tréguer, P., Bowler, C., Moriceau, B., Dutkiewicz, S., Gehlen, M., Aumont, O., Bittner, L., Dugdale, R., Finkel, Z., Iudicone, D., Jahn, O., Guidi, L., Lasbleiz, M., Leblanc, K., Levy, M., & Pondaven, P. (2018). Influence of diatom diversity on the ocean biological carbon pump. *Nature Geoscience*, *11*(1), 27–37. https://doi.org/10.1038/s41561-017-0028-x

Tsimplis, M. N., Shaw, A. G. P., Flather, R. A., & Woolf, D. K. (2006). The influence of the North Atlantic Oscillation on the sea-level around the northern European coasts reconsidered: The thermosteric effects. *Philosophical Transactions of the Royal Society A: Mathematical, Physical and Engineering Sciences*, *364*(1841), 845–856. https://doi.org/10.1098/rsta.2006.1740

Van den Eynde D Lauwaert B, Pichot G, K. F. (2007). *Ontwikkeling van de zandbank ter hoogte van Heist. Eindrapport*.

Van Oostende, N., Harlay, J., Vanelslander, B., Chou, L., Vyverman, W., & Sabbe, K. (2012). Phytoplankton community dynamics during late spring coccolithophore blooms at the continental margin of the Celtic Sea (North East Atlantic, 2006-2008). *Progress in Oceanography*, *104*, 1–16. https://doi.org/10.1016/j.pocean.2012.04.016

Wang, Q., Garrity, G. M., Tiedje, J. M., & Cole, J. R. (2007). Naïve Bayesian classifier for rapid assignment of rRNA sequences into the new bacterial taxonomy. *Applied and Environmental Microbiology*, *73*(16), 5261–5267. https://doi.org/10.1128/AEM.00062-07

Weiss, S., Xu, Z. Z., Peddada, S., Amir, A., Bittinger, K., Gonzalez, A., Lozupone, C., Zaneveld, J. R., Vázquez-Baeza, Y., Birmingham, A., Hyde, E. R., & Knight, R. (2017). Normalization and microbial differential abundance strategies depend upon data characteristics. *Microbiome*, *5*(1), 1–18. https://doi.org/10.1186/s40168-017-0237-y

Widdicombe, C. E., Eloire, D., Harbour, D., Harris, R. P., & Somerfield, P. J. (2010). Long-term phytoplankton community dynamics in the Western English Channel. *Journal of Plankton Research*, *32*(5), 643–655. https://doi.org/10.1093/plankt/fbp127

Wilks, J. V., & Armand, L. K. (2017). Diversity and taxonomic identification of Shionodiscus spp. in the Australian sector of the Subantarctic Zone. *Diatom Research*, *32*(3), 295–307. https://doi.org/10.1080/0269249X.2017.1365015

Winder, M., & Sommer, U. (2012). Phytoplankton response to a changing climate. *Hydrobiologia*, *698*(1), 5–16. https://doi.org/10.1007/s10750-012-1149-2

Wright, S., & Jeffrey, S. (1996). Phytoplankton Pigments in Oceanography:Guidelines To Modern Methods. *Unesco Publishing*.

Wright, S. W., W., J. S., R.F.C, M., C., L. C., T., B., D., R., Wel, & N., S. (1991). Improved HPLC method for the analysis of chlorophylls and carotenoids from marine phytoplankton. *Marine Ecology Progress Series Mar. Ecol. Prog. Ser.*, *77*(183–196). http://www.embase.com/search/results?subaction=viewrecord&from=export&id=L614090177%0Ahttp://library.deakin.edu.au/resserv?sid=EMBASE&issn=10976868&id=doi:&atitle=Perinatal+outcomes+of+twin+twin+transfusion+syndrome+based+on+gestational+age+at+time+of+sel

Yahia-Kéfi, O. D., Souissi, S., De Stefano, M., & Yahia, M. N. D. (2005). Bellerochea horologicalis and Lithodesmioides polymorpha var. tunisiense var. nov. (Coscinodiscophyceae, Bacillariophyta) in the Bay of Tunis: Ultrastructural observations and spatio-temporal distribution. *Botanica Marina*, *48*(1), 58–72. https://doi.org/10.1515/BOT.2005.009

APPENDIX

Appendix 1: Sampling protocol

In general

- Sample stations 120, ZG02, 700 en 780
- At every station before sampling, rinse all used material with local sea water from the hose while the CTD is being taken (E.g. rinse barrel, beakers, phytoplankton net, measuring cylinder, bucket,…)
- Ask for 2 CTD's and put them together in the big black barrel so there will be enough water (the CTD only needs to be on the first time it goes down)
- Gently stir the water in the barrel every time you take water for a sample.
- The barrel with the liquid nitrogen needs to be tied somewhere so it does not fall over. Make sure you never get liquid nitrogen on your skin as it can cause burns and try to avoid inhaling it.
- Take the samples in the following order
- The sampling takes about 25 minutes in total

2 x 100 ml sample

- stir water and take 2 times 100 ml with a measuring cylinder
- put the 100 ml in a bottle and fix both bottles with 1 ml Lugol
- There are no special labels for these samples, just write: date + station+ "100ml" on the bottles and caps in marker.
- Store in fridge

2x DNA samples

- Try to work on a clean surface of tin foil when handling the filters
- Prepare the following steps beforehand:
- Clean tweezers, syringe and filter heads for filters with milliQ water, use gloves

  Put the 3µm and 0.8 µm filters in the filter heads, put the ring on top and close the filter heads. Remember which filter is in which head (you can write the size on the filter heads if you want). The filter papers are separated by matte papers in between so make sure you use the filters which are glossy.

  Stir water in barrel and take 2L of water with the beaker and pre-filter it over a 50µm mesh (it looks like a big bottle cut in half with a red, cut out cap in which a mesh is screwed)
- Mix the water in the beaker and fill the syringe with 60 ml of this filtrate

- Put the filter heads on (in correct order: the 3µm filter on top of the syringe and the 0.8µm filter on top of the 3µm filter) and push the water through the filters. Repeat this as much as possible and keep track of the volume filtered. This will become progressively harder and will require some muscle. Sometimes it helps if you put the back of the syringe against a wall and push it against the wall with your bodyweight. On shore stations, especially at Zeebrugge will be hard because of the sediment.
- When finished, blow dry air through to filters to dry them
- Open the filter heads and take the filters out with rinse tweezers and gloves, only touch the edge of the filters. Fold the filters and put them in separate cryovails
- There are special labels for the cryovails . Write the: date + station+ fraction (3µm or 0.8µm) + volume on the white side of the label. Stick this side around the cryovail and then cover this with the transparent side.
- Store in liquid nitrogen

2 Net samples

- Try to rinse the net well between the stations
- Put a bottle on the bottom of the net.
- Filter as much water as possible through 10µm plankton net until it clogs (keep track of the sampled volume by using 2L beakers). If the net clogs too much you can gently beat it or tilt the net so the water can leak out on the top part.
- (If you want to save some time you could already fill the net with as much water as possible right after you take the 2L for the DNA sampling. You can then hang the net somewhere so the water can leak out while you do the DNA sampling with the syringe)
- Use some water to rinse the sides of the net so that the phytoplankton is in the bottle and not on the net
- Unscrew the bottle and split the filtrate in half so you have 2 bottles. Fix one bottle with 1% Lugol, the other bottle is a live sample and needs no fixation. (For one 1% Lugol: measure the volume you want to fix and add 1% of that volume of Lugol e.g. 1ml of lugol in 100ml sample)
- There are no special labels for these samples, just write: date + station+ volume + life or lugol + “net” on the bottle and cap.
- Store in fridge

Packing list

- LN_2 container
- 100 ml sample bottles (4 per station = 16)
- 100 ml measuring cylinder
- Lugol solution in dropper bottle
- Plastic Pasteur pipettes
- Marker
- Tin foil
- Tweezers
- Syringe
- 2 filter holders + 1 back-up
- Filters
    - 0.8µm membrane
    - 3.0 µm membrane
- Barrel
- Sampling bucket with cord
- Cut-off filter with 50µm mesh
- Cryovails (2 per station = 4 + some back-up)
- Cryolabels
- 10µm Plankton net
- 2L Beakers
- Cooler + cooling elements

Appendix 2: DNA extraction protocol

DNeasy Powerlyzer Microbial Kit (Qiagen, Hilden, Germany)[2]
Note: step 1 to 4 are adjusted because we sample DNA with the use of filters. We chose to add the beads from the Glass PowerBead Tube to an Eppendorf tube with the filters. Subsequently we added 300 µl PowerBead solution and 50 µl solution SL and shaking the tubes in a beadbeater for 3 min. at a frequency of 30Hz. Tubes were put on ice and we proceeded from step 5 onwards with the protocol from the manufacturer (see below).

[2] https://www.qiagen.com/us/products/discovery-and-translational-research/dna-rna-purification/dna-purification/microbial-dna/dneasy-powerlyzer-microbial-kit/#technicalspecification

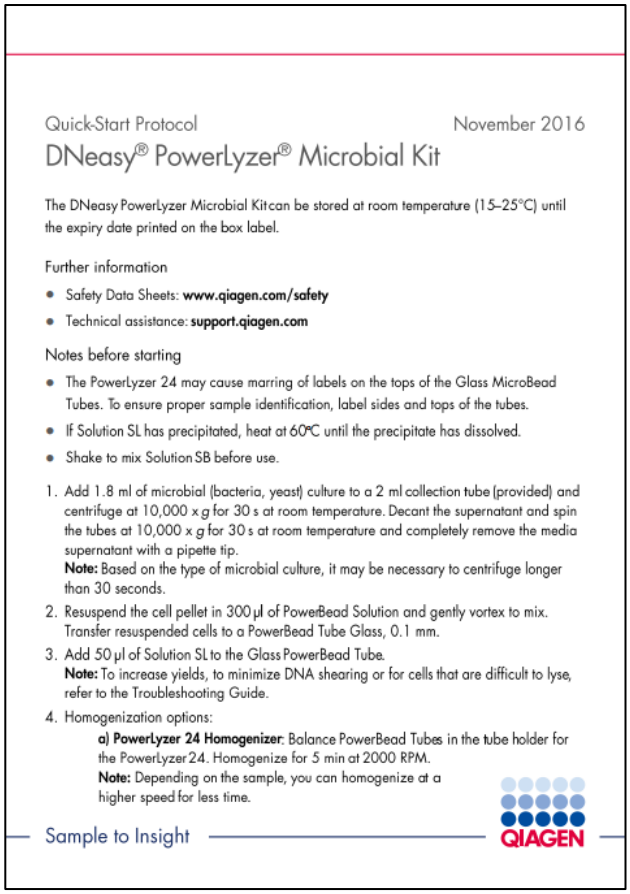

Quick-Start Protocol November 2016

DNeasy® PowerLyzer® Microbial Kit

The DNeasy PowerLyzer Microbial Kit can be stored at room temperature (15–25°C) until the expiry date printed on the box label.

Further information

- Safety Data Sheets: **www.qiagen.com/safety**
- Technical assistance: **support.qiagen.com**

Notes before starting

- The PowerLyzer 24 may cause marring of labels on the tops of the Glass MicroBead Tubes. To ensure proper sample identification, label sides and tops of the tubes.
- If Solution SL has precipitated, heat at 60°C until the precipitate has dissolved.
- Shake to mix Solution SB before use.

1. Add 1.8 ml of microbial (bacteria, yeast) culture to a 2 ml collection tube (provided) and centrifuge at 10,000 x *g* for 30 s at room temperature. Decant the supernatant and spin the tubes at 10,000 x *g* for 30 s at room temperature and completely remove the media supernatant with a pipette tip.
   Note: Based on the type of microbial culture, it may be necessary to centrifuge longer than 30 seconds.
2. Resuspend the cell pellet in 300 µl of PowerBead Solution and gently vortex to mix. Transfer resuspended cells to a PowerBead Tube Glass, 0.1 mm.
3. Add 50 µl of Solution SL to the Glass PowerBead Tube.
   Note: To increase yields, to minimize DNA shearing or for cells that are difficult to lyse, refer to the Troubleshooting Guide.
4. Homogenization options:
   a) PowerLyzer 24 Homogenizer: Balance PowerBead Tubes in the tube holder for the PowerLyzer 24. Homogenize for 5 min at 2000 RPM.
   Note: Depending on the sample, you can homogenize at a higher speed for less time.

Sample to Insight

QIAGEN

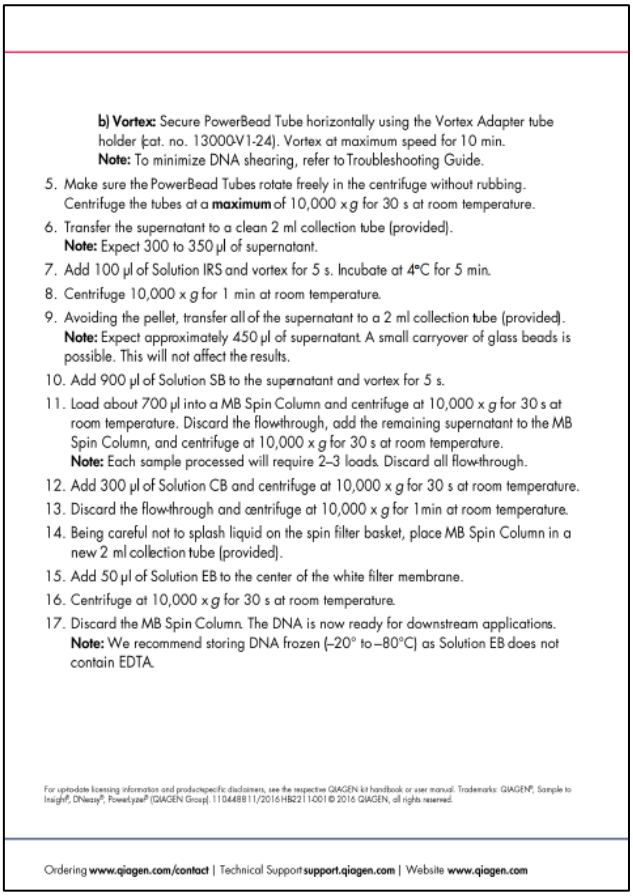

b) Vortex: Secure PowerBead Tube horizontally using the Vortex Adapter tube holder (cat. no. 13000-V1-24). Vortex at maximum speed for 10 min.
Note: To minimize DNA shearing, refer to Troubleshooting Guide.

5. Make sure the PowerBead Tubes rotate freely in the centrifuge without rubbing. Centrifuge the tubes at a **maximum** of 10,000 x *g* for 30 s at room temperature.
6. Transfer the supernatant to a clean 2 ml collection tube (provided).
   Note: Expect 300 to 350 µl of supernatant.
7. Add 100 µl of Solution IRS and vortex for 5 s. Incubate at 4°C for 5 min.
8. Centrifuge 10,000 x *g* for 1 min at room temperature.
9. Avoiding the pellet, transfer all of the supernatant to a 2 ml collection tube (provided).
   Note: Expect approximately 450 µl of supernatant. A small carryover of glass beads is possible. This will not affect the results.
10. Add 900 µl of Solution SB to the supernatant and vortex for 5 s.
11. Load about 700 µl into a MB Spin Column and centrifuge at 10,000 x *g* for 30 s at room temperature. Discard the flowthrough, add the remaining supernatant to the MB Spin Column, and centrifuge at 10,000 x *g* for 30 s at room temperature.
    Note: Each sample processed will require 2–3 loads. Discard all flow-through.
12. Add 300 µl of Solution CB and centrifuge at 10,000 x *g* for 30 s at room temperature.
13. Discard the flow-through and centrifuge at 10,000 x *g* for 1 min at room temperature.
14. Being careful not to splash liquid on the spin filter basket, place MB Spin Column in a new 2 ml collection tube (provided).
15. Add 50 µl of Solution EB to the center of the white filter membrane.
16. Centrifuge at 10,000 x *g* for 30 s at room temperature.
17. Discard the MB Spin Column. The DNA is now ready for downstream applications.
    Note: We recommend storing DNA frozen (–20° to –80°C) as Solution EB does not contain EDTA.

Ordering **www.qiagen.com/contact** | Technical Support **support.qiagen.com** | Website **www.qiagen.com**

Appendix 3: PCR protocol

Mix:

- Buffer: 2.5 µl
- dNTP's: 2.5 µl
- primer: 2* 2µl
- water: 14.75 µl
- Taq: 0.25 µl
- DNA: 1µl for 35 cycles 2µl for 40 cycles

PCR program:

- 94°C for 5min (denaturation)

For 35-40 cycles:

- 94°C for 1 min
- 57°C-52°C for 1 min (annealing) (we go down 0.5°C each cycles for 10 cycles, then 30 cycles at lowest temperature)
- 72°C for 3 min (elongation)
- 72°C for 20m (for equal elongation of all sequences)

Appendix 4: Protocol Library prep

Mix:

- Buffer: 5µl
- dNTP's: 5µl
- tags: 3.5µl each
- water: 25 µl
- DNA: 7.5µl
- Taq: 0.5 µl

➔ End volume of 50µl in each well

PCR program :

94°C for 5 min

For 14-16 cycles:

- 94°C for 1 min
- 55°C for 1 min
- 72°C for 3 min
- 72°C for 20 min

➔ For samples 2E, 5F, 5H, 6A, 6B, 6C, 6D, 6E, 6F, 6G, 6H, 7A, 7B, and 7C 14 cycles didn't suffice, so these samples were run for 16 cycles

Table 9: Plate library prep. Legend see below.

	lib prep tag	N716	N718	N719	N720	N721	N722	N723
lib prep tag		1	2	3	4	5	6	7
S502	A	13	22	38	7	A7	31(1)	6
S503	B	14	23	39	17 (1)	A6	32(1)	11
S505	C	15	24	44	37 (1)	A8	33	42
S506	D	16	26	17 (2)	8	A12	34(1)	(-)
S507	E	17 (2)	27	37 (2)	12	19	35	
S508	F	18	28	1	A9	25	40	
S510	G	20	36	2	A11	29	41	
S511	H	21	37 (2)	5	A5	30 (1)	43	

Legend plate:

Control PCR:

- Samples 17 and 37 were replicated 5 times and added 3 times each in the well plate (number of replicates per well indicated between brackets)
- Negative PCR product was added indicated by (-)

Control library prep:

- Samples starting with A are samples from a previous campaign who were already extracted and sequenced but the PCR product was added to check for the accuracy of the library prep

PCR notes:

- Grey: 35 PCR cycles
- Blue: 40 PCR cycles
- For some samples we could only get one replicate, indicated by (1)

Appendix 5 : microscopic count data on oxidized slides

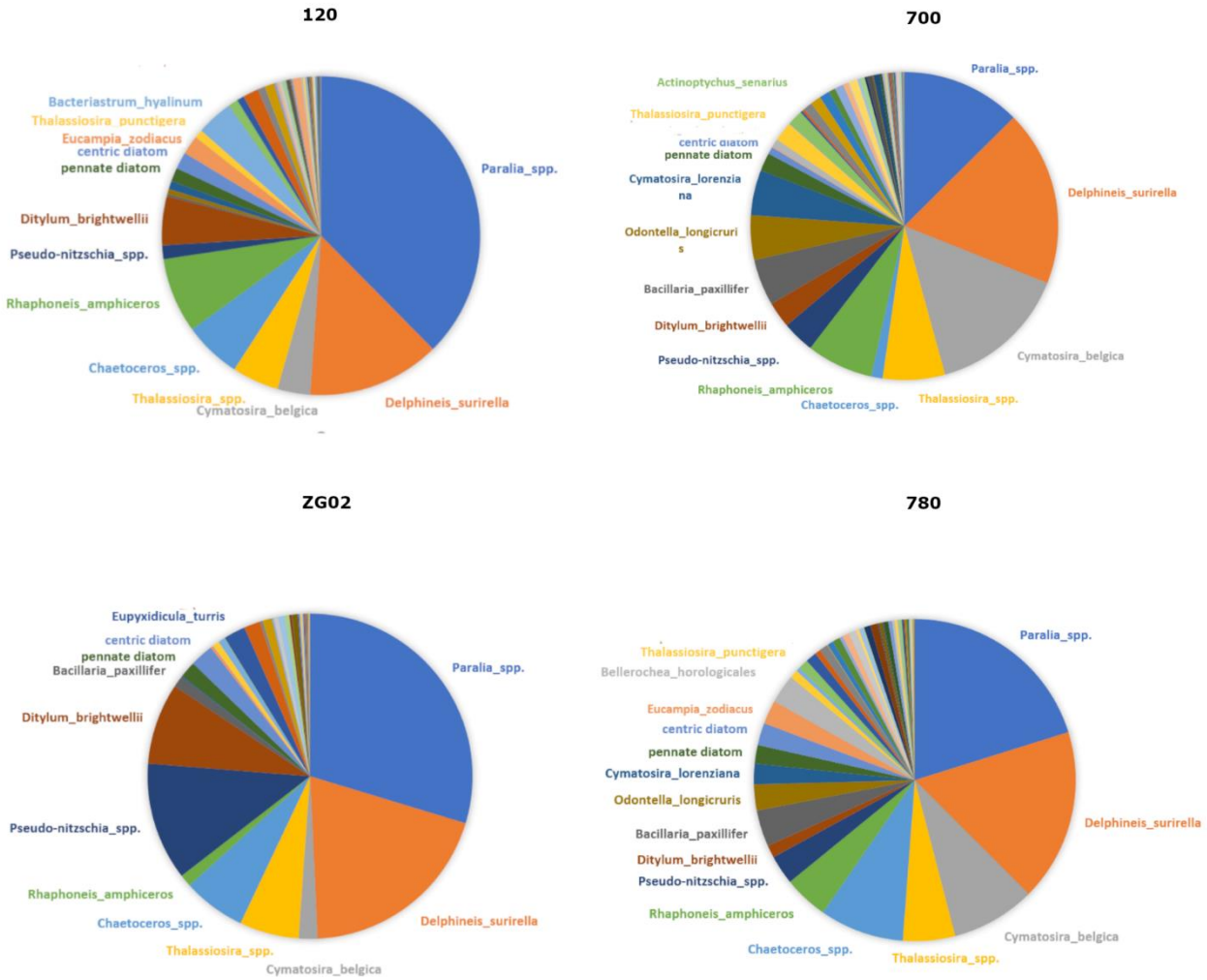

Figure 39:Relative abundance of species in the microscopic count data on oxidized material displayed for the 4 different stations. Only the names of the most abundant species are displayed.

Appendix 6: ordinations amplicon sequencing

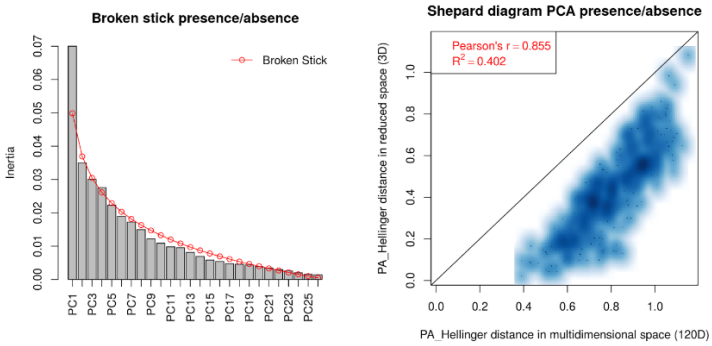

Figure 40: Broken stick model and Shepard diagram for presence/absence ordinations.

A

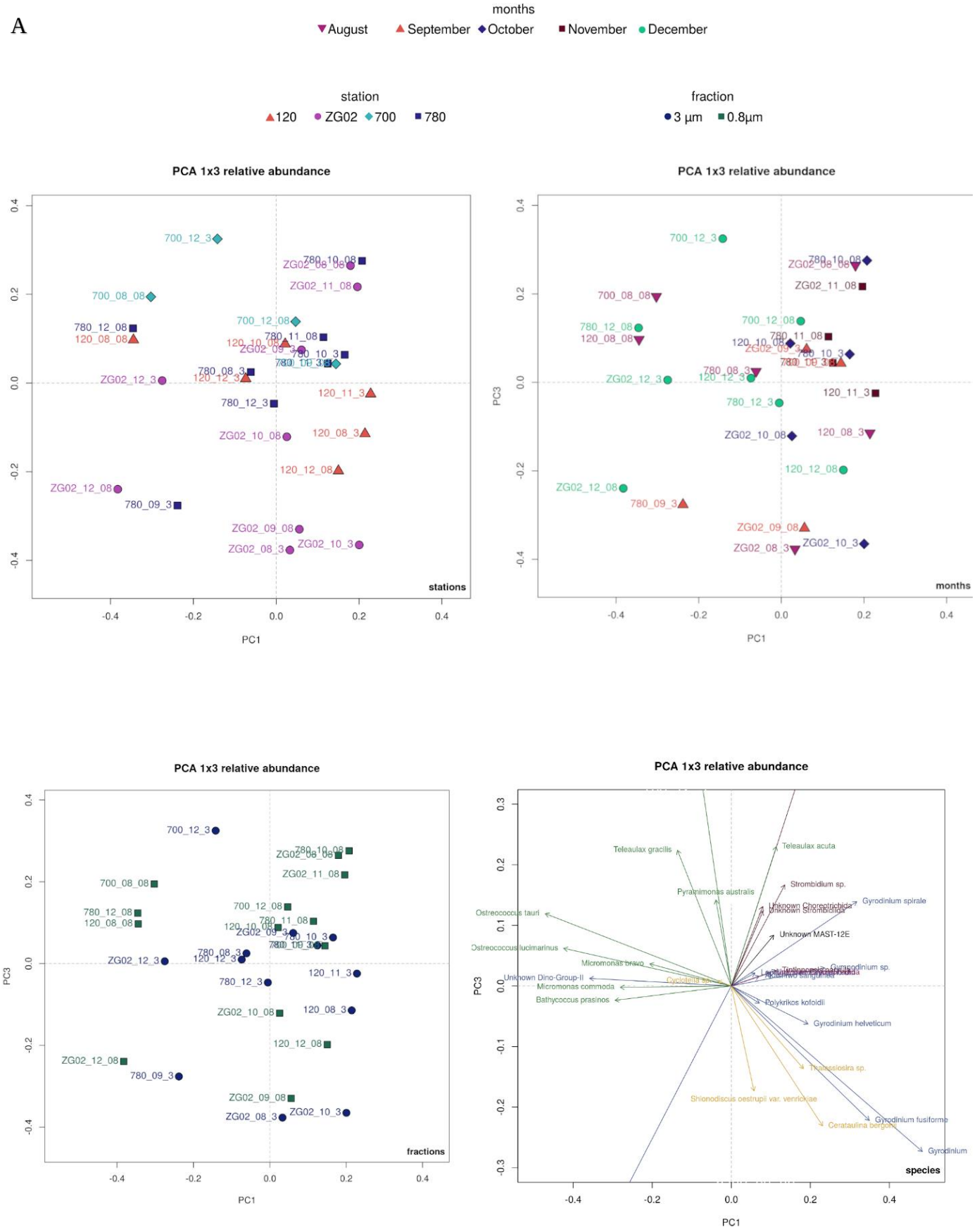
months
August
September
October
November
December
station
120
ZG02
700
780
fraction
3 µm
0.8µm
PCA 1x3 relative abundance
stations
months
fractions
species
PC1
PC3
700_12_3
700_08_08
780_12_08
120_08_08
ZG02_12_3
780_12_3
ZG02_10_08
ZG02_12_08
780_09_3
ZG02_09_08
ZG02_08_3
ZG02_10_3
ZG02_11_08
700_12_08
780_11_08
780_08_3
120_12_3
120_11_3
120_08_3
120_12_08
Teleaulax gracilis
Teleaulax acuta
Pyramimonas australis
Strombidium sp.
Gyrodinium spirale
Ostreococcus tauri
Ostreococcus lucimarinus
Micromonas bravo
Micromonas commoda
Bathycoccus prasinos
Unknown MAST-12E
Gymnodinium sp.
Polykrikos kofoidii
Gyrodinium helveticum
Gyrodinium fusiforme
Gyrodinium

B

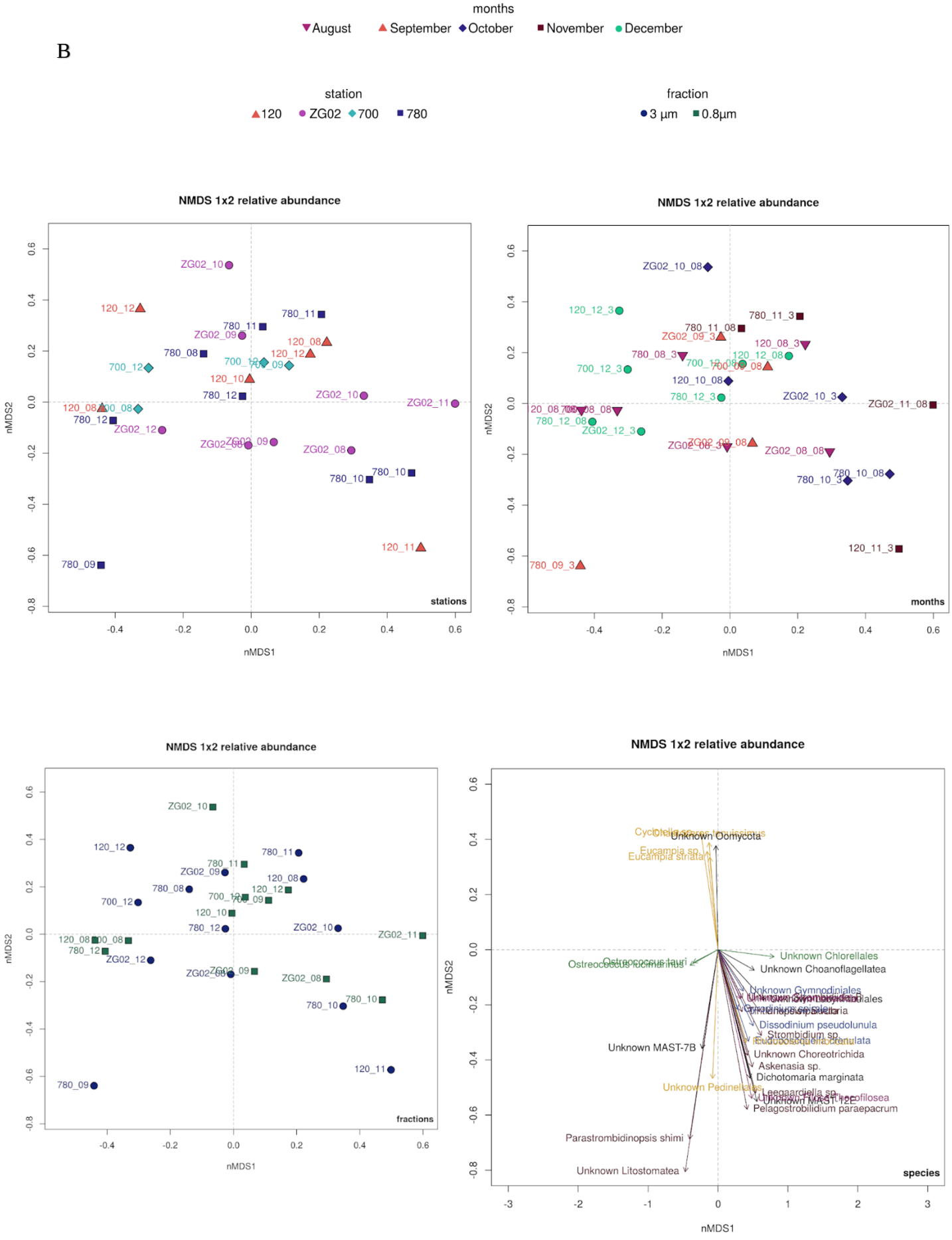
months
August
September
October
November
December
station
120
ZG02
700
780
fraction
3 µm
0.8µm
NMDS 1x2 relative abundance
stations
months
fractions
species
nMDS1
nMDS2
Unknown Oomycota
Eucampia sp.
Eucampia striata
Unknown Chlorellales
Unknown Choanoflagellatea
Unknown Gymnodiniales
Dissodinium pseudolunula
Strombidium sp.
Unknown MAST-7B
Unknown Choreotrichida
Askenasia sp.
Dichotomaria marginata
Unknown Litostomatea
Pelagostrobilidium paraepacrum
Parastrombidinopsis shimi

C

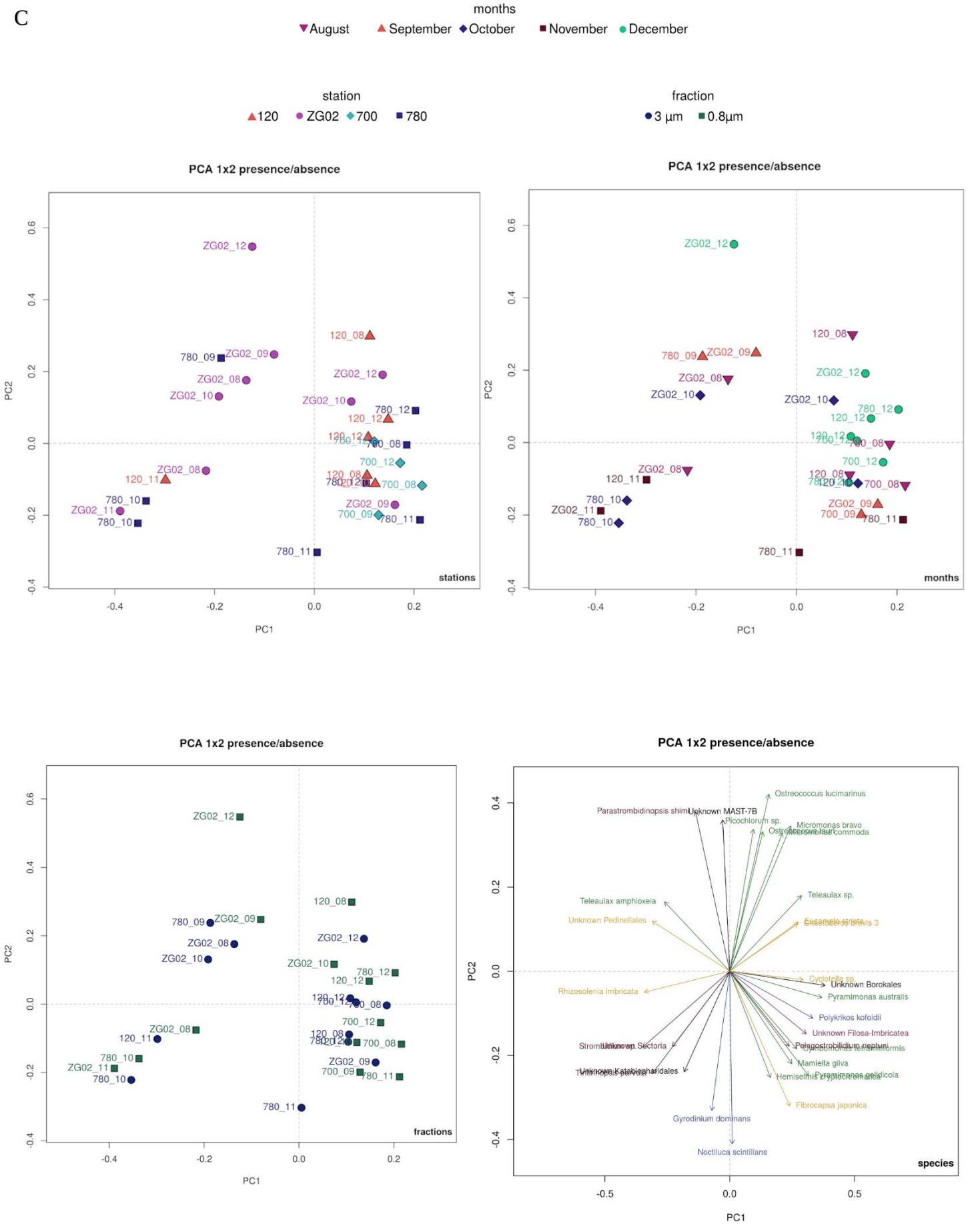
months
August
September
October
November
December
station
120
ZG02
700
780
fraction
3 µm
0.8µm
PCA 1x2 presence/absence
stations
months
fractions
species
PC1
PC2
Ostreococcus lucimarinus
Parastrombidinopsis shimi
Unknown MAST-7B
Picochlorum sp.
Micromonas bravo
Teleaulax amphioxeia
Teleaulax sp.
Unknown Pedinellales
Cyclotella sp.
Unknown Borokales
Rhizosolenia imbricata
Pyramimonas australis
Polykrikos kofoidii
Unknown Filosa-Imbricatea
Mamiella gilva
Fibrocapsa japonica
Gyrodinium dominans
Noctiluca scintillans

D

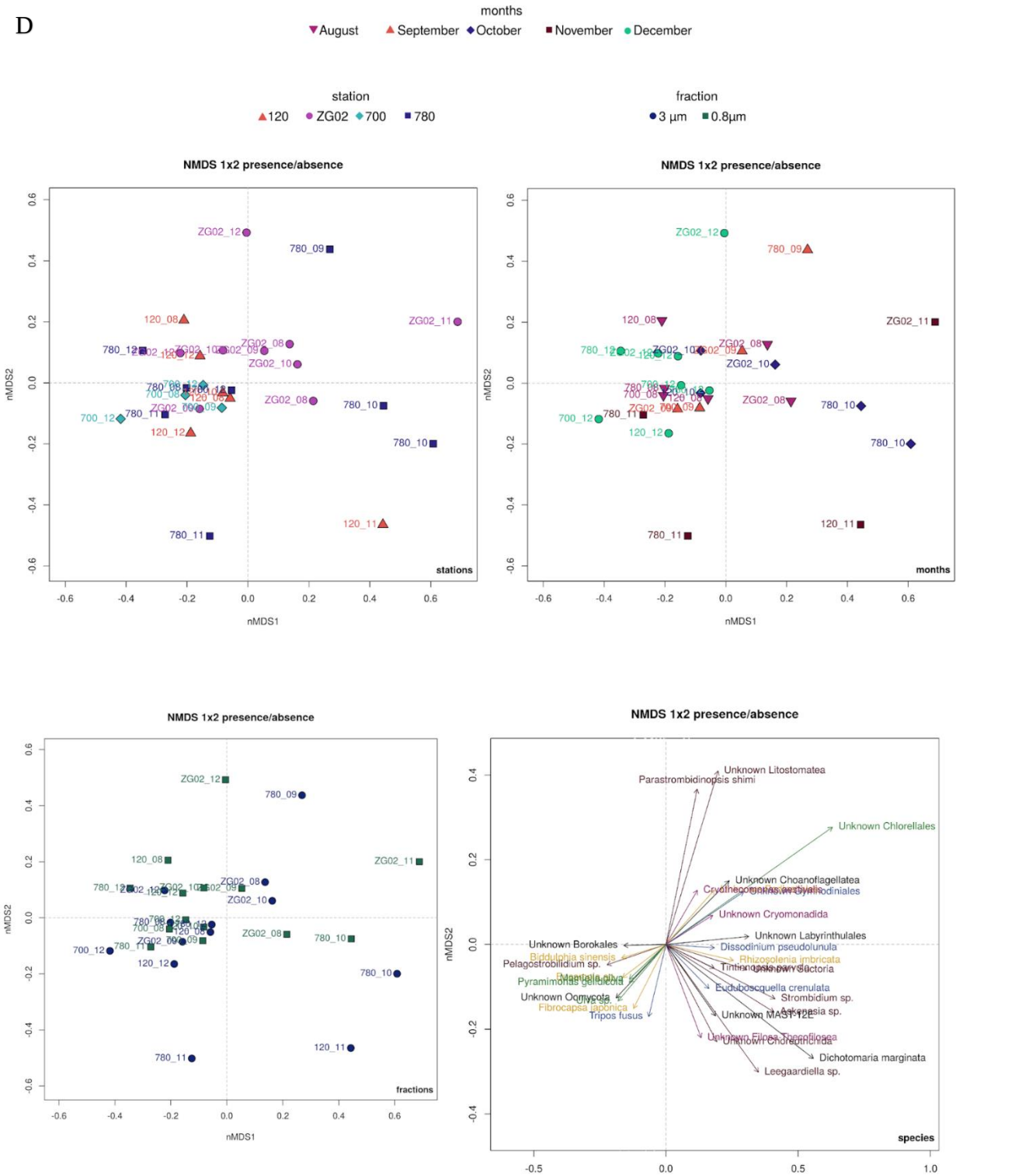

Figure 41: Ordinations for amplicon sequencing based on Hellinger transformed Euclidean distance count tables. Symbols and colours for stations, months and fractions as indicated in the right bottom corner of the first three graphs. The 30 most relevant species plotted for community structure are displayed in the fourth graph, species names are coloured for divisions. Species displayed have a relative abundance higher than 1% for at least one of the samples.

A.PCA for relative abundance 1x3 B. NMDS for relative abundance. C. PCA for presence/absence. D. NMDS for presence/absence.

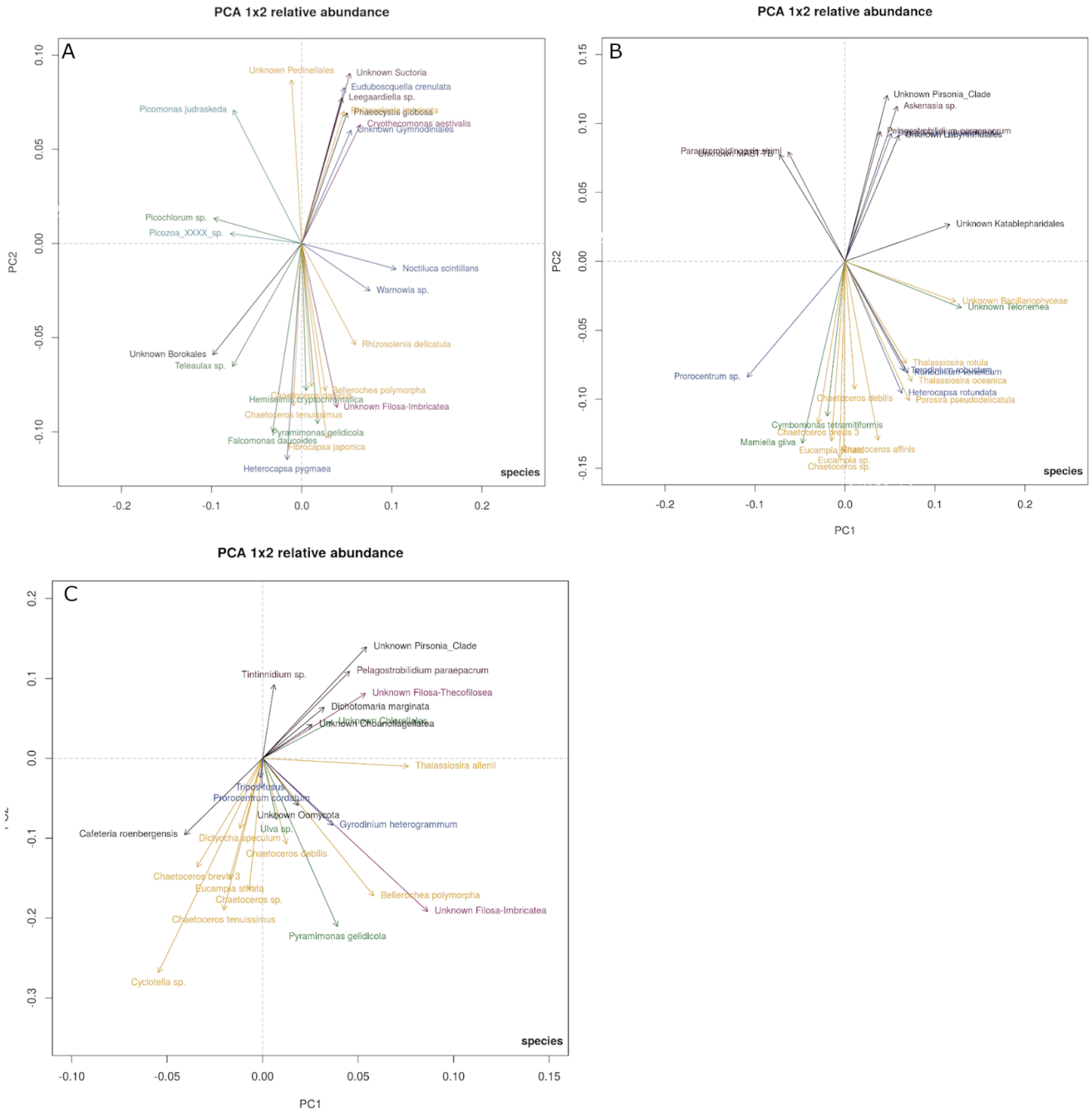

Figure 42: Species 31-104 for the PCA on Hellinger transformed relative abundance. Names and arrows are coloured according to division. For display purposes the species are divided over 3 plots, in decreasing order. Plot A species 31-60, plot B species 61-80, plot C species 81-104.

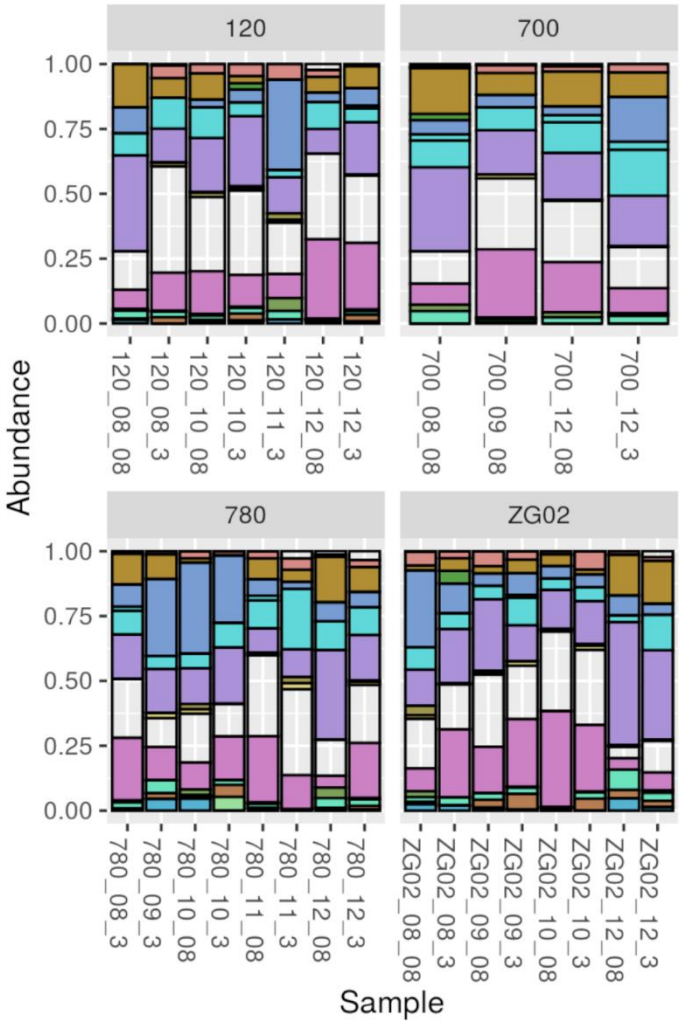

stations

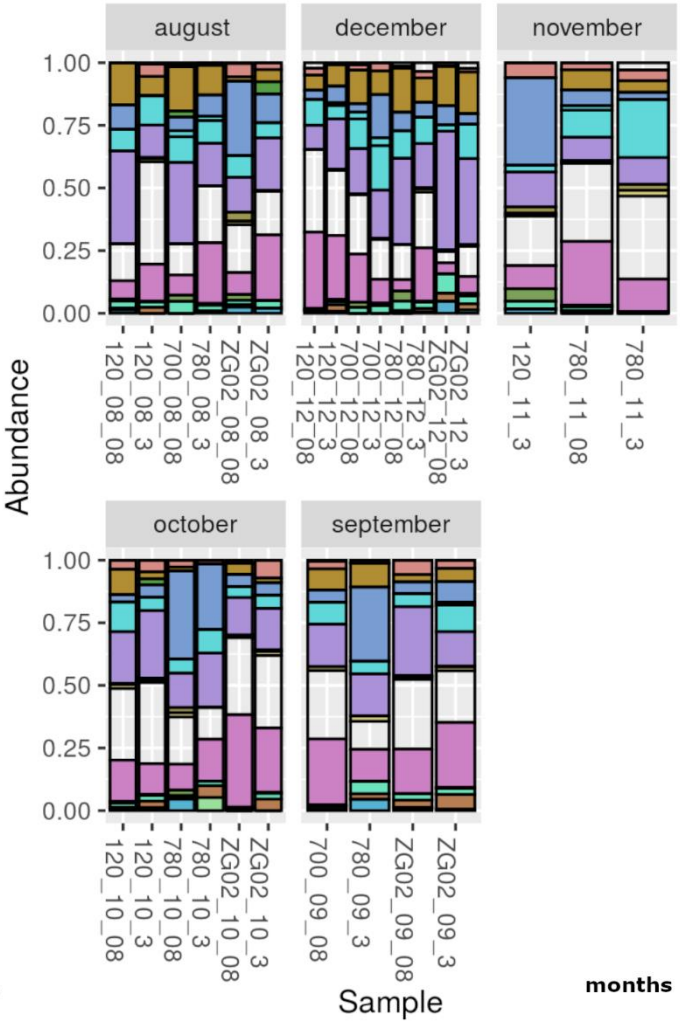

months

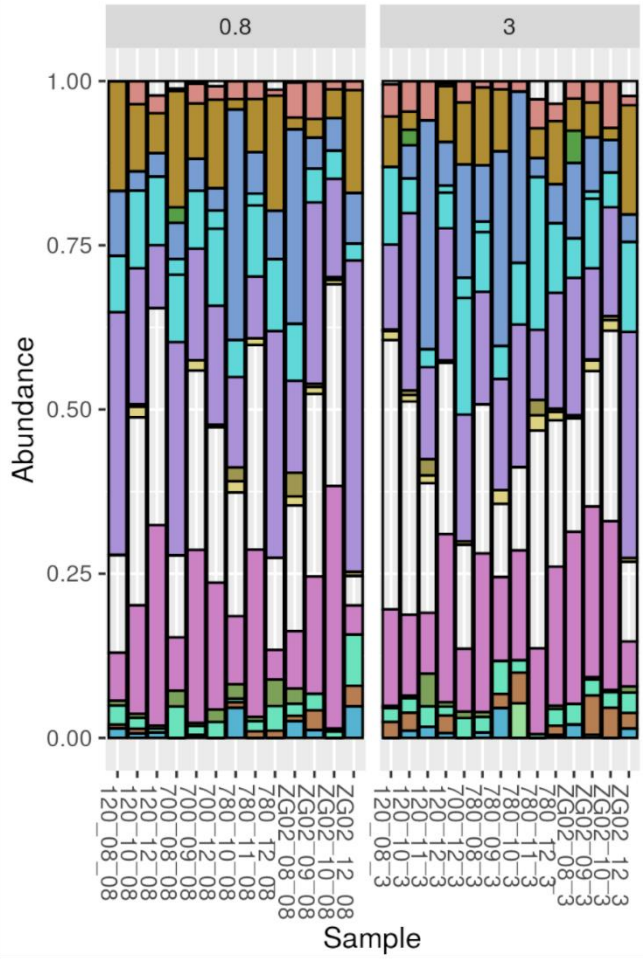

fractions

legend

Division

- Bigyra
- Cercozoa
- Chlorophyta
- Choanoflagellida
- Ciliophora
- Cryptophyta
- Dinoflagellata
- Haptophyta
- Katablepharidophyta
- Myzozoa
- Ochrophyta
- Opalozoa
- Picozoa
- Pseudofungi
- Rhodophyta
- Sagenista

Figure 43: Bar graphs indication abundances of divisions, split for stations, months and fractions (see bottom right). Divisions are displayed in same order in graphs and in legend. Some months and stations have more samples than others, this because some samples had to be deleted from the dataset because they comprised of only few species or had a very low number of reads.

Appendix 7: Amplicon sequencing species-based inventory

Table 10: Light version of amplicon sequencing species inventory. Displayed are taxonomic levels Supergroup, Division, Order, Species, Abundance mean over all samples, and number of ASVs that match to each species.

Supergroup	Division	Order	Species	Abundance_mean
Alveolata	Dinoflagellata	Dino-Group-II	*Unknown Dino-Group-II*	0,098701314
Alveolata	Myzozoa	Gymnodiniales	*Gymnodinium sp.*	0,090354658
Hacrobia	Cryptophyta	Pyrenomonadales	*Plagioselmis prolonga*	0,056205775
Alveolata	Dinoflagellata	Dino-Group-I	*Unknown Dino-Group-I*	0,056046012
Alveolata	Myzozoa	Gymnodiniales	*Gyrodinium fusiforme*	0,046902029
Alveolata	Myzozoa	Gymnodiniales	*Gyrodinium dominans*	0,041279549
Alveolata	Myzozoa	Gymnodiniales	*Gyrodinium spirale*	0,025847296
Alveolata	Ciliophora	Strombidiida_B	*Unknown Strombidiida_B*	0,025086825
Hacrobia	Cryptophyta	Pyrenomonadales	*Teleaulax acuta*	0,020797486
Alveolata	Myzozoa	Peridiniales	*Heterocapsa pygmaea*	0,018504407
Hacrobia	Cryptophyta	Pyrenomonadales	*Teleaulax gracilis*	0,01605249
Archaeplastida	Chlorophyta	Mamiellales	*Ostreococcus tauri*	0,015957006
Stramenopiles	Ochrophyta	Hemiaulales	*Cerataulina bergonii*	0,015828417
Hacrobia	Cryptophyta	Cryptomonadales	*Teleaulax amphioxeia*	0,0138889
Alveolata	Ciliophora	Strombidiida	*Unknown Strombidiida*	0,013644881
Hacrobia	Picozoa	Picomonadida	*Picomonas judraskeda*	0,01320692
Stramenopiles	Ochrophyta	Thalassiosirales	*Thalassiosira sp.*	0,013201171
Stramenopiles	Ochrophyta	Bacillariophyta_X	*Shionodiscus oestrupii var. venrickiae*	0,013078269
Alveolata	Myzozoa	Gymnodiniales	*Gyrodinium helveticum*	0,012543961
Archaeplastida	Chlorophyta	Mamiellales	*Ostreococcus lucimarinus*	0,012441976
Alveolata	Myzozoa	Gymnodiniales	*Polykrikos kofoidii*	0,010593219
Rhizaria	Cercozoa	Cryomonadida	*Cryothecomonas aestivalis*	0,009818921
Alveolata	Dinoflagellata	NA	*Unknown Dinophyceae*	0,009608415
Alveolata	Myzozoa	Gymnodiniales	*Lepidodinium chlorophorum*	0,009514513
Hacrobia	Picozoa	Picozoa_XX	*Picozoa_XXXX_sp.*	0,008561869
Archaeplastida	Chlorophyta	Mamiellales	*Bathycoccus prasinos*	0,007871531
Alveolata	Myzozoa	Noctilucales	*Noctiluca scintillans*	0,007733867
Stramenopiles	Ochrophyta	Thalassiosirales	*Cyclotella sp.*	0,007681758
Stramenopiles	Ochrophyta	Rhizosoleniales	*Rhizosolenia delicatula*	0,007620306
Alveolata	Dinoflagellata	Dino-Group-III	*Unknown Dino-Group-III*	0,007372287
Stramenopiles	Ochrophyta	Chaetocerotanae incertae sedis	*Chaetoceros sp.*	0,00712448
Archaeplastida	Chlorophyta	Mamiellales	*Micromonas bravo*	0,006906351
Archaeplastida	Chlorophyta	Mamiellales	*Micromonas commoda*	0,006580727

Hacrobia	Cryptophyta	Pyrenomonadales	*Falcomonas daucoides*	0,006423862
Rhizaria	Cercozoa	Cryomonadida	*Unknown Cryomonadida*	0,006184601
Alveolata	Myzozoa	Prorocentrales	*Prorocentrum sp.*	0,005968552
Rhizaria	Cercozoa	Filosa-Imbricatea_X	*Unknown Filosa-Imbricatea*	0,005942137
Alveolata	Dinoflagellata	Gymnodiniales	*Unknown Gymnodiniales*	0,005912629
Hacrobia	Cryptophyta	NA	*Unknown Telonemea*	0,005482148
Alveolata	Myzozoa	Peridiniales	*Heterocapsa rotundata*	0,005290629
Stramenopiles	Ochrophyta	Pedinellales	*Unknown Pedinellales*	0,004897059
Alveolata	Myzozoa	Gymnodiniales	*Torodinium robustum*	0,004792835
Archaeplastida	Chlorophyta	Chlorellales	*Picochlorum sp.*	0,004769604
Hacrobia	Cryptophyta	Cryptomonadales	*Unknown Cryptomonadales*	0,004474523
Alveolata	Myzozoa	Gymnodiniales	*Warnowia sp.*	0,004400547
Stramenopiles	Ochrophyta	Chaetocerotanae incertae sedis	*Chaetoceros tenuissimus*	0,004372283
Stramenopiles	Ochrophyta	NA	*Unknown Chrysophyceae*	0,004157047
Stramenopiles	Ochrophyta	NA	*Unknown Bacillariophyceae*	0,003992243
Alveolata	Ciliophora	Oligotrichida	*Strombidium sp.*	0,003788566
Archaeplastida	Chlorophyta	Pyramimonadales	*Pyramimonas australis*	0,003779435
Stramenopiles	Opalozoa	MAST-12E	*Unknown MAST-12E*	0,00332892
Stramenopiles	Opalozoa	Borokales	*Unknown Borokales*	0,003280167
Stramenopiles	Ochrophyta	Chaetocerotanae incertae sedis	*Chaetoceros danicus*	0,003247906
Hacrobia	Cryptophyta	Pyrenomonadales	*Teleaulax sp.*	0,003051488
Alveolata	Ciliophora	Choreotrichida	*Tintinnopsis parvula*	0,002982935
Stramenopiles	Ochrophyta	Hemiaulales	*Bellerochea polymorpha*	0,002934218
Rhizaria	Cercozoa	Filosa-Thecofilosea_X	*Unknown Filosa-Thecofilosea*	0,002901075
Stramenopiles	Pseudofungi	NA	*Unknown Pirsonia_Clade*	0,002800912
Hacrobia	Katablepharidophyta	Katablepharidales	*Unknown Katablepharidales*	0,002779022
Alveolata	Dinoflagellata	Dino-Group-I	*Eduboscquella crenulata*	0,002708568
Alveolata	Myzozoa	Gymnodiniales	*Akashiwo sanguinea*	0,002644807
Alveolata	Ciliophora	Choreotrichida	*Unknown Choreotrichida*	0,002607837
Alveolata	Ciliophora	Cyclotrichiida	*Askenasia sp.*	0,002492043
Stramenopiles	Sagenista	NA	*Unknown MAST-6*	0,002427997
Stramenopiles	Ochrophyta	Hemiaulales	*Eucampia striata*	0,00230735
Stramenopiles	Ochrophyta	Bacillariophyta_X	*Chaetoceros brevis 3*	0,002074813
Archaeplastida	Chlorophyta	Mamiellales	*Mamiella gilva*	0,002039499
Stramenopiles	Pseudofungi	Oomycota_X	*Unknown Oomycota*	0,001959538
Alveolata	Myzozoa	Gymnodiniales	*Gymnodinium dorsalisulcum*	0,00193906
Stramenopiles	Ochrophyta	Dictyochales	*Dictyocha speculum*	0,001925625
Hacrobia	Cryptophyta	Pyrenomonadales	*Hemiselmis cryptochromatica*	0,001914419
Alveolata	Ciliophora	Choreotrichida	*Leegaardiella sp.*	0,001888166
Stramenopiles	Ochrophyta	NA	*Cylindropyxis profunda*	0,00188713
Stramenopiles	Ochrophyta	Thalassiosirales	*Thalassiosira rotula*	0,001849978
Stramenopiles	Ochrophyta	Chattonellales	*Fibrocapsa japonica*	0,001842801
Stramenopiles	Sagenista	Labyrinthulales	*Unknown Labyrinthulales*	0,001841351

Stramenopiles	Ochrophyta	Thalassiosirales	*Thalassiosira oceanica*	0,001831667
Alveolata	Ciliophora	Suctoria	*Unknown Suctoria*	0,001802858
Hacrobia	Haptophyta	Phaeocystales	*Phaeocystis globosa*	0,00179558
Stramenopiles	Ochrophyta	Bacillariophyta_X	*Porosira pseudodelicatula*	0,00179036
Archaeplastida	Chlorophyta	Pyramimonadales	*Pyramimonas gelidicola*	0,0017236
Stramenopiles	Ochrophyta	Chaetocerotanae incertae sedis	*Chaetoceros affinis*	0,001705975
Hacrobia	Cryptophyta	Pyrenomonadales	*Rhodomonas sp.*	0,001705497
Alveolata	Myzozoa	Gymnodiniales	*Karlodinium veneficum*	0,001677
Stramenopiles	Ochrophyta	Thalassiosirales	*Thalassiosira allenii*	0,001672911
Archaeplastida	Chlorophyta	Mamiellales	*Micromonas pusilla*	0,00165653
Alveolata	Myzozoa	Gymnodiniales	*Gyrodinium heterogrammum*	0,001653672
Alveolata	Ciliophora	Oligotrichida	*Strombidium R sp.*	0,001647024
Stramenopiles	Ochrophyta	Lithodesmiales	*Ditylum brightwellii*	0,001636761
Opisthokonta	Choanoflagellida	Acanthoecida	*Unknown Acanthoecida*	0,001587481
Rhizaria	Cercozoa	Ventricleftida	*Unknown Ventricleftida*	0,001548204
Alveolata	Ciliophora	Choreotrichida	*Tintinnidium sp.*	0,001516172
Stramenopiles	Ochrophyta	Hemiaulales	*Eucampia sp.*	0,00149552
Stramenopiles	Ochrophyta	Coscinodiscales	*Coscinodiscus trioculatus*	0,001461566
Stramenopiles	Ochrophyta	Triceratiales	*Odontella aurita*	0,001441103
Alveolata	Ciliophora	Choreotrichida	*Pelagostrobilidium sp.*	0,001409317
Stramenopiles	Sagenista	MAST-7B	*Unknown MAST-7B*	0,001386986
Stramenopiles	Pseudofungi	MAST-1C	*Unknown MAST-1C*	0,001382769
Stramenopiles	Ochrophyta	Thalassiosirales	*Thalassiosira lundiana*	0,001382612
Stramenopiles	Bigyra	Bicoecida	*Cafeteria roenbergensis*	0,001378956
Alveolata	Ciliophora	Oligotrichida	*Laboea strobila*	0,001366908
Alveolata	Ciliophora	Choreotrichida	*Strombidinopsis acuminata*	0,001340544
Alveolata	Myzozoa	Peridiniales	*Archaeperidinium minutum*	0,00132391
Rhizaria	Cercozoa	Marimonadida	*Unknown Marimonadida*	0,001304364
Alveolata	Dinoflagellata	Peridiniales	*Unknown Peridiniales*	0,001300208
Archaeplastida	Chlorophyta	Pyramimonadales	*Cymbomonas tetramitiformis*	0,001252221
Stramenopiles	Ochrophyta	Biddulphiales	*Biddulphia sinensis*	0,001194525
Alveolata	Ciliophora	Choreotrichida	*Pelagostrobilidium neptuni*	0,001156349
Stramenopiles	Ochrophyta	Parmales	*Unknown Parmales*	0,001130786
Opisthokonta	Choanoflagellida	NA	*Unknown Choanoflagellatea*	0,001102125
Stramenopiles	Ochrophyta	Ethmodiscales	*Ethmodiscus punctiger*	0,001039135
Alveolata	Ciliophora	Choreotrichida	*Parastrombidinopsis shimi*	0,001024221
Stramenopiles	Opalozoa	MAST-3A	*Unknown MAST-3A*	0,000984963
Archaeplastida	Chlorophyta	Pseudoscourfieldiales	*Unknown Pseudoscourfieldiales*	0,000975726
Alveolata	Ciliophora	NA	*Unknown Litostomatea*	0,00097528
Alveolata	Myzozoa	Gymnodiniales	*Gyrodinium sp.*	0,000945875
Stramenopiles	Opalozoa	MAST-3E	*Unknown MAST-3E*	0,000903584
Alveolata	Myzozoa	Gonyaulacales	*Tripos fusus*	0,000889632
Stramenopiles	Ochrophyta	Rhizosoleniales	*Rhizosolenia imbricata*	0,000886214

Rhizaria	Cercozoa	Cercozoa_XX	*Cercozoa_XXXX_sp.*	0,000878731
Rhizaria	Cercozoa	Ebriida	*Unknown Ebriida*	0,000869191
Hacrobia	Cryptophyta	NA	*Leucocryptos marina*	0,000853975
Stramenopiles	Ochrophyta	Chaetocerotanae incertae sedis	*Chaetoceros debilis*	0,000844976
Alveolata	Ciliophora	Philasterida	*Myxophyllum sp.*	0,000786524
Stramenopiles	Ochrophyta	Thalassiosirales	*Thalassiosira minima*	0,000777318
Alveolata	Ciliophora	Strombidiida_F	*Unknown Strombidiida_F*	0,000773977
Stramenopiles	Opalozoa	MAST-3C	*Unknown MAST-3C*	0,00077159
Stramenopiles	Bigyra	Anoecida	*Caecitellus paraparvulus*	0,000770245
Rhizaria	Cercozoa	Phagomyxida	*Phagomyxa odontellae*	0,000744709
Stramenopiles	Ochrophyta	Bacillariales	*Pseudo-nitzschia sp.*	0,000739542
Alveolata	Myzozoa	Prorocentrales	*Prorocentrum cordatum*	0,000736641
Alveolata	Myzozoa	Pyrocystales	*Dissodinium pseudolunula*	0,000727019
Alveolata	Ciliophora	Strombidiida_G	*Unknown Strombidiida_G*	0,000720404
Stramenopiles	Ochrophyta	Thalassiosirales	*Thalassiosira curviseriata*	0,00069407
Alveolata	Myzozoa	Syndiniales	*Syndinium sp.*	0,000687452
Stramenopiles	Sagenista	MAST-7A	*Unknown MAST-7A*	0,00067291
Alveolata	Ciliophora	Choreotrichida	*Pelagostrobilidium paraepacrum*	0,00067019
Archaeplastida	Chlorophyta	Pyramimonadales	*Pyramimonas sp.*	0,000667997
Alveolata	Ciliophora	Choreotrichida	*Parastrombidinopsis sp.*	0,000654459
Stramenopiles	Ochrophyta	Rhaponeidales	*Delphineis sp.*	0,000637854
Stramenopiles	Ochrophyta	Thalassiosirales	*Thalassiosira tenera*	0,000628248
Stramenopiles	Ochrophyta	Thalassiosirales	*Skeletonema sp.*	0,000614321
Archaeplastida	Chlorophyta	Ulvales	*Ulva sp.*	0,000599614
Stramenopiles	Ochrophyta	Thalassiosirales	*Thalassiosira eccentrica*	0,00059689
Alveolata	Ciliophora	Tintinnida	*Unknown Tintinnida*	0,000596511
Stramenopiles	Ochrophyta	Chaetocerotales	*Tenuicylindrus belgicus*	0,000588601
Stramenopiles	Ochrophyta	Chaetocerotanae incertae sedis	*Chaetoceros decipiens*	0,000578042
Stramenopiles	Pseudofungi	MAST-1B	*Unknown MAST-1B*	0,000569592
Rhizaria	Cercozoa	Thaumatomonadida	*Reckertia filosa*	0,000564118
Archaeplastida	Chlorophyta	Trebouxiales	*Trebouxia sp.*	0,000558973
Rhizaria	Cercozoa	Cryomonadida	*Cryothecomonas sp.*	0,000558095
Opisthokonta	Mesomycetozoa	Ichthyosphonida	*Unknown Ichthyosphonida*	0,000555965
Hacrobia	Cryptophyta	Cryptomonadales	*Goniomonas amphinema*	0,000552322
Stramenopiles	Ochrophyta	Leptocylindrales	*Leptocylindrus sp.*	0,000551698
Hacrobia	Centroheliozoa	Pterocystida	*Unknown Pterocystida*	0,000547156
Stramenopiles	Opalozoa	MAST-12A	*Unknown MAST-12A*	0,000533936
Stramenopiles	Opalozoa	MAST-3D	*Unknown MAST-3D*	0,000529138
Stramenopiles	Ochrophyta	Leptocylindrales	*Leptocylindrus minimus*	0,000510999
Archaeplastida	Chlorophyta	Chlorellales	*Unknown Chlorellales*	0,000503001
Stramenopiles	Ochrophyta	Coscinodiscales	*Actinocyclus curvatulus*	0,000495911
Archaeplastida	Rhodophyta	Nemaliales	*Dichotomaria marginata*	0,000466361
Stramenopiles	Sagenista	Thraustochytriales	*Unknown Thraustochytriales*	0,000457627

Alveolata	Ciliophora	Oligotrichida	*Strombidium K sp.*	0,000452905
Archaeplastida	Chlorophyta	Nephroselmidales	*Nephroselmis pyriformis*	0,000444335
Stramenopiles	Opalozoa	MAST-3I	*Unknown MAST-3I*	0,000438582
Alveolata	Myzozoa	Suessiales	*Biecheleria cincta*	0,000437118
Stramenopiles	Sagenista	MAST-4D	*Unknown MAST-4D*	0,000435553
Stramenopiles	Opalozoa	Bicoecales	*Unknown Bicoecales*	0,000432799
Alveolata	Dinoflagellata	Suessiales	*Unknown Suessiales*	0,000430845
Opisthokonta	Choanoflagellida	Craspedida	*Unknown Craspedida*	0,000401515
Stramenopiles	Bigyra	Thraustochytrida	*Aplanochytrium sp.*	0,000399737
Rhizaria	Ochrophyta	Raphidophyceae incertae sedis	*Thaumatomastix salina*	0,000398165
Alveolata	Myzozoa	Gymnodiniales	*Pelagodinium sp.*	0,000392164
Stramenopiles	Sagenista	MAST-4E	*Unknown MAST-4E*	0,000384903
Alveolata	Ciliophora	Prorodontida	*Urotricha sp.*	0,000379407
Alveolata	Myzozoa	Peridiniales	*Scrippsiella sp.*	0,000376314
Stramenopiles	Ochrophyta	Rhizosoleniales	*Rhizosolenia similoides*	0,00037429
Alveolata	Ciliophora	Choreotrichida	*Rimostrombidium_A_sp.*	0,000373005
Stramenopiles	Ochrophyta	Thalassiosirales	*Thalassiosira delicatula*	0,000369549
Opisthokonta	Fungi	Chytridiomycotina	*Clydaea vesicula*	0,000368243
Hacrobia	Katablepharidophyta	Katablepharidales	*Katablepharis japonica*	0,000364866
Alveolata	Ciliophora	Oligotrichida	*Strombidium M sp.*	0,000363935
Alveolata	Dinoflagellata	Dinophysiales	*Unknown Dinophysiales*	0,000361994
Stramenopiles	Ochrophyta	Chaetocerotanae incertae sedis	*Bacteriastrum hyalinum*	0,000358121
Stramenopiles	Opalozoa	MAST-3F	*Unknown MAST-3F*	0,000357624
Stramenopiles	Ochrophyta	Leptocylindrales	*Leptocylindrus convexus*	0,000346993
Stramenopiles	Ochrophyta	Thalassiosirales	*Lauderia pumila*	0,000343368
Alveolata	Ciliophora	NA	*Unknown CONTH_7*	0,000335648
Alveolata	Myzozoa	Tovelliales	*Woloszynskia sp.*	0,000333567
Alveolata	Ciliophora	Cyrtophoria_1	*Unknown Cyrtophoria_1*	0,000329022
Alveolata	Myzozoa	Gymnodiniales	*Pelagodinium bei*	0,000321401
Stramenopiles	Ochrophyta	Rhizosoleniales	*Rhizosolenia fallax*	0,000318452
Archaeplastida	Chlorophyta	Dolichomastigales	*Unknown Dolichomastigales*	0,000317434
Stramenopiles	Bigyra	Anoecida	*Caecitellus parvulus*	0,0003158
Rhizaria	Cercozoa	Chlorarachniophyceae_X	*Unknown Chlorarachniophyceae*	0,00031367
Rhizaria	Radiolaria	NA	*Unknown Acantharea*	0,000313423
Stramenopiles	Opalozoa	MAST-3J	*Unknown MAST-3J*	0,000311993
Rhizaria	Cercozoa	Filosa_X	*Discomonas retusa*	0,000311045
Stramenopiles	Ochrophyta	Bacillariales	*Cylindrotheca sp.*	0,000298691
Alveolata	Myzozoa	Peridiniales	*Crypthecodinium sp.*	0,000295791
Hacrobia	Centroheliozoa	Centroheliozoa_XX	*Centroheliozoa_XXXX_sp.*	0,000294983
Alveolata	Ciliophora	OLIGO5	*Unknown OLIGO5*	0,000289592
Apusozoa	Apusomonadidae	NA	*Unknown Apusomonadidae_Group-1*	0,000284375
Alveolata	Myzozoa	Peridiniales	*Pentapharsodinium sp.*	0,000276904
Stramenopiles	Pseudofungi	MAST-2D	*Unknown MAST-2D*	0,000274922

Stramenopiles	Ochrophyta	NA	*Unknown MOCH-3*	0,00027067
Stramenopiles	Ochrophyta	Chaetocerotanae incertae sedis	*Chaetoceros sporotruncatus*	0,000264312
Stramenopiles	Ochrophyta	Naviculales	*Navicula lanceolata*	0,000262415
Stramenopiles	Ochrophyta	Chaetocerotanae incertae sedis	*Chaetoceros elegans*	0,00025756
Alveolata	Ciliophora	Apostomatia	*Synophrya_sp.*	0,000255957
Hacrobia	Cryptophyta	Pyrenomonadales	*Hemiselmis andersenii*	0,000249179
Amoebozoa	Amoebozoa	Nolandida	*Nolandella sp.*	0,000248543
Archaeplastida	Rhodophyta	Halymeniales	*Grateloupia sp.*	0,000247992
Stramenopiles	Ochrophyta	Naviculales	*Navicula membranacea*	0,000243707
Alveolata	Ciliophora	Choreotrichida	*Lynnella semiglobulosa*	0,000241269
Alveolata	Myzozoa	NA	*Stoeckeria algicida*	0,000239096
Stramenopiles	Sagenista	MAST-4B	*Unknown MAST-4B*	0,000238643
Alveolata	Apicomplexa	Colpodellida	*Voromonas pontica*	0,000234556
Rhizaria	Cercozoa	Marimonadida	*Pseudopirsonia sp.*	0,000232899
Alveolata	Myzozoa	Suessiales	*Biecheleria halophila*	0,000232284
Stramenopiles	Sagenista	NA	*Unknown MAST-10*	0,000232158
Stramenopiles	Opalozoa	MAST-12D	*Unknown MAST-12D*	0,000231211
Stramenopiles	Ochrophyta	Chaetocerotanae incertae sedis	*Chaetoceros lorenzianus*	0,000223126
Alveolata	Ciliophora	NA	*Holosticha diademata*	0,000217196
Alveolata	Myzozoa	NA	*Protodinium simplex*	0,000208733
Alveolata	Ciliophora	Choreotrichida	*Strombidinopsis sp.*	0,000206089
Stramenopiles	Opalozoa	Bicoecales	*Bicosoeca vacillans*	0,000205596
Stramenopiles	Ochrophyta	Chromulinales	*Paraphysomonas imperforata*	0,000201784
Stramenopiles	Sagenista	MAST-4A	*Unknown MAST-4A*	0,000200146
Opisthokonta	Fungi	Chytridiomycotina	*Rhyzophidiales_sp.*	0,00020014
Alveolata	Apicomplexa	Eugregarinorida	*Unknown Eugregarinorida*	0,000198147
Alveolata	Ciliophora	Oligotrichida	*Strombidium capitatum*	0,000198041
Stramenopiles	Opalozoa	Anoecales	*Unknown Anoecales*	0,000192888
Stramenopiles	Ochrophyta	Chaetocerotanae incertae sedis	*Chaetoceros contortus*	0,00019183
Alveolata	Myzozoa	Gymnodiniales	*Gymnodinium microreticulatum*	0,000190088
Hacrobia	Haptophyta	Prymnesiales	*Chrysochromulina sp.*	0,000186755
Stramenopiles	Ochrophyta	Bacillariales	*Nitzschia sp.*	0,000183381
Stramenopiles	Ochrophyta	Rhizosoleniales	*Rhizosolenia robusta*	0,000182307
Alveolata	Ciliophora	Suctoria	*Acineta_1_sp.*	0,000179119
Stramenopiles	Ochrophyta	Thalassiosirales	*Thalassiosira hendeyi*	0,000176961
Archaeplastida	Chlorophyta	Ulvales	*Pseudendoclonium arthopyreniae*	0,000175192
Opisthokonta	Fungi	Chytridiomycotina	*Unknown Chytridiomycotina*	0,000174419
Alveolata	Ciliophora	Haptoria_4	*Unknown Haptoria_4*	0,00017235
Stramenopiles	Sagenista	MAST-8A	*Unknown MAST-8A*	0,000168693
Stramenopiles	Ochrophyta	Dictyochophyceae_X	*Dictyocha globosa*	0,00016796
Stramenopiles	Ochrophyta	Triceratiales	*Triceratium intricatum*	0,000165903
Rhizaria	Cercozoa	Marimonadida	*Pseudopirsonia mucosa*	0,000164146
Stramenopiles	Ochrophyta	Coscinodiscales	*Coscinodiscus angustelineatus*	0,000163187

Rhizaria	Cercozoa	Chlorarachnida	*Minorisa minuta*	0,00015777
Rhizaria	Cercozoa	Thaumatomonadida	*Peregrinia sp.*	0,00015456
Alveolata	Ciliophora	Nassophorea_X	*NASSO_1_sp.*	0,000154342
Opisthokonta	Choanozoa	Craspedida	*Choanoeca perplexa*	0,000154288
Alveolata	Myzozoa	Coccidiniales	*Eudubosquella cachonii*	0,000153464
Stramenopiles	Ochrophyta	Bacillariales	*Pseudo-nitzschia pungens*	0,000153295
Archaeplastida	Chlorophyta	Prasinococcales	*Unknown Prasinococcales*	0,000147687
Alveolata	Perkinsea	Perkinsida_X	*Parvilucifera prorocentri*	0,000147246
Hacrobia	Cryptophyta	Pyrenomonadales	*Geminigera cryophila*	0,000147073
Stramenopiles	Ochrophyta	Chromulinales	*Paraphysomonas sp.*	0,000145913
Alveolata	Myzozoa	Peridiniales	*Heterocapsa sp.*	0,000139217
Alveolata	Ciliophora	Choreotrichida	*Schmidingerella sp.*	0,000135485
Stramenopiles	Ochrophyta	Thalassiosirales	*Thalassiosira minuscula*	0,000135395
Stramenopiles	Ochrophyta	Bacillariales	*Pseudo-nitzschia delicatissima*	0,000134781
Alveolata	Ciliophora	Choreotrichida	*Tintinnidium mucicola*	0,00013402
Alveolata	Ciliophora	Choreotrichida	*Eutintinnus sp.*	0,00013283
Stramenopiles	Ochrophyta	Naviculales	*Navicula sp.*	0,000128444
Archaeplastida	Chlorophyta	Pyramimonadales	*Unknown Pyramimonadales*	0,000127412
Alveolata	Ciliophora	Hypotrichia	*Unknown Hypotrichia*	0,000126163
Alveolata	Ciliophora	Choreotrichida	*Eutintinnus tubulosus*	0,000123709
Alveolata	Myzozoa	Dinophysiales	*Phalacroma rotundatum*	0,000121398
Stramenopiles	Ochrophyta	Chromulinales	*Paraphysomonas butcheri*	0,000119573
Alveolata	Myzozoa	Gymnodiniales	*Proterythropsis sp.*	0,000115256
Rhizaria	Cercozoa	Euglyphida	*Paulinella sp.*	0,000112147
Rhizaria	Cercozoa	Ebriida	*Ebria tripartita*	0,00010926
Opisthokonta	Choanozoa	Acanthoecida	*Savillea micropora*	0,000108772
Apusozoa	Apusomonadidae	Apusomonadidae_Group-1_X	*Amastigomonas debruynei*	0,000106086
Archaeplastida	Chlorophyta	Trebouxiophyceae ordo incertae sedis	*Choricystis sp.*	0,000105571
Alveolata	Ciliophora	Cyrtolophosidida	*Aristerostoma sp.*	0,000103476
Apusozoa	Hilomonadea	Planomonadidae	*Micronuclearia podoventralis*	0,000103004
Opisthokonta	Fungi	Cryptomycotina	*Unknown Cryptomycotina*	0,000101675
Stramenopiles	Ochrophyta	Chaetocerotanae incertae sedis	*Bacteriastrum mediterraneum*	0,000101409
Alveolata	Myzozoa	Thoracosphaerales	*Luciella sp.*	1,00E-04
Stramenopiles	Ochrophyta	NA	*Unknown MOCH-1*	9,91E-05
Alveolata	Myzozoa	Noctilucales	*Spatulodinium pseudonoctiluca*	9,82E-05
Stramenopiles	Pseudofungi	MAST-2B	*Unknown MAST-2B*	9,78E-05
Alveolata	Myzozoa	Suessiales	*Ansanella granifera*	9,74E-05
Archaeplastida	Chlorophyta	Ulvales	*Dilabifilum sp.*	9,68E-05
Hacrobia	Cryptophyta	Goniomonadales	*Unknown Goniomonadales*	9,56E-05
Stramenopiles	Ochrophyta	Rhizosoleniales	*Rhizosolenia flaccida*	9,47E-05
Stramenopiles	Ochrophyta	Pedinellales	*Pseudopedinella elastica*	9,44E-05
Alveolata	Ciliophora	Oligotrichida	*Spirostrombidium agathae*	9,18E-05

Alveolata	Ciliophora	Oligotrichida	*Varistrombidium kielum*	9,08E-05
Archaeplastida	Chlorophyta	Halosphaerales	*Pterosperma sp.*	9,07E-05
Alveolata	Ciliophora	Haptorida	*Cyclotrichium cyclokaryon*	8,93E-05
Stramenopiles	Ochrophyta	Florenciellales	*Florenciella parvula*	8,86E-05
Stramenopiles	Ochrophyta	Naviculales	*Pleurosigma sp.*	8,83E-05
Stramenopiles	Bigyra	Bicoecida	*Bicosoeca sp.*	8,79E-05
Stramenopiles	Ochrophyta	NA	*Syndendrium diadema*	8,73E-05
Stramenopiles	Ochrophyta	Pedinellales	*Apedinella radians*	8,71E-05
Stramenopiles	Ochrophyta	Rhizosoleniales	*Rhizosolenia setigera*	8,58E-05
Alveolata	Apicomplexa	Gregarines	*Selenidium1_sp.*	8,45E-05
Alveolata	Myzozoa	Peridiniales	*Protoperidinium monovelum*	8,36E-05
Alveolata	Ciliophora	Tintinnida	*Tintinnopsis kiangsuensis*	8,29E-05
Alveolata	Myzozoa	Perkinsida	*Perkinsus sp.*	8,23E-05
Stramenopiles	Ochrophyta	Achnanthales	*Cocconeis sp.*	8,13E-05
Stramenopiles	Ochrophyta	Triceratiales	*Odontella mobiliensis*	7,88E-05
Alveolata	Myzozoa	Dinophyceae incertae sedis	*Azadinium sp.*	7,88E-05
Archaeplastida	Chlorophyta	Chlorodendrales	*Unknown Chlorodendrales*	7,84E-05
Stramenopiles	Ochrophyta	Bacillariales	*Pseudo-nitzschia multiseries*	7,84E-05
Stramenopiles	Ochrophyta	Bacillariophyta_X	*Chaetoceros lorenzianus 2*	7,66E-05
Stramenopiles	Opalozoa	NA	*Unknown MAST-12*	7,65E-05
Alveolata	Ciliophora	Prorodontida	*Plagiocampa sp.*	7,61E-05
Archaeplastida	Chlorophyta	Ulvales	*Ulva intestinalis*	7,55E-05
Stramenopiles	Ochrophyta	Florenciellales	*Pseudochattonella sp.*	7,54E-05
Stramenopiles	Ochrophyta	Chattonellales	*Heterosigma akashiwo*	7,48E-05
Alveolata	Myzozoa	Peridiniales	*Islandinium tricingulatum*	7,46E-05
Alveolata	Myzozoa	Gymnodiniales	*Paragymnodinium shiwhaense*	7,23E-05
Stramenopiles	Ochrophyta	Florenciellales	*Pseudochattonella verruculosa*	7,21E-05
Apusozoa	Apusomonadidae	Apusomonadidae_Group-1_X	*Apusomonas proboscidea*	7,17E-05
Alveolata	Myzozoa	Peridiniales	*Diplopsalis caspica*	7,13E-05
Amoebozoa	Amoebozoa	Himatismenida	*Parvamoeba sp.*	7,11E-05
Stramenopiles	Ochrophyta	Chaetocerotanae incertae sedis	*Chaetoceros anastomosans*	6,79E-05
Stramenopiles	Ochrophyta	Chattonellales	*Chattonella marina*	6,75E-05
Stramenopiles	Ochrophyta	Chromulinales	*Spumella sp.*	6,72E-05
Stramenopiles	Ochrophyta	Chromulinales	*Paraphysomonas bandaiensis*	6,50E-05
Archaeplastida	Chlorophyta	Trebouxiales	*Asterochloris phycobiontica*	6,38E-05
Stramenopiles	Chlorophyta	Cladophorales	*Symbiomonas scintillans*	6,36E-05
Opisthokonta	Fungi	Pucciniomycotina	*Unknown Pucciniomycotina*	6,33E-05
Alveolata	Myzozoa	Peridiniales	*Archaeperidinium saanichii*	6,30E-05
Stramenopiles	Ochrophyta	Melosirales	*Stephanopyxis turris*	6,26E-05
Alveolata	Ciliophora	Scuticociliatia_1	*Unknown Scuticociliatia_1*	6,18E-05
Alveolata	Apicomplexa	Gregarines	*Selenidium1 serpulae*	6,17E-05
Rhizaria	Cercozoa	Cercomonadida	*Cercomonas braziliensis*	6,17E-05
Rhizaria	Cercozoa	Vampyrellida	*Vampyrellida_sp.*	6,07E-05

Stramenopiles	Ochrophyta	NA	*Vibrio paxillifer*	6,06E-05
Alveolata	Myzozoa	Gonyaulacales	*Gonyaulax spinifera*	6,01E-05
Alveolata	Myzozoa	Coccidiniales	*Eudubosquella sp.*	6,00E-05
Archaeplastida	Chlorophyta	Microthamniales	*Unknown Microthamniales*	6,00E-05
Stramenopiles	Ochrophyta	Lithodesmiales	*Helicotheca tamesis*	5,97E-05
Stramenopiles	Ochrophyta	Thalassiosirales	*Cyclotella striata*	5,95E-05
Hacrobia	Cryptophyta	Telonemida	*Telonema subtile*	5,94E-05
Stramenopiles	Opalozoa	MAST-12B	*Unknown MAST-12B*	5,91E-05
Stramenopiles	Ochrophyta	Cymbellales	*Cymbella sp.*	5,89E-05
Archaeplastida	Chlorophyta	Chlorellales	*Leptosira sp.*	5,83E-05
Stramenopiles	Ochrophyta	Paraliales	*Paralia sulcata*	5,70E-05
Alveolata	Ciliophora	Peritrichia_2	*Unknown Peritrichia_2*	5,68E-05
Stramenopiles	Bigyra	Thraustochytrida	*Oblongichytrium sp.*	5,62E-05
Alveolata	Myzozoa	Peridiniales	*Protoperidinium claudicans*	5,61E-05
Archaeplastida	Chlorophyta	NA	*Chloropicon roscoffensis*	5,49E-05
Archaeplastida	Chlorophyta	Prasinococcales	*Prasinoderma coloniale*	5,40E-05
Archaeplastida	Chlorophyta	Trebouxiophyceae ordo incertae sedis	*Coccomyxa sp.*	5,38E-05
Rhizaria	Cercozoa	Vampyrellida	*Unknown Vampyrellida*	5,30E-05
Archaeplastida	Chlorophyta	Halosphaerales	*Pterosperma cristatum*	5,30E-05
Alveolata	Ciliophora	Choreotrichida	*Helicostomella subulata*	5,30E-05
Rhizaria	Cercozoa	Cryptofilida	*Nanofila sp.*	5,20E-05
Alveolata	Ciliophora	Scuticociliatia_1	*Porpostoma notata*	4,90E-05
Alveolata	Myzozoa	Gonyaulacales	*Gonyaulax sp.*	4,77E-05
Stramenopiles	Ochrophyta	Bacillariophyta_X	*Chaetoceros cf tortissimus*	4,77E-05
Rhizaria	Ochrophyta	Raphidophyceae incertae sedis	*Thaumatomastix sp.*	4,72E-05
Stramenopiles	Ochrophyta	Thalassiosirales	*Cyclotella choctawhatcheeana*	4,63E-05
Stramenopiles	Ochrophyta	NA	*Unknown MOCH-2*	4,61E-05
Archaeplastida	Chlorophyta	Dolichomastigales	*Crustomastigaceae-C_sp.*	4,61E-05
Stramenopiles	Ochrophyta	Cymatosirales	*Papiliocellulus sp.*	4,57E-05
Alveolata	Ciliophora	Choreotrichida	*Tintinnopsis major*	4,56E-05
Rhizaria	Cercozoa	Chlorarachnida	*Unknown Chlorarachnida*	4,51E-05
Stramenopiles	Ochrophyta	Thalassiosirales	*Thalassiosira concaviuscula*	4,42E-05
Stramenopiles	Ochrophyta	Chaetocerotanae incertae sedis	*Chaetoceros costatus*	4,39E-05
Rhizaria	Cercozoa	Thaumatomonadida	*Unknown Thaumatomonadida*	4,33E-05
Alveolata	Myzozoa	Gymnodiniales	*Torodinium sp.*	4,31E-05
Alveolata	Myzozoa	Gonyaulacales	*Tripos furca*	4,31E-05
Alveolata	Myzozoa	Dinophyceae incertae sedis	*Levanderina fissa*	4,22E-05
Stramenopiles	Ochrophyta	Thalassiosirales	*Skeletonema marinoi*	4,22E-05
Alveolata	Myzozoa	Dinophysiales	*Dinophysis acuminata*	4,18E-05
Rhizaria	Cercozoa	Filosa-Granofilosea_X	*Unknown Filosa-Granofilosea*	4,12E-05
Stramenopiles	Ochrophyta	Chaetocerotanae incertae sedis	*Chaetoceros eibenii*	4,02E-05
Stramenopiles	Ochrophyta	Chaetocerotanae incertae sedis	*Chaetoceros pseudocurvisetus*	4,00E-05

Stramenopiles	Ochrophyta	Bacillariales	*Psammodictyon sp.*	3,99E-05
Rhizaria	Cercozoa	Ventricleftida	*Verrucomonas_sp.*	3,98E-05
Stramenopiles	Ochrophyta	Coscinodiscales	*Coscinodiscus radiatus*	3,95E-05
Stramenopiles	Ochrophyta	Anaulales	*Eunotogramma laevis*	3,93E-05
Rhizaria	Cercozoa	Euglyphida	*Unknown Euglyphida*	3,91E-05
Hacrobia	Haptophyta	Prymnesiales	*Haptolina sp.*	3,86E-05
Alveolata	Myzozoa	Peridiniales	*Scrippsiella acuminata*	3,85E-05
Archaeplastida	Chlorophyta	Trebouxiales	*Myrmecia sp.*	3,79E-05
Hacrobia	Haptophyta	Syracosphaerales	*Unknown Syracosphaerales*	3,78E-05
Stramenopiles	Ochrophyta	Coscinodiscales	*Actinocyclus sp.*	3,66E-05
Stramenopiles	Ochrophyta	Bacillariophyta_X	*Chaetoceros curvisetus 2b*	3,64E-05
Stramenopiles	Pseudofungi	MAST-1A	*Unknown MAST-1A*	3,57E-05
Apusozoa	Hilomonadea	Planomonadidae	*Unknown Planomonadidae*	3,51E-05
Stramenopiles	Ochrophyta	Bacillariales	*Cylindrotheca closterium*	3,50E-05
Rhizaria	Cercozoa	Cercomonadida	*Eocercomonas_sp.*	3,41E-05
Stramenopiles	Sagenista	Thraustochytriales	*Amphifilidae_sp.*	3,40E-05
Stramenopiles	Ochrophyta	Chaetocerotanae incertae sedis	*Chaetoceros lauderi*	3,31E-05
Opisthokonta	Mesomycetozoa	Rhynosporida	*Unknown Rhynosporida*	3,30E-05
Stramenopiles	Oomycota	Saprolegniales	*Haliphthoros sp.*	3,26E-05
Rhizaria	Cercozoa	Euglyphida	*Paulinella chromatophora*	3,26E-05
Opisthokonta	Mesomycetozoa	Ichthyosphonida	*Pseudoperkinsus tapetis*	3,25E-05
Amoebozoa	Lobosa	Lobosa_XX	*Unknown Lobosa_X*	3,18E-05
Stramenopiles	Sagenista	MAST-7C	*Unknown MAST-7C*	3,08E-05
Rhizaria	Cercozoa	Cryomonadida	*Protaspa sp.*	3,00E-05
Rhizaria	Cercozoa	Thecofilosea incertae sedis	*Mataza hastifera*	2,94E-05
Stramenopiles	Bigyra	Thraustochytrida	*Thraustochytrium sp.*	2,94E-05
Stramenopiles	Ochrophyta	Dictyochales	*Dictyocha sp.*	2,93E-05
Alveolata	Dinoflagellata	Gymnodiniales	*Gyrodinium jinhaense*	2,86E-05
Archaeplastida	Chlorophyta	Trebouxiales	*Trebouxia arboricola*	2,85E-05
Rhizaria	Cercozoa	Cercomonadida	*Unknown Cercomonadida*	2,82E-05
Alveolata	Ciliophora	Prorodontida	*Tiarina sp.*	2,82E-05
Alveolata	Ciliophora	Exogenida	*Ephelota mammillata*	2,77E-05
Archaeplastida	Streptophyta	Streptophyta_XX	*Streptophyta_XXXX_sp.*	2,76E-05
Archaeplastida	Chlorophyta	Dolichomastigales	*Crustomastix didyma*	2,76E-05
Stramenopiles	Ochrophyta	Fragilariales	*Asterionella glacialis*	2,72E-05
Hacrobia	Cryptophyta	Telonemida	*Telonema antarcticum*	2,57E-05
Stramenopiles	Ochrophyta	Chaetocerotanae incertae sedis	*Chaetoceros curvisetus*	2,57E-05
Alveolata	Myzozoa	Peridiniales	*Protoperidinium sp.*	2,55E-05
Alveolata	Myzozoa	Peridiniales	*Pentapharsodinium tyrrhenicum*	2,47E-05
Archaeplastida	Chlorophyta	Mamiellales	*Ostreococcus mediterraneus*	2,42E-05
Stramenopiles	Ochrophyta	Rhizosoleniales	*Proboscia alata*	2,41E-05
Rhizaria	Cercozoa	Cryptofilida	*Unknown Cryptofilida*	2,39E-05
Apusozoa	Apusomonadidae	Apusomonadidae_Group-1_X	*Amastigomonas_sp.*	2,37E-05

Alveolata	Myzozoa	Syndiniales	*Hematodinium sp.*	2,36E-05
Alveolata	Dinoflagellata	Noctilucales	*Unknown Noctilucales*	2,33E-05
Stramenopiles	Oomycota	Developayellales	*Developayella sp.*	2,31E-05
Stramenopiles	Ochrophyta	Sarcinochrysidales	*Unknown Sarcinochrysidales*	2,28E-05
Archaeplastida	Chlorophyta	Sphaeropleales	*Desmodesmus sp.*	2,23E-05
Alveolata	Myzozoa	NA	*Polyplicarium curvarae*	2,21E-05
Archaeplastida	Chlorophyta	Chlamydomonadales	*Chloromonas sp.*	2,19E-05
Stramenopiles	Ochrophyta	Chaetocerotanae incertae sedis	*Chaetoceros protuberans*	2,17E-05
Archaeplastida	Chlorophyta	Prasinococcales	*Prasinoderma sp.*	2,13E-05
Alveolata	Ciliophora	Choreotrichida	*Amphorellopsis acuta*	2,11E-05
Alveolata	Ciliophora	Philasterida	*Pseudocohnilembus persalinus*	2,09E-05
Alveolata	Myzozoa	Peridiniales	*Protoperidinium americanum*	1,99E-05
Opisthokonta	Chytridiomycota	Chytridiales	*Chytridium polysiphoniae*	1,93E-05
Stramenopiles	Ochrophyta	Pedinellales	*Pseudopedinella sp.*	1,91E-05
Stramenopiles	Ochrophyta	Naviculales	*Pleurosigma intermedium*	1,84E-05
Alveolata	Myzozoa	Dinophyceae incertae sedis	*Qia lebouriae*	1,82E-05
Archaeplastida	Chlorophyta	Chlorellales	*Chloroidium ellipsoideum*	1,79E-05
Hacrobia	Haptophyta	Prymnesiophyceae_Clade_D	*Unknown Prymnesiophyceae_Clade_D*	1,78E-05
Alveolata	Myzozoa	Peridiniales	*Amphidiniopsis rotundata*	1,77E-05
Stramenopiles	Bigyra	Bicoecida	*Pseudobodo sp.*	1,75E-05
Stramenopiles	Ochrophyta	Dictyotales	*Newhousia imbricata*	1,75E-05
Stramenopiles	Ochrophyta	Thalassiosirales	*Thalassiosira guillardii*	1,73E-05
Stramenopiles	Ochrophyta	Mischococcales	*Monodus sp.*	1,73E-05
Stramenopiles	Bigyra	Thraustochytrida	*Aplanochytrium haliotidis*	1,69E-05
Hacrobia	Haptophyta	Isochrysidales	*Gephyrocapsa oceanica*	1,69E-05
Opisthokonta	Choanozoa	NA	*Sphaeroforma sp.*	1,54E-05
Archaeplastida	Chlorophyta	Prasiolales	*Stichococcus bacillaris*	1,50E-05
Stamenopiles	Ochrophyta	Thalassiosirales	*Minidiscus variabilis*	1,49E-05
Stramenopiles	Ochrophyta	Parmales	*Triparma pacifica*	1,49E-05
Rhizaria	Euglenozoa	Eubodonida	*Cercomonas sp.*	1,46E-05
Rhizaria	Cercozoa	Marimonadida	*Auranticordis quadriverberis*	1,45E-05
Alveolata	Myzozoa	Gymnodiniales	*Gyrodinium gutrula*	1,43E-05
Stramenopiles	Ochrophyta	Thalassiosirales	*Lauderia annulata*	1,43E-05
Stramenopiles	Ochrophyta	Corethrales	*Corethron hystrix*	1,42E-05
Amoebozoa	Amoebozoa_X	UI13E03-lineage	*Unknown UI13E03-lineage*	1,41E-05
Amoebozoa	Conosa	ATCC50593-Flamella-WIM80-lineage	*Unknown ATCC50593-Flamella-WIM80-lineage*	1,41E-05
Stramenopiles	Ochrophyta	Parmales	*Triparma laevis clade*	1,39E-05
Rhizaria	Cercozoa	Novel-clade-12	*Unknown Novel-clade-12*	1,38E-05
Archaeplastida	Chlorophyta	Mamiellales	*Mantoniella squamata*	1,38E-05
Alveolata	Ciliophora	NA	*Unknown Phyllopharyngea*	1,34E-05
Hacrobia	Cryptophyta	Pyrenomonadales	*Hemiselmis sp.*	1,33E-05
Archaeplastida	Chlorophyta	Dolichomastigales	*Crustomastigaceae-AB_sp.*	1,32E-05

Opisthokonta	Fungi	Pezizomycotina	*Unknown Pezizomycotina*	1,31E-05
Stramenopiles	Ochrophyta	Triceratiales	*Triceratium alternans f. alternans*	1,30E-05
Stramenopiles	Ochrophyta	Chromulinales	*Paraphysomonas foraminifera*	1,29E-05
Alveolata	Apicomplexa	Colpodellida	*Colpodellidae2_sp.*	1,28E-05
Rhizaria	Radiolaria	Chaunacanthida	*Unknown Chaunacanthida*	1,24E-05
Alveolata	Myzozoa	Dinophysiales	*Phalacroma porodictyum*	1,23E-05
Opisthokonta	Ascomycota	Saccharomycetales	*Saccharomyces cerevisiae*	1,23E-05
Stramenopiles	Ochrophyta	Chromulinales	*Spumella vulgaris*	1,23E-05
Alveolata	Apicomplexa	Apicomplexa_XX	*Apicomplexa_XXXX_sp.*	1,21E-05
Stramenopiles	Sagenista	MAST-4C	*Unknown MAST-4C*	1,18E-05
Archaeplastida	Chlorophyta	Ulvales-relatives	*Unknown Ulvales-relatives*	1,16E-05
Archaeplastida	Chlorophyta	Mamiellales	*Unknown Mamiellales*	1,15E-05
Hacrobia	Cryptophyta	Cryptomonadales	*Cryptomonas curvata*	1,14E-05
Rhizaria	Cercozoa	Phytomyxea incertae sedis	*Phagomyxa sp.*	1,13E-05
Rhizaria	Cercozoa	Leucodictyida	*Massisteria sp.*	1,10E-05
Stramenopiles	Ochrophyta	Thalassionematales	*Thalassionema sp.*	1,10E-05
Stramenopiles	Ochrophyta	Surirellales	*Entomoneis sp.*	1,10E-05
Stramenopiles	Opalozoa	NA	*Unknown MAST-3*	1,06E-05
Archaeplastida	Chlorophyta	Trentepohliales	*Trentepohlia sp.*	1,06E-05
Opisthokonta	Fungi	Pucciniomycotina	*Kondoa malvinella*	1,06E-05
Hacrobia	Cryptophyta	Cryptophyceae_X	*Unknown Cryptophyceae*	1,04E-05
Alveolata	Ciliophora	Apostomatia	*Unknown Apostomatia*	1,04E-05
Amoebozoa	Lobosa	Dermamoebida	*Unknown Dermamoebida*	1,01E-05
Stramenopiles	Opalozoa	MAST-3H	*Unknown MAST-3H*	1,00E-05
Stramenopiles	Bigyra	Bicoecida	*Pseudobodo tremulans*	9,96E-06
Alveolata	Myzozoa	Oxyrrhinales	*Oxyrrhis marina*	9,66E-06
Hacrobia	Cryptophyta	Pyrenomonadales	*Rhodomonas salina*	9,60E-06
Alveolata	Myzozoa	Eugregarinorida	*Lecudina phyllochaetopteri*	9,51E-06
Hacrobia	Haptophyta	Phaeocystales	*Phaeocystis cordata*	9,36E-06
Amoebozoa	Lobosa	Leptomyxida	*Unknown Leptomyxida*	9,22E-06
Stramenopiles	Ochrophyta	Rhizosoleniales	*Guinardia blavyana var. blavyana*	9,17E-06
Alveolata	Ciliophora	Cyrtophoria_7	*Unknown Cyrtophoria_7*	8,95E-06
Opisthokonta	Choanoflagellida	Choanoflagellida_XX	*Choanoflagellida_XXXX_sp.*	8,88E-06
Stramenopiles	Ochrophyta	Eustigmatales	*Nannochloropsis granulata*	8,87E-06
Alveolata	Ciliophora	Philasterida	*Pseudocohnilembus longisetus*	8,72E-06
Archaeplastida	Chlorophyta	Synurales	*Microglena monadina*	8,54E-06
Rhizaria	Cercozoa	Glissomonadida	*Allantion sp.*	8,53E-06
Stramenopiles	Opalozoa	MAST-3L	*Unknown MAST-3L*	8,48E-06
Stramenopiles	Ochrophyta	Thalassiosirales	*Thalassiosira pseudonana*	8,28E-06
Alveolata	Ciliophora	Philasterida	*Cinetochilum ovale*	8,23E-06
Opisthokonta	Fungi	Chytridiomycotina	*Lobulomyces_sp.*	8,11E-06
Rhizaria	Cercozoa	Aconchulinida	*Thalassomyxa sp.*	7,80E-06
Stramenopiles	Ochrophyta	Rhaponeidales	*Rhaphoneis amphiceros*	7,70E-06

Stramenopiles	Ochrophyta	Triceratiales	*Odontella sp.*	7,62E-06
Amoebozoa	Breviatea	Breviatea_XX	*Unknown Breviatea_X*	7,57E-06
Alveolata	Ciliophora	Cyrtophoria_8	*Dysteria_2_sp.*	7,56E-06
Archaeplastida	Chlorophyta	Nephroselmidales	*Unknown Nephroselmidales*	7,45E-06
Hacrobia	Haptophyta	Prymnesiales	*Prymnesium sp.*	7,34E-06
Archaeplastida	Chlorophyta	Prasinococcales	*Prasinoderma singularis*	7,33E-06
Amoebozoa	Amoebozoa	Leptomyxida	*Rhizamoeba saxonica*	7,33E-06
Hacrobia	Cryptophyta	Pyrenomonadales	*Hemiselmis rufescens*	7,32E-06
Stramenopiles	Ochrophyta	Chromulinales	*Spumella elongata*	7,22E-06
Alveolata	Ciliophora	Chlamydodontida	*Pseudochilodonopsis sp.*	6,98E-06
Alveolata	Ciliophora	NA	*Unknown CONTH_3*	6,95E-06
Rhizaria	Cercozoa	Thaumatomonadida	*Esquamula lacrimiformis*	6,94E-06
Apusozoa	Apusomonadidae	Apusomonadidae_Group-1_X	*Amastigomonas mutabilis*	6,93E-06
Rhizaria	Cercozoa	Novel-clade-9	*Unknown Novel-clade-9*	6,73E-06
Amoebozoa	Amoebozoa	Leptomyxida	*Paraflabellula sp.*	6,06E-06
Rhizaria	Cercozoa	Limnofilida	*Limnofila_sp.*	5,87E-06
Rhizaria	Cercozoa	NA	*Unknown Filosa*	5,81E-06
Archaeplastida	Chlorophyta	Chlamydomonadales	*Unknown Chlamydomonadales*	5,69E-06
Stramenopiles	Pseudofungi	MAST-2C	*Unknown MAST-2C*	5,64E-06
Stramenopiles	Ochrophyta	Triceratiales	*Odontella regia*	5,62E-06
Alveolata	Apicomplexa	Eimeriida	*Unknown Eimeriida*	5,61E-06
Archaeplastida	Chlorophyta	Mamiellales	*Micromonas clade B3*	5,61E-06
Alveolata	Myzozoa	Gymnodiniales	*Torodinium teredo*	5,58E-06
Opisthokonta	Fungi	Fungi_XX	*Fungi_XXXX_sp.*	5,56E-06
Rhizaria	Cercozoa	Glissomonadida	*Neoheteromita globosa*	5,53E-06
Stramenopiles	Oomycota	Olpidiopsidales	*Olpidiopsis sp.*	5,53E-06
Stramenopiles	Ochrophyta	Pelagomonadales	*Aureococcus anophagefferens*	5,43E-06
Hacrobia	Cryptophyta	Cryptomonadales	*Goniomonas avonlea*	5,35E-06
Stramenopiles	Ochrophyta	NA	*Unknown Raphidophyceae*	5,27E-06
Apusozoa	Apusomonadidae	Apusomonadidae_Group-2B	*Unknown Apusomonadidae_Group-2B*	5,23E-06
Rhizaria	Cercozoa	Ventricleftida	*Verrucomonas bifida*	5,23E-06
Stramenopiles	Sagenista	MAST-9D	*Unknown MAST-9D*	5,19E-06
Alveolata	Myzozoa	Lophodiniales	*Biecheleriopsis adriatica*	5,18E-06
Alveolata	Perkinsea	NA	*Unknown Perkinsida*	5,17E-06
Alveolata	Ciliophora	Philasterida	*Mesanophrys carcini*	5,08E-06
Opisthokonta	Fungi	Ustilaginomycotina	*Malassezia restricta*	5,08E-06
Stramenopiles	Ochrophyta	Bacillariophyta_X	*Chaetoceros debilis 1*	4,95E-06
Alveolata	Ciliophora	NA	*Stylonychia lemnae*	4,74E-06
Hacrobia	Haptophyta	Prymnesiales	*Chrysochromulina leadbeateri*	4,69E-06
Archaeplastida	Chlorophyta	Trentepohliales	*Trentepohlia umbrina*	4,67E-06
Alveolata	Ciliophora	NA	*Spirotrachelostyla tani*	4,62E-06
Alveolata	Myzozoa	Peridiniales	*Scrippsiella precaria*	4,55E-06
Archaeplastida	Chlorophyta	Nephroselmidaceae	*Unknown Nephroselmidaceae*	4,55E-06

Alveolata	Ciliophora	Peniculia	*Paramecium nephridiatum*	4,45E-06
Alveolata	Myzozoa	Gonyaulacales	*Alexandrium sp 01*	4,45E-06
Rhizaria	Cercozoa	Cryomonadida	*Protaspa obliqua*	4,36E-06
Stramenopiles	Opalozoa	MAST-3G	*Unknown MAST-3G*	4,36E-06
Archaeplastida	Chlorophyta	Chlorellales	*Nannochloris sp.*	4,27E-06
Stramenopiles	Opalozoa	Pseudodendromonadales	*Paramonas globosa*	4,27E-06
Stramenopiles	Ochrophyta	Pelagomonadales	*Pelagomonas calceolata*	4,24E-06
Stramenopiles	Sagenista	MAST-8B	*Unknown MAST-8B*	4,24E-06
Opisthokonta	Fungi	Pucciniomycotina	*Rhodotorula minuta*	4,23E-06
Excavata	Euglenozoa	Diplonemida	*Diplonema sp.*	3,98E-06
Stramenopiles	Ochrophyta	Hemiaulales	*Eucampia zodiacus*	3,92E-06
Alveolata	Myzozoa	Gymnodiniales	*Lepidodinium viride*	3,88E-06
Alveolata	Myzozoa	Gymnodiniales	*Spiniferodinium sp.*	3,87E-06
Alveolata	Apicomplexa	Colpodellida	*Unknown Colpodellida*	3,79E-06
Rhizaria	Cercozoa	Limnofilida	*Limnofila anglica*	3,76E-06
Archaeplastida	Chlorophyta	Pyramimonadales	*Pyramimonas disomata*	3,76E-06
Alveolata	Myzozoa	Peridiniales	*Islandinium sp.*	3,49E-06
Apusozoa	Hilomonadea	Planomonadidae	*Ancyromonas micra*	3,48E-06
Alveolata	Ciliophora	Sessilida	*Pseudovorticella sinensis*	3,44E-06
Stramenopiles	Ochrophyta	Chaetocerotanae incertae sedis	*Chaetoceros sp Clade Na11C3*	3,44E-06
Stramenopiles	Ochrophyta	Rhizosoleniales	*Rhizosolenia sp.*	3,38E-06
Alveolata	Dinoflagellata	Dino-Group-IV	*Hematodinium perezi*	3,34E-06
Rhizaria	Cercozoa	Cryomonadida	*Protaspa grandis*	3,34E-06
Stramenopiles	Ochrophyta	Bacillariophyta_X	*Guinardia solstherfothii*	3,32E-06
Stramenopiles	Sagenista	MAST-8D	*Unknown MAST-8D*	3,30E-06
Stramenopiles	Opalozoa	MAST-3K	*Unknown MAST-3K*	3,25E-06
Stramenopiles	Ochrophyta	Chaetocerotanae incertae sedis	*Chaetoceros didymus*	3,24E-06
Stramenopiles	Ochrophyta	Naviculales	*Navicula phyllepta*	3,18E-06
Stramenopiles	Ochrophyta	Triceratiales	*Plagiogramma vanheurckii*	3,12E-06
Alveolata	Ciliophora	NA	*Unknown Oligohymenophorea*	3,12E-06
Excavata	Percolozoa	Schizopyrenida	*Heteramoeba clara*	3,05E-06
Archaeplastida	Chlorophyta	Pyramimonadales	*Pyramimonas subg. Pyramimonas propulsa*	3,03E-06
Stramenopiles	Ochrophyta	Chaetocerotanae incertae sedis	*Chaetoceros jonquieri*	2,85E-06
Hacrobia	Haptophyta	Prymnesiophyceae_Clade_E	*Unknown Prymnesiophyceae_Clade_E*	2,84E-06
Opisthokonta	Fungi	Blastocladiomycotina	*Unknown Blastocladiomycotina*	2,77E-06
Alveolata	Ciliophora	Philasterida	*Uronema elegans*	2,76E-06
Opisthokonta	Fungi	Chytridiomycotina	*Rhizophydium chlorogonii*	2,74E-06
Alveolata	Myzozoa	Perkinsida	*Perkinsus qugwadii*	2,74E-06
Alveolata	Ciliophora	Plagiopylea_X	*Trimyema compressum*	2,65E-06
Alveolata	Myzozoa	Prorocentrales	*Prorocentrum nanum*	2,65E-06
Stramenopiles	Ochrophyta	NA	*Unknown MOCH-4*	2,63E-06
Alveolata	Myzozoa	Blastodiniales	*Oodinium pouchetii*	2,54E-06

Stramenopiles	Ochrophyta	Lithodesmiales	*Lithodesmium undulatum*	2,53E-06
Hacrobia	Haptophyta	Prymnesiales	*Unknown Prymnesiales*	2,36E-06
Rhizaria	Cercozoa	Plasmodiophorida	*Spongospora_sp.*	2,34E-06
Stramenopiles	Ochrophyta	NA	*Unknown Phaeophyceae*	2,34E-06
Alveolata	Ciliophora	Choreotrichida	*Eutintinnus lusus-undae*	2,32E-06
Alveolata	Ciliophora	Peniculia	*Frontonia_1_sp.*	2,27E-06
Amoebozoa	Amoebozoa	Euamoebida	*Hartmannella abertawensis*	2,27E-06
Stramenopiles	Ochrophyta	Bacillariophyta_X	*Chaetoceros pumilum*	2,24E-06
Alveolata	Ciliophora	Choreotrichida	*Pelagostrobilidium minutum*	2,21E-06
Hacrobia	Haptophyta	NA	*Unknown Prymnesiophyceae*	2,18E-06
Hacrobia	Cryptophyta	Pyrenomonadales	*Falcomonas sp.*	2,15E-06
Alveolata	Myzozoa	Gymnodiniales	*Lepidodinium sp.*	2,10E-06
Hacrobia	Cryptophyta	NA	*Leucocryptos sp.*	2,07E-06
Opisthokonta	Fungi	Ustilaginomycotina	*Tilletiopsis pallescens*	2,03E-06
Amoebozoa	Conosa	Variosea_X	*Nematostelium ovatum*	2,02E-06
Rhizaria	Cercozoa	Plasmodiophorida	*Woronina pythii*	2,00E-06
Alveolata	Myzozoa	Gymnodiniales	*Polykrikos schwartzii*	1,99E-06
Stramenopiles	Ochrophyta	Chaetocerotanae incertae sedis	*Chaetoceros circinalis*	1,96E-06
Stramenopiles	Ochrophyta	Rhizosoleniales	*Guinardia sp.*	1,96E-06
Alveolata	Perkinsea	Perkinsida_X	*Parvilucifera infectans*	1,89E-06
Amoebozoa	Amoebozoa	Stygamoebida	*Vermistella sp.*	1,75E-06
Archaeplastida	Chlorophyta	NA	*Chloropicon laureae*	1,75E-06
Stramenopiles	Ochrophyta	Biddulphiales	*Biddulphia rostrata var. rostrata*	1,73E-06
Apusozoa	Hilomonadea	Planomonadidae	*Ancyromonas kenti*	1,64E-06
Rhizaria	Cercozoa	Metromonadida	*Micrometopion nutans*	1,64E-06
Archaeplastida	Chlorophyta	Ulvales	*Blidingia dawsonii*	1,63E-06
Archaeplastida	Chlorophyta	NA	*Chloroparvula pacifica*	1,56E-06
Hacrobia	Haptophyta	Prymnesiophyceae_Clade_F	*Unknown Prymnesiophyceae_Clade_F*	1,56E-06
Alveolata	Ciliophora	Pleuronematida	*Cyclidium glaucoma*	1,52E-06
Amoebozoa	Conosa	Variosea_X	*Unknown Variosea*	1,52E-06
Archaeplastida	Chlorophyta	Pedinomonadales	*Marsupiomonas sp.*	1,52E-06
Hacrobia	Cryptophyta	NA	*Katablepharis remigera*	1,52E-06
Alveolata	Myzozoa	Gymnodiniales	*Polykrikos tanit*	1,49E-06
Hacrobia	Cryptophyta	Cryptomonadales	*Goniomonas sp.*	1,42E-06
Stramenopiles	Ochrophyta	Pedinellales	*Pteridomonas danica*	1,41E-06
Alveolata	Ciliophora	Choreotrichida	*Strombidinopsis batos*	1,39E-06
Stramenopiles	Ochrophyta	Triceratiales	*Cerataulus smithii*	1,37E-06
Stramenopiles	Ochrophyta	Thalassiosirales	*Stephanodiscus sp.*	1,37E-06
Stramenopiles	Ochrophyta	Bacillariophyta_X	*Chaetoceros debilis 3*	1,37E-06
Stramenopiles	Ochrophyta	Thalassiosirales	*Skeletonema pseudocostatum*	1,34E-06
Stramenopiles	Ochrophyta	Bacillariophyta_X	*Skeletonema menzellii*	1,34E-06
Alveolata	Myzozoa	Torodiniales	*Kapelodinium vestifici*	1,32E-06
Stramenopiles	Pseudofungi	Pirsonia_Clade_X	*Pirsonia guinardiae*	1,29E-06

Alveolata	Myzozoa	Eugregarinorida	*Lecudina tuzetae*	1,14E-06
Alveolata	Ciliophora	Choreotrichida	*Stenosemella pacifica*	1,08E-06
Amoebozoa	Breviatea	NA	*Unknown NAMAKO-1-lineage*	1,01E-06
Stramenopiles	Pseudofungi	Hyphochytrydiales	*Hyphochytrium_sp.*	9,48E-07
Archaeplastida	Chlorophyta	Sphaeropleales	*Desmodesmus communis*	9,15E-07
Stramenopiles	Ochrophyta	Naviculales	*Halamphora coffeaeformis*	9,15E-07
Hacrobia	Cryptophyta	Pyrenomonadales	*Plagioselmis nannoplanctica*	8,72E-07
Alveolata	Myzozoa	Gymnodiniales	*Gymnodinium aureolum*	8,32E-07
Alveolata	Myzozoa	Noctilucales	*Noctiluca sp.*	8,32E-07
Stramenopiles	Pseudofungi	Oomycota_X	*Olpidiopsis porphyrae*	8,13E-07
Alveolata	Myzozoa	Peridiniales	*Protoperidinium conicum*	7,58E-07
Apusozoa	Mantamonadidea	Mantamonadida_X	*Mantamonas plastica*	7,12E-07
Alveolata	Ciliophora	Sessilida	*Vorticella microstoma*	6,10E-07
Opisthokonta	Ascomycota	Saccharomycetales	*Metschnikowia sp.*	6,10E-07
Amoebozoa	Amoebozoa	Nolandida	*Nolandella hibernica*	5,08E-07
Alveolata	Myzozoa	Gymnodiniales	*Nematodinium sp.*	4,46E-07
Opisthokonta	Fungi	Pucciniomycotina	*Sporobolomyces roseus*	4,46E-07
Alveolata	Myzozoa	Peridiniales	*Protoperidinium thulesense*	4,07E-07
Alveolata	Ciliophora	Oligotrichida	*Strombidium triquetrum*	3,79E-07
Amoebozoa	Lobosa	Dactylopodida	*Vexillifera tasmaniana*	3,79E-07
Opisthokonta	Fungi	Saccharomycotina	*Yarrowia lipolytica*	3,05E-07
Stramenopiles	Ochrophyta	Bacillariophyta_X	*Rhaphoneis belgicae*	3,05E-07
Stramenopiles	Sagenista	MAST-4F	*Unknown MAST-4F*	2,73E-07
Stramenopiles	Ochrophyta	Rhizosoleniales	*Rhizosolenia pungens*	2,23E-07
Stramenopiles	Ochrophyta	Bacillariales	*Nitzschia thermalis*	1,36E-07